This is to certify that the

dissertation entitled

Use of Scaling Theory in Predictive Methods to
Efficiently Construct Two- and Three-Phase
Constitutive Relationships

presented by

Herr Soeryantono

has been accepted towards fulfillment
of the requirements for

Ph.D. degree in Civil Engineering

Roger B. Wallace
Major professor

Date April, 1995

Use of Scaling Theory in Predictive Methods to Efficiently Construct Two- and Three-Phase Constitutive Relationships

by

Herr Soeryantono

A DISSERTATION

Submitted to
Michigan State University
in partial fulfillment of the requirements
for the degree of

DOCTOR OF PHILOSOPHY

Department of Civil and Environmental Engineering

1995

Roger B. Wallace

ABSTRACT

Use of Scaling Theory in Predictive Methods to Efficiently Construct Two- and Three-Phase Constitutive Relationships

by

Herr Soeryantono

Scaling theory (*Parker et al.*, 1987) combined with *Leverette*'s (1941) predictive method permits prediction of the relative permeability-saturation-pressure (k_r-S-P) relationship of any two- or three-phase system from P-S data of a particular two-phase system and interfacial tension data. Implementation of the theory is studied by comparing the two- and three-phase k_r-S-P curves constructed with *Leverette*'s predictive method with and without the use of scaling theory. The observations include predictions which are based on air-water or air-oil P-S data using two soils: uniform graded Ottawa sand and loamy sand Metea soil.

Comparison of the k_r-S-P curves obtained with and without the scaling theory showed that, at least for the investigated cases, the use of air-oil system as the basis of prediction is only suggested for a well-graded soil. When involving a uniform grain type soil the use of air-water system as the basis of prediction is preferable.

The required *P-S* data were measured in a pressure cell using the pressure equilibrium method. This method reverses the conventional technique (*Klute*, 1986) by imposing rapid finite desaturation and subsequently allowing hydrostatic equilibrium under a zero flux boundary conditions. Theoretical verification showed that this method is more efficient than the conventional technique. Laboratory experiments confirmed the theoretical result and showed that the *P-S* relation obtained from the data, statistically, indistinguishable from that obtained by conventional method.

To Ibu, Christina, Titon and Nino

ACKNOWLEDGMENT

I gratefully acknowledge the contributions of those who have made this dissertation possible. My deepest gratitude goes to Dr. Roger B. Wallace, Associate Professor, Department of Civil and Environmental Engineering, Michigan State University, my dissertation director and advisor during my course work. I appreciate his fatherly advice, patience, and continual encouragement throughout my entire graduate program and his stamina in reviewing a great many drafts. He was instrumental to the successful completion of this dissertation.

I would also like to thank Dr. Thomas C. Voice, Associate Professor Department of Civil and Environmental Engineering; Dr. David C. Wiggert, Professor, Department of Civil and Environmental Engineering; and Dr. Raymond J. Kunze, Professor, Department of Crops and Soil Science, Michigan State University for serving in my dissertation committee and for their extremely valuable comments in this study.

For the further development of pressure saturation measurement apparatus which was essential in this study I owe Dr. Arthur T. Corey, Profesor Emeritus, Department of Agricultural Engineering, Colorado State University. Dr. Mokma, Professor, Department of Crop and Soil Sciences helped to select the soil types I used.

Research funding was obtained from several sources. I wish to thank the Second Higher Education Development Project, Ministry of Education and Culture Republic of Indonesia that provided support for the first three years of my doctoral program. This research could not have been completed without support from the National Institute for

Environmental Health Sciences (Grant ES04911) and the Michigan State University Institute for Environmental Toxicology.

Ruth Dukesbury and Kahlil Rowter helped in proofreading. For that I am very grateful. To Mike Annable, Lizzette Chevalier, Reza Rakhshandehroo, Munjed Maraqa, Michel Hsu, Yao J.J, Linda Steinmann and Brenda Minott, my colleagues in the Department of Civil and Environmental Engineering, Michigan State University, I would like to express my deep appreciation to for all their support and encouragement

Finally, I want to thank my wife and children: Christina, Titon and Nino for their love, care, support and understanding.

TABLE OF CONTENT

Tabl

Tabl

Tabl

LIST OF TABLES

Figure

Figur

Figur

Figur

Figur

Figure

Figure

Figure

Figur

LIST OF FIGURES

LIST OF SYMBOLS

α, α_{pq}	*P-S* parameter of *van Genuchten* (1982) *P-S* function in two phase system *pq*.
α_{aw}	α of air-water *P-S* curve.
α_{ow}	α of oil-water *P-S* curve.
α_{ao}	α of air-oil *P-S* curve.
β	scaling factor.
β_{ao}	air-oil scaling factor.
B_o	air-water scaling factor.
β_{ow}	oil-water scaling factor.
ε_α	uncertainty limits of parameter α.
ε_n	uncertainty limits of parameter *n*.
ε_S	uncertainty limits of saturation.
ε_{Sr}	uncertainty limits of residual saturation.
λ	*Brooks and Corey* (1964) pore size index.
ϕ	porosity.
ρ^*	specific density of the reference phase.
ρ_p	specific density of phase *p*.
σ	interfacial tension.
σ_{aw}	air-water interfacial tension.
σ_{ow}	oil-water interfacial tension.
σ_{ao}	air-oil interfacial tension.
σ_{ow}	oil-water interfacial tension.
$\forall$	accumulated outflow volume.
$\forall_d$	target outflow volume in simulation.
ω	contact angle.
$[C]$	covariance matrix $[C]=(F^T.F)^{-1}$

[F]	jacobian matrix $[\mathbf{F}]=\left[\frac{\partial S(h_i)}{\partial S_\mathrm{r}} \quad \frac{\partial S(h_i)}{\partial \alpha} \quad \frac{\partial S(h_i)}{\partial n}\right]$
d	grain size scale factor in similar media concept.
df	degree of freedom.
g	gravitational acceleration
h	pressure head.
h_a	air phase pressure head.
h_ao	capillary pressure head of air-water system.
h_aw	capillary pressure head of air-water system.
h_o	oil phase pressure head.
h_ow	capillary pressure head of air-water system.
h_p	prescribed pressure head lower boundary condition.
h_{pq}	capillary pressure head in two-phase system pq.
h_w	water phase pressure head.
i, j	summation index, i, j=1, 2, 3, . . .
$\mathrm{J}(S^*)$	Leverette J function.
k	saturated relative permeability.
k_{ij}	saturated permeability tensor.
k_r	relative permeability.
$k_\mathrm{ro}^\mathrm{ao}$	oil relative permeability in air-oil system.
$k_\mathrm{ro}^\mathrm{ow}$	oil relative permeability in oil-water system.
$k_\mathrm{ro}^\mathrm{aow}$	oil relative permeability in three-phase system.
$k_{\mathrm{r}p}$	relative permeability of phase p.
$k_\mathrm{rw}^\mathrm{aow}$	water relative permeability in three-phase system.
$k_\mathrm{rw}^\mathrm{aw}$	water relative permeability in air-water system.
$k_\mathrm{rw}^\mathrm{ow}$	water relative permeability in oil-water system.
m, m_{pq}	P-S parameter of *van Genuchten* (1982) P-S function in two phase system pq.
n, n_{pq}	P-S parameter of *van Genuchten* (1982) P-S function in two phase system pq.
P	capillary pressure.

p	phase type, p = air, oil, water.
P_d	displacement capillary pressure.
P_p	wetting-phase pressure.
P_{pq}	capillary pressure in two-phase system pq.
P_q	nonwetting-phase pressure.
pq	two-phase system p=oil, water. q=air, oil.
q	wetting phase flux.
R.	macroscopic radius of curvature.
R_c	microscopic radius of curvature, radius of curvature interfaces in capillary tube.
S	degree of saturation.
$S(P_\mathrm{pq})$	degree of saturation as a function of capillary pressure in two phase system pq.
$S(R)$	saturation as a function of macroscopic radius of curvature, pore size distribution function.
$S(t_\mathrm{d})$	water saturation profile at t_d.
$S(t_\mathrm{e})$	water saturation profile at t_e.
$S(t_\mathrm{o})$	water saturation profile at t_o.
S_e	effective saturation $S_\mathrm{e} \equiv (S-S_\mathrm{r})/(1-S_\mathrm{r})$.
S_o^ao	oil phase saturation in air-oil system.
$S_\mathrm{o}^\mathrm{aow}$	oil phase saturation in three-phase system.
S_p	degree of saturation of phase p.
S_r, $S_{\mathrm{r}\text{-}pq}$	residual saturation, residual saturation of wetting phase p in two phase system pq.
sse	sum of squared error
$S_\mathrm{t}^\mathrm{aow}$	total liquid saturation, saturation of oil phase plus water phase in three-phase system.
$\bar{S}_\mathrm{t}^\mathrm{aow}$	total liquid effective saturation in three-phase system.
$S_\mathrm{w}^\mathrm{aow}$	water phase saturation in three phase system.
S_w^aw	water phase saturation in air-water system.
$\bar{S}_\mathrm{w}^\mathrm{aow}$	water phase effective saturation in three-phase system.

$S_{\mathrm{w}}^{\mathrm{ow}}$	water phase saturation in oil-water system.
t	time.
t_{d}	time required to drain $\forall_{\mathrm{d}}$, drainage time.
$t_{df}^{2.5}$	student **t** value at 95% probability and degree of freedom *df.*
t_{e}	time required to reach equilibrium.
t_{o}	initial time.
x	direction in Cartesian coordinates.
z	vertical distance.

CHAPTER I

INTRODUCTION

1.1. BACKGROUND

Volatile organic contaminants (VOCs) are extensively present in waste dumps. Some of the VOCs exist in the form of non-aqueous phase liquid (NAPL). When NAPL is allowed to infiltrate the soil, some fraction will partition into and contaminate the water phase that exist in soil pores. Due to its immiscible nature with water and gas, the remaining fraction will stay as a separate liquid phase. This fraction will migrate further leaving a trail of residual NAPL in the soil pore. This residual fraction will become a long-term source of ground water contamination and further NAPL migration will extend the contaminated region.

As a special case in immiscible flow problems, the coexistence of gas-NAPL-water in porous medium is referred to as a three-phase system. The phases involved in such a system are commonly referred to as air, oil and water phases with the VOC being the oil phase. According to *Gee et al.* (1991) the development of a mathematical model to accurately assess the spatial and temporal quantification of these contaminants is impeded by the lack of three-phase constitutive information relating relative permeability (k_r), saturation (S) and capillary pressure (P). As pointed out by *Abriola* (1989), the primary difficulty is in measuring the capillary pressure of an individual phase in a three-phase system. Therefore, most analyses of constitutive properties governing three-phase flow

(*Corey, et al.*, 1956; *Stone*, 1973; *Azis and Settari*, 1979) are based on predictive methods which extend the information obtained from two-phase measurements.

The predictive method conceptualizes the three-phase system as two separate interdependent two-phase systems; air-total liquid and oil-water. The degree of total liquid saturation (ie. the saturation of the oil and water altogether) is assumed to be dictated only by the air-oil capillary pressure and that the degree of water saturation is dictated only by the oil-water capillary pressure. Thus, a complete set of two- and three phase k_r-S-P relationships can be determined based only on the two-phase P-S information. *Parker et al.* (1987) proposed a scaling theory which simplifies the implementation of the predictive method even further. Within the same porous medium, the scaling theory permits prediction of the P-S relationship of any two-phase system from the P-S relationship of a particular two-phase system provided that the pertaining scaling factor is known. The scaling theory determines the scaling factors from interfacial tension data. Therefore, when the P-S data of one two-phase system is available the k_r-S-P information involving any fluids in any combinations can be determined. The additional data required are only the interfacial tension data.

The scaling theory was incorporated in a versatile numerical three-phase flow model (*Kaluarachi et al.*, 1990), which was further improved and has been shown valid for both desaturation and imbibition scanning paths (*Parker and Lenhard*, 1987b) and to accept multi component organic chemical transport (*Parker and Kaluarachchi*, 1990). This model is one among the few formulated to predict DNAPL movement (*Huling and*

Weaver, 1991). Incorporation of scaling theory into the model eliminates the necessity to provide air-oil and oil-water *P-S* information. It allows the use of air-water *P-S* and interfacial tension data only.

NAPL contamination assessment in the unsaturated zone most likely involves unconsolidated soils. Air-water *P-S* measurement on an unconsolidated soil sample is a common practice among soil scientist and the measurement protocol for this case is well established. Thus, air-water *P-S* data are commonly available. Interfacial tension measurement can also be considered standard measurements with an established protocol as described by *Adamson* (1976). Considering that the data requirements are less, scaling theory greatly improves the applicability of the multi-phase and multi-component model by *Kaluarachi et al.* (1990).

Beside the advantages stated above, however, the use of scaling theory in the predictive method may contribute to additional loss in accuracy of the obtained k_r-S relationship as *Lenhard etal.* (1987) has suggested. Scaling theory regards the soil matrix as a rigid porous medium. Accordingly, the pore size distribution is also assumed constant with respect to time. This assumption is widely adopted in the ares of ground water engineering. However, as noted in *Lenhard et al.* (1987), the k_r-S relationship prediction via scaling theory might be sensitive to any disturbance in the pore size distribution. Small changes in pore size distributions, such as that due to swelling, which is not clearly evidenced in the *P-S* plot might affect the prediction of k_r-S curves significantly. On the other hand, the pore size distribution is inherent in *P-S* relationship and this relationship is represented only by the *P-S* parameters. Therefore, any error or bias in these parameters might also affect the prediction of k_r-*S* curves significantly such as the effect of pore size distribution changes. Note that, k_r-*S-P* relationship prediction via scaling theory is based on *P-S* parameters measured in one two-phase system only. These parameters are referred to as base parameters. The above discussion suggests the importance of a study to investigate the effect of error or bias embodied in the base parameters to the prediction of the k_r-*S-P* curves via the scaling theory.

The magnitude of error and the potential of obtaining bias parameters can be deduced from the precision of those parameters. Accuracy and precision in determining the *P-S* parameters might be affected by soil texture and the type of the immiscible fluid involved. A study by *McCuen et al.* (1981), based on 1,085 samples measured by *Rawls et al.* (1976) and *Holtan et al.* (1968), observed distinct *P-S* parameter variance between soil texture classes. As observed in the measurement result reported by *Lenhard and Parker* (1987), the *P-S* parameters derived from air-water data possessed higher variation than those determined from either air-oil or oil-water data . If the accuracy and precision of the *P-S* parameters differs from one two-phase or from one porous medium to the other, so does the performance of the prediction of the k_r-*S-P* relationship. In turn, the scaling theory might perform differently when it is implemented on different soil texture using base parameters from different two-phase system.

In providing the three-phase k_r-S-P relationship information the predictive method relies on the availability of two-phase *P-S* information. When involving unconsolidated soil samples, which is typical for subsurface soil samples, *P-S* measurement of the air-water system is more common than the air-oil or oil-water system. Therefore, air-water *P-S* data in general is widely available. When information of air-oil or oil-water *P-S* relationship are required, in most cases, measurements should be conducted. On the other hand, established *P-S* measurement, such as that by *Klute* (1986), are primarily intended to measure air-water system. The characteristics of an air-water measurement protocol are: suitable only for a low wetting phase volatility, limited to gaseous type of non-wetting phase, and takes a considerable amount of time. In parallel with current growing interest in the multiphase flow problem, it is desirable to have an efficient *P-S* measurement technique that measures not only air-water systems but also air-oil and oil-water systems.

Conventionally, *P-S* data are measured by allowing saturation to equilibrate under a series of fixed pressures imposed at the boundaries. While this technique is considered to be standard, a considerable amount of time is required to measure the entire *P-S* relationship. Typically, time required to obtain sufficient data to adequately represent the desaturation scanning path is approximately two weeks (*Su and Brooks*, 1980; *Bear*, 1982). Such a disadvantage significantly constrains the gathering a large amount of data, sample replication, and to measure data near the region of residual saturation. Yet, it is desirable to include these measurements. Replication and a large number of data insure a representative sample mean as well as knowledge about the variance. Inclusion of data from the region near residual saturation reduces the risk of bias.

The time required to measure *P-S* data using the conventional method is primarily dictated by the time required for the system to reach hydrostatic equilibrium. Evidently, any measurement readings in other than the hydrostatic equilibrium state would not represent the primary drainage or imbibition *P-S* relationships. (*Topp et al.*, 1967; *Smiles et al.*, 1971; *Corey and Brooks*, 1975; *Parker et al.*, 1985). A *P-S* measurement method devised by *A.T. Corey*, as reported by *White et al.* (1970) is capable of reducing the measurement time while obtaining data that are representative of primary drainage. This technique reverses the conventional method by requiring capillary pressure to equilibrate under a series of fixed externally imposed saturation. Henceforth in this dissertation (based on the phenomenon to deduce the equilibrium state of the sample), the conventional method is referred to as the saturation equilibrium method. The method devised by *Corey* is referred to as the pressure equilibrium method. The pressure equilibrium method has been employed by *White et al.* (1970) and *White et al.* (1972) and was improved upon by *Su and Brooks* (1980). Typical total time required to measure 9 data points in air-water desaturation and imbibition scanning paths was less than 24 hours (*Su and Brooks*, 1980).

While the pressure equilibrium technique has been shown capable of reducing the measurement time significantly, the obtained data have never been formally compared to that obtained using the conventional method. As such, the time reduction achieved may only be the result of a premature reading which might be biased relative to the conventional measurement. If the converse was true and experimental time was indeed shortened, this technique offers an efficient method which might be further improved to measure any type of immiscible fluid.

1.2. GENERAL OBJECTIVES, APPROACHES AND PRESENTATION ORGANIZATION

This study focuses on the effects of incorporating scaling theory in the predictive method to construct the three-phase k_r-S-P relationship. Without using scaling theory, the P-S parameters required by the predictive method should be determined from P-S desaturation data of air-water, oil-water and air-oil systems. With scaling theory, however, only one of those systems is required to be measured. This study investigates the alternative of using either the air-water or air-oil systems as the base system. The air-water system is not directly involved in a three phase system. However, air-water data are commonly available. Conversely, the air-oil system involves in a three-phase system but P-S data of this system are not as widely available as that of air-water. The performances of these alternatives are investigated in two soil textures. The textures chosen are sand with uniform grain size distribution and loamy sand. *Lenhard and Parker* (1987) proposed the scaling theory as a way of improving the efficiency of the predictive method. Accordingly, the discussion throughout this dissertation is in the context of testing the hypothesis that the predictive methods with and without the scaling theory are not different regardless of the usage of the two-phase system to obtain the base parameters and the involvement of soil texture.

Additionally, this study verifies the pressure equilibrium measurement technique against the conventional measurement method as part of an effort of developing an efficient *P-S* measurement technique. The *Su and Brooks* (1980) apparatus is modified and improved to make it suitable for air-water, oil-water and air-oil *P-S* desaturation measurement. The concept of the modification is verified theoretically. An unsaturated mathematical model based on Richard's equation is developed to simulate *P-S* measurement employing the pressure equilibrium method as well as the saturation equilibrium method. The modified apparatus is used to measure *P-S* data of air-water and air-oil systems. The pressure equilibrium is proposed to provide an efficient two-phase *P-S* measurement technique substituting the conventional saturation equilibrium method. As such, discussion in this dissertation is focused to observe whether the pressure equilibrium method is capable of reducing the time required to measure two-phase *P-S* data while conserving the characteristic of the primary desaturation.

The two major issues addressed pertain to the implementation of the scaling theory and the verification of the pressure equilibrium measurement method. These two issues are discussed in Chapter II and Chapter III. Each of these chapters is presented as a self-contained section. Each one contains a concise discussion of the background, description of the material and method used and subsequently discusses the results and findings specific to the particular issue. Experimental protocols, measurement result, data reduction and statistical calculations are presented in the appendices.

Background of the issue is presented in three separate sections. First, the Definition and General Overview section in this chapter clarifies the terminology used and summarizes the major existing concepts pertaining to the pressure-saturation scaling theory. It is intended to draw a frame work from a broad point of view. Additional background, more specific to the separate issues is presented concisely in the introductory sections of Chapters II and III. These sections are intended to put the addressed issues in perspective.

1.3. DEFINITIONS AND GENERAL OVERVIEW.

As mentioned above, this dissertation is concerned with the scaling method in the context of its implementation in the predictive method. The predictive method is a concept to provide an alternative means for solving multiphase flow equations. Prior to discussing the existing methods to scale the *P-S* relationship, the subsequent sections describes some terminology pertaining to multiphase flow used in this dissertation. Following that, the involvement of the predictive method in solving the multiphase flow is presented. The last section reviews the existing methods to scale the *P-S* relationship and highlights the porous medium hydraulic properties that are postulated by some authors as being the factors in the scaling method. The notations used in the presentation, generally follow the symbols used in *Parker* (1989).

1.3.1. Multiphase System

When two or more fluids coexist in a soil pore and one or more of those fluids are in motion, the types of flow possible are either miscible or immiscible displacements (*Bear*, 1972). Miscible displacement refers to the case where the fluids are completely

soluble in each other. A distinct fluid-fluid interface which separates those fluids does not exist. In the immiscible displacement, each fluid for practical purpose exists separately. As such, a distinct interface between fluids exists and the interfacial tension between the two fluids is not zero.

Fluid motion accompanying immiscible displacement is commonly referred to as multiphase flow. In this dissertation the term phase is used specifically to refer to the fluids involved and not the soil grains. A multiphase system refers to the coexistence of two or more phases in soil pore in conjunction with the multiphase flow concept. A multiphase system in general may involve two or more fluid types. However, a conceptualization of multiphase system which considers only three types of fluid is commonly regarded as sufficient and representative as the most general form of a multiphase system. This dissertation uses the term three-phase system in this context. In conjunction with an interest in subsurface contamination assessment, the three fluids involved in a three-phase system are often classified as water, NAPL and gaseous phases. The NAPL and gaseous phase are commonly referred to as oil and air phases respectively. Henceforth, the terms air, oil and water are used to refer to the phases involved in the three-phase system.

A two-phase system is a multiphase system involving only two phases. The phases in a two-phase system are referred to as wetting-and nonwetting. The phase that tends to have direct contact with the solid is referred to as the wetting phase. The two-phase system consisting of air and water is a special case. This system describes condition in the unsaturated zone prior to contamination. The water and the air phases are the wetting- and nonwetting-phases, respectively. Unsaturated flow is a particular case of two-phase flow. In this case, the interest is focused on the water phase motion only and the air phase is assumed stagnant at atmospheric pressure.

1.3.2. Multiphase Flow Equation and the Predictive Method.

The equation governing the multiphase flow is derived from the generalization of Darcy's equation combined with the continuity equation. (*Bear*, 1972; *Corey*, 1982; *Parker*, 1989). According to *Parker* (1989), the governing equation of the multiphase flow in a non-deformable porous medium, under the assumption of no sources or sinks of the phases involved, is given by:

$$\phi \frac{\partial(\rho_p \cdot S_p)}{\partial t} = \frac{\partial}{x_i} \rho_p \cdot k_{rp} k_{ij} \left[\frac{\partial h_p}{\partial x_j} + \rho_p \cdot \frac{\partial z}{\partial x_j} \right]$$

The subscript p is reserved to indicate the fluid phase (p=a, o, w) while i and j indicates directions (i, j=1,2,3) with repeating values indicating summation in tensor notation, x is the Cartesian coordinate, z is the vertical elevation, ϕ denotes the porosity of the medium, t is time, ρ_p is the phase density, k_{rp} is the phase relative permeability, k_{ij} is the intrinsic permeability tensor, S_p is the degree of saturation by the phase which is the fraction of the soil pore occupied by phase p, and h_p is the pressure head of phase p.

Note that h, S and k_r are interrelated. When capillary pressure h increases the saturation is decreased. Saturation decrement reduce the pore volume that participate in providing the channel for the fluid in question to flow. The relationship between k_r-S-h is formulated in the constitutive equations. The constitutive equation governing multiphase flow consists of two functional relationships. The first relationship is a function relating the saturation of a particular phase and the pressure heads of the phases involved. The second is the relationship between the relative permeability and the saturation. The first function is referred to as pressure-saturation (*P-S*) function. In a three-phase system, this function is formulated as:

$$S_p = \mathrm{f}(h_a, h_o, h_w). \qquad [1\text{-}1]$$

The *P-S* function in a two-phase system is a special case that involves only the pressures of the wetting and nonwetting phases. Interaction between these pressures can be represented only by the capillary pressure which is defined as:

$$P_{pq} \equiv P_p - P_q$$

Here P_{pq} is the capillary pressure, P_p is the pressure of the nonwetting phase p and P_q is the pressure of the wetting phase q. The capillary pressure P_{pq} is commonly expressed in terms of pressure head relative to some reference phase as:

$$h_{pq} = P_{pq} (g \rho^*)^{-1}$$

where h_{pq} is the capillary pressure of the pertaining immiscible phases pq in term of pressure head, g is the gravitational force, and ρ^* is the density of the reference phase. The two-phase *P-S* function will then take a simple form as:

$$S = \mathrm{f}(h_{pq}). \qquad [1\text{-}2]$$

The procedure to solve the flow equation commonly involves a step to reduce the nonlinearity of that function by applying the chain rule to the term of the derivative of saturation with respect to time. The form of the chain rule for the case of three-phase flow is written as:

$$\frac{\partial S_o}{\partial t} = \frac{\partial S_o}{\partial h_a}\frac{\partial h_a}{\partial t} + \frac{\partial S_o}{\partial h_o}\frac{\partial h_o}{\partial t} + \frac{\partial S_o}{\partial h_w}\frac{\partial h_w}{\partial t} \qquad [1\text{-}3]$$

This means that the constitutive equation that describe the relation of oil saturation and the capillary pressure heads should be formulated in the form of Eqn 1-1. Construction of such a relationship requires direct measurement of the saturation and the pressure head of the air, oil and water phases simultaneously. This requires three phase measurements which are not commonly made. Furthermore an established protocol and technique to conduct three-phase *P-S* measurement is not yet available. *Lenhard and Parker* (1988) are the only investigators to report three-phase measurements for *P-S* relationships.

The common method for solving the three-phase flow equation is by employing the predictive method proposed by *Leverett* (1941). The predictive method assumes that the soil matrix is a hydrophilic porous medium. Under this assumption, the water phase has a direct contact with the soil grain while the oil phase always resides between the water and the air phases. Provided that the oil volume is high enough to cover the water surface, the air phase would have no direct contact with the water phase. The predictive method further assumes that the total liquid saturation (ie. oil plus water) is dictated only by the air-oil capillary pressure and that the water saturation is dictated only by the oil-water capillary pressure.

Employing the above point of view, a three-phase system consisting of air, oil and water can be conceptualized as two interdependent two-phase systems. The first system is a two-phase system consisting of a total liquid phase and an air phase. Since the saturation of the total liquid is a function of the air-oil capillary pressure only, the total liquid-air system is assumed to be identical to an air-oil system. Secondly, within the total liquid phase, the oil-water two-phase system exists. Employing this approach, the above chain rule would only involve the derivative of total saturation with respect to air-oil capillary pressure and derivatives of water saturation with respect to oil-water capillary pressure. Therefore, it only requires knowledge of the air-oil and oil-water *P-S* relationship. These relationships are easier to measure compared to a true three-phase *P-S* relationship.

1.3.3. Methods to Scale the Pressure-Saturation Relationship.

1.3.3.1. General Formulation of the Pressure-Saturation Scaling

P-S scaling theory was developed to relate a *P-S* curve across porous media hydraulic system. This knowledge allows transformation of the *P-S* relationship from certain system to another system. Prerequisite to this knowledge is an understanding of any determinants that dictate the *P-S* relationship. According to *Bear* (1972), because of the dependency of capillary pressure P on interfacial tension σ and radius of curvature R_c on a microscopic level, macroscopically it depends on (a) the geometry of the void space, (b) the nature of the soil-fluid interaction and (c) the degree of saturation S. On a macroscopic level, the porous medium property associated with the characteristic of the void space geometry is the pore size distribution. The factor of soil-fluid interaction includes contact angle ω as suggested by *Morrow* (1976) and *Demond and Roberts*

(1990) among others and wettability as suggested by *Scheideger* (1969) and *Adamson* (1967). The study by *Anderson* (1987), however, concluded that the *P-S* relationship was insensitive to the wettability at large saturation ranges as it is overwhelmed by the effect of surface roughness. This dissertation assumes that the effect of wettability is insignificant. The third factor which is the dependency of capillary pressure to the saturation, is formulated in the form of *P-S* relationship curve. Therefore, it is obvious that inherent in the *P-S* relationship there exist interactions between P, R_c, σ, ω and S. The following paragraphs discuss further the conceptualization of these interaction.

Capillary phenomena in a soil matrix are commonly explained based on Laplace's equation. Under this concept, the capillary pressure P_{pq} is related to the radius of curvature R_c of the interface by:

$$P_{pq} = \frac{2\,\sigma}{R_c} \qquad [1\text{-}4]$$

Note that, a *P-S* relationship describes the relationship between the capillary pressure and saturation at a macroscopic level. Hence, a given capillary pressure does not necessarily refer to a particular radius of curvature in a particular soil pore. On a macroscopic level, R_c is rather the radius of a conceptual capillary interface in the soil-fluid system that exits as the response of the system when subjected to that capillary pressure. To distinguish between the microscopic and the macroscopic radius of curvature let the macroscopically measure be denoted as R. *Corey* (1982) defined R as the hydraulic radius equivalent to that commonly used in hydraulic engineering. *Bear* (1982) put this R in the context of "statistical average taken over the void space in the vicinity of a considered point in the porous medium". The most important characteristic of R is that it decreases as the capillary pressure P_{pq} increase and when R decreases S decreases proportionally. The conceptual relation between S and R is commonly associated with pore size distribution and is taken to be a porous medium dependent parameter. In this dissertation the term of pore size distribution function is used specifically to refer a function that relates S and R in the form of $R(S)$.

Based on the conception above, a P-S relationship in the form of saturation as a function of capillary pressure $S(P_{pq})$ can be factored into two relationships. The first relationship relates the capillary pressure and the radius of curvature $P_{pq}(R)$. This relationship is formulated following the concept behind Equation 1-4. The second relates the macroscopic radius of curvature and a function of saturation which is conceptualized as the pore size distribution function $R(S)$. Therefore, the function of $S(P_{pq})$ can be viewed as the result of substituting the $R(S)$ into $P_{pq}(R)$.

Following this conceptualization, an $S^{\mathbf{A}}(P_{pq}^{\mathbf{A}})$ curve of soil-fluids system **A** can be transformed to become $S^{\mathbf{B}}(P_{pq}^{\mathbf{B}})$ of soil-fluids system **B** by scaling their capillary pressures such that at any given S there exist a relation of $P_{pq}^{\mathbf{B}}(R) = \beta(S)\ P_{pq}^{\mathbf{A}}(R)$. The factor β is referred to as scaling factor and hence is defined as:

$$\beta(S) \equiv P_{pq}^{\mathbf{B}}(R)/P_{pq}^{\mathbf{A}}(R). \qquad [1\text{-}5]$$

The general formulation of the scaling factor can be obtained by substituting Equation 1-4 into Equation 1-5 and is written as:

$$\beta(S)=\left(\frac{\sigma^{\mathbf{B}}}{\sigma^{\mathbf{A}}}\right)\left[\frac{R^{\mathbf{A}}(S)}{R^{\mathbf{B}}(S)}\right] \qquad [1\text{-}6]$$

Within a soil-fluid system the interfacial tension is commonly regarded as a constant. The macroscopic radius of curvature R, however, varies as the saturation changes. When the saturation in the system **A** and **B** is changed with the same amount, the R in systems **A** and **B** is not necessarily changed with the same amount. Therefore, the ratio $R^{\mathbf{A}}/R^{\mathbf{B}}$ varies when the saturation is varied. Equation 1-6 accommodates this characteristic by expressing the macroscopic radius of curvature R as the pore size distribution function $R(S)$. Therefore, to obtain a scaling factor that transform *P-S* curves across two different two-phase systems and porous media requires knowledge of the interfacial tensions and pore size distribution functions.

The scaling factor as formulated in Equation 1-6 might obscure its practical value. To date, most common technique to deduce the pore size distribution function requires *P-S* data. When *P-S* data are measured and available for both systems **A** and **B**, scaling procedures are not required. Some investigators have proposed relating the pore size distribution function to the grain size distribution. For example, *Smith* (1933) and *White et al.* (1970a) simplify the shape of the soil grain into sphere shapes to formulate the void structure. Even after such simplification, the results were still too complex for practical use and yet too specific to serve any general purpose. Apparently, procedures for scaling the *P-S* curve are only feasible within identical soils or at least within similar porous media as defined in the similar media concept by *Miller and Miller* (1956).

1.3.3.2. Leverette (1941) J Function

Leverette (1941) proposed a function, referred to as **J** function, to represent a general form of the *P-S* relations. This function is given as:

$$\mathbf{J}(S^{*}) = \left(\frac{P_{pq}}{\sigma}\right)\left(\sqrt{\frac{k}{\phi}}\right) \qquad [1\text{-}7]$$

Here *k* is the saturated permeability and ϕ is the porosity. In his report, *Laverette* (1941) showed that Equation 1-7 coalesced the *P-S* curves measured in several unconsolidated sands. Based on this notion, the **J** function is commonly regarded as function that can be used to scale *P-S* curves not only across the two-phase system but also across porous media.

To scale *P-S* relationship, Equation 1-6 utilizes a factor which transforms *P-S* relationship of a particular soil-fluids system to another. The **J** function follows different approach. This method transforms any *P-S* curve into its standard form, which is the J function as written in Equation 1-7. In order to compare the scaling concept behind Equation 1-6 and Equation 1-7, the scaling factor is reformulated based on Equation 1-7. The factor which scales the capillary pressure in system **A** into system **B** at a given **J**(*S**) is given by:

$$\beta = \frac{\sigma^{\mathbf{B}}}{\sigma^{\mathbf{A}}} \cdot \frac{\sqrt{k^{\mathbf{A}} / \phi^{\mathbf{A}}}}{\sqrt{k^{\mathbf{B}} / \phi^{\mathbf{B}}}} \qquad [1\text{-}8]$$

According to *Bear* (1972) and *Corey* (1982), based on the concept of relative permeability proposed by *Burdine* (1956), the term of $(k_r/\phi)^{1/2}$ is equivalent to *R* at

saturation in which the unsaturated permeability is k_r. When k_r is substituted by the saturated permeability k, the term $(k/\phi)^{1/2}$ can be interpreted as the macroscopic radius of curvature when the effective porosity are fully filled with the wetting phase. If this particular radius of curvature is denoted as $R_{\max}$, Equation 1-8 becomes:

$$\beta = \frac{\sigma^{\mathbf{B}}}{\sigma^{\mathbf{A}}} \cdot \frac{R_{\max}^{\mathbf{A}}}{R_{\max}^{\mathbf{B}}} \qquad [1\text{-}9]$$

When comparing Equation 1-9 with Equation 1-6, it shows that the **J** function scales the *P-S* relationship across porous media using a constant (the ratio of $R_{\max}$) rather than using the pore size distribution function. It is expected that this particular scaling method will not always hold. In a later study using air-water system in various consolidated and unconsolidated porous media (*Rose and Bruce*, 1949), shows that plots of the **J** function are unique to the porous medium type. Based on this, further studies (*Rapoport* 1955; *Richardson*, 1961) that advocated the use of this function to scale the *P-S* curves, restricted the use of their method for identical porous medium. Under this restriction the ratio of $R_{\max}$ becomes unity. In turn *P-S* scaling by **J** function accommodates the scaling across two-phase systems only and excludes the feature of across porous media.

1.3.3.3. Similar Media Concept by Miller and Miller (1956)

Miller and Miller (1956) proposed the similar media concept as a method to scale the unit of a physical model to simulate unsaturated flow in porous media. Here two porous media are considered as similar when the grain size axis of their grain size frequency distribution curves can be scaled to each other by a constant factor *d*.

According to this method, all *P-S* curves within similar media will coalesce into a standard curve when their capillary pressures are scaled by:

$$\dot{P} = \left(\frac{P_{pq}}{\sigma} \right) d \qquad [1\text{-}10]$$

where $\dot{P}$ is the scaled capillary pressure. Using superscript **A** and **B** to denote the oil-fluids systems, the scaling factor equation derived based on Equation 1-10 will take form of:

$$\beta = \frac{\sigma^{\mathbf{B}}}{\sigma^{\mathbf{A}}} \cdot \frac{d^{\mathbf{A}}}{d^{\mathbf{B}}} \qquad [1\text{-}11]$$

This formulation is equivalent to that formulated in Equation 1-9 where the scaling across porous media is accommodated by including the term of the ratio of *d*. It should be noted, however, to satisfy the similar media condition the two porous media should have similar grain size frequency distribution. Inherently, this condition requires that the two porous media have similar shape pore size distribution curve. When this condition is applied in Equation 1-6, the term of the ratio of the pore size distribution functions will be constant. As the result the scaling factor β in Equation 1-6 will take form of constant rather than function. Thus, the scaling factor as formulated in Equation 1-6 is in agreement with that in Equation 1-11.

Study by *Klute and Wilkinson* (1958) confirmed that when the criterion of similar media was satisfied *P-S* curves of several different-but-similar sands were coalesced. The study by *Elrick et al.* (1959) using soil containing not only sand fractions but also silt and clay, however, concluded that when the theory was checked against condition far from ideal a deviation was observed. Moreover, this study demonstrated the sensitivity of the scaling procedure to any pore size distribution variation.

1.3.3.4. Brooks and Corey (1964) Pressure-Saturation Function as A Scaling Method

A special case of interest in scaling the *P-S* curve is when this curve is expressed following the equation proposed by *Brooks and Corey* (1964). Here the *P-S* relationship is formulated as:

$$S_e = \left(\frac{P_d}{P_{pq}} \right)^{\lambda} \qquad [1\text{-}12]$$

where S_e is the effective saturation which is defined as $(S-S_r)/(1-S_r)$, S_r is the residual saturation, P_d is the displacement pressure and λ is the pore size index. All the required parameters to scale the *P-S* curve are already inherent in this formula since all parameters involved have a clear physical interpretation. When S is expressed in term of S_e the differences between the two *P-S* curves due to their differences in S_r are factored out. Thus *P-S* curves from any two-phase system will have common range of S_e from 1 at full saturation to zero at residual saturation.

The displacement pressure P_d is the capillary pressure associated with the largest pore in the soil-fluid system in question. When the capillary pressure in a *P-S* plot is factored by P_d, a standard capillary pressure equivalent to $\dot{P}$ used in *Miller and Miller* (1956) is obtained. The parameter λ represents the pore size distribution characteristic and was postulated to be a porous medium dependent parameter. In turn, any two *P-S* curves that have identical λ will satisfy the requirement for similar media. Therefore, if those two curves are expressed in term of effective saturation and reduced capillary pressure they will coalesce into a single curve. Based on this particular characteristic, the parameters P_d and λ are often used as parameters upon which the characteristic of the scaling method is observed such as in studies by *Demond and Roberts* (1990), *Lenhard and Parker* (1987) among others.

Even though *P-S* formulation given by Eqn 1-12 provides all properties required for scaling procedure, the use of this function to conduct scaling across porous media is not practical. When a scaling equation comparable to Equation 1-6 is derived based on Equation 1-12, the resulting equation will be a function of λ. This means that the knowledge of pore size indexes of the porous media involved is required. As mention previously, to date, these indexes can only be obtained by means of *P-S* measurement.

1.3.3.5. Lenhard and Parker (1987) Scaling Theory.

As part of their effort to develop an efficient method to construct a three-phase constitutive relationship, *Lenhard and Parker* (1987) proposed their scaling theory. This method was intended to scale the *P-S* curves across two-phase systems within a single porous medium. Therefore, their scaling factor took the form of Equation 1-6 in which the term of $R^{\mathbf{A}}(S)/R^{\mathbf{B}}(S)$ is set to unity since the soil in systems **A** and **B** are identical. Further detail description of their theory is presented as part of Chapter III.

1.3.3.6. The Issue of Contact Angle.

In its original form, the contact angle ω is involved in the Laplace equation. When ω is included, Equation 1-1 takes the form:

$$\beta(S) = \left(\frac{\sigma^{\mathbf{B}} \cdot \cos\omega^{\mathbf{B}}}{\sigma^{\mathbf{A}} \cdot \cos\omega^{\mathbf{A}}} \right) \left[\frac{R^{\mathbf{A}}(S)}{R^{\mathbf{B}}(S)} \right] \qquad [1\text{-}13]$$

Among investigators, the inclusion of contact angle ω is still a point of controversy. Several investigators who worked with artificial unconsolidated porous medium (*Bethel and Calhoun*, 1953; *Morrow*, 1976; *Demond*, 1988; and *Demond and Roberts*, 1990) observed the effect of ω on the *P-S* relationship. Subsequent work (*Demond and Roberts*, 1991) on a sand-organic liquid-water system showed the discrepancy between the observed and scaled displacement pressure when ω was excluded.

Exclusion of ω (*Leverette*, 1941; *Rapoport*, 1955; *Parker*, 1987) was based on the argument that conceptualization of soil pore geometry as a tube was not appropriate. Hence, the radius of tube should be expressed in term of radius of curvature. Arithmetically, when the radius of tube is expressed in term of radius of curvature the contact angle ω will be canceled out. By not including contact angle ω, *Dumore and Schols* (1974) were able to successfully scale their data of heptane-water and toluane-water in consolidated sample. *Anderson* (1987) observed that both in strongly water-wet and oil-wet consolidated rock sample, the capillary pressure is insensitive to ω at large range values of ω, especially in the drainage path.

It is interesting that most of the investigations that reported an observable effect of ω, used an artificial unconsolidated porous medium or clean sand. On the contrary, those who used natural rock core or unconsolidated soil concluded that due to the existence of surface roughness, the apparent effect of contact angle is almost non-existent. In this dissertation the effect of contact angle ω is assumed negligible.

1.3.3.7. Dependency of Scaling Method on Soil Texture

Several studies indicate the dependency of the parameters P_d and λ on soil texture. This dependency is based on the assumption that in an air-water system, the pore size distribution characteristic is strongly affected by the grain size frequency distribution. Several studies even advocated deduction of the *P-S* curve based on the parameters associated with the grain size distribution (*McCueen et al.*, 1981; *Campbell*, 1985; *Mishra et al.*, 1989 among others).These approaches were based on regressing an empirical function onto grain size distribution data. *Brakensiek et al.* (1981) used the *Brooks-Corey* (1964) equation as their regression function. In this study the parameters P_d and λ were classified into the twelve Soil Conservation Service textural classes. A study by *Cosby et al.*, (1984) confirmed that, statistically, the magnitudes of P_d and λ were strongly dictated by the soil texture. Similarly, the study by *McCueen et al.*, (1981) found that these parameters are unique for each soil texture class.

CHAPTER II

THE ACCEPTABILITY OF THE PRESSURE EQUILIBRIUM METHOD TO MEASURE DRAINAGE PATH OF SOIL PRESSURE-SATURATION

2.1. BACKGROUND

The pressure-saturation (*P-S*) relationship is one of the constitutive relationships governing multiphase flow through unsaturated porous media. It expresses the functional relationship of the equilibrium wetting phase saturation at a given capillary pressure. Petroleum engineers employ the *P-S* relationship (*Collins*, 1961), while soil scientists present the same information in a water retention or moisture characteristic curve (*Child*, 1940). The soil scientist's term, however, is commonly restricted to air-water systems, while the more general *P-S* relationship is employed with a variety of immiscible fluid systems. In parallel with current growing interest in a multiphase flow problem, it is desirable to have an efficient *P-S* measurement method that measures not only air-water systems but also air-oil and oil-water systems.

Conventionally, the *P-S* data are measured by allowing saturation to equilibrate under a series of fixed pressure gradients imposed at a boundary. While this technique is considered to be a standard, it is a very time_consuming method. The typical time period required to obtain sufficient data to adequately represent the desaturation scanning path is approximately two weeks (*Su and Brooks*, 1980). Such a disadvantage places significant limitations in collecting larger numbers of data, replicating the sample, and measuring the data near the residual saturation region. Replication and the large numbers of data are desirable to obtain representative mean and to increase precision reliability. An inclusion of data from the region near residual saturation eliminates the risk of bias.

The length of experimental time in the conventional *P-S* measurement is primarily dictated by the length of time required for the system to reach equilibrium. Up to this time, studies that investigated the feasibility of conducting measurements during the transient state have had qualified success. At a given saturation, capillary pressure measured under dynamic flow tended to be higher than those in a static condition (*Topp et al.*, 1967; *Smiles et al.*, 1971; *Corey and Brooks*, 1975; *Parker et al.*, 1985). Apparently, in order to obtain *P-S* data that share similar characteristic to the conventional method, any alternative method that measures the *P-S* relationship under an equilibrium state is more sound.

An alternative method that measures the *P-S* relationship under the equilibrium state was devised by *A.T. Corey* (*White et al.*, 1970). This method had been used in *White et al.* (1970) and *White et al.* (1972) and was improved by *Su and Brooks* (1980). In contrast to the conventional method, suction was applied in two stages. In the first stage suction was set to drive a reasonably quick desaturation. While in the second stage, after a volume of desaturation had been obtained, the suction was adjusted to balance the equilibrium wetting phase pressure. Implementing this method to measure air-water data using 50 different soils covering a wide range of properties, *Su and Brooks* (1980), observed that typical experimental time to complete both desaturation and imbibition scanning paths was less than 24 hours. The transient time for the pressure to reach

equilibrium after the desaturation step took only a few minutes at high saturation and a few hours at low saturation region.

While this technique significantly shortens the experimental time, the obtained data have never been formally compared to data using the conventional method. As such, the time reduction achieved may only be the result of a premature reading which could introduce bias relative to the conventional measurement. If the converse were true and experimental time was indeed shortened, this technique offers an efficient method which might be further improved to measure any type of immiscible fluids. Note that in the *Su and Brooks* (1980) apparatus, a wetting phase evaporation was allowed to accelerate the desaturation rate. If the wetting phase is a volatile liquid, the desaturation might be dominated by evaporation. This condition may introduce a problem in adjusting the second stage suction. Furthermore, this approach prohibits the use of a liquid nonwetting phase. However, applying a high positive pressure on the nonwetting phase to desaturate the sample may resolve those problems. This modification, however, is only justified providing that it will not affect the characteristics of the method for reaching equilibrium quickly.

According to *Su and Brooks* (1980), the equilibrium state was quickly reached due to the adjustment made in applying the second stage suction. Unfortunately, no further explanation was given. In their measurement technique this adjustment was conducted in the following manner. After a finite volume had been drained from the sample, the outflow was directed toward a vertical capillary glass tube containing the meniscus of the air-wetting phase interface. At this instance, the air pressure on that interface was adjusted to maintain the meniscus level at a prescribed datum until this meniscus became stationary. Leveling the meniscus during the transient state will permit determination of the wetting phase pressure. In our opinion leveling the meniscus changes the condition at the external face of the plate from a constant head to a zero flux condition. This suggests that the important behavior underlying the *Su and Brooks* (1980) method is that the transient state within the soil sample which occurs under a no-flow boundary condition will be terminated more quickly than it would under a constant head boundary condition as in the conventional method.

Based on this premise, applying a positive pressure to desaturate the sample should give no effect to the basic principle of the method. Furthermore, replacing the capillary tube with a zero displacement pressure transducer seems to be more effective in providing a zero-flux boundary condition while monitoring the wetting phase pressure. Furthermore, the use of a transducer eliminates the laborious second stage suction adjustment. If the transducer used is capable of measuring the pressure difference between the wetting and nonwetting pressure, a more efficient measurement protocol can be obtained.

In order to distinguish between the *Corey* method and the conventional method based on the phenomenon used to indicate the equilibrium state of the system, the *Corey* method will be referred to as the pressure equilibrium (PE) method and the conventional one as the saturation equilibrium (SE) method. The current paper studies the implementation of the PE method by developing a *P-S* measurement apparatus based on the concept referred to in the previous paragraph. The apparatus developed was tested to measure air-water, air-oil and oil-water desaturation *P-S* relationships in a natural loamy sand soil. To justify the acceptability of the PE method, the air-water and air-oil data obtained were compared to those obtained by the SE method. In addition, a 1-D unsaturated flow mathematical model was used to verify the method theoretically.

2.2. MEASUREMENT METHOD AND MATERIAL

The PE method measures the *P-S* desaturation data by imposing a finite desaturation on a presaturated sample and subsequently allowing the fluids in the sample to equilibrate under a no-flow boundary conditions prior to recording the equilibrium data. The equilibrium state in this case is indicated by a stationary wetting-nonwetting pressure difference. With the SE method, desaturation is allowed to occur under a fixed wetting-nonwetting pressure difference imposed at the boundaries until equilibrium is reached as indicated by an outflow diminishment. In order to compare the performance of these two methods, a *P-S* measurement device capable of performing either PE or SE methods in measuring air-water, oil-water or air-oil desaturation data was developed.

This device was developed utilizing a standard pressure cell by Soil Moisture (Model No: 1400) as shown in detail in Figure 2-1. The connection between the pressure cell and the other parts of the device is shown in Figure 2-2. Three pressurized fluid sources are available: air, oil and water. The air phase source is obtained from the building line through a cascade of coarse and fine regulators. The oil and water phase pressure chambers provide the source of the oil and water phases respectively. The pressures of these liquids are governed by the air pressure in the chamber. This pressure

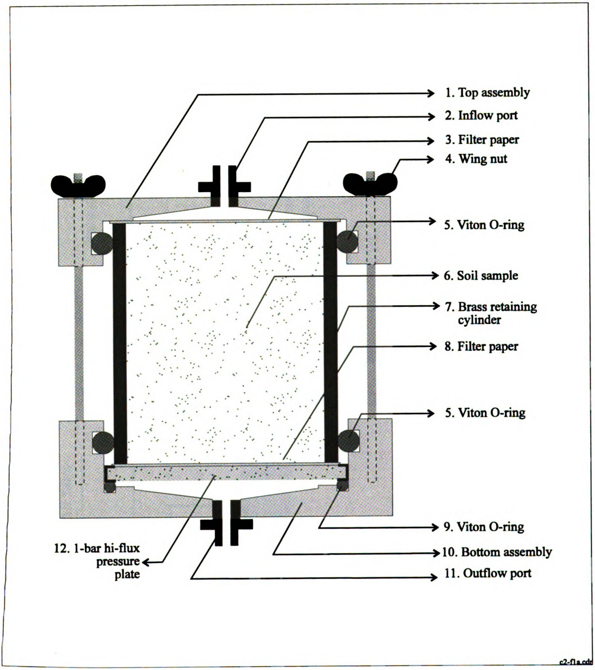

Figure 2-1: Pressure cell detail

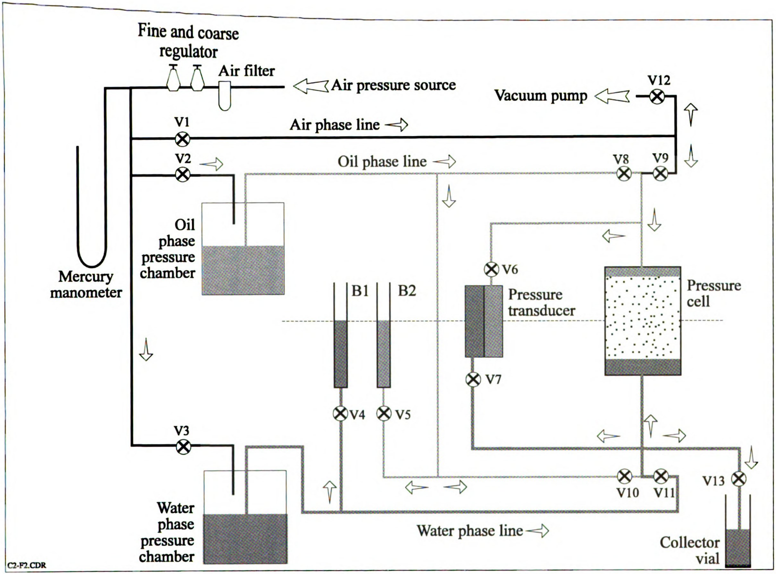

Figure 2-2: The apparatus set up

can be altered utilizing the building pressurized air. The zero pressure of these liquids is defined as the pressure which level the air-liquids interface in burettes B1 and B2 (Figure 2-2) at the center of the cell. The applied building air pressure at any instance is monitored via a mercury manometer.

The connections between the fluid sources and the cell are designed such that the air and water phases can be used as the nonwetting and the wetting phases respectively, while the oil phase may function as either one. The nonwetting phase line is connected to the top of the cell. The positive pressure applied on the nonwetting phase drains the wetting phase from the bottom of the cell. The outflow is directed into a vial collector in which the pressure is atmospheric. The outflow line to the vial is controlled by a valve, referred to as the collector valve. The collector valve is opened only when desaturation is permitted. A differential pressure transducer is installed to measure the pressure gradient between the wetting and the nonwetting phase pressures.

Typical procedures in conducting measurement are: packing the sample, saturating the sample, calibrating the transducer, conducting *P-S* measurement based on PE or SE method, and determining the residual saturation by an independent means. Note that in the SE method the nonwetting phase pressure is determined using a mercury manometer. Therefore, transducer calibration is not required.

The loose soil sample with approximately 2-3% water content was packed in a brass retaining cylinder (2¼"OD, 0.065" wall thickness, and 3 cm height) using a compactor with a 1.6 kg weight falling 10 times from a 7 cm height. This procedure proved to be effective in maintaining consistent bulk density between samples.

Subsequently, the packed soil in the retaining cylinder was assembled with the other pressure cell parts. The pressure plate was oven dried prior to being installed in the cell. The final cell assembly (Figure 2-1) was placed and connected to the other part of the measurement device and ready to be saturated.

To saturate the sample, the top of the cell was connected to a vacuum source. The bottom of the cell was connected to the wetting phase line and the wetting phase pressure was adjusted to be atmospheric at the center of the cell. Subsequently, in order to evacuate the soil's pore gas, a 900 mbar vacuum was applied to the nonwetting phase without allowing wetting phase to flow into the cell (the valves V10 and V11 were closed, see Figure 2-2). After several hours, wetting phase absorption was allowed, by opening either V0 or V11, until the top surface of the soil sample became slightly oversaturated. At this instance, the suction was dropped to atmospheric pressure. Using this technique, air bubbles trapped during the advancement of the wetting phase were confined and collapsed. Next, the cell was removed and weighed in order to obtain what is referred as the initial weight of the cell. Subsequently, the cell was reconnected to the wetting and non-wetting phase lines. These lines, including the voids in the transducer, were filled with the pertinent fluid and the pressure of each fluid was set to zero. The cell was then left to equilibrate at this setting for approximately 14 hours after which the transducer was calibrated.

The transducer is calibrated against a mercury manometer in the following manner: The wetting phase pressure, either water or oil phase pressure, is fixed at zero. Once this pressure is set, the cell is removed and the wetting and nonwetting phase lines to the cell are sealed. Subsequently, the non-wetting phase pressure is varied stepwise from zero to maximum and back to zero. The transducer reading then, is calibrated against the applied nonwetting pressure as indicated by the manometer. This calibration is conducted prior to any experimental run.

The PE method is employed to determine the *P-S* relationship in the following manner. After the transducer is calibrated, the nonwetting phase pressure is increased to approximately twice the displacement pressure without permitting any desaturation; this aspect of the procedure will be discussed in the Result and Discussion section. Since no desaturation has occurred, the increment in the nonwetting phase pressure should not affect the transducer reading even though a small disturbance may be registered. Once the fluctuation due to this disturbance has diminished, the first capillary pressure measurement is taken. The initial capillary pressure and saturation are therefore known. The subsequent desaturation is initiated by opening the collector valve. After a finite volume has been collected the valve is closed. The collected wetting phase is weighed to determine the current state of saturation in the sample. The capillary pressure reading is taken after the transducer reading stabilizes. The procedure is repeated again starting at the step of opening the collector valve. When the drainage rate becomes too low, the non-wetting phase pressure is increased. The desaturation process is continued until saturation in the sample is near residual saturation.

With the SE method, the saturated cell is connected to the wetting phase burette and the air phase lines are left open to the atmosphere. The pressure in the wetting phase fluid is adjusted to place the interface in the burette at the center of the cell and the fluids are allowed to equilibrate overnight. The wetting phase pressure at the center of the cell being atmospheric results in a calculated pressure difference, relative to the air pressure, of zero. This what is recorded as the capillary pressure at initial saturation.

The next desaturation point is obtained by applying an incremental step of positive pressure to the non-wetting phase while the outflow is directed to the collector vial and the line to the burette is closed. Drainage is permitted for at least 22 hours. Either the mercury manometer or the transducer can be used to determined the nonwetting phase pressure. However, it is preferable to use the manometer, since it does not require calibration. The wetting phase pressure is the distance of the wetting phase fluid surface in the vial to the center of the cell. The saturation in the sample is determined from the weight of the drained wetting phase. The procedure is repeated for the subsequent desaturation points. After the last measurement point is obtained, the cell is weighed. The difference between this weight and the initial weight of the cell reflects the total amount of the wetting phase drained. The agreement between this amount and the sum of the wetting phase collected in the vial is used to determined the mass balance error. The cell is then taken apart and all the soil in the retaining cylinder is weighed prior to being oven dried. The difference in weight before and after oven drying is the residual saturation and the oven dried weight divided by the brass retainer volume is the bulk density.

This apparatus was used to examine the performance of the pressure equilibrium method in measuring air-water and air-oil pressure-saturation data. Likewise, the same apparatus was used to conduct the saturation equilibrium method measurements of the air-water and air-oil systems. The porous medium used was Metea soil with a texture of 6% non-expansive clay, 11% silt and 83% sand. It contained 1.1% organic matter after dry sieving to pass 850 micron to exclude larger gravel and other organic matter. In order to have a stable packed sample, the water-phase used was a deaerated 0.005 *M* $CaSO_4$ solution as suggested by *Klute* (1986). The oil-phase was tetrachloroethylene (PCE) at 99.99% purity with a density of 1.623 g/cm^3. Building air was used as the air phase.

2.3. RESULT AND DISCUSSION

2.3.1. Pressure-Saturation Measurement Simulation.

The PE method is based on the premise that transient saturation profiles within the soil sample will reach equilibrium relatively quickly when occurring under a zero flux boundary condition. To verify this notion theoretically, a numerical model was developed and used to compare the time required by the PE and SE methods to collect *P-S* data.

This model was a 1-D finite difference model, in which the air mass density and viscosity are assumed to be negligible. The air pressure and water mass density are assumed constant with respect to time and space. The appropriate governing equation for this case is given by Richard equation:

$$\varnothing \cdot \frac{\partial S}{\partial t} = -\frac{\partial}{\partial z}\left(k_s \cdot k_r\left(\frac{\partial h}{\partial z} - 1\right)\right) \qquad [2\text{-}1]$$

where $\varnothing$ is the porosity (cm^3/cm^3), k_s is the saturated hydraulic conductivity (cm/sec), t is the time (sec), h is the pressure head of water (cm) and z is the vertical distance (cm). The

bottom of the soil sample was set at z=0 cm and the top was at z= 3 cm. This height was divided into 10 uniform elements.

The water saturation (S) and relative permeability (k_r) are assumed to follow *van Genuchten* (1980) closed-form relations:

$$S = S_r + (1 + S_r)[1 + (\alpha h)^n]^{1-1/n} \qquad [2\text{-}2]$$

$$k_r = S_e^{1/2}\left[1 - \left(1 - S_e^{n/(n-1)}\right)^{(n-1)/n}\right]^2 \qquad [2\text{-}3]$$

where S_e is the effective saturation defined as $(S- S_r)/(1-S_r)$. Here S_r, α (cm^{-1}) and n are the van Genuchten P-S parameters. Note that the model was simplified by omitting hysteresis in the P-S relationship and Equation 2-2 was assumed to hold regardless of the saturation history.

A simulation of the transient conditions within the cell when the PE method is employed begins at time t_0 when drainage is initiated by opening the collector valve. The initial pressure head distribution $h(z, t<t_0)$ was hydrostatic and based on the pressure head specified at the lower boundary, prior to initiating the drainage. At t_0 the lower boundary pressure head is reduced to h_p. The finite difference formulation of Equation 2-1 was solved to determine pressure head $h(z, t)$, saturation $S(z, t)$ and accumulated outflow volume $\forall(t)$. To simulate the effect of collector valve closure in the PE measurement, when the outflow volume exceeded the specified drained volume $\forall_d$ the boundary condition was switched from h_p to a no flow boundary. This was the end of drainage which occurs at time t_d. The execution was continued to simulate transient during

saturation redistribution. A PE measurement simulation was executed to determine transient history in a hypothetical sample. The dimensions used were identical to the pressure cell as described in the Material and Method section. The parameters describing the soil-water system used were obtained from air-water *P-S* measurement using Metea soil. In the simulation, the sample was initially at hydrostatic equilibrium with lower boundary pressure head at -35 cmH_2O. Pressure head of h_p=-50 cmH_2O was applied at the lower boundary to desaturate 0.945 cm^3 of water. This scenario is equivalent to reduce the saturation from 89% to 85%.

Alternatively, the pressure head profile at final equilibrium after desaturation can be determined via mass conservation equation. Calculation based on this equation shows that; desaturation of $\forall_d$=0.945 cm^3 reduced the initial pressure head by 2.13 cmH_2O at any point in the modeled domain. The pressure head at the lower boundary, then, would be reduced from an initiall -35 to -37.13 cmH_2O by the time the new equilibrium was reached. Having known this, the SE measurement simulation was conducted by re-executing the above PE measurement simulation using h_p= -37.13 cmH_2O. As such, it was expected that an accumulation of outflow as much as $\forall_d$ would only be obtained at the time when the new equilibrium had been reached. Therefore, in this particular simulation, the lower boundary condition was never switched to a no flow boundary.

In order to contrast the transient characteristics of the PE and SE measurement methods Figure 2-3 was plotted. The top plot shows the pressure head at node z=0.15 cm obtained for the PE and SE simulations. The right vertical axis, labeled as the Error axis, indicates the percentage discrepancies between the pressure heads obtained by each

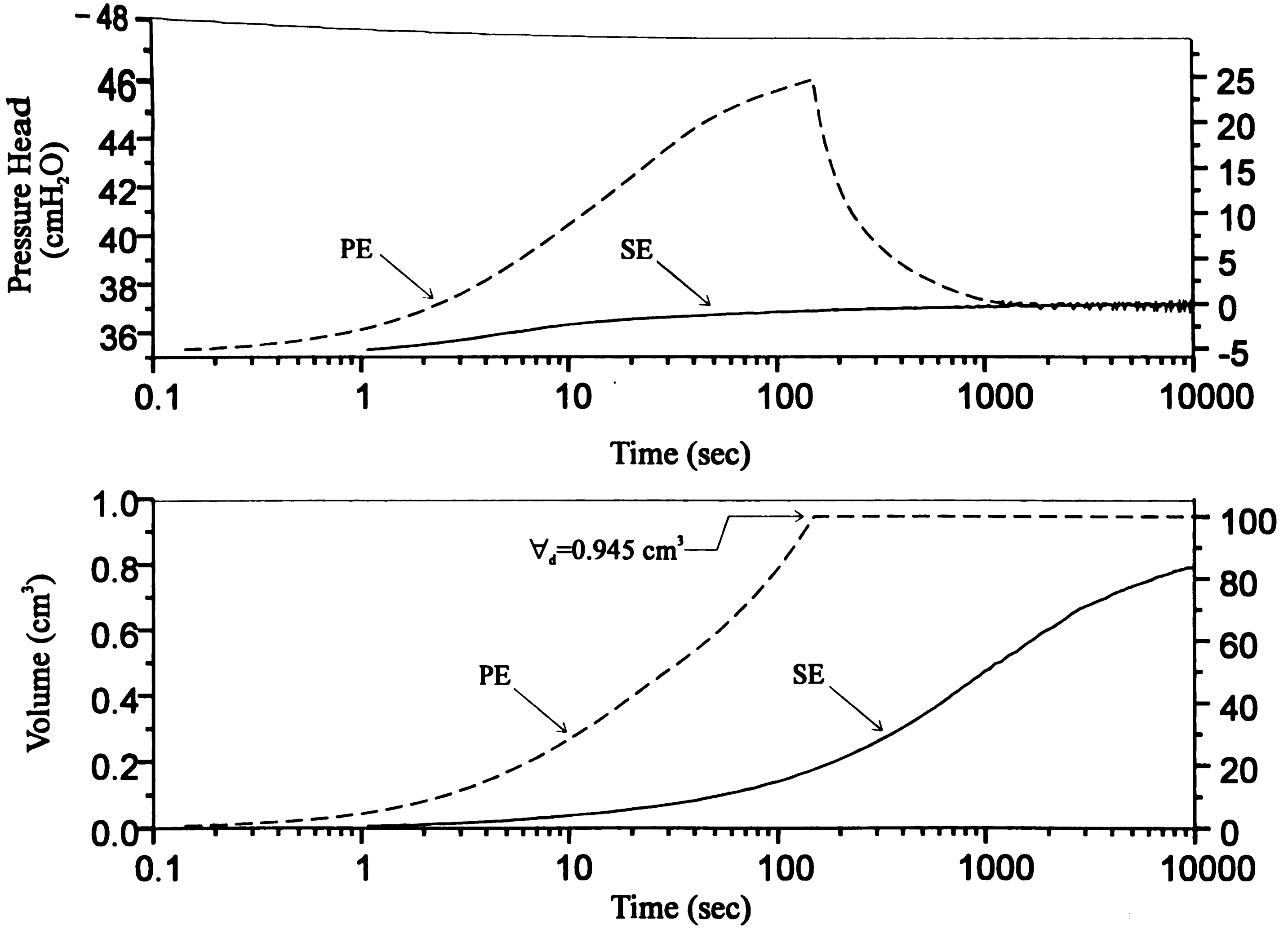

Figure2- 3: Pressure head at z= 0.15 cm and accumulated outflow with respect to time obtained from the PE and SE method simulations using h_p=-50 cmH$_2$O and h_p=-37 cm H$_2$O respectively

m-se&pe.cdr

simulation relative to the equilibrium pressure head at any instance. The equilibrium pressure head was that obtained via the mass balance equation. The bottom plot in Figure 2-3 plots the accumulated outflow predicted by the two simulations. The scale of the right vertical axis in this plots indicates percentage of the target volume $\forall_d$ fulfilled by the accumulated outflow at any given time. These plots shows that, when the PE method was employed, the pressure head at this node was initially decreased effected by the imposed lower boundary condition. During this time range, the accumulated outflow increase and reached the target volume $\forall_d$ at t_d= 149 seconds. At this instance, the lower boundary condition was switched to the no flow boundary condition. This change appears as constant accumulated outflow volume in the bottom plot. The pressure head, as shown in the top plot, was increased exponentially converging toward the equilibrium pressure head. At time t larger than 1000 seconds the discrepancies in the pressure head to the equilibrium head were already insignificant.

The pressure head curve obtained by the SE measurement simulation shows an identical trend to the desaturation range in the curve of the PE case where the pressure head was decreased effected by the imposed lower boundary condition. Differently from the PE case, the pressure head curve of the SE case converged directly toward the equilibrium pressure head since the boundary condition never changed. The accumulated outflow increased slowly. For example, at the time when the PE measurement had already accumulated 100% of the target volume at t_d= 149 seconds, the SE measurement volume was only capable in accumulating approximately 20% of the target volume. At time t=1000 seconds, when the PE method was employed, the pressure reading can be taken at that time since the error has become insignificant. When the SE method was employed instead, at that instance, additional time was still required to accumulate approximately 50% more outflow volume. Note that, to accumulate this volume the time required was significantly increased. At 10,000 seconds the SE method accumulated only 83% of the target volume.

2.3.2. Hysteretic Issue in the P-S Measurement Employing the Pressure Equilibrium Method

The above simulations suggest that the time required to measure *P-S* data can be reduced by implementing the PE method. This time reduction, however, would be gained at the cost of losing accuracy due to the hysteresis problem. To illustrate this problem, several saturation profiles obtained by simulations were plotted. Figure 2-4a plots the profiles obtained by the SE simulation The rightmost curve is the initial saturation profile $S(t_0)$ and the leftmost is the final profile $S(t_e)$ which is the saturation profile at the end of the simulation. The four curves between these two profiles were the transient profiles during time $t_0<t<t_e$. The order of these profiles, from right to left, shows the changing of the saturation profile with respect to time. The position of these profiles relative to the initial profiles suggest that, when the SE method was employed, saturation in any location consistently decreased until the new hydrostatic equilibrium was reached. This means that the flow was continuously controlled by the desaturation mechanism at any time during transient throughout the modeled domain. Thus, the data obtained indeed reflected the primary drainage characteristic of the *P-S* relationship.

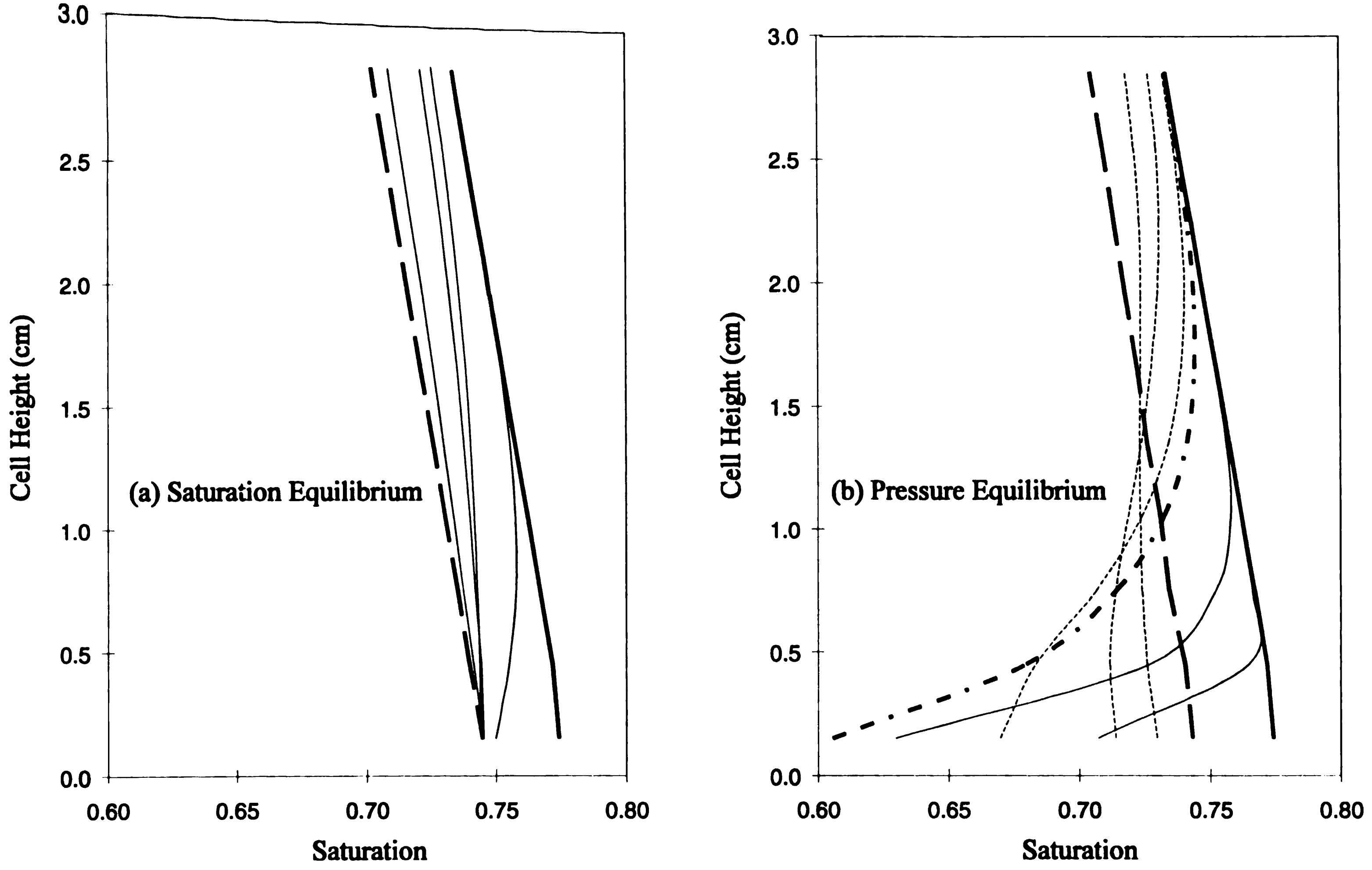

Figure 2-4: Saturation profiles obtained from the saturation equilibrium and the pressure equilibrium simulations at initial time (heavy solid lines), during desaturation stage (light solid lines), at the end of desaturation stage (heavy dash-dotted lines), during redistribution stage (light dashed line) and at simulation end time (heavy dashed lines).

c2-profl.cdr

Figure 2-4b plots the saturation profiles obtained by the PE simulation. Different from those obtained by the SE simulation, prior to becoming the final profile $S(t_e)$, the initial profile $S(t_o)$ changed to the profile at the end of desaturation stage $S(t_d)$. Therefore, Figure 2-4b contains two type of transient profiles: those obtained during desaturation transient between time $t_o<t<t_d$ and those during redistribution transient between time $t_d<t<t_e$. The position of the desaturation transient profiles relative to the initial profile suggest that during time $t_o<t<t_d$ the saturation throughout the modeled domain decreased until the $S(t_d)$ profile was formed at the end of desaturation stage. After that, at $t>t_d$, the $S(t_d)$ profile changed to becoming the redistribution transient profile and formed the final profile at the end of simulation time. The relative position of these transient profiles relative to the final profile suggest that, in the region of z bellow approximately 1 cm, saturation was increasing. As a result, the data obtained in the PE case might not represent the true primary drainage and a bias relative to the SE data would then be observed.

The hysteresis issue may not be the only determinant which could bias the data obtained by the PE method. The dynamic state of the fluids at the time when the measurement readings were taken might also be an important factor. *Topp* (1967), *Smiles et al.* (1971) and *Corey and Brooks* (1975) observed that *P-S* measurements taken under unsteady, steady and hydrostatic states yielded different data sets. They found that at any given saturation, capillary pressure measured in a steady or unsteady state was higher than that measured in hydrostatic equilibrium. The model developed cannot be used to address any discrepancy associated with these hysteretic and dynamic state issues. The hysteresis was omitted in the model so that similarity in the final saturation profile $S(t_e)$ obtained by the PE and SE simulations was artificially imposed. With the model, the occurrence of the hydrostatic equilibrium state can be precisely determined by monitoring the change in the pressure distribution profile. During an actual measurement, however, such a profile might not be practical to be acquired since the height of the pressure cell is only 3 cm. Thus, any means used to infer the state of hydrostatic equilibrium during the actual measurement could be less accurate than that employed in the model. In turn, the *P-S* point obtained in the actual measurement employing the PE method might be unintentionally taken while the fluids were still at an unsteady state condition. As the model cannot be used to address theses issues, it is necessary to conduct an inspection on data obtained from experimental measurements.

2.3.3. Pressure-Saturation Measurement employing the Pressure Equilibrium and the Saturation Equilibrium methods.

To verify the PE method experimentally, the method was implemented to measure *P-S* data for air-water and air-oil systems using Metea soil. The PE method would be justified if it was unbiased relative to the SE method. In order to achieve this condition, the following criteria should be satisfied. First, the measurement should be taken as close as possible to the hydrostatic equilibrium state. Second, any discrepancies observed should still be within tolerable limits such that the *P-S* information obtained is statistically comparable. This information would include the *P-S* curve derived from the measured data and the *P-S* parameters describing that curve. Subsequent discussions will be presented from this point of view.

2.3.3.1. Equilibrium Time in the Pressure Equilibrium Method

In order to verify the sufficiency of the time given for the system to reach hydrostatic equilibrium for each measurement with the PE method, the transient behavior of the capillary pressure as indicated by the transducer during redistribution was recorded approximately every 5 minutes. Typical plots of such data are shown in Figure 2-5. The open squares in Figures 2-5a through 2-5d denote the capillary pressure readings. The series of points belonging to a particular desaturation step end with a solid point for which hydrostatic equilibrium was assumed to be achieved. The criterion for identifying these end points was that the rate of capillary pressure change be less than 0.25 mbar per minute. If this rate was achieved at the second point, additional readings were taken. The label next to each solid point shows the degree of saturation at that step. At $S = 0.62$ and 0.25, the pressures were equilibrated overnight (785 minutes). The horizontal lines indicate the pressure level at which the non-wetting phase pressure was set (labeled as h_p in the Figure 2-5).

Having knowledge of the trend of the pressure head profile in the vicinity of the pressure plate as shown in Figure 2-3, it was possible to reconstruct the redistribution curve of each desaturation step. Each redistribution curve in Figure 2-5 (solid line) was traced manually through the open points that belong to a particular step ending at the solid point. The beginning and the end points of this solid curve were then manually extrapolated (shown as dotted lines) so that at the beginning of each desaturation step it crossed h_p and at the end point it continued the trend of the solid line. It is assumed that the quasi-equilibrium state was already reached at the points where the redistribution

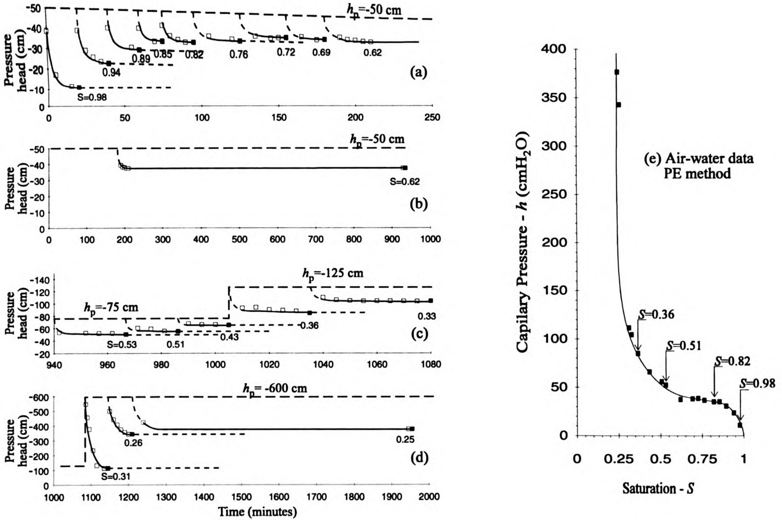

Figure 2-5: (a)-(d) Water pressure head changes with respect to time as recorded by the transducer during redistribution time in a measurement employing the PE method and (e) the obtained *P-S* data from that particular measurement superimposed with the fitted *P-S* function by *van Genuchten* (1981).

c2-f4.cdr

curves became horizontal. Beyond these points, the rate of the capillary pressure change was assumed to be insignificant. It was observed that the solid points were laid in the horizontal region of the curve. This indicates that the criteria of 0.25 mbar per minute was sufficient to assure the quasi-equilibrium state of the system. Inspection of the constructed curve indicates that, with the air pressure setting h_p as shown in Figure 2-5, in an air-water system with high saturation (S>80%), 20 minutes was sufficient to reach quasi-equilibrium. At moderate saturation (30%<S<80%), it was 40 minutes and 60 minutes at lower saturation. In a similar manner of analysis in an air-oil system, those values were approximately 15, 30 and 45 minutes respectively.

2.3.3.2. Comparison of the P-S curves Obtained by the Pressure Equilibrium and the Saturation Equilibrium Method

Comparison of the *P-S* curves obtained by the PE and SE method is presented in Figure 2-6a and 2-6b. The solid curves in these figures are the best fit curve of Equation 2-2 for the *P-S* data measured using the SE method, pooled from 5 replications of air-water measurements (Figure 2-6a) and 4 replications of air-oil measurements (Figure 2-6b). The dashed lines were similar to the solid curves but determined from data obtained by the PE measurement. In this case, the obtained *P-S* curves for the air-water and air-oil systems were based on pooled data from 7 and 4 replications respectively.

The shaded areas are regions within the 95% confidence limits of the solid curves which were determined based on *Seber and Wild* (1988):

$$\varepsilon_S = t_{df}^{2.5} \cdot \sqrt{\frac{sse}{df} \cdot \left[1 + \mathbf{f}_h^{\mathrm{T}} \left(\mathbf{F}^{\mathrm{T}} \cdot \mathbf{F} \right)^{-1} \cdot \mathbf{f}_h \right]}$$

The term $t_{df}^{2.5}$ is the student *t* value at 95% confidence intervals with degree of freedom *df*, and *sse* is the sum of the squared error. Since Equation 2-2 was used to describe the *P-S* relationship, the covariance matrix **F** is defined as:

$$[\mathbf{F}]=\left[\frac{\partial S(h_i)}{\partial S_r} \quad \frac{\partial S(h_i)}{\partial \alpha} \quad \frac{\partial S(h_i)}{\partial n}\right]$$

where *i* is the data index number. The matrix **f** is the covariance matrix at a given pressure.

Prior to comparing the *P-S* curves obtained by the methods, the characteristic of the curve obtained by the reference method, i.e. the SE method, will be discussed. The solid lines in Figure 2-6 are assumed as the best estimate of the population primary desaturation curves of the air-water and air-oil systems when measured in the Metea soil. The confidence limits of this curves bound an area in which, within 95% probability, a different best estimate curve might be laid if a different data set from the same population were used. At a given pressure, the width of the confidence limits is dictated by the variability of the saturation data across sample replications. In general, this variability might be due to the deference from one replica to the next as to their: 1) applied pressure, 2) equilibrium state when the readings were taken, 3) pore size distribution and 4) precision in determining the saturation. In conducting the SE experiment, five replications were run simultaneously. A single air pressure source was regulated and distributed to each replica using a manifold. Therefore, it is assumed that each replica received identical load of air pressure in each desaturation step. As mentioned in the Materials and Methods section of this chapter, with the SE method the samples are

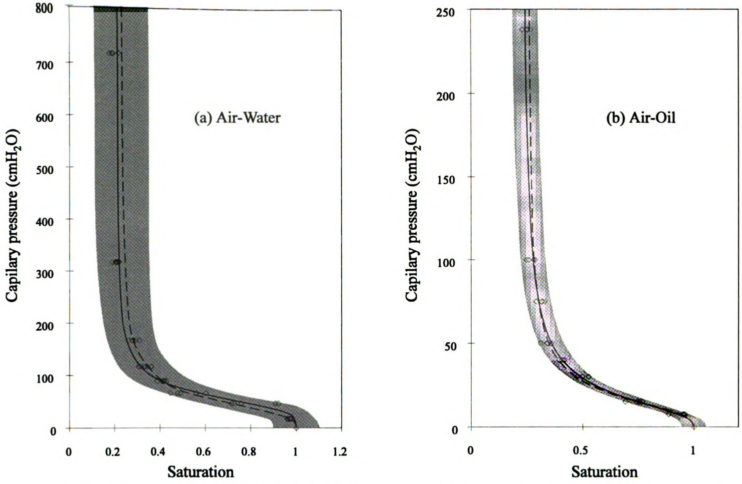

Figure 2-6: *P-S* curves obtained by the PE method (dashed lines) superimposed with those obtained by the SE method (solid lines). The confidence limits (shaded area) were based on regression upon the SE data (diamond marker).

c2-f5a.cdr

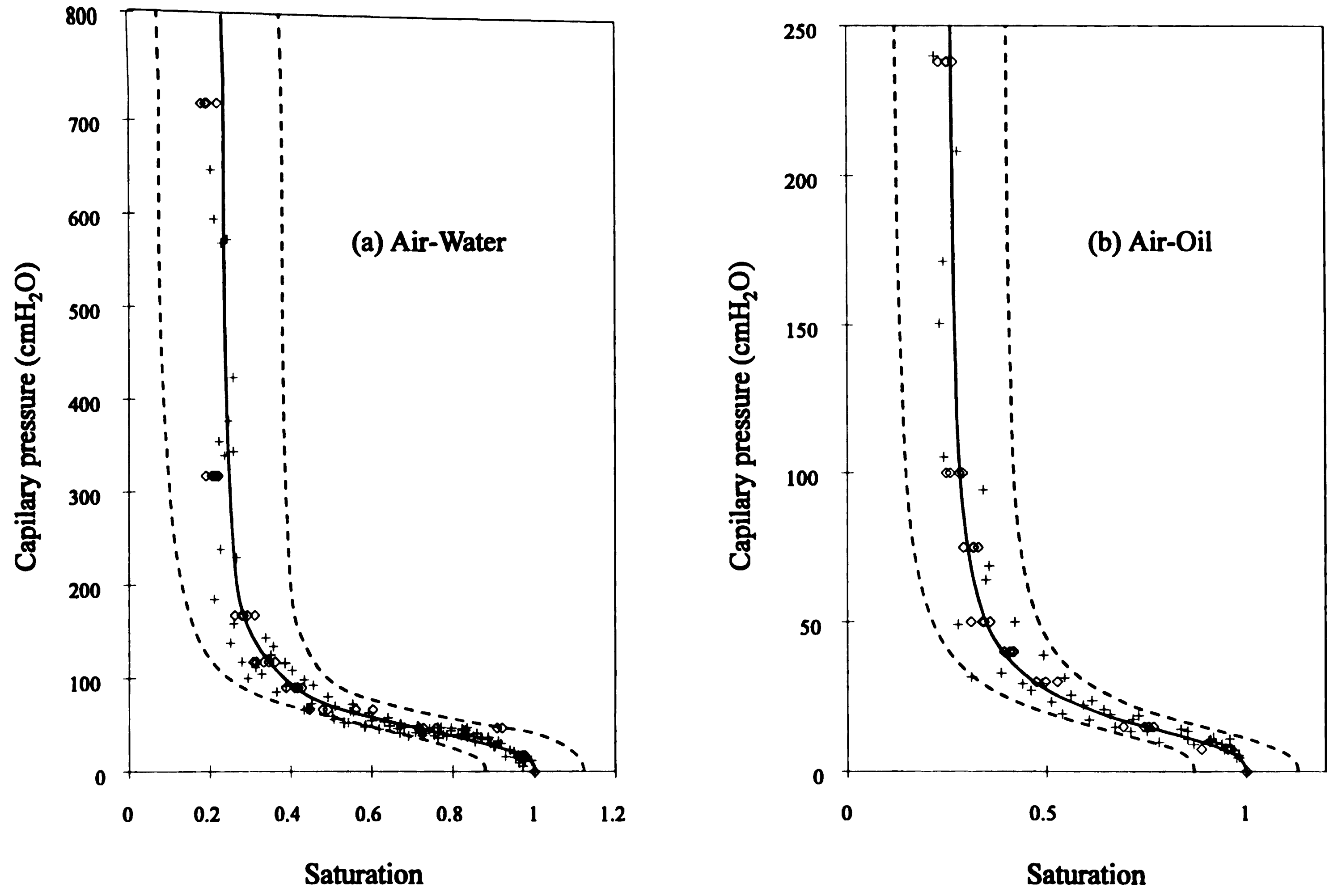

Figure 2-7: *P-S* data obtained from measurement using the PE method (plus marker) and the SE method (diamond marker). The *P-S* curves (solid lines) and 95% confidence limits (dashed lines) were based on regression upon the PE data (plus marker).

c2-f5.cdr

permitted to equilibrate for at least 22 hours. Subsequently, the saturation in each replica was determined one at a time. The time different between the first and the last replica was not more than 5 minutes. It is unlikely that this difference contributed a significant effect. If we assumed that 22 hours given in each desaturation step was sufficient to equilibrate the sample, then the width of the confidence limits were affected only by the variation in the pore size distribution across the replication and the precision in determining the saturation. Across the replication, the variation in the pore size distribution is due to the inability to produce the same pore geometry from one sample to the next.

To discriminate the effect of these two determinants on the obtained confidence limits the saturation measurement precision was inspected. The discrepancy between the total mass of the wetting-phase released by the soil sample to that accumulated in the collector vial in each replica was determined. This discrepancy is the total saturation loss in one replica. It is true that the fraction of this loss that occurs in each desaturation step was unknown. It is assumed that this provides a conservative reasonable etimate of the error that could occur at any step. Out of 5 replications of air-water measurements the maximum saturation error in the worst replica was only 0.009. The plot in Figure 2-6, on the other hand, shows that the narrowest band width of the confidence limits in the air-water curve was 0.184. For the case of air-oil the maximum measurement error from 4 replications was only 0.017 compare to 0.105 of the narrowest confidence limits. It appear that the maximum measurement errors were small when compared to the confidence limits band width. Thus, the confidence limits of the *P-S* curve obtained via the SE method was mostly affected by the pore size distribution variation across the replication rather than the measurement error.

As mention previously, the PE method could be justified if it is capable of producing data so that any *P-S* information derived from these data are as good as those determined from data measured via the SE method. It is observed in Figures 2-6a and 2-6b that the discrepancies in the *P-S* curves estimated by the two methods are small compared to the band width of the confidence limits of the reference curve. For example, in the case of the air-water system, the highest discrepancy between the two curves was only 0.03 which occurs at capillary pressure h=800 cmH_2O. On the other hand, the width of the confidence intervals of the SE curve at this pressure was 0.230. In the case of the air-oil system, the highest discrepancy was 0.021 at h=30 cmH_2O while the confidence limits width was 0.110. As stated before, the confidence limits define the area in which, within 95% probability, any best estimate curve from the same population might be laid. Therefore, small discrepancies relative to the confidence limits band width, such as those observed in the investigated cases, suggest that the obtained *P-S* curves via the PE and SE methods were derived from two data set which came from the same population. As such, the data obtained by the two methods were not deferent statistically.

Additionally, the relative position of the *P-S* curve obtained via the PE method to that by the SE method, was not indicative of any consistent bias. Any bias associated with the hysteretic issue would be observed as a departure with consistent direction from the reference curve. The effect of hysteresis would shift the curve toward the primary imbibition scanning path. Thus, in Figure 2-6, it would appear as a consistent departure toward the left side of the reference curve. Such a consistent tendency was not observed in any of the above cases investigated. It is speculated that the effect of hysteresis, if any, was overwhelmed by the variation due to sample replication. This suggests that, at least for the investigated case, the effect of hysteresis is insignificant compared to the pore size distribution variation across replication.

2.3.3.3. Comparison of the P-S Parameters Obtained by the Pressure Equilibrium and the Saturation Equilibrium Method

Typically, the purpose of a *P-S* measurement is to obtain information to determine the *P-S* relationship. In most cases, this information is required in the form of a *P-S* parameters set. Note that the comparison plots in Figure 2-6 reveal only the effect of parameters discrepancies when they are used to construct a *P-S* curve. A different use, such as to determine unsaturated hydraulic conductivity, might result in a different level of agreement. However, if those parameters came from the same population, any disagreement associated between the discrepancy of the PE and SE methods could be regarded as just variation within one SE measurement to the next. Therefore, it is necessary to inspect whether the *P-S* parameters determined from the obtained PE data are comparable to those obtained by the SE method. The following paragraphs discuss this issue.

The *P-S* parameters used to construct the *P-S* curve in Figure 2-6 are listed in Table 2-1 along with their 95% confidence limits. These limits were determined following *Seber and Wild* (1988):

$$\begin{bmatrix} \varepsilon_{S_r} \\ \varepsilon_{\alpha} \\ \varepsilon_{n} \end{bmatrix} = t_{df}^{2.5} \cdot \sqrt{\frac{sse}{df}} \cdot [\mathrm{C}]$$

where ε_{Sr}, ε_{α}, and ε_n are the 95% confidence limits of parameters S_r, α and n respectively and [C] is the diagonal of the covariance matrix $(F^T.F)^{-1}$.

Table 2-1: The best estimated air-water and air-oil *P-S* parameters based on the pooled data measured using the PE and SE methods

	SE Method	PE Method
Air-Water		
S_r	0.193±0.059	0.229±0.058
n	2.91±0.68	3.12±0.58
α	0.0213±0.0032	0.0218±0.0014
Replication	5	7
Air-Oil		
S_r	0.231±0.047	0.257±0.058
n	2.50±0.38	2.80±0.83
α	0.0646±0.0081	0.0637±0.0101
Replication	4	4

Following the current approach, the parameters determined from data measured using the SE method are assumed to represent the characteristic of the population's parameters. As shown in Table 2-1, in all cases, the parameters estimated from data measured via the PE method are within the confidence limits obtained in the case of SE method. It is also observed that the width of the confidence limits of the parameters in the PE case are comparable to those in the SE case. This indicates that the parameters from the PE and SE cases share similar statistical properties. None of the investigated cases suggests that the parameter set estimated from the PE data is different from those estimated from the SE data. Based on this, it is concluded that the obtained parameters estimated from data measured via the PE and SE method are comparable. In turn, the PE measurement method is capable of providing data as good as the SE method.

2.4. SUMMARY AND CONCLUSION

An alternative method to reduce the *P-S* measurement time based on the pressure equilibrium (PE) method developed by *Su and Brooks* (1980) was investigated. Theoretical verification using a mathematical model confirmed the feasibility of this method. To justify its acceptability, the performance of this method was compared to the conventional saturation equilibrium (SE) method. In order to conduct this comparison, the *Su and Brooks* (1980) apparatus was modified and used to measure air-oil and air-water desaturation data employing the PE and SE method. The soil used was Metea soil with loamy sand texture and the oil phase was tetrachloroethylene.

A mathematical model was developed to simulate the transient flow during *P-S* measurement using either the PE or SE method. The simulated measurements suggest that the time required to measure *P-S* data can be reduced by implementing the PE method. The simulation indicated that the PE method was able to reduce the saturation from 89% to 85% within 149 seconds. During this time only 20% of the target volume was accumulated by the SE method. At time t= 1000 seconds, the pressure head error in measurement employing the PE method was already insignificant while in the SE method additional time was still required to accumulate approximately 50% more outflow volume.

This time reduction, however, would be gained at the cost of losing accuracy due to hysteresis. The simulation suggests that during the redistribution stage in the PE method the saturation in the lower region of the sample was increased. As a result, the data obtained in the PE case might not represent the true primary drainage and a bias relative to the SE data would then be observed.

Comparison of the *P-S* curves obtained by the PE and SE method, however, did not show any indication of bias. It is speculated that the effect of hysteresis, if any, was overwhelmed by the variation due to sample replication. This suggests that, at least for this uncosolidated soil, the effect of hysteresis was insignificant compared to the pore size distribution variation across replication.

None of the investigated cases suggests that the parameters estimated from the PE data are significantly different from those estimated from the SE data. Based on this, it is concluded that the obtained parameters estimated from data measured via the PE and SE method were comparable. In turn, the PE measurement method is capable of providing data as good as the SE method.

The effective time required to measure 19 desaturation data points by the PE method was only about 12 hours. Compared to the 108 hours required by the conventional method, this was a significant improvement. This time reduction was theoretically confirmed. Implementation of this method to determined the air-water and air-oil *P-S* relationship in loamy sand Metea soil demonstrate the capability of this method to substitute the conventional method. Based on this, it is concluded that the PE method provides a more efficient alternative for measuring *P-S* data.

CHAPTER III

THE ACCEPTABILITY OF SCALING THEORY IMPLEMENTATION IN PREDICTING THREE-PHASE CONSTITUTIVE EQUATIONS FROM TWO-PHASE PRESSURE-SATURATION DATA.

3.1. BACKGROUND

Recently, *Parker, et al.* (1987) proposed a predictive method employing scaling theory to construct three-phase constitutive information relating relative permeability (k_r), saturation (*S*) and capillary pressure (*P*). The predictive method (*Leverette*, 1941) assumes that when air, oil and water phases coexist in soil pore, the water saturation is a function of oil-water capillary pressure only and the sum of water and oil saturation is a function of air-oil capillary pressure. Therefore, the three phase *P-S* relationship information can be obtained from two-phase *P-S* measurements. Once the three-phase *P-S* relationship is known, the three-phase k_r-*S* relationship can be determined using various formulations.

Simplification through the predictive method is widely utilized (*Corey, et al.*, 1956; *Stone*, 1973; *Azis and Settari*, 1979; *Parker, et al.*, 1987) primarily due to difficulty in directly measuring the capillary pressure of an individual phase in a three-phase system (*Abriola*, 1989). Even in utilizing the predictive methods, the experimental burden remains substantial. For this reason, *Parker, et al.* (1987) proposed a predictive method employing scaling theory. In this method, a complete set of two- and three-phase k_r-*S*-*P* equations for the desaturation scanning path for a particular porous medium were formulated as dependent solely upon the *P-S* desaturation parameters for a single two-phase system and scaling factors. When the scaling factors are predicted from interfacial tension measurements, the experimental burden is reduced substantially.

This scaling theory is based on the premise that in a porous medium there exists a scaling factor (β) which transforms the *P-S* curve from a particular two-phase system into a different two-phase system (*Leverette*, 1941; *Purcel*, 1942; *Miller and Miller*, 1955). *Parker et al.* (1987) further postulated that β can be predicted from the ratio of the interfacial tensions (σ) of the immiscible fluids involved. *Lenhard and Parker* (1987) validated this notion by comparing the scaled two-phase *P-S* curves to those obtained from direct measurements. The incorporation of scaling theory into the predictive method was validated by *Lenhard and Parker* (1988). This validation was conducted by comparing the water and total liquid *P-S* data measured in three-phase systems to those constructed via the scaling method. These validation studies support the use of scaling theory.

The k_r-*S*-*P* relationships constructed via the predictive method employing scaling theory are based on a rigid porous medium assumption. This assumption states that the soil pore structure is constant with respect to time. According to *Parker, et al.* (1987), the prediction of k_r-*S* relationships are sensitive to any disturbance in pore size distribution such as that due to swelling. Rather small changes in pore size distribution, which may not be clearly evident in *P-S* relations, may markedly affect the permeability functions. If this notion is true, it might have significant impact on the implementation of the scaling theory. Note that, the characteristics of the soil pore structure is constituted in the *P-S* parameters. To obtain these parameters, the scaling theory relies on data that are measured in one system only. Therefore, any small error in these parameters might significantly biases the prediction of the k_r-*S-P* relationships. From this point of view, the accuracy and precision of the *P-S* parameters measured in that single two-phase system appear to be important. From here on, these parameters are referred to as base parameters.

The accuracy and precision of the *P-S* parameters are affected by the soil texture involved (*McCuen et al.*, 1981). The parameters determined in a soil containing fractions of sand, silt and clay tend to give less variation than those determined in uniform grain size soil. The accuracy and precision might also vary from one immiscible fluid system to another. For example, displacement pressure measured by *Demond and Roberts* (1991) possesses higher variations in air-water system than in oil-water system. *Lenhard and Parker* (1987) observed that their *P-S* measurements involving benzyl alcohol were inferior compared to other systems they had investigated. They concluded that this was due to the characteristics of benzyl-alcohol which drains at a relatively low capillary pressure.

The variances of the base parameters might be different when measured in different soil textures or different fluid pairs. In turn, the k_r-*S-P* relationship predicted based on these parameters might also possesses different accuracy and precision. This chapter describes the investigation of the implementation of scaling theory in the predictive method to predict the k_r-S-P relationships when either air-water or air-oil systems were used as the base system. These two approaches, ie. using air-water or air-oil in implementing the scaling theory, are referred to as method 2 and method 3, respectively. The obtained relationships were compared to those obtained via the predictive method without utilizing scaling theory. The latter approach served as the reference method and was referred to as method 1. These comparisons were conducted utilizing two soils that have a contrast in their textures; loamy sand Metea soil and uniform grain Ottawa sand.

Using either the air-water or air-oil systems as the base system has an advantage over the use of an oil-water system. Air-water P-S information is considered as the most common data available compared to the other two systems. Also a well established measurement protocol such as that by *Klute* (1986) is available. When lacking air-water data, an air-oil system is more attractive for two reasons. First, the air-oil P-S parameters are directly involved in the three-phase k_r-S-P equations. Secondly, compared to the oil-water system, the air-oil measurement technique is more similar to the well established air-water P-S measurement.

The scaling theory has been incorporated in a versatile numerical three-phase flow model (*Kaluarachchi et al.*, 1990). This model was improved in becoming valid for both the desaturation and imbibition scanning paths (*Parker and Lenhard*, 1987; *Lenhard and Parker*, 1987; *Lenhard et al.*, 1989) and accepting multi-component organic chemical transport (*Parker and Kaluarachchi*, 1990). This model is one among a few that accepts dense non-aqueous phase liquids (DNAPL) as the oil phase (*Huling and Weaver*, 1991). Unfortunately, most of the scaling theory studies use light non-aqueous phase liquids (LNAPL) as their oil phase. The only instances of DNAPL uses were tricholoroethylene (*Parker and Lenhard*, 1987a) and benzyl alcohol (*Lenhard and Parker*, 1987). However, the density of benzyl alcohol is only 1.046 g/cc which is very close to the density threshold of the LNAPL type of oil (< 1.00 g/cc). Thus, the small contrast offered by benzyl alcohol may not be sufficient to reveal the characteristic of DNAPL. Based on this, tetrachloroethylene, which ha denity of 1.6 g/cc, was selected in this study as the oil phase to broaden the type of dense NAPL involved in the scaling theory study.

3.2. THEORETICAL BACKGROUND.

Parker et al., (1987) described a predictive method to construct the three-phase k_r-*S*-*P* relationships from *P-S* data of the two-phase system. The subsequent paragraphs summarize the theory in conjunction with its application and focus on monotonic desaturation involving DNAPL in the oil phase.

The scaling factor (β) was defined as a constant which transforms the *P-S* curve of a particular two-phase system into a different two-phase system in a single porous medium. Specifically, this constant relates the capillary pressure of two two-phase systems at a given saturation. The saturation which measures the fraction of soil pore occupied by the nonwetting-phase, is dictated by the interfacial surface and pore geometry. In turn, identical saturation implies identical pore geometry and radius of curvature (R_c) of the interfacial surface. Employing the Laplace theory, the ratio of the capillary pressures of two two-phase systems at a given R_c is equal to the inverse of the interfacial tension ratio. If air-water is chosen as the reference system, that statement can be formulated as follows:

$$\beta_{pq} \equiv \left.\frac{h_{\mathrm{aw}}}{h_{pq}}\right|_{R_c} = \frac{\sigma_{\mathrm{aw}}}{\sigma_{pq}} \qquad [3\text{-}1]$$

In which the h_{pq} are the capillary pressures of any arbitrary two-phase system pq (=aw, ow, ao) expressed in terms of water capillary head.

The scaling factor can also be expressed in the term of the *P-S* functional relationship equation. *van Genuchten* (1981) formulated the *P-S* functional relationship as follows:

$$S_q^{pq}\left(h_{pq}\right) = S_{\mathrm{r}\text{-}pq} + \left(1 - S_{\mathrm{r}\text{-}pq}\right)\left[1 + \left(\alpha_{pq} h_{pq}\right)^{n_{pq}}\right]^{1/n_{pq}-1} \qquad [3\text{-}2]$$

This equation is referred to as the *P-S* model. The constants $S_{\mathrm{r}\text{-}pq}$, α_{pq}, and n_{pq} are the curve fitting parameters. Employing this equation, the ratio of h_{aw} and h_{pq} becomes:

$$\frac{h_{\mathrm{aw}}}{h_{pq}} = \left[\frac{\alpha_{pq}}{\alpha_{\mathrm{aw}}}\right] \cdot \left[\frac{f\left(S_{\mathrm{w}}^{\mathrm{aw}}, S_{\mathrm{r}\text{-}\mathrm{aw}}, n_{\mathrm{aw}}\right)}{f\left(S_p^{pq}, S_{\mathrm{r}\text{-}pq}, n_{pq}\right)}\right]$$

At the same saturation and assuming $S_{\mathrm{r}\text{-}\mathrm{aw}}=S_{\mathrm{r}\text{-}pq}$ and $n_{\mathrm{aw}}=n_{pq}$ for identical porous medium, the second bracket on the right hand side is unity. This derivation leads to an alternative way of formulating the scaling factor, which is:

$$\beta_{pq} \equiv \left.\frac{h_{\mathrm{aw}}}{h_{pq}}\right|_{S_p^{pq}=S_{\mathrm{w}}^{\mathrm{aw}}} = \frac{\alpha_{pq}}{\alpha_{\mathrm{aw}}} \qquad [3\text{-}3a]$$

The α_{aw} and α_{pq} can be obtained by regressing the pertinent *P-S* data into the VG model. Combining Equation 3-1 and 3-3a leads to:

$$\alpha_{pq} = \beta_{pq}\alpha_{\mathrm{aw}} \approx \frac{\sigma_{\mathrm{aw}}}{\sigma_{pq}}\alpha_{\mathrm{aw}} \qquad [3\text{-}3b]$$

Incorporating Equation 3-3b into Equation 3-2 leads to:

$$S_q^{pq}\left(\beta_{pq}, h_{pq}\right) = S_{\mathrm{r}} + \left(1 - S_{\mathrm{r}}\right)\left[1 + \left(\alpha_{\mathrm{aw}}\frac{\sigma_{\mathrm{aw}}}{\sigma_{pq}}h_{pq}\right)^{n}\right]^{1/n-1} \qquad [3\text{-}4]$$

This equation permits prediction of the *P-S* curve of the system *pq* from air-water parameters. Note that, in incorporating Equation 3-2 into the scaling theory the parameter S_{r} was assumed to be independent of fluid properties or saturation history. The parameter *n* was also formulated without any designation of the fluid system. Several studies, such as those by *van Genuchten* (1980), *van Genuchten and Nielsen* (1985) and *Parker and Lenhard* (1989), showed that *n* is equivalent to the parameter λ in the *Brooks and Corey* (1964) *P-S* model. The parameter λ was postulated as an empirical parameter used as the index of pore size distribution (*Corey*, 1986). In turn, *n* was also regarded as a porous medium-dependent parameter.

Following the notion in Equation 3-2 and Equation 3-4, the prediction of oil-water and air-oil systems from an air-water system can be expressed in the following manner:

$$S_{\mathrm{o}}^{\mathrm{ao}}\left(h_{\mathrm{ao}}\right) \approx S_{\mathrm{o}}^{\mathrm{ao}}\left(\beta_{\mathrm{ao}}, h_{\mathrm{ao}}\right) \qquad [3\text{-}5]$$

$$S_{\mathrm{w}}^{\mathrm{ow}}\left(h_{\mathrm{ow}}\right) \approx S_{\mathrm{w}}^{\mathrm{ow}}\left(\beta_{\mathrm{ow}}, h_{\mathrm{ow}}\right) \qquad [3\text{-}6]$$

The left hand side reflects the direct measurement, while the right hand side expresses the prediction using the scaling theory. The predictions of the three-phase *P-S* relationship from the two-phase *P-S* information were given by:

$$S_{\mathrm{t}}^{\mathrm{aow}} \equiv S_{\mathrm{o+w}}^{\mathrm{aow}} \tag{3-7a}$$

$$\approx S_{\mathrm{o}}^{\mathrm{ao}}(h_{\mathrm{ao}}) \tag{3-7b}$$

$$S_{\mathrm{w}}^{\mathrm{aow}} \approx S_{\mathrm{w}}^{\mathrm{ow}}(h_{\mathrm{ow}}) \tag{3-8}$$

$$S_{\mathrm{o}}^{\mathrm{aow}} = S_{\mathrm{t}}^{\mathrm{aow}} - S_{\mathrm{w}}^{\mathrm{aow}} \tag{3-9a}$$

$$\approx S_{\mathrm{o}}^{\mathrm{ao}}(h_{\mathrm{ao}}) - S_{\mathrm{w}}^{\mathrm{ow}}(h_{\mathrm{ow}}) \tag{3-9b}$$

The subscript t denotes the total saturation of the oil plus water phases in the three-phase system. The superscripts indicate the pertinent phase systems, either a three-phase (aow) or a two-phase (ao, ow) system.

Once the three-phase *P-S* relationships were obtained, the *k-S* relationships can be constructed. Employing the VG parameters, such a procedure was formulated so that:

$$k_{\mathrm{ro}}^{\mathrm{aow}} = \left(\bar{S}_{\mathrm{t}}^{\mathrm{aow}} - \bar{S}_{\mathrm{w}}^{\mathrm{aow}}\right)^{1/2} \left\{\left[1 - \left(\bar{S}_{\mathrm{w}}^{\mathrm{aow}}\right)^{1/m}\right]^{m} - \left[1 - \left(\bar{S}_{\mathrm{t}}^{\mathrm{aow}}\right)^{1/m}\right]^{m}\right\}^{2} \tag{3-10}$$

$$k_{\mathrm{rw}}^{\mathrm{aow}} = \left(\bar{S}_{\mathrm{w}}^{\mathrm{aow}}\right)^{1/2} \left\{1 - \left[1 - \left(\bar{S}_{\mathrm{w}}^{\mathrm{aow}}\right)^{1/m}\right]^{m}\right\}^{2} \tag{3-11}$$

where m=1-1/n, $k_{\mathrm{rw}}^{\mathrm{aow}}$ and $k_{\mathrm{ro}}^{\mathrm{aow}}$ denote the relative permeability of the water and the oil phase in a three-phase system receptively. Omitting the superscript, the effective saturation $\bar{S}_q$ is defined as $(S_q\text{-}S_r)/(1\text{-}S_r)$.

Note that, a three-phase system with $\bar{S}_{\mathrm{t}}^{\mathrm{aow}}$ = 1 is equivalent to a two-phase oil-water system. In this particular case, when the oil and water phases are regarded just as the nonwetting and the wetting phases of a two-phase system, Equation 3-10 becomes the equation for the nonwetting phase relative permeability k_{rq}^{pq}. In this two-phase form the saturation $\bar{S}_{w}^{aow}$ becomes saturation of the wetting phase S_{p}^{pq}. Likewise, at $\bar{S}_{w}^{aow} = 0$ any three-phase system becomes a two-phase air-oil system. In this case the oil phase act as the wetting phase and since $\bar{S}_{t}^{aow}$ contains only the oil phase it becomes saturation of the wetting phase S_{p}^{pq}. In this situation Equation 3-10 becomes the equation for the wetting phase relative permeability k_{rp}^{pq}. Thus, the two-phase relative permeabilities k_{rw}^{aw}, k_{rw}^{ow}, k_{ro}^{ow} and k_{ro}^{ao} can be calculated using Equation 3-10 by substituting appropriate saturation.

Previous investigators focused their studies by testing the hypotheses as formulated in Equations. 3-5, 3-6, 3-7b, 3-8 and 3-9b. *Lenhard and Parker* (1987) studied the agreement of the mean response of the direct measurements (the left hand side of Equation 3-5 and Equation 3-6) and the predicted ones (the right hand side of Equations 3-5 and 3-6). Later, *Lenhard and Parker* (1988) focused their study on the validity of Equations 3-7b, 3-8 and 3-9b. The favorable agreements they observed deteriorated slightly when the right hand side of those equations was substituted in Equation 3-5 and Equation 3-6. Nevertheless, they showed the possibilities of constructing three-phase k_r-S-P relationships when a set of parameters S_r, n, α_{ow} and α_{ao} is given. By predicting the scaling factor from interfacial tension and choosing the air-water as the reference system the required parameters are S_r, n, β_{ow}, β_{ao} and α_{aw}.

3.3. MATERIAL AND METHOD.

In order to obtain the parameters required to construct the k_r-S-P relationship using methods 1, 2 and 3 which were discussed previously, P-S measurements of air-water, oil-water and air-oil systems were conducted using Ottawa sand and Metea soil. Ottawa sand is a relatively uniform sand. About 85% of its grain diameter is 0.33 mm and no grains are smaller than 50 μ. Metea soil has a loamy sand texture with 6% being non-expansive clay, 11% silt and 83% sand. It is a structureless soil that contains 1.1% organic matter after it is dried and sieved to pass 850 μ. The water-phase used was a 0.005 M $CaSO_4$ solution as suggested by Klute (1986). Prior to being used in the experiment, this solution was subjected to a 750 mbar vacuum for at least two hours in order to minimize the amount of dissolved air. Tetrachloroethylene (PCE) at 99.99% purity and density of 1.623 gr/cm^3 was used as the oil-phase.

The P-S measurement protocol was based on the pressure equilibrium method as described in more detail in the Materials and Methods section of Chapter II. Conventionally, the P-S measurement in a pressure cell is conducted by measuring the saturation at its equilibrium state under a certain imposed capillary pressure. The pressure equilibrium method, which is based on the method proposed by *White et al.*, (1970b) and *Su and Brooks* (1980), reverses the conventional measurement method. In this method the equilibrium state of the capillary pressure is measured under a series of desaturation steps which are externally controlled. By employing this method, large numbers of P-S data can be obtained in a relatively short time.

The mentioned protocol was applied to measure the *P-S* relationship in a soil sample which was placed in a pressure cell. The pressure cells used were the Tempe cells by Soil Moisture type no.1400 made from Plexiglas. All standard rubber o-rings of the cells were replaced with Viton o-rings to avoid dissolution and to minimize PCE absorption. A 1-bar pressure plate made by Soil Moisture (part no. 1430B1M3) was used as the nonwetting-phase barrier. The loose soil sample was placed in a brass retaining cylinder (2¼"OD, 0.065" wall thickness and 3 cm height) and packed using a 1.6 kg. falling weight dropped 10 times from 7 cm high. With this method, replicable bulk density of ±1.67 gr/cm^{-3} for Ottawa sand and ±1.44 gr/cm^{-3} for Metea soil was achieved. The packed samples in the cells were vacuum saturated and were equilibrated at zero capillary pressure for at least 12 hours. A pressure transducer, which had been calibrated against a mercury manometer prior to any measurement, was used to monitor the capillary pressure. Measurements of each system were replicated four to eight times. Out of these, the three replicates that yielded the least mass balance error were selected to be used for further analyses.

The *P-S* parameters used in method 1 were determined by regressing the VG equation into the measured *P-S* data. The regression procedure was constrained to yield common values of S_r and n in all two-phase systems from the same soil type. This was necessary to accommodate the assumption which states that S_r and n are porous medium-dependent parameters. To achieve this, the sum of the squared error in predicting the air-water, oil-water and air-oil parameters was minimized simultaneously (pooled regression). The parameters S_r, *n* and α_{aw} required by method 2 were obtained from regression upon air-water *P-S* data only (individual regression). The α_{ow} and α_{ao} were determined via Equation 3-3b. For method 3, the required parameters were obtained in a similar manner but the air-water system was replaced by the air-oil system.

The precision limits of method 1 for S_w^{aw}, S_w^{ow} and S_o^{ao} were the 95% confidence limits of the regression determined using the procedure as explained by *Seber* (1988). For the other constitutive variables, those limits were determined by propagating the 95% confidence limits of the parameters involved. The procedure employed was based on error propagation method utilizing the first order of Taylor series expansion. An identical propagation method was also used to determine prediction precision by methods 2 and 3.

To obtain the interfacial tension data required by methods 2 and 3, the air-water oil-water and air-oil interfacial tensions were measured using the pendant drop method by *Adamson* (1976). Values of σ_{ow} were measured at 20 °C using oil and water taken from the air-oil and oil-water *P-S* experiments. The fluid samples used to determined σ_{ao} and σ_{aw} were taken from the air-oil and the air-water *P-S* experiments. As such, the liquid had been put in contact with the porous medium material for about 60 hours.

3.4. RESULT AND DISCUSSION

To verify the acceptability of method 2 or 3 relative to method 1, each method was implemented to construct the k_r-*S*-*P* relationships. The *P-S* and interfacial tension data were measured. Subsequently, the *P-S* parameters and scaling factor values including their precision limits were determined. Table 3-1 lists the results obtained both for Ottawa sand and Metea soil. Based on these values the constitutive variables $S_{\mathrm{w}}^{\mathrm{aw}}(h)$, $S_{\mathrm{w}}^{\mathrm{ow}}(h)$, $S_{\mathrm{a}}^{\mathrm{ao}}(h)$, $S_{\mathrm{o}}^{\mathrm{aow}}(h)$, $k_{\mathrm{rw}}^{\mathrm{aw}}(h)$, $k_{\mathrm{rw}}^{\mathrm{ow}}(h)$, $k_{\mathrm{ro}}^{\mathrm{ao}}(h)$ and $k_{\mathrm{ro}}^{\mathrm{aow}}(h)$ were plotted and superimposed with their uncertainty limits (Figure 3-1 through Figure 3-9).

Table 3-1: The obtained interfacial tensions, *P-S* parameters and scaling factors [a]

	Ottawa sand		Metea soil	
Interfacial tension				
σ_{aw} (dyne/cm^2)	71.60	±1.661	69.09	±5.512
σ_{ow} (dyne/cm^2)	38.03	±3.001	38.62	±4.591
σ_{ao} (dyne/cm^2)	26.40	±1.762	25.29	±1.650
Method 1				
S_{r}	0.11	±0.048	0.22	±0.036
α_{aw} (cm^{-1})	0.053	±0.0037	0.023	±0.0015
α_{ow} (cm^{-1})	0.093	±0.0061	0.045	±0.0031
α_{ao} (cm^{-1})	0.134	±0.0322	0.058	±0.0040
n	4.33	±0.741	3.10	±0.352
Method 2				
S_{r}	0.08	±0.075	0.21	±0.065
α_{aw} (cm^{-1})	0.053	±0.0045	0.022	±0.0016
α_{ow} (cm^{-1})	0.099	±0.0117[b]	0.040	±0.0064[b]
α_{ao} (cm^{-1})	0.142	±0.0158[b]	0.060	±0.0067[b]
n	4.13	±1.116	3.38	±0.775
β_{ow}	1.88	±0.155[b]	1.79	±0.256[b]
β_{ao}	2.71	±0.192[b]	2.73	±0.281[b]
Method 3				
S_{r}	0.14	±0.077	0.23	±0.068
α_{aw} (cm^{-1})	0.037	±0.0051[b]	0.023	±0.0033[b]
α_{ow} (cm^{-1})	0.068	±0.0108[b]	0.041	±0.0069[b]
α_{ao} (cm^{-1})	0.099	±0.0118	0.063	±0.0062
n	3.00	±0.728	2.882	±0.540
β_{aw}	0.37	±0.026[b]	0.37	±0.038[b]
β_{ow}	0.69	±0.072[b]	0.65	±0.089[b]

[a]) Except where indicated, all values were given as mean ±95% confidence limit from parameter estimation procedure.

[b]) The values given as mean ± uncertainty from error propagation employing the first order of the Taylor series.

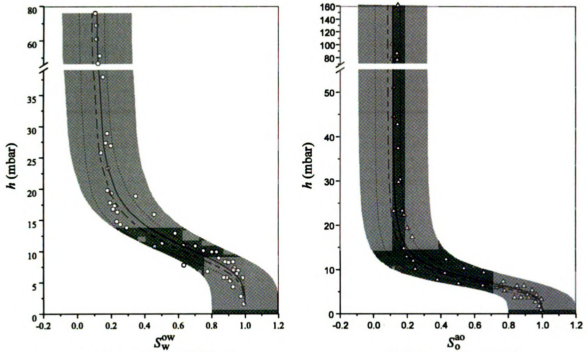

(a) Ottawa Sand: Oil-Water

(b) Ottawa Sand: Air-Oil

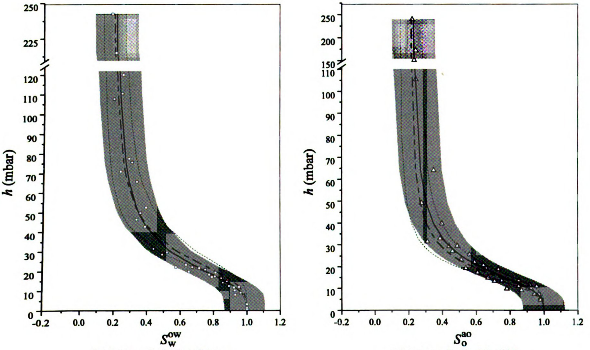

(c) Metea Soil: Oil-Water

(d) Metea Soil: Air-Oil

Figure 3-1: Two-phase oil-water and air-oil pressure-saturation curves obtained by method 1 (solid lines) with their 95% confidence limis (shaded area) superimposed with those obtained by method 2 (heavy dashed lines) with their uncertainty limits (light dashed lines) and the measured data.

ps2-12.cdr

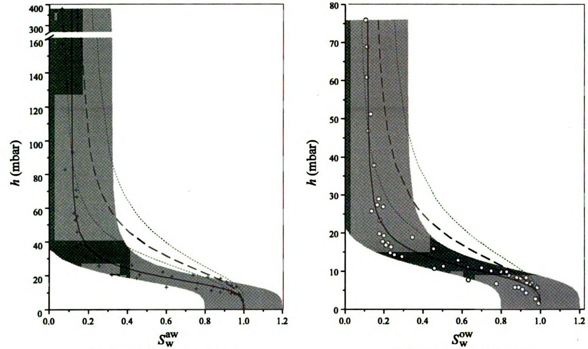

(a) Ottawa Sand: Air-Water

(b) Ottawa Sand: Oil-Water

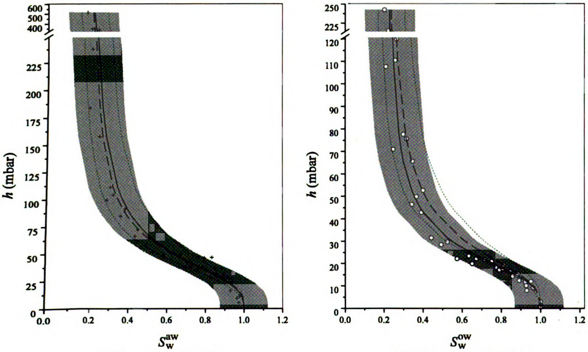

(c) Metea Soil: Air-Water

(d) Metea Soil: Oil-Water

Figure 3-2: Two-phase air-water and oil-water pressure-saturation curves obtained by method 1 (solid lines) with their 95% confidence limis (shaded area) superimposed with those obtained by method 3 (heavy dashed lines) with their uncertainty limits (light dashed lines) and the measured data.

ps2-13.cdr

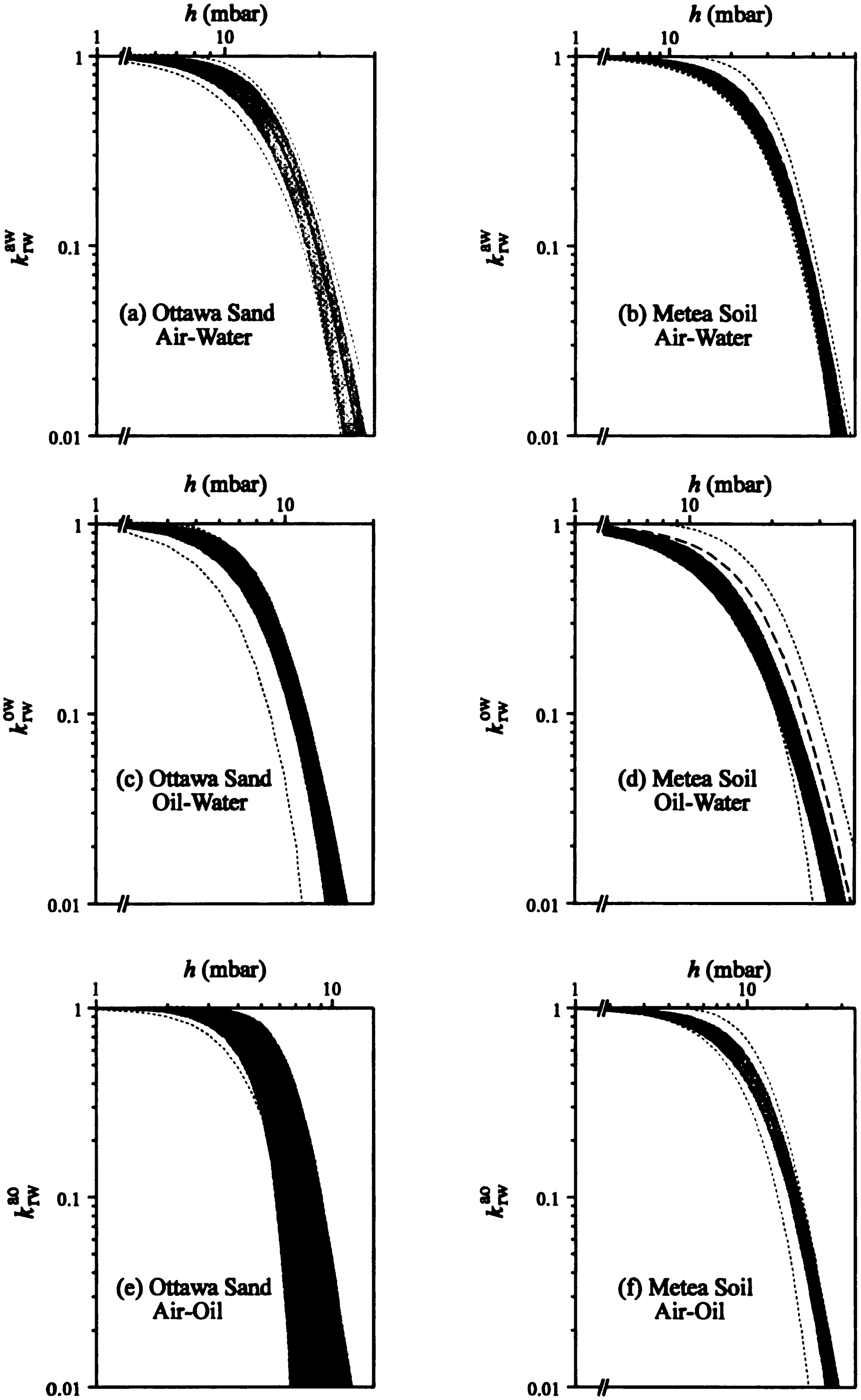

Figure 3-3: Two-phase air-water, oil-water and air-oil relative permeability curves obtained by method 1 (solid lines) with their uncertainty limits (shaded area) superimposed with those obtained by method 2 (heavy dashed lines) with their uncertainty limits (light dashed lines).

k2-12.cdr

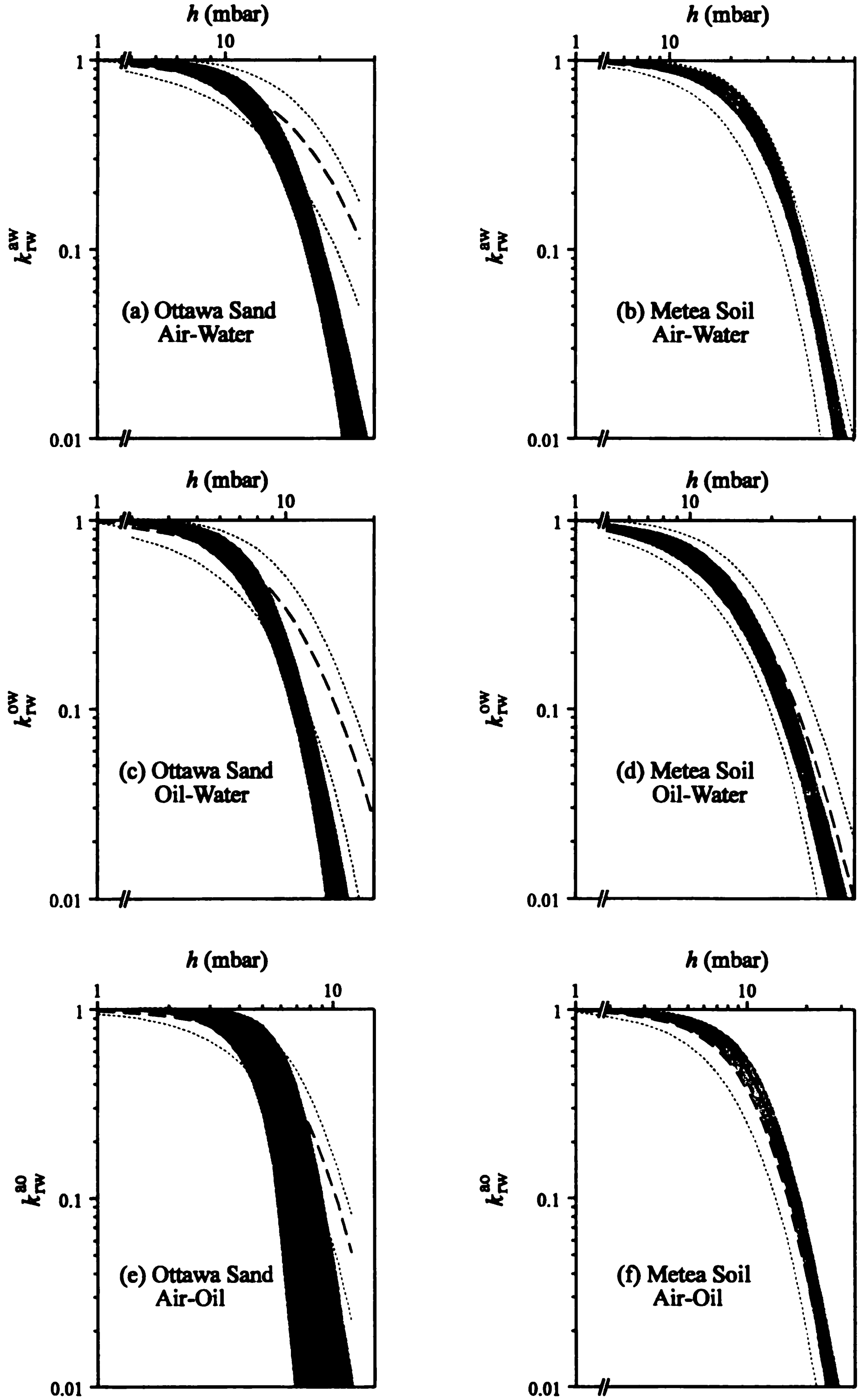

Figure 3-4: Two-phase air-water, oil-water and air-oil relative permeability curves obtained by method 1 (solid lines) with their uncertainty limits (shaded area) superimposed with those obtained by method 3 (heavy dashed lines) with their uncertainty limits (light dashed lines).

k2-13.cdr

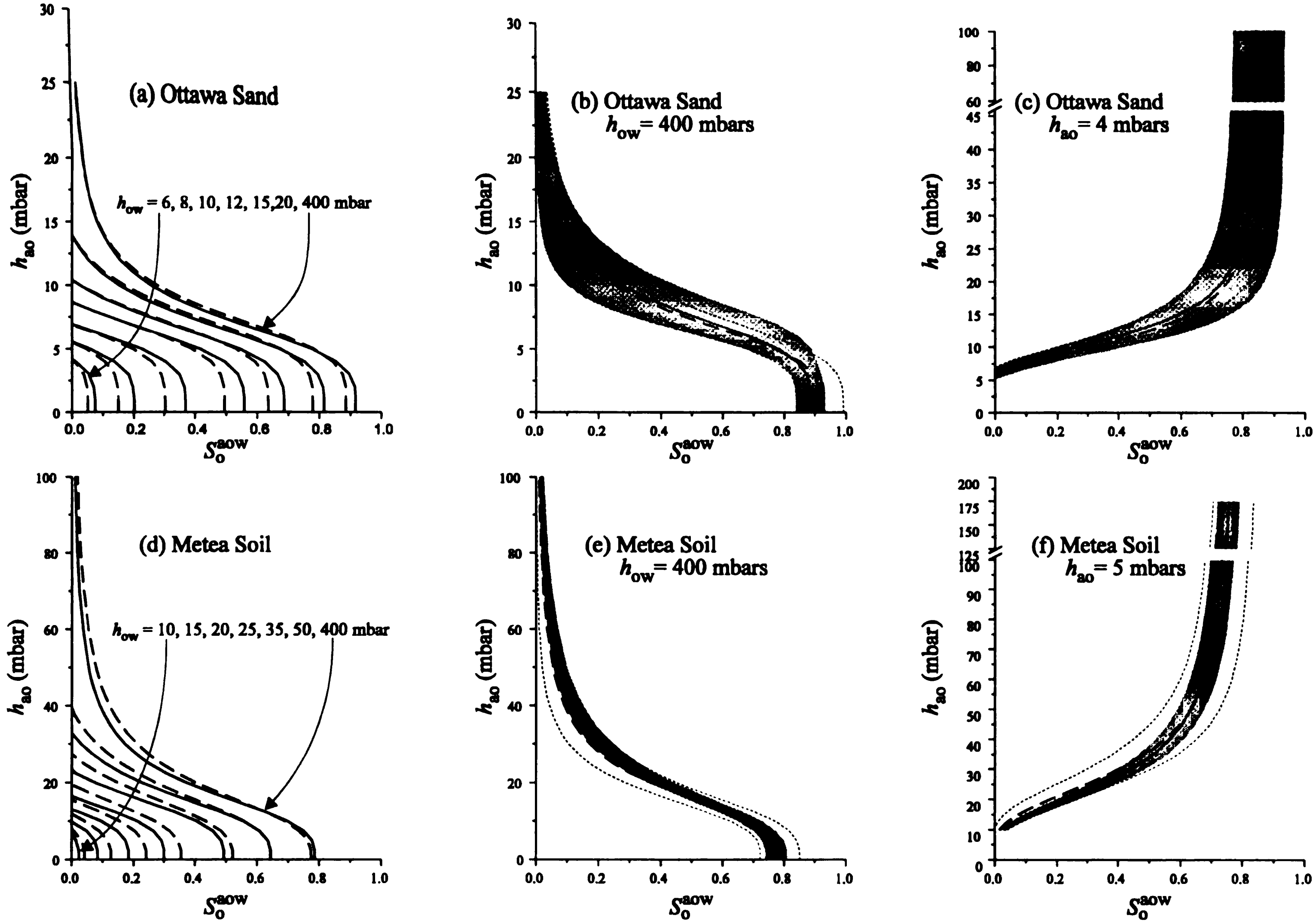

Figure 3-5: Three-phase oil saturation curves obtained by method 1 (solid lines) with their uncertainty limits (shaded area) superimposed with those obtained by method 2 (heavy dashed lines) with their uncertainty limits (light dashed lines).

pa3-12.cdr

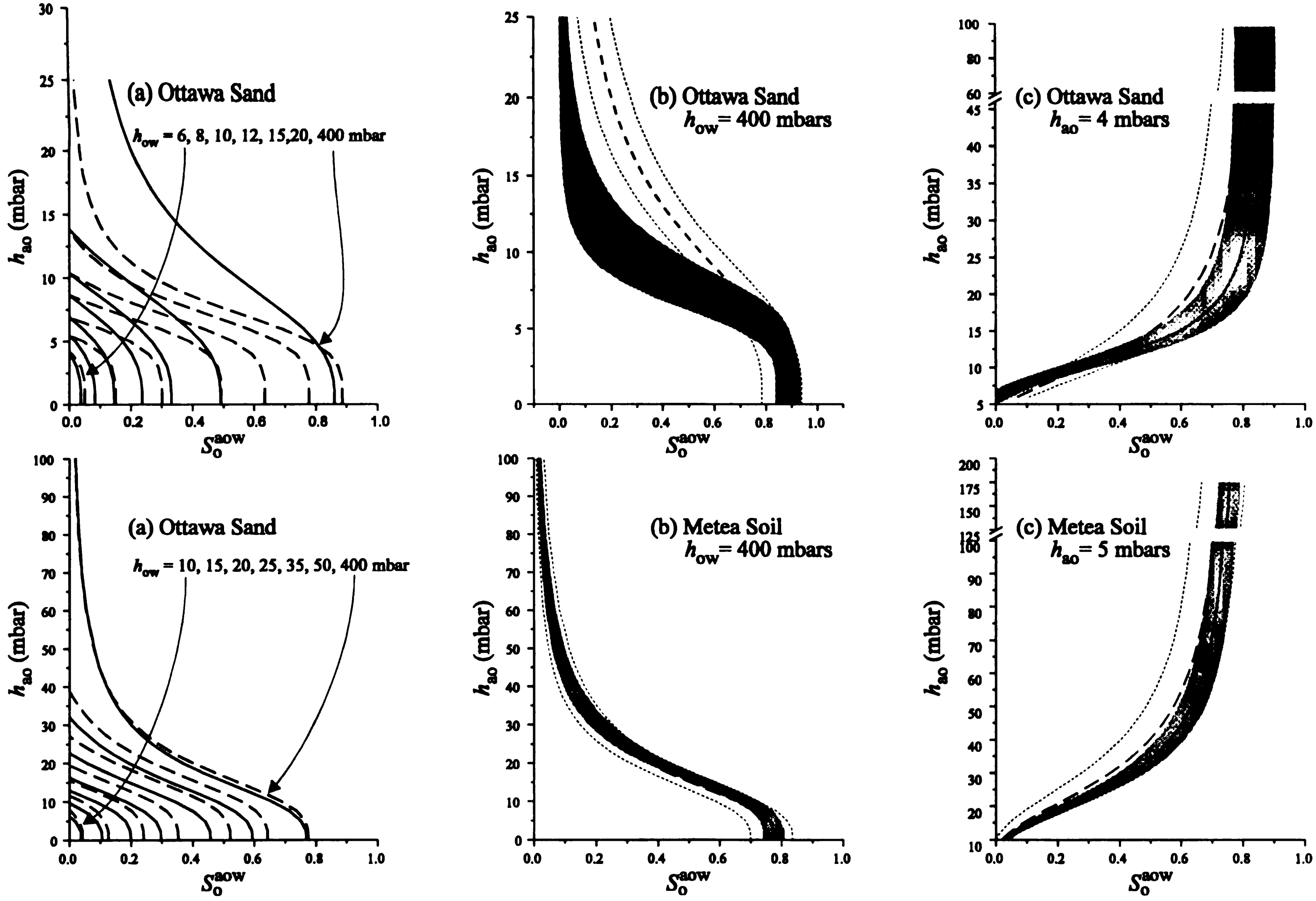

Figure 3-6: Three-phase oil saturation curves obtained by method 1 (solid lines) with their uncertainty limits (shaded area) superimposed with those obtained by method 3 (heavy dashed lines) with their uncertainty limits (light dashed lines).

ps3-13.cdr

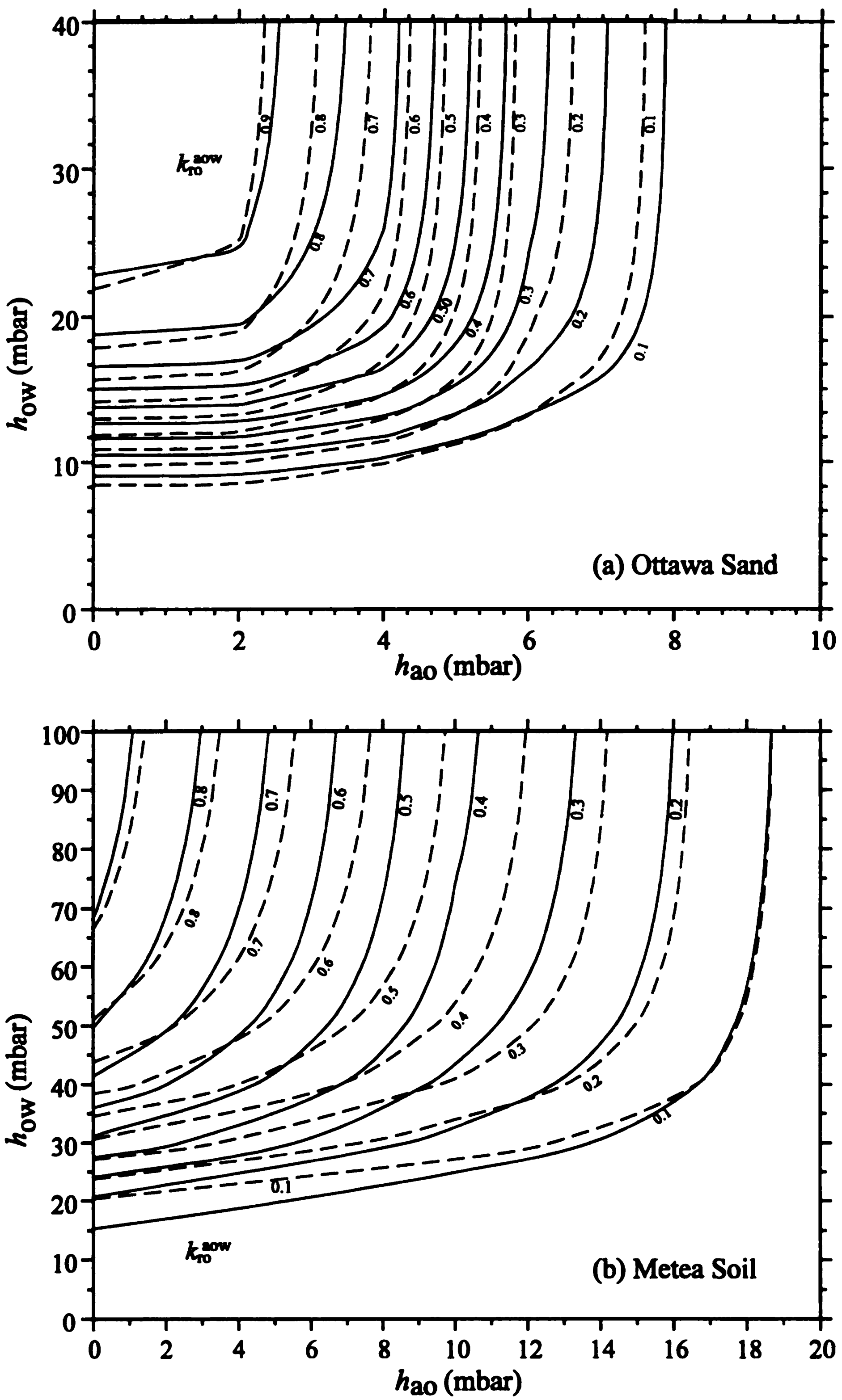

Figure 3-7: Three-phase oil relative permeability obtained by method 1 (solid lines) and method 2 (dashed lines).

k3-12-3d.cdr

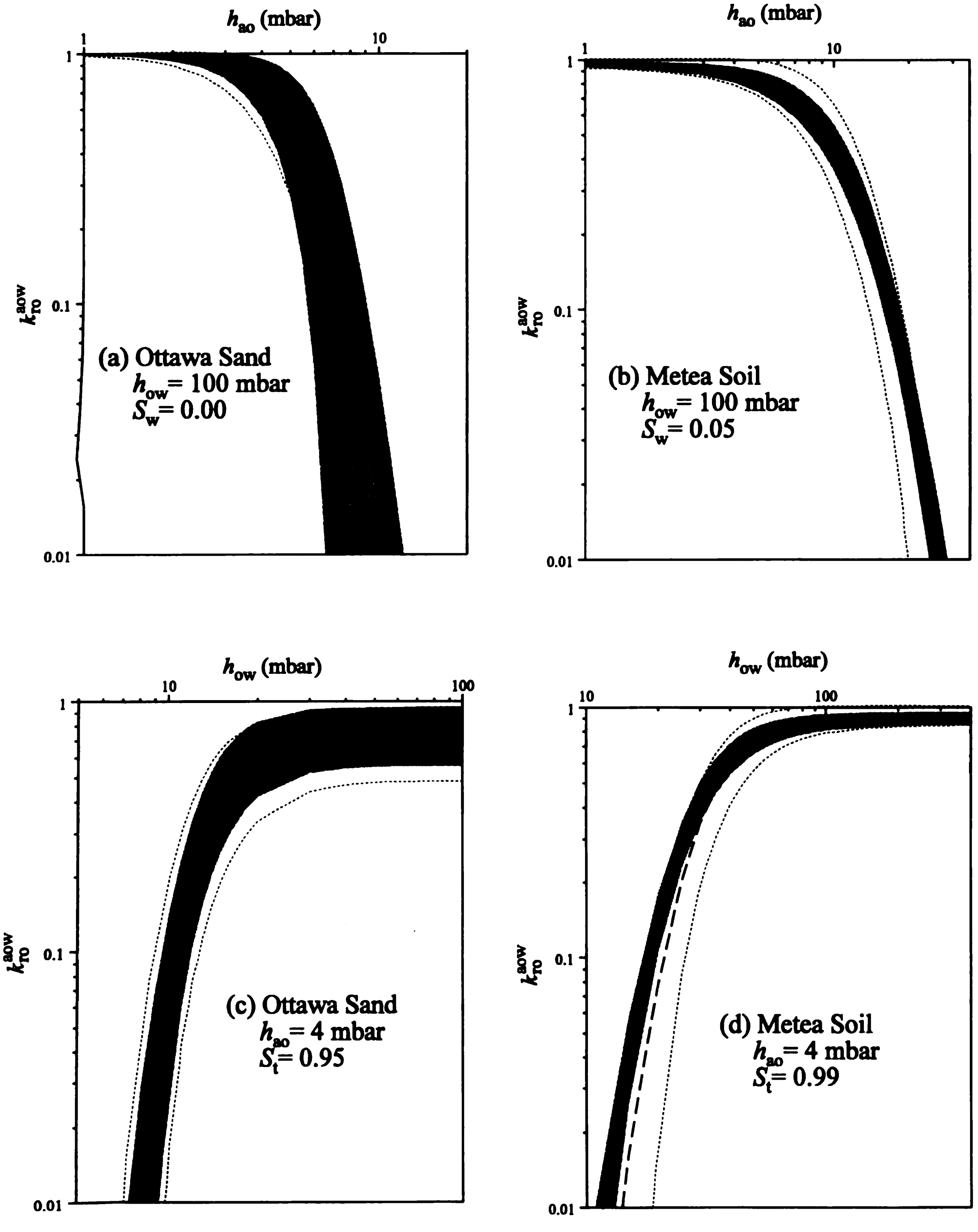

Figure 3-8: Three-phase oil relative permeability obtained by method 1 (solid lines) with their uncertainty limits (shaded area) and those obtained by method 2 (heavy dashed lines) with their uncertainty limits (light dashed lines).

k3-12.cdr

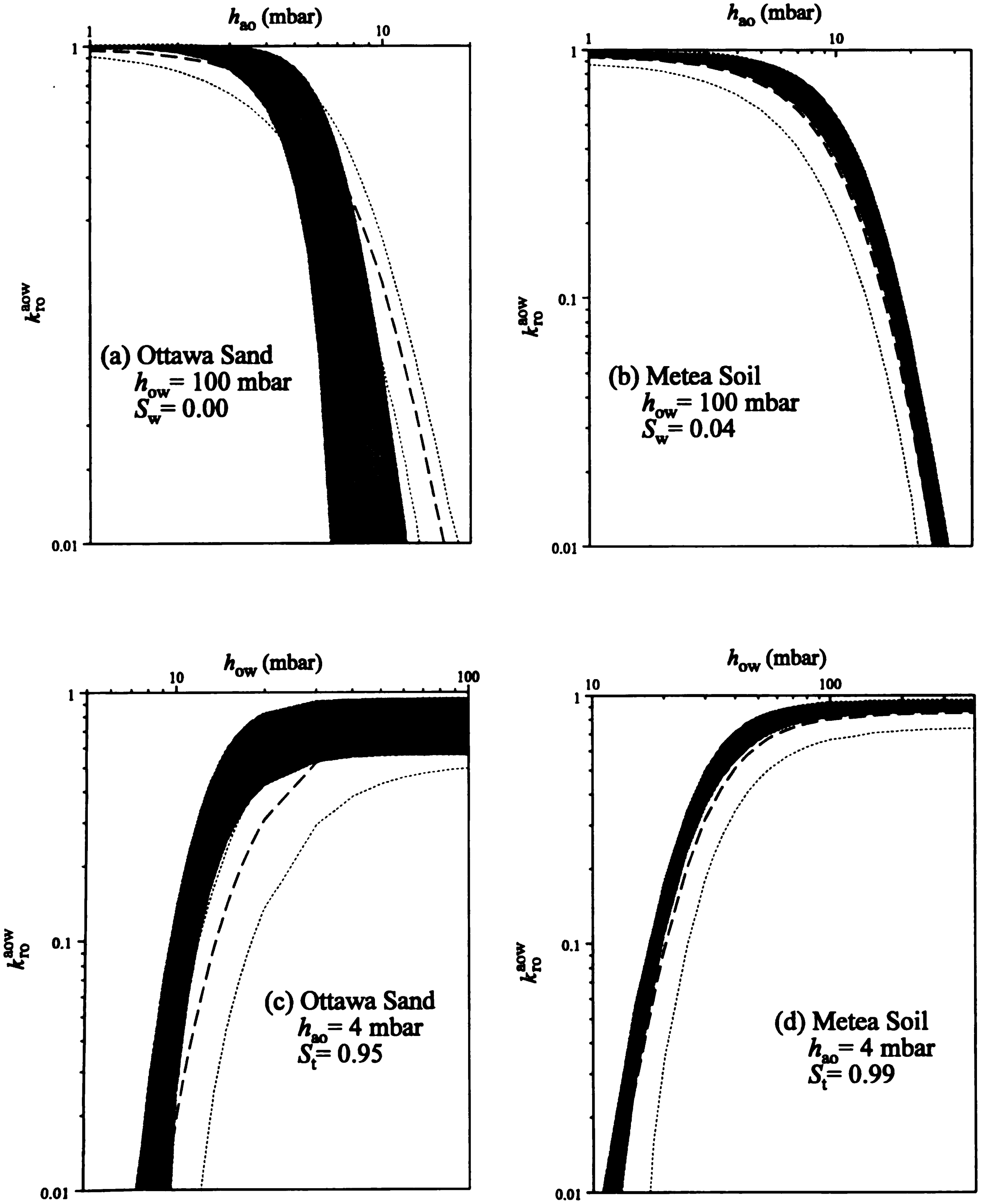

Figure 3-9: Three-phase oil relative permeability obtained by method 1 (solid lines) with their uncertainty limits (shaded area) and those obtained by method 3 (heavy dashed lines) with their uncertainty limits (light dashed lines).

k3-13.cdr

In method 2, the base parameters were used to construct the curves of water saturation S_{w}^{aw} against capillary pressure h for the air-water system using Equation 3-2. The 95% confidence limits obtained during regression were used as the uncertainty limits of the curve prediction. The same base parameters plus the measured interfacial tension were used to plot the air-oil S_{o}^{ao} and oil-water S_{w}^{ow} curves using Equation 3-4. The uncertainty limits of these curves were determined based on the uncertainty in the base parameters and the scaling factors. The uncertainty limits of the base parameters were assumed to be identical to their confidence limits obtained in the parameter estimation procedure. The uncertainty limits of the scaling factors were determined by propagating the confidence limits of the interfacial tension values.

The two-phase relative permeability curves k_{rw}^{aw} k_{ro}^{ao} and k_{rw}^{ow} were plotted employing the two-phase form of Equation 3-10. With this two-phase form, the terms of $\bar{S}_{t}^{aow}$ and $\bar{S}_{w}^{aow}$ in Equation 3-10 were substituted by S_{a}^{aw}, S_{w}^{ow} or S_{o}^{ao} as necessary. Note that, the saturation S_{a}^{aw}, S_{w}^{ow} or S_{o}^{ao} were substituted in the form of Equation 3-2 and Equation 3-4. As such the relative permeability functions were expressed in term of the capillary pressure, base parameters and interfacial tension. This expanded function was used to determined the relative permeability at a given capillary pressure. This function also served as the base function to propagate the error of the base parameters and the scaling factors in order to determine the uncertainty limits. Similar procedures were employed to construct the rest of the constitutive functions and to determine their uncertainty limits.

In general, method 3 and method 1 followed similar procedures to construct the constitutive curves. The base parameters used in method 3, however, were the air-oil parameters obtained from the individual regression while those used in method 1 were from the pooled regression. Each of the saturation functions $S_{\mathrm{w}}^{\mathrm{aw}}$, $S_{\mathrm{o}}^{\mathrm{ao}}$ or $S_{\mathrm{w}}^{\mathrm{ow}}$ in method 1 has its own base parameter set. Therefore, these curves were constructed in a similar manner to those used in the case of $S_{\mathrm{w}}^{\mathrm{aw}}$ in method 2.

As shown in the previous section, the three-phase oil saturation ($S_{\mathrm{o}}^{\mathrm{aow}}$) and relative permeability ($k_{\mathrm{ro}}^{\mathrm{aow}}$) functions are formulated as functions of the oil-water and air-oil capillary pressures (h_{ow} and h_{ao}). When h_{ow} and h_{ao} are varied, a family of $S_{\mathrm{o}}^{\mathrm{aow}}$ or $k_{\mathrm{ro}}^{\mathrm{aow}}$ curves are obtained (Figures 3-5a, 3-5d, 3-6a, 3-6d and 3-7). Among these curves, two which allow the widest range of oil saturation change were selected for further analysis. The selected curves were referred to as vadose zone and saturated zone curves. The vadose zone curves were plotted by increasing h_{ao} while holding h_{ow} constant at high capillary pressure (Figures 3-5b, 3-5e, 3-6b and 3-6e for $S_{\mathrm{o}}^{\mathrm{aow}}$ and Figures 3-8a, 3-8b, 3-9a, and 3-9b for $k_{\mathrm{ro}}^{\mathrm{aow}}$). These plots represent oil desaturation as the air saturation increased at constant low water saturation. In the field, this case might occur in the vadose zone when the water phase is at residual saturation and the oil phase percolates as it is driven by gravitational force. The saturated zone curves were plotted reversing the vadose zone situation, ie., h_{ow} was increased but h_{ao} was held constant at low capillary pressure (3-5c, 3-5f, 3-6c and 3-6f for S_o^{aow} and Figures 3-8c, 3-8d, 3-9c, and 3-9d for k_{ro}^{aow}). In this setting the oil saturation was increased as water desaturation occurs at constant high total liquid saturation. Such a situation may occur when the DNAPL penetrates below the capillary fringe zone and replaces the water volume in the soil pore.

Table 3-2: Summary of the agreement between prediction outcomes by methods 2 or 3 to method 1

	Ottawa Sand		**Metea Soil**	
	Method 2	**Method 3**	**Method 2**	**Method 3**
S_w^{aw}	-	●	-	○
S_o^{ao}	○	-	○	-
S_w^{ow}	○	●	○	○
k_{rw}^{aw}	○	●	○	○
k_{ro}^{ao}	○	●	○	○
k_{rw}^{ow}	○	●	⊙	⊙
S_o^{aow} in vadose zone	○	●	○	○
S_o^{aow} in sat'd zone	○	⊙	○	⊙
k_{ro}^{aow} in vadose zone	○	●	○	⊙
k_{ro}^{aow} in sat'd zone	○	●	⊙	⊙

Note: ● poor agreement, no overlapping uncertainty limits in most of the range.
⊙ fair agreement, overlapping uncertainty limits.
○ good agreement, the mean laid within the uncertainty limit of method 1.
- no prediction required

Table 3-2 summarizes the subjective interpretation of the agreement between method 1 and 2 as well as between method 1 and 3 as observed on the obtained curves. The agreement levels in this table were classified into three categories. A good agreement score was given for the cases where the mean responses of the prediction curves (method 2 or 3) were laid within the uncertainty limits of the reference curve (method 1). A fair agreement score was given for the cases in which the mean of the prediction curve was slightly off of the uncertainty limits of the reference curve, however, their uncertainty limits overlapped each other in all of the observed ranges. If those uncertainty limits were off at some parts of the observed ranges, a poor agreement score was given.

The Ottawa sand and Metea soil columns in Table 3-2 contrast the effect of soil texture. The columns labeled as Method 2 and Method 3 show the effects of using air-water and air-oil as the system basis for prediction, respectively. The arrangement of the constitutive variables listed in the rows of Table 3-2, from top to bottom, were sorted according to the order of the procedure followed in constructing the two- and three-phase k_r-S-P relationships. The variables which were potentially affected more by the error in the base parameters propagated along the prediction were placed in the lower rows. The subsequent sections discuss the issue associated with soil texture, and are followed by discussion concerning the methods. The characteristic of the error propagation along the prediction procedure is discussed in the last sections.

3.4.1. Comparison Across the Soil Types

Table 3-2 shows that, when the Metea soil was used as the porous medium, all of the obtained k_r-S-P curves were in the categories of good or fair. When the Ottawa sand was used, however, the outcomes range from good to poor. It appears that the soil texture affects the prediction outcomes. The Metea soil has loamy sand texture while the size of the Ottawa sand grains are practically uniform. Study by *McCuen et al.* (1981), based on

1,085 samples measured by *Rawls et al.*, (1976) and *Holtan et al.*, (1968), found that the standard error of the squared root of the *Brooks and Corey's* (1964) λ (which is equivalent to *van Genuchten's* parameter n) for sand was 0.039. Compared to 0.013 for loamy sand, that for the sand was 300% higher.

The pooled regressions regressed the air-water, oil-water and air-oil simultaneously. As such, any factor associated with a two-phase type involved was lumped. Accordingly, any differences in the estimated parameters including their statistical properties should be related to the soil type. The entries under sub-heading Method 1 in Table 3-1 list the confidence limits of the *P-S* parameters estimated by the pooled regression for the investigated soil. It is observed in the table that the confidence limits of all parameters obtained in the Ottawa sand were in almost in all cases wider than those measured in the Metea soil. A wider confidence limit suggests a higher possibility of obtaining various outcomes when a number of data sets are used to estimate the parameters. This explaines the pattern exhibited by the scoring outcomes across the soil type in Table 3-2. In Ottawa sand cases, where the confidence limits of the base parameters used were relatively wide, the outcomes were varied in a wider range of outcomes: from good to poor. A favorable outcome may be obtained (Method 2-Ottawa sand in Table 3-1). Yet, there was also a risk of obtaining unfavorable outcome (Method 3-Ottawa sand in Table 3-1). In contrast, the outcomes of the Metea soil cases, where the confidence limits of the base parameters used were relatively narrow, were consistently favorable. This evidence suggests that when prediction via scaling theory was implemented in a uniform graded porous medium the obtained result may vary. At the extreme case, an unfavorable result such as those observed in the case of Ottawa sand might be obtained.

3.4.2. Comparison Across the Methods

Across the methods, as observed in Table 3-2, method 2 received a greater number of good scores compared to method 3. This tendency was consistently observed in both soils. This scoring outcome might suggest that method 2 is a better substitute for method 1 than is method 3. The major difference between method 2 and 3 was in the two-phase type from which the base parameters were determined. If it is true that the superiority of method 2 over method 3 is due to the use of the two-phase type, then a parallel tendency should also be observed in their base parameters.

The following discussion inspects any possible correlation between the base parameters used in methods 2 and 3 and the superiority of method 2 over method 3. Except the scaling factor β, the other parameters S_r, n and α_{aw} (method 2) or α_{ao} (method 3) were inspected. At this stage, each of these parameters is assumed to have potential for influencing the difference in the scores across the two methods. As shown in Equation 3-5 and Equation 3-6 the scaling factors β were involved in the scaling procedure. These factors, however, were determined using the interfacial tension data and the same interfacial tension data was used by the two methods. Based on this, it is unlikely that β has potential to influence the difference between methods.

Table 3-3: Discrepancies between the base parameters used in method 2 and 3 relative to those used in method 1.

Base Parameters	Ottawa sand Method 2	Ottawa sand Method 3	Metea soil Method 2	Metea soil Method 3
S_r	27 %	20 %	5 %	2 %
α_{aw}	1 %	-	4 %	-
α_{ao}	-	26 %	-	8 %
n	5 %	31 %	9 %	7 %

Table 3-3 shows the discrepancies of the base parameters S_r, n and α_{aw} or α_{ao} employed by the two methods relative to the base parameters used in method 1. The magnitude of these descrepancies are regarded as the level of the error of those parameters. As observed in this table, the discrepancies in the parameters S_r and n were not consistent with the scoring outcome observed in Table 3-2. For example, while method 2 received a better score than method 3, the errors of the S_r employed in method 2 was higher than those employed in method 3.

That S_r and n cannot be associated to the two-phase type involved appears to be in agreement with the assumption which states that these parameters are porous medium dependent parameters rather than the two-phase type (*Lenhard and Parker*, 1987). Note that, methods 2 and 3 estimate the *P-S* parameters using the individual regression procedure. This procedure did not pool the data according to the soil type. The S_r and n used in method 2 were obtained from air-water measurements while those used in method 3 were from air-oil measurements. To permit more general inspection, S_r and n estimated by the individual regression upon each of the air-water, air-oil and oil-water data were

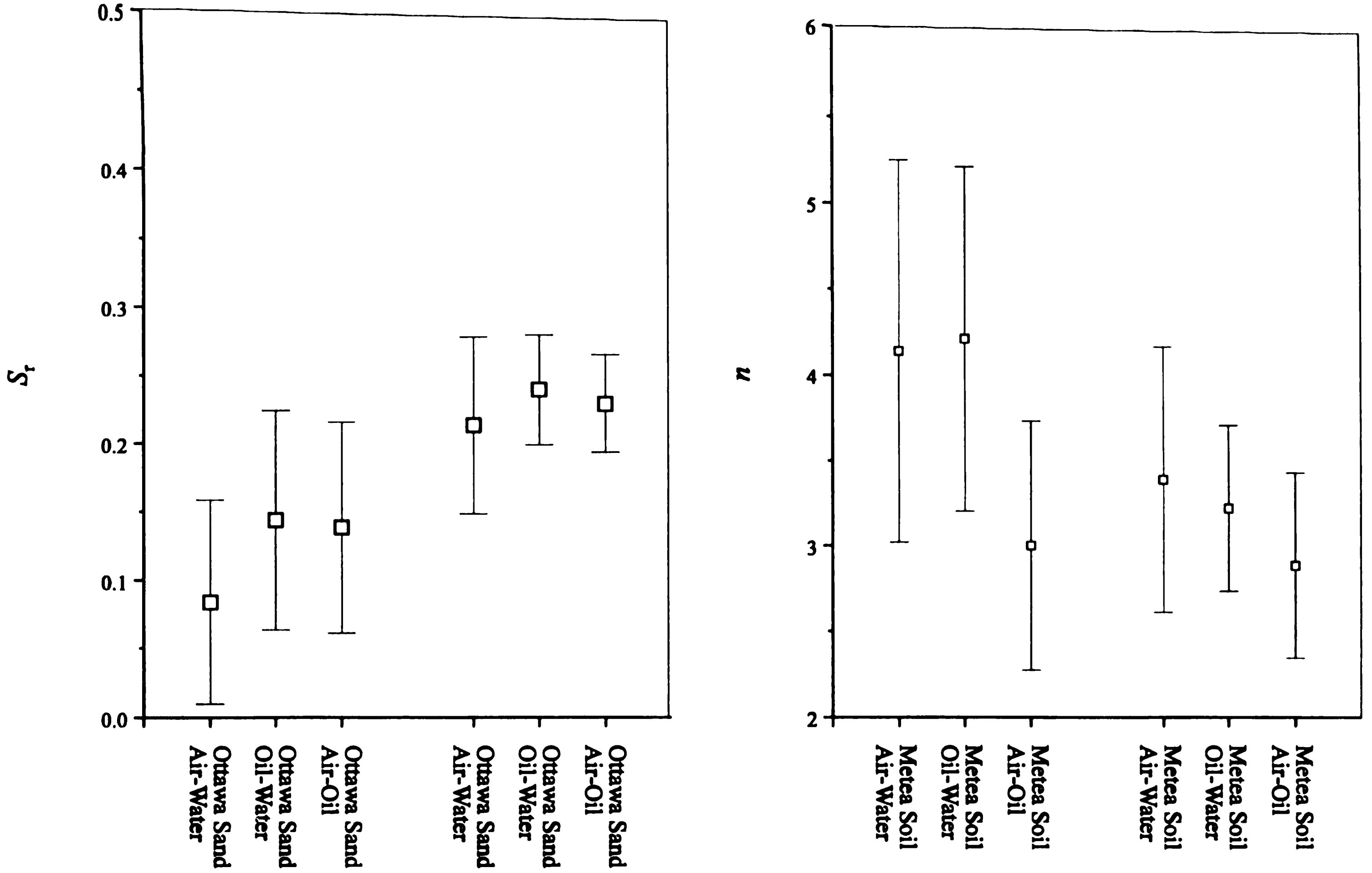

Figure 3-10: Parameters S_r and n estimated by the individual regression with their 95% confidence limit.s

sr-n.cdr

plotted in Figure 3-10. With the individual regression procedure, neither their independence to the two-phase type nor their correlation to the soil type was artificially imposed. However, as observed in Figure 3-10, except in the case of n_{ao} of the Ottawa sand, S_r and n appear to be more consistent across the soil types than across the methods. Based on all of the mentioned evidence, it is concluded that S_r and n are independent of the two-phase type used. As such, the outcome across the two methods observed in Table 3-2 was unlikely to be the signature of the errors of S_r and n. Unfavorable scores in the cases of method 2 using Ottawa sand migh be strongly influenced by the error in n_{ao}. However, it is viewed as more characteristic of the soil type rather than the methods.

The discrepancies in the parameter α in Table 3-3, on the other hand, appear to be correlated to the differences in the scores obtained by the two methods. Method 2, which received overall good results had α discrepancies of only 1% and 4%. Method 3, however, received overall poorer results and had α discrepancies of 26% and 8%. It appears that good result might be correlated to low discrepancies, whereas poorer results to high discrepancies.

As concluded in the previous section, S_r and n appeared to be porous medium dependent parameters. The pooled regression accommodates this condition. Thus, α_{aw} α_{ow} and α_{ao} obtained via pooled regression are regarded as the most representative α. As such, any discrepancies relative to these α can be used to measure the level of errors embodied in α. Additionally, the width of the confidence limits of the α obtained by the pooled regression indicates the range in which different outcomes from different data sets might be obtained. The wider these limits the more the risk of obtaining higher discrepancies. In turn it also indicates higher risk of obtaining stronger errors.

The parameters listed under sub-heading Method 1 in Table 3-1 were obtained via pooled regression. An inspection on α values in this list, shows that the order of the magnitude of α was $\alpha_{ao}>\alpha_{ow}>\alpha_{aw}$ and the width of the confidence limits of those obtained by the pooled regression followed the same order. These patterns were consistently observed in both soils. The observed pattern suggest that the higher the magnitude of α the lower its precision. A study by *van Genuchten and Nielsen* (1985) postulated that α is inversely proportional to displacement capillary pressure($\alpha \approx P_d^{-1}$). Utilizing this relationship, the observed pattern indicated that low P_d value possesses low accuracy. *Lenhard and Parker* (1987) observed similar problems. Their *P-S* measurement using benzyl alcohol as the oil phase covering the lowest range of capillary pressures among the measured two-phase systems, suffered the highest uncertainties.

In the investigated cases, the α_{aw} in method 2 was equivalent to P_d= 43.5 mbars for the Metea soil and 17.1 for the Ottawa sand. In method 3, α_{ao} was equivalent to 18.7 (Metea soil) and 7.5 mbars (Ottawa sand). In order to anticipate 200 mbar maximum capillary pressure measurement in the air-oil system of the Ottawa sand, a 5 psi (≈345 mbar) rated pressure transducer membrane was used. While it gave a good resolution for low pressure measurement, it lacked accuracy due to a zero shift problem. On the average, the calibration in the air-oil measurement setting indicated a ±0.7 mbar standard error of estimate. When this standard error of estimate is expressed as 95% confidence limits it is equivalent to approximately 20% of the P_d of the air-oil system in the case of Ottawa sand. For the air-water system, on the other hand, it equivalent to only 3.5% of P_d. Based on this inspection, it is concluded that α_{ao} was less reliable compared to α_{aw}.

Method 3 used α_{ao} while method 2 used α_{aw}. When identical S_r and n were employed in the two methods and since α_{ao} was less reliable than α_{aw}, the chance of obtaining bias in the prediction outcome is higher in method 3 than in method 2. As observed in Table 3-2, method 2 performed reasonably well not only when a well-graded soil such as Metea soil was used but also when the poorly graded Ottawa sand was used. Method 3 appears to be acceptable only when Metea soil was used.

The source of discrepancies between methods 1 and 2 or methods 1 and 3 was due to the discrepancies in the P-S parameters used. When method 3 was applied using Ottawa sand, the base parameters used suffered the combination of two problems; less precision in the parameters S_r and n due to the texture of the soil and low accuracy in α_{ao} due to difficulty in measuring low capillary pressure. As a result, the parameters determined solely from the air-oil data measured in a uniform grain soil might not be representative enough to be used as the scaling reference compared to those derived from the air-water data.

As presented in the previous section the two- and three-phase oil saturation S_o and relative permeability k_{ro} are functions of the two-phase oil saturation in an air-oil system (S_{ao}) and water saturation in an oil-water system (S_{ow}). In method 2 both S_{ao} and S_{ow} are prediction curves while in method 3 only S_{ow} is a prediction curve. Thus, in obtaining S_o and k_{ro}, method 2 would propagate any error embodied in the base parameters more than would method 3. Based on this, prediction via method 3 should not be inferior when compared to the prediction via method 2. The scoring outcome on Table 3-2, however, shows that method 2 was better than method 3. As concluded previously, method 3 has a problem in determining the parameter α_{ao}. Apparently, the difficulty of measuring low capillary pressure has a stronger effect upon the outcome than when this additional source of error is induced.

3.4.3. Effect of Propagated Error on the Constitutive Variables

Parker et al. (1987) postulated that prediction of the relative permeability function might be sensitive to any disturbance in the base *P-S* parameters. The arrangement of the rows in Table 3-2, as mentioned previously, roughly reflects the sequential steps in constructing the two- and three-phase constitutive relationship curves. In turn, it also reflects the way the errors in the base parameters and scaling factors were propagated. The constitutive variables in the lower rows were functions of the variables in the upper rows. Therefore, the lower row variables possessed the uncertainty of the variables in the upper rows. Thus, the lower row variables possessed greater uncertainties as the error that embodied in the base parameters and the scaling factors were propagated further.

The columns under the Metea Soil heading in Table 3-2 show the above trend. The upper rows, up to variable k_{ro}^{ao}, were scored in the category good. Below this row, some scores of fair were observed. This pattern indicates that the errors propagated up to variable k_{ro}^{ao} produced only insignificant bias. Further propagation slightly increased the bias. The bias resulting from this increment at the end point (the three-phase oil relative permeability), however, is still within tolerable limits. This was possible as the error embodied in the original bias was relatively small. Therefore, it follows that the magnitude of error of the base parameters as tabulated in the pertaining columns in Table 3-3 can be regarded as small.

It is interesting to observe that 27% error in the S_r, as shown in the column Ottawa Sand - Method 2 in Table 3-3, yields insignificant bias in all of the prediction curves. This is only possible, however, if the accuracy of the other parameter was high. Nevertheless, this particular case suggests the insensitivity of the employed prediction methods employed to the parameter S_r. It is speculated that the bias in the prediction curve associated with error in this parameter is localized in the vicinity of the low saturation region. On the other hand, even with parameter estimation based on measured data the uncertainty in this region is high due to the non-linearity of the constitutive relation function.

The errors of the base parameters in the case of Ottawa sand - Method 3 (Table 3-2) were high. The predictions employing these parameters, as shown in Table 3-2, were unfavorable. Despite the significant discrepancy observed in the prediction curves the errors of the base parameters in this particular case was not clearly evident in the *P-S* curves plot. Figure 3-11 was plotted to demonstrate this issue. This figure plots the measured data and the fitted *P-S* curves on these data via the pooled regression (dashed line) superimposed by the curves obtained via the individual regressions (solid line). The parameters used by the pooled regression curves were the parameters employed in method 1. Those used by the individual regression curves were the base parameters used in methods 2 or 3. Thus, the parameter discrepancies listed in Table 3-3 were the discrepancies of the parameters used by the dashed and shaded areas.

In Figure 3-11 the discrepancy between the solid and dashed curves in the case of the air-oil system in Ottawa sand appears to be comparable, for example, to the case of the air-water system in Metea soil. As a *P-S* plot, error as high as 20%, 26% and 31% in parameters S_r, n and α appears similar to errors of 5%, 4% and 9% (Table 3-3). If these errors were included in the scaling procedure, however, a significant difference in outcomes would be clearly observed. In the same example, the air-oil and air-water systems were scaled to predict the oil-water *P-S* curve. The resulting curves were the plots in Figure 3-2a and Figure 3-1c, respectively. It is observed that the plot in Figure 3-2a was significantly worse than that in Figure 3-1c. Note that, the errors of the scaling factors involved in constructing Figure 3-2a was only 0.02% while in Figure 3-1c it was 9.5%. Therefore, it is believed that the errors observed in Figure 3-2a and Figure 3-1c were strongly affected by the errors in their base parameters rather than to the errors in their scaling factors.

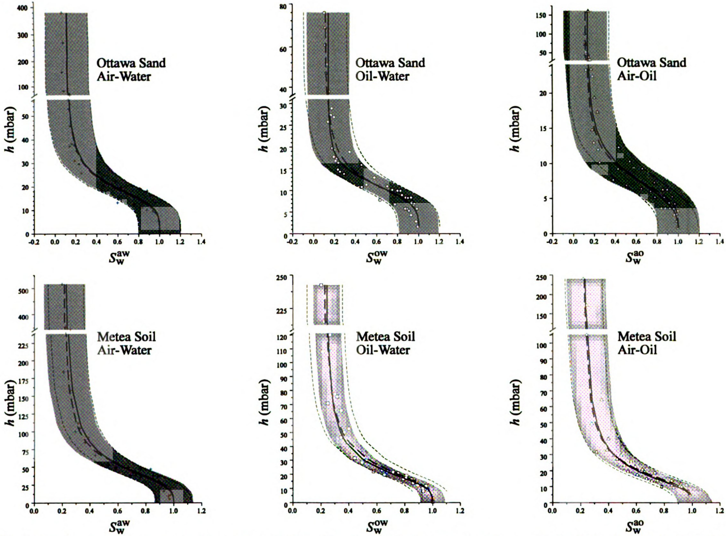

Figure 3-11: Two-phase pressure-saturation curves obtained by the pooled regression (heavy dashed lines) with their 95% confidence limits (light dashed lines) and those obtained by the individual regression (solid lines) with their 95% confidence limits (shaded area)

ps2-reg.cdr

In the actual implementation of the scaling theory, only one system is required to be measured. When data is available from only one system, the goodness of the obtained base parameters can only be verified through an inspection of the agreement upon the best estimated *P-S* curve against the data points. As demonstrated above, this technique might not be sufficient to reveal even errors as high as 20%, 26% and 31% in parameters S_r, n and α. Based on this, in order to increase the possibility of obtaining more representative parameters, it is necessary to replicate the sample.

3.5. SUMMARY AND CONCLUSION

Parker et al. (1987) proposed a predictive method employing scaling theory. Using their theory, a complete set of two- and three-phase k_r-*S*-*P* relationships can be constructed based only on one set of *P-S* parameters, referred to as the base parameters, measured in one two-phase system plus the pertaining interfacial tension data. Two alternatives to implement this theory were investigated, referred to as method 2 and 3 respectively. Method 2 uses the air-water system to determined the base parameters while Method 3 uses the air-oil system.

Method 2 was regarded as the most efficient alternative in the case where air-water *P-S* data are available. The base parameters S_r, n, α_{aw} were determined from the available data and the parameters α_{ow} and α_{ao} were predicted via interfacial tension measurements. Method 3 was similar to method 2, but the S_r, n, α_{ao} were determined from air-oil *P*-*S* data while the α_{aw} and α_{ow} were predicted. This alternative might be suitable in cases where sufficient data are not available, yet more efficient procedures than those used in method 2 are desired.

These methods were tested to predict the two- and three phase k_r-*S*-*P* relationships using two contrasting soils: uniform grain Ottawa sand and loamy sand Metea. As the reference to justify the performance of methods 2 and 3, the obtained prediction curves were compared to those obtained via method 1 which is a predictive method without employing the scaling theory.

When the Metea soil was used as the porous medium, the prediction of the k_r-*S*-*P* curves yielded a favorable outcome. For the cases where Ottawa sand was used the outcomes vary. At the extreme case, an unfavorable result such as those observed in the case of Ottawa sand with method 3 might be obtained. Inspection of the statistical properties of the base parameters, suggests that determination of these parameters in a poorly graded soil, such as Ottawa sand, might result in a high variation. In turn, the risk of obtaining less representative parameters is also high.

The investigated cases suggest that the parameters S_r and n were independent of the two-phase system used. The deference between the outcomes obtained via methods 2 and 3 was associated with the errors in their values of the parameter α. Determination of α in the air-water system was more reliable than in the air-oil system. This was due to the difficulty of measuring low capillary pressure. As a result, prediction by method 2 which is based on air-water data appears to be superior over method 3.

When method 3 was applied using Ottawa sand, the base parameters used suffered the combination of two problems; less precision in parameters S_r and n due to the texture of the soil and low accuracy in α_{ao} due to the difficulty in measuring low capillary pressure. As a result, the parameters determined solely from the air-oil data measured in a uniform grain soil might not be representative enough to be used as the scaling reference compared to those derived from the air-water data.

A less representative parameters set may not deteriorate in agreement between the data points and the regressed *P-S* curve, however, it may cause a problem if used as the basis of prediction. Hence, the use of method 3 should be limited to a well-graded soil. For a uniform grain type soil, it is more rigorous to employ method 2 which gives better assurances in providing representative parameters. Furthermore, the issue of difficulty in measuring low capillary pressure inherent in method 3 has a more significant effect than the error propagated by the additional step required in method 2.

BIBLIOGRAPHY

Anderson, W.G. 1987. Wettability literature survey Part 4: Effects of wettability on capilary pressure. *J. of Petrol. Technol., 39, 10*:1283-1300.

Azis, K., and A. Settari. 1979 Petroleum Reservoir simulation. *Applied Science Publisher*. London

Bear, J. 1982. 1972. Dynamics of Porous Media. American Elsevier Publishing Co. Inc.

Beck, J.V., and K.J. Arnold. 1976. *Parameter Estimation in Engineering and Science*. 501 pp. John Wiley and Son Inc. New York.

Bethel, F.T., and J.C. Calhoun. 1953. Capilary desaturation in unconsolidated beads. *Petroleum Transaction., 198*:197-202

Brakensiek, D.L., R.L. Engleman, W.J. Rawls. 1981. Variation within texture classes of soil water parameters, *Trans, ASAE*, 24,2:335-339.

Brooks, R.H., and A.T. Corey. 1964. Hydraulic properties of porous media. *Hydrology papers no. 3.*, Colorado State University., Forth Collins., Colorado.

Burdine, N.T. 1953. Relative permeability calculations from pore size distribution data. *Petroleum Transaction, AIME., 198*:71-78

Corey, A.T. 1986. *Mechanics of immiscible fluids in porous media.* Water Resource Publ.Chelsea. Michigan.

Corey, A.T., and R.H. Brooks. 1975. Drainage characteristics of soils. *Soil Sci. Soc. Amer. Proc., 39*:251-255

Corey, A.T., C.H. Rathjens, and J.H. Anderson. 1956. Technical note: Three-phase relative permeability. *Petroleum Transaction, AIME., 207*:349-351

Cosby, B.J., G.M. Hornberger, R.B. Clapp, and T.R. Ginn. 1984. A statistical exploration of the relationships of soil moisture characteritics to the physical properties of soils. *Water Resour. Res., 20, 6*:682-690.

Demond, A.H., and P.V. Roberts. 1991. Effect of interfacial forces on two-phases capillary pressure-saturation relationships. *Water Resour. Res., 27, 3*:423-437

Dumore, J.M., and R.S. Schols. 1974. Drainage capillary presure functions and the influence of connate water. *Soc. of Petrol. Eng. J., 14, 5*:437-444

Elrick, D.E. J.H. Scandrett, and E.E. Miller. 1959. Test of capillary flow scaling. *Soil Sci. Soc. Amer. Proc., 23*:329-332

Gee, G.W., C.T. Kincaid, R.J. Lenhard, and C.S. Simmons.1992 Recent studies of flow and transport in the vadose zone.

Kaluarachchi, J.J., and J.C. Parker. 1989. An efficient finite element method for modeling multiphase flow. *Water Resour. Res., 25, 1*:43-54

Kia, S.F., and A. Abdul. 1990. Retention of diesel fuel in aquifer material. *J. Hydraul. Eng., 116, 7*:881-894

Klute, A. 1986. Water retention laboratory methods; Methods of soil analysis, Part I: Physical and mineralogical methods., *Amer. Soc. of Agron., Madison., 26*:635-661

Klute, A, and J.E. Wilkinson. 1958. Some tests of the similar media concept of capillary flow: I. Reduced capillary conductivity and moisture characteristic data. *Soil Sci. Soc. Amer. Proc., 22*:278-281

Kool, J.B., J.C. Parker, and M.T. van Genuchten. 1985. Determining soil hydraulic properties from one-step outflow experiments by parameter estimation: I. Theory and numerical studies. *Soil Sci. Soc. Am. J., 49*:1348-1354.

Lenhard, R.J., and J.C. Parker. 1987. Measurement and prediction of saturation-pressure relationships in three-phase porous media systems. *J. Contam. Hydrol., 1*:407-424.

Lenhard, R.J., J.C. Parker, and J.J. Kaluarachchi. 1989. A model for hysteretic constitutive relations governing multiphase flow. 3. Refinements and numerical simulations. *Water Resour. Res. J., 25, 7*:1727-1736.

Lenhard, R.J., J.C. Parker. 1988. Experimental validation of the theory of extending two-phase saturation-pressure relations to three-phase fluid phase systems for monotonic drainage paths. *Water Resour. Res. J., 24, 3*:373-380.

Lenhard, R.J., J.C. Parker. 1988a. Experimental validation of the theory of extending two-phase saturation-pressure relations to three-phase fluid phase systems for monotonic drainage paths. *Water Resour. Res. J., 24, 3*:373-380.

Lenhard, R.J., J.H. Dane, J.C. Parker, and J.J. Kaluarachchi. 1988b. Measurement and simulation of one dimensional transient three-phase flow for monotonic liquid drainage. *Water Resour. Res. J., 24*, 6:853-863.

Leverrett, M.C. 1942. Capillary behavior in porous solids. *Trans. Amer. Ins. of Mining Eng., 142*:152-169

Luckner, L., M.Th. van Genuchten, and D.R. Nielssen. 1989. A consisten set of parametric models for the two-phase flow of immicible fluids in the suburface. *Water Resour. Res. J., 25*, 10:2187-2193.

McCueen R.H., W.J. Rawls, and T.L. Brakensiek. 1981. Statistical analysis of the Brooks-Corey and the Green-Ampt parameters across soil textures. *Water Resour. Res. J., 17*, 4:1005-1013.

Mercer, J.W., and R.M. Cohen.1990. A riview of immiscible fluids in the subsurface: properties, models, characteristization and remediation. *J. of Contam. Hydrol., 6*:107-163

Miller, E.E., and R.D. Miller. 1956. Physical theory for capillary flow phenomena. *J. of Applied Physics., 27*, 4:324-332

Mishra, S., and J.C. Parker. 1989. Parameter estimation for coupled unsaturated flow and transport. *Water Resour. Res., 25*, 3: 385-396

Morrow , N. R. 1976. Capillary pressure correlation for uniformly wetted porous media. *J. Can. Pet. Technol., 15, 4*:49-69

Mualem, Y. 1976. A new model for predicting the hydraulic conductivity of unsaturated porous media. *Water Resour. Res. J., 12, 3*:513-521.

Parker, J.C. 1986. Hydrostatic of porous media. *Soil physical chemistry.*, Ed. D.L. Sparks., CBC Press.

Parker, J.C., and R.J. Lenhard. 1987. A model for hysteretic constitutive relations governing multiphase flow. I. Saturation-pressure relations. *Water Resour. Res. J., 23, 12*:2187-2196

Parker, J.C., J.B. Kool, and M.T. van Genuchten. 1985. Determining soil hydraulic properties from one-step outflow experiments by parameter estimation: II. Experimental studies. *Soil Sci. Soc. Am. J., 49*:1354-1359.

Parker, J.C., R.J. Lenhard, and T. Kuppusamy. 1987. A parametric model for constitutive properties governing multiphase flow in porous media. *Water Resour. Res. J., 23, 4*:618-624

Parker, J.C., R.J. Lenhard, and T. Kuppusamy. 1987a. A parametric model for constitutive properties governing multiphase flow in porous media. *Water Resour. Res. J., 23, 4*:618-624

Pinder, G.F. 1982. Groundwater Hydrology -- Research Needs for the Next Decade. *Fundamental Research Needs for Water and Waste Water Systems*, AEEP/NSF Conference, M.S. Switzenbaum, ed., Arlington, Virginia

Purcell, W.R. 1949. Capillary pressure - their measurement using mercury and the calculation of permeability therefrom. *Petroleum Trans, TP 2544, 186*:39-48

Rawls, W.J., D.L. Brakensiek, and K.E. Saxton. 1981 Soil water characteristics. Paper no. 81-2510, *ASCE.*, St. Joseph, MI.

Rapoport, L.A. 1955. Scaling laws for use in design and operation of water-oil flow models. *Petroleum Trans, AIME 204*:143-150

Russo, D. 1988. Determining soil hydraulic properties by parameter estimation : On the selection of a model for the hydraulic properties. *Water Resour. Res. J., 24*, 3:453-459.

Schwille, F. 1967. Petroleum Contamination of the Subsoil - A Hydrological Problem. *Joint Problem of Oil and Water Industries.*, P. Hepple, ed., Elsevier Publ. Co., New York.

Seber, G.A.F, and C.J. Wild. 1988. *Nonlinear Regression.* 768 pp. John Weley & Sons Inc. New York.

Smiles, D.E., G. Vachaud, M. Vauclin. 1971. A test of the uniqueness of the soil moisture characteristic during transient, nonhysteretic flow of water in a rigid soil. *Soil Sci. Soc. Amer. Proc., 35*:534-539

Smith, W.O. 1933. Minimum capillary rise in an ideal uniform soil. *Physics*, *4*:184-193

Smith, W.O. 1933. The final distribution of retained liquid in an ideal uniform soil. *Physics*, *4*:425-438

Stone, H.L. 1973. Probability model for estimating three-phase relative permeability. *J. Petrol. Technol.*, *20*:214-218

Su, C., and R.H. Brooks. 1980. Water retention measurement for soils. *J. Irrig. Drain. Div.*, 105-112.

Topp, G.C., A. Klute, and D. B. Peters. 1967. Comparison of water content-pressure head data obtained by equilibrium, steady-state, and unsteady-state methods. *Soil Sci. Soc. Amer. Proc.*, *31*:312-314.

van Genuchten, M.T. 1980. A closed-form equation for predicting the hydraulic conductivity of unsaturated soils. *Soil Sci. Soc. Am. J.*, *44*:892-898.

van Genuchten, M.T., and D.R. Nielsen. 1985. On describing and predicting the hydraulic properties of unsaturated soils. *Annales Geophysicae.*, *3*, *5*:615-628

Warrick, A.W., J.J. Mullen, and D.R. Nielsen. 1977. Scaling field-measured soil hydraulic properties uing a similar media concept. *Water Resour. Res. J.*, *13*, 2:355-362

White, N.F., D.K. Sunada, H.R. Duke, and A.T. Corey. 1970b. Boundary effects in desaturation of porous media. *Soil Science.*, *113*:7-12.

White, N.F., H.R. Duke, D.K. Sunada, and A.T. Corey. 1970a. Physics of desaturation in porous materials. *J. Irrig. Drain. Div.*, 165-190.

Wilkinson, J.E., and A. Klute. 1959. Some tests of the similar media concept of ccapillary flow: II. Flow system data. *Soil Science.*, *23*:434-437

APPENDICES

A. PRESSURE-SATURATION MEASUREMENT SIMULATION

A.1. Model Conceptualization.
A.2. Simulation Flowchart
A.3. Program Listing in Excel Worksheet.

A.1. MODEL CONCEPTUALIZATION

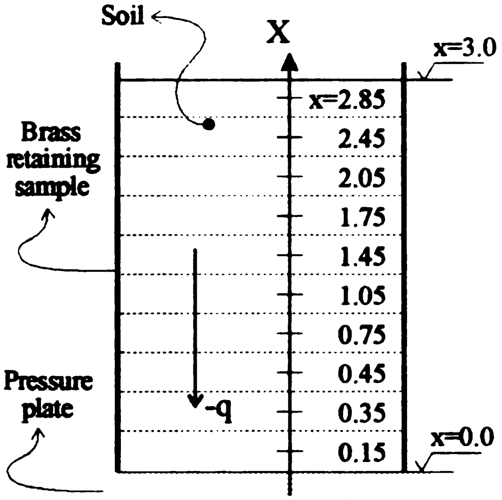

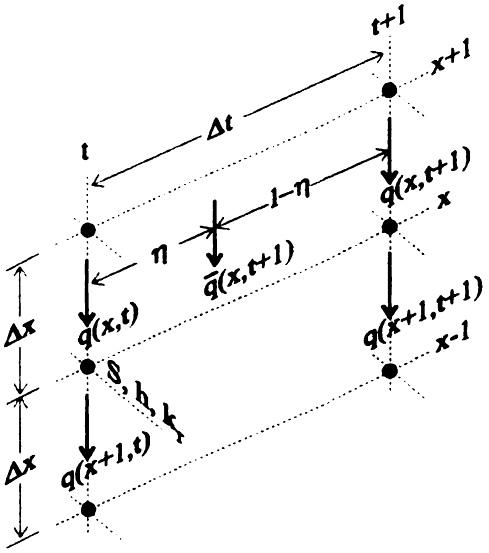

Governing equation:

$$\varphi \frac{\partial S}{\partial t} = \frac{\partial}{\partial x}\left\{k_s \cdot k_r\left(\frac{\partial h}{\partial x} - 1\right)\right\}$$

Constitutive equation:

$$S_e = \frac{S - S_r}{1 - S_r} = \left\{1 + (\alpha h)^n\right\}^{1/n - 1}$$

$$k_r = S_e^{1/2}\left\{1 - \left(1 - S_e^{(n-1)/n}\right)^{n/(n-1)}\right\}^2$$

Boundary condition:

a) SE method $t \geq 0 \rightarrow q_{x=3} = 0$

$t \geq 0 \rightarrow h_{x=0} = h_{\text{prescribed}}$

b) PE method $t \geq 0 \rightarrow q_{x=3} = 0$

$0 < t < t_{\text{desat.}} \rightarrow h_{x=0} = h_{\text{prescribed}}$

$t > t_{\text{desat.}} \rightarrow q_{x=0} = 0$

Initial condition: Hydrostatic profile with $h_{x=0} = h_{\text{prescribed}}$

A.2. SIMULATION FLOWCHART

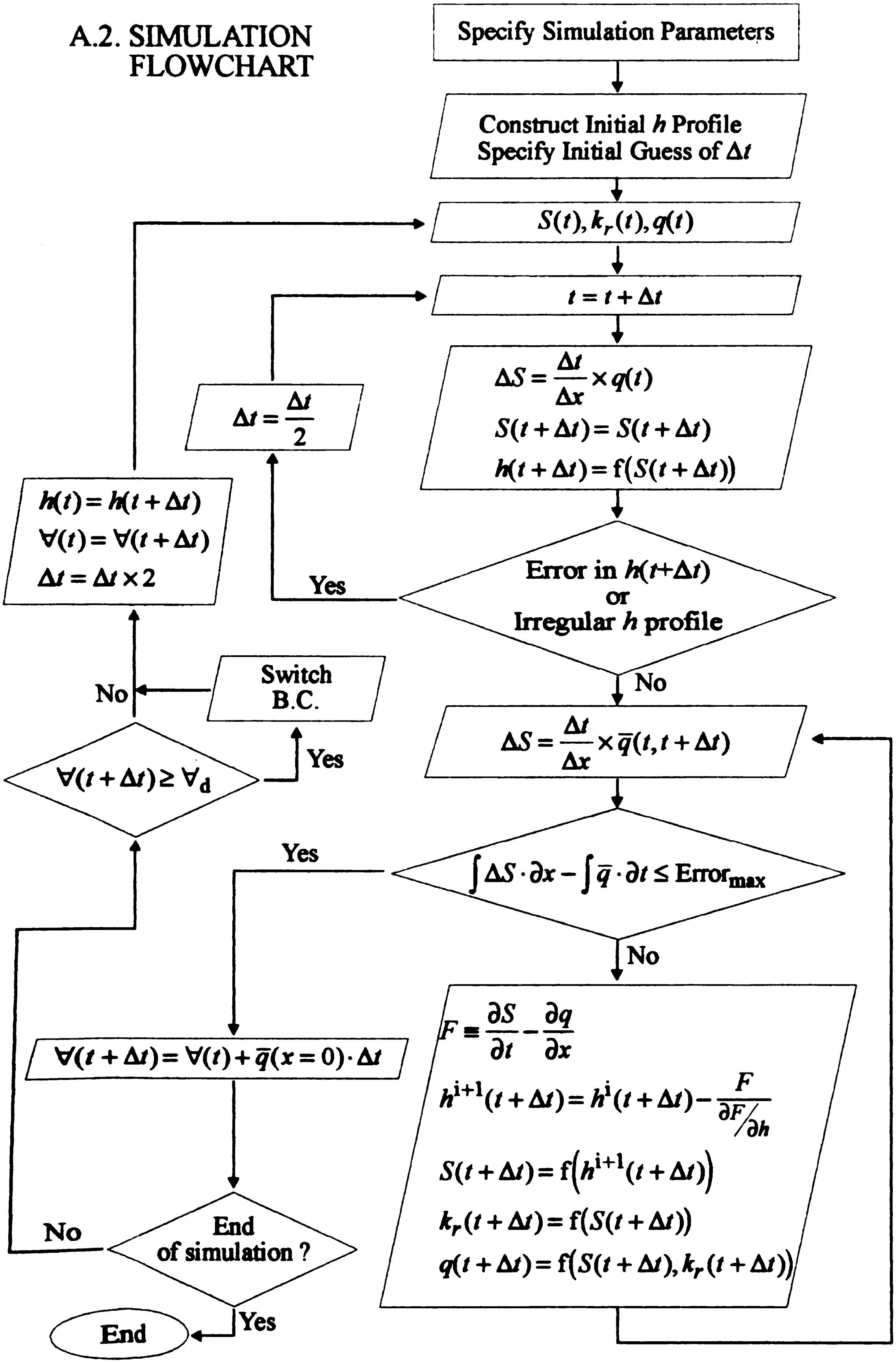

A.3. PROGRAM LISTING IN EXCEL WORKSHEET

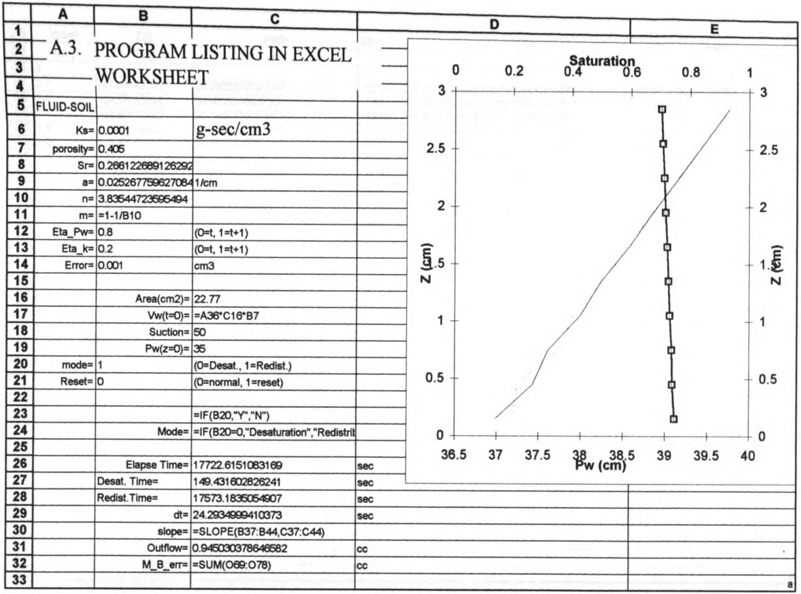

	A	B	C	D	E
1					
2					
3					
4					
5	FLUID-SOIL				
6	Ks=	0.0001	g-sec/cm3		
7	porosity=	0.405			
8	Sr=	0.266122689126292			
9	a=	0.0252677596270841	1/cm		
10	n=	3.83544723595494			
11	m=	=1-1/B10			
12	Eta_Pw=	0.8	(0=t, 1=t+1)		
13	Eta_k=	0.2	(0=t, 1=t+1)		
14	Error=	0.001	cm3		
15					
16		Area(cm2)=	22.77		
17		Vw(t=0)=	=A36*C16*B7		
18		Suction=	50		
19		Pw(z=0)=	35		
20	mode=	1	(0=Desat., 1=Redist.)		
21	Reset=	0	(0=normal, 1=reset)		
22					
23			=IF(B20,"Y","N")		
24		Mode=	=IF(B20=0,"Desaturation","Redistrib		
25					
26		Elapse Time=	17722.6151083169	sec	
27		Desat. Time=	149.431602826241	sec	
28		Redist.Time=	17573.1835054907	sec	
29		dt=	24.2934999410373	sec	
30		slope=	=SLOPE(B37:B44,C37:C44)		
31		Outflow=	0.945030378646582	cc	
32		M_B_err=	=SUM(O69:O78)	cc	
33					a

	A	B	C	D	E
34	X(cm)	Z(i)	Pw(t)	S(t)	Se(t)
35	(cm)	(cm)	(cm)		
36	3				
37	2.7	=(A36+A37)/2	39.7633233797947	=$B$8+(1-$B$8)*(1+($B$9*C37)^$B$10)^(-$B$11)	=(D37-$B$8)/(1-$B$8)
38	2.4	=(A37+A38)/2	39.4623978647256	=$B$8+(1-$B$8)*(1+($B$9*C38)^$B$10)^(-$B$11)	=(D38-$B$8)/(1-$B$8)
39	2.1	=(A38+A39)/2	39.1650735158902	=$B$8+(1-$B$8)*(1+($B$9*C39)^$B$10)^(-$B$11)	=(D39-$B$8)/(1-$B$8)
40	1.8	=(A39+A40)/2	38.8586312134561	=$B$8+(1-$B$8)*(1+($B$9*C40)^$B$10)^(-$B$11)	=(D40-$B$8)/(1-$B$8)
41	1.5	=(A40+A41)/2	38.5727396257418	=$B$8+(1-$B$8)*(1+($B$9*C41)^$B$10)^(-$B$11)	=(D41-$B$8)/(1-$B$8)
42	1.2	=(A41+A42)/2	38.2445694357327	=$B$8+(1-$B$8)*(1+($B$9*C42)^$B$10)^(-$B$11)	=(D42-$B$8)/(1-$B$8)
43	0.9	=(A42+A43)/2	37.995716674058	=$B$8+(1-$B$8)*(1+($B$9*C43)^$B$10)^(-$B$11)	=(D43-$B$8)/(1-$B$8)
44	0.6	=(A43+A44)/2	37.6129748107039	=$B$8+(1-$B$8)*(1+($B$9*C44)^$B$10)^(-$B$11)	=(D44-$B$8)/(1-$B$8)
45	0.3	=(A44+A45)/2	37.4311649969377	=$B$8+(1-$B$8)*(1+($B$9*C45)^$B$10)^(-$B$11)	=(D45-$B$8)/(1-$B$8)
46	0	=(A45+A46)/2	36.9884186532764	=$B$8+(1-$B$8)*(1+($B$9*C46)^$B$10)^(-$B$11)	=(D46-$B$8)/(1-$B$8)
47			=C18		
48					
49			Pw(t+1)		Se(t+1)
50			=(1-$B$12)*C37+$B$12*I37		=(1+($B$9*C50)^$B$10)^(-$B$11)
51			=(1-$B$12)*C38+$B$12*I38		=(1+($B$9*C51)^$B$10)^(-$B$11)
52			=(1-$B$12)*C39+$B$12*I39		=(1+($B$9*C52)^$B$10)^(-$B$11)
53			=(1-$B$12)*C40+$B$12*I40		=(1+($B$9*C53)^$B$10)^(-$B$11)
54			=(1-$B$12)*C41+$B$12*I41		=(1+($B$9*C54)^$B$10)^(-$B$11)
55			=(1-$B$12)*C42+$B$12*I42		=(1+($B$9*C55)^$B$10)^(-$B$11)
56			=(1-$B$12)*C43+$B$12*I43		=(1+($B$9*C56)^$B$10)^(-$B$11)
57			=(1-$B$12)*C44+$B$12*I44		=(1+($B$9*C57)^$B$10)^(-$B$11)
58			=(1-$B$12)*C45+$B$12*I45		=(1+($B$9*C58)^$B$10)^(-$B$11)
59			=(1-$B$12)*C46+$B$12*I46		=(1+($B$9*C59)^$B$10)^(-$B$11)
60					
61					
62					
63					
64					
65					
66					
67					b

	F	G
34	k(t)	
35		k_avg_z(t)
36	0	
37	=$B$6*(E37)^0.5*(1-(1-(E37)^($B$10/($B$10-1)))^(($B$10-1)/$B$10))^2	0
38	=$B$6*(E38)^0.5*(1-(1-(E38)^($B$10/($B$10-1)))^(($B$10-1)/$B$10))^2	=2*F37*F38/(F37+F38)
39	=$B$6*(E39)^0.5*(1-(1-(E39)^($B$10/($B$10-1)))^(($B$10-1)/$B$10))^2	=2*F38*F39/(F38+F39)
40	=$B$6*(E40)^0.5*(1-(1-(E40)^($B$10/($B$10-1)))^(($B$10-1)/$B$10))^2	=2*F39*F40/(F39+F40)
41	=$B$6*(E41)^0.5*(1-(1-(E41)^($B$10/($B$10-1)))^(($B$10-1)/$B$10))^2	=2*F40*F41/(F40+F41)
42	=$B$6*(E42)^0.5*(1-(1-(E42)^($B$10/($B$10-1)))^(($B$10-1)/$B$10))^2	=2*F41*F42/(F41+F42)
43	=$B$6*(E43)^0.5*(1-(1-(E43)^($B$10/($B$10-1)))^(($B$10-1)/$B$10))^2	=2*F42*F43/(F42+F43)
44	=$B$6*(E44)^0.5*(1-(1-(E44)^($B$10/($B$10-1)))^(($B$10-1)/$B$10))^2	=2*F43*F44/(F43+F44)
45	=$B$6*(E45)^0.5*(1-(1-(E45)^($B$10/($B$10-1)))^(($B$10-1)/$B$10))^2	=2*F44*F45/(F44+F45)
46	=$B$6*(E46)^0.5*(1-(1-(E46)^($B$10/($B$10-1)))^(($B$10-1)/$B$10))^2	=2*F45*F46/(F45+F46)
47		=F46
48	k(t+1)	k_avg_z(t+1)
49	0	0
50	=$B$6*E50^0.5*(1-(1-E50^($B$10/($B$10-1)))^(($B$10-1)/$B$10))^2	=2*F50*F51/(F50+F51)
51	=$B$6*E51^0.5*(1-(1-E51^($B$10/($B$10-1)))^(($B$10-1)/$B$10))^2	=2*F51*F52/(F51+F52)
52	=$B$6*E52^0.5*(1-(1-E52^($B$10/($B$10-1)))^(($B$10-1)/$B$10))^2	=2*F52*F53/(F52+F53)
53	=$B$6*E53^0.5*(1-(1-E53^($B$10/($B$10-1)))^(($B$10-1)/$B$10))^2	=2*F53*F54/(F53+F54)
54	=$B$6*E54^0.5*(1-(1-E54^($B$10/($B$10-1)))^(($B$10-1)/$B$10))^2	=2*F54*F55/(F54+F55)
55	=$B$6*E55^0.5*(1-(1-E55^($B$10/($B$10-1)))^(($B$10-1)/$B$10))^2	=2*F55*F56/(F55+F56)
56	=$B$6*E56^0.5*(1-(1-E56^($B$10/($B$10-1)))^(($B$10-1)/$B$10))^2	=2*F56*F57/(F56+F57)
57	=$B$6*E57^0.5*(1-(1-E57^($B$10/($B$10-1)))^(($B$10-1)/$B$10))^2	=2*F57*F58/(F57+F58)
58	=$B$6*E58^0.5*(1-(1-E58^($B$10/($B$10-1)))^(($B$10-1)/$B$10))^2	=2*F58*F59/(F58+F59)
59	=$B$6*E59^0.5*(1-(1-E59^($B$10/($B$10-1)))^(($B$10-1)/$B$10))^2	=F59
60		
61		
62		
63		
64		
65		
66		
67		c

	H	I	J
34	Se(t+1)	Pw(t+1)	t
35		(cm)	
36			
37	=((D37-G4)-$B$8)/(1-$B$8)	=1/$B$9*(H37^(-1/$B$11)-1)^(1/$B$10)	=IF(F4=0,1000000000000000,ABS((B37-B38)/F4))
38	=((D38-G5)-$B$8)/(1-$B$8)	=1/$B$9*(H38^(-1/$B$11)-1)^(1/$B$10)	=IF(F5=0,1000000000000000,ABS((B38-B39)/F5))
39	=((D39-G6)-$B$8)/(1-$B$8)	=1/$B$9*(H39^(-1/$B$11)-1)^(1/$B$10)	=IF(F6=0,1000000000000000,ABS((B39-B40)/F6))
40	=((D40-G7)-$B$8)/(1-$B$8)	=1/$B$9*(H40^(-1/$B$11)-1)^(1/$B$10)	=IF(F7=0,1000000000000000,ABS((B40-B41)/F7))
41	=((D41-G8)-$B$8)/(1-$B$8)	=1/$B$9*(H41^(-1/$B$11)-1)^(1/$B$10)	=IF(F8=0,1000000000000000,ABS((B41-B42)/F8))
42	=((D42-G9)-$B$8)/(1-$B$8)	=1/$B$9*(H42^(-1/$B$11)-1)^(1/$B$10)	=IF(F9=0,1000000000000000,ABS((B42-B43)/F9))
43	=((D43-G10)-$B$8)/(1-$B$8)	=1/$B$9*(H43^(-1/$B$11)-1)^(1/$B$10)	=IF(F10=0,1000000000000000,ABS((B43-B44)/F10))
44	=((D44-G11)-$B$8)/(1-$B$8)	=1/$B$9*(H44^(-1/$B$11)-1)^(1/$B$10)	=IF(F11=0,1000000000000000,ABS((B44-B45)/F11))
45	=((D45-G12)-$B$8)/(1-$B$8)	=1/$B$9*(H45^(-1/$B$11)-1)^(1/$B$10)	=IF(F12=0,1000000000000000,ABS((B45-B46)/F12))
46	=((D46-G13)-$B$8)/(1-$B$8)	=1/$B$9*(H46^(-1/$B$11)-1)^(1/$B$10)	=IF(F13=0,1000000000000000,ABS((B46-B47)/F13))
47	=MAX(H37:H46)		=MIN(J37:J46)
48			
49			
50	=((D37-G17)-$B$8)/(1-$B$8)	=1/$B$9*(H50^(-1/$B$11)-1)^(1/$B$10)	=ABS((B37-B38)/(F3+F17)/2)
51	=((D38-G18)-$B$8)/(1-$B$8)	=1/$B$9*(H51^(-1/$B$11)-1)^(1/$B$10)	=ABS((B38-B39)/(F4+F18)/2)
52	=((D39-G19)-$B$8)/(1-$B$8)	=1/$B$9*(H52^(-1/$B$11)-1)^(1/$B$10)	=ABS((B39-B40)/(F5+F19)/2)
53	=((D40-G20)-$B$8)/(1-$B$8)	=1/$B$9*(H53^(-1/$B$11)-1)^(1/$B$10)	=ABS((B40-B41)/(F6+F20)/2)
54	=((D41-G21)-$B$8)/(1-$B$8)	=1/$B$9*(H54^(-1/$B$11)-1)^(1/$B$10)	=ABS((B41-B42)/(F7+F21)/2)
55	=((D42-G22)-$B$8)/(1-$B$8)	=1/$B$9*(H55^(-1/$B$11)-1)^(1/$B$10)	=ABS((B42-B43)/(F8+F22)/2)
56	=((D43-G23)-$B$8)/(1-$B$8)	=1/$B$9*(H56^(-1/$B$11)-1)^(1/$B$10)	=ABS((B43-B44)/(F9+F23)/2)
57	=((D44-G24)-$B$8)/(1-$B$8)	=1/$B$9*(H57^(-1/$B$11)-1)^(1/$B$10)	=ABS((B44-B45)/(F10+F24)/2)
58	=((D45-G25)-$B$8)/(1-$B$8)	=1/$B$9*(H58^(-1/$B$11)-1)^(1/$B$10)	=ABS((B45-B46)/(F11+F25)/2)
59	=((D46-G26)-$B$8)/(1-$B$8)	=1/$B$9*(H59^(-1/$B$11)-1)^(1/$B$10)	=ABS((B46-B47)/(F12+F26)/2)
60	=MAX(H50:H59)		=MIN(J50:J59)
61			
62			
63			
64			
65			
66			
67			d

	K	L	M	N
34	P Profile Slope Sign	Count on Slope Change		
35				
36				
37	=SIGN(I37-I38)	=IF(K37=K38,0,1)		
38	=SIGN(I38-I39)	=IF(K38=K39,0,1)		
39	=SIGN(I39-I40)	=IF(K39=K40,0,1)		
40	=SIGN(I40-I41)	=IF(K40=K41,0,1)		
41	=SIGN(I41-I42)	=IF(K41=K42,0,1)		
42	=SIGN(I42-I43)	=IF(K42=K43,0,1)		
43	=SIGN(I43-I44)	=IF(K43=K44,0,1)		
44	=SIGN(I44-I45)	=IF(K44=K45,0,1)		
45	=SIGN(I45-I46)	=IF(K45=K46,0,1)		
46	=SIGN(I46-I47)	=SUM(L37:L45)		
47				
48				
49				
50	=SIGN(I50-I51)	=IF(K50=K51,0,1)		
51	=SIGN(I51-I52)	=IF(K51=K52,0,1)		
52	=SIGN(I52-I53)	=IF(K52=K53,0,1)		
53	=SIGN(I53-I54)	=IF(K53=K54,0,1)		
54	=SIGN(I54-I55)	=IF(K54=K55,0,1)		
55	=SIGN(I55-I56)	=IF(K55=K56,0,1)		
56	=SIGN(I56-I57)	=IF(K56=K57,0,1)		
57	=SIGN(I57-I58)	=IF(K57=K58,0,1)		
58	=SIGN(I58-I59)	=IF(K58=K59,0,1)		
59	=SIGN(I59-#REF!)	=SUM(L50:L58)		
60				
61				
62				
63				
64				
65				
66				
67				e

	F	G
1	q(t)	dS(t)
2	(cm/sec)	
3	0	
4	=G37*((C37-C38)/(B37-B38)-1)	=1/$B$7*$C$29*(F3-F4)/(B37-B38)
5	=G38*((C38-C39)/(B38-B39)-1)	=1/$B$7*$C$29*(F4-F5)/(B38-B39)
6	=G39*((C39-C40)/(B39-B40)-1)	=1/$B$7*$C$29*(F5-F6)/(B39-B40)
7	=G40*((C40-C41)/(B40-B41)-1)	=1/$B$7*$C$29*(F6-F7)/(B40-B41)
8	=G41*((C41-C42)/(B41-B42)-1)	=1/$B$7*$C$29*(F7-F8)/(B41-B42)
9	=G42*((C42-C43)/(B42-B43)-1)	=1/$B$7*$C$29*(F8-F9)/(B42-B43)
10	=G43*((C43-C44)/(B43-B44)-1)	=1/$B$7*$C$29*(F9-F10)/(B43-B44)
11	=G44*((C44-C45)/(B44-B45)-1)	=1/$B$7*$C$29*(F10-F11)/(B44-B45)
12	=G45*((C45-C46)/(B45-B46)-1)	=1/$B$7*$C$29*(F11-F12)/(B45-B46)
13	=IF($B$20=0,G46*((C46-C47)/B46-1),0)	=1/$B$7*$C$29*(F12-F13)/(B46-B47)
14		
15	q(t+1)	dS(t+1)
16		
17	=((1-$B$13)*G37+$B$13*G50)*((C50-C51)/(B37-B38)-1)	=1/$B$7*$C$29*(F16-F17)/(B37-B38)
18	=((1-$B$13)*G38+$B$13*G51)*((C51-C52)/(B38-B39)-1)	=1/$B$7*$C$29*(F17-F18)/(B38-B39)
19	=((1-$B$13)*G39+$B$13*G52)*((C52-C53)/(B39-B40)-1)	=1/$B$7*$C$29*(F18-F19)/(B39-B40)
20	=((1-$B$13)*G40+$B$13*G53)*((C53-C54)/(B40-B41)-1)	=1/$B$7*$C$29*(F19-F20)/(B40-B41)
21	=((1-$B$13)*G41+$B$13*G54)*((C54-C55)/(B41-B42)-1)	=1/$B$7*$C$29*(F20-F21)/(B41-B42)
22	=((1-$B$13)*G42+$B$13*G55)*((C55-C56)/(B42-B43)-1)	=1/$B$7*$C$29*(F21-F22)/(B42-B43)
23	=((1-$B$13)*G43+$B$13*G56)*((C56-C57)/(B43-B44)-1)	=1/$B$7*$C$29*(F22-F23)/(B43-B44)
24	=((1-$B$13)*G44+$B$13*G57)*((C57-C58)/(B44-B45)-1)	=1/$B$7*$C$29*(F23-F24)/(B44-B45)
25	=((1-$B$13)*G45+$B$13*G58)*((C58-C59)/(B45-B46)-1)	=1/$B$7*$C$29*(F24-F25)/(B45-B46)
26	=IF($B$20=0,((1-$B$13)*G46+$B$13*G59)*((C59-C47)/B46-1),0)	=1/$B$7*$C$29*(F25-F26)/(B46-B47)
27		
28		
29		
30		
31		
32		
33		f0

	A	B	C	D	E
68					
69		ITERATION (Newton-Raphson: F=n dS/dt-dq/dx Pw new = Pw old - F/(dF/dP) ALL entry is determined at t+1	P	S(P)	Se(P)
70	F=f(Pw)		39.7628371518624	=$B$8+(1-$B$8)*(1+($B$9*C70)^$B$10)^(-$B$11)	=(D70-$B$8)/(1-$B$8)
71	dP=	0.1	39.4643357752804	=$B$8+(1-$B$8)*(1+($B$9*C71)^$B$10)^(-$B$11)	=(D71-$B$8)/(1-$B$8)
72			39.1600044584684	=$B$8+(1-$B$8)*(1+($B$9*C72)^$B$10)^(-$B$11)	=(D72-$B$8)/(1-$B$8)
73			38.8704392458761	=$B$8+(1-$B$8)*(1+($B$9*C73)^$B$10)^(-$B$11)	=(D73-$B$8)/(1-$B$8)
74			38.5476140457246	=$B$8+(1-$B$8)*(1+($B$9*C74)^$B$10)^(-$B$11)	=(D74-$B$8)/(1-$B$8)
75			38.2932857279685	=$B$8+(1-$B$8)*(1+($B$9*C75)^$B$10)^(-$B$11)	=(D75-$B$8)/(1-$B$8)
76			37.9106415626996	=$B$8+(1-$B$8)*(1+($B$9*C76)^$B$10)^(-$B$11)	=(D76-$B$8)/(1-$B$8)
77			37.744954080971	=$B$8+(1-$B$8)*(1+($B$9*C77)^$B$10)^(-$B$11)	=(D77-$B$8)/(1-$B$8)
78			37.2540270678381	=$B$8+(1-$B$8)*(1+($B$9*C78)^$B$10)^(-$B$11)	=(D78-$B$8)/(1-$B$8)
79			37.1853252004612	=$B$8+(1-$B$8)*(1+($B$9*C79)^$B$10)^(-$B$11)	=(D79-$B$8)/(1-$B$8)
80			=C47		
81					
82			P+dP10	(P+dp10)	SE(P+dp10)
83	F=f(P+dP10)	=$B$71	=$C$70+B83	=$B$8+(1-$B$8)*(1+($B$9*C83)^$B$10)^(-$B$11)	=(D83-$B$8)/(1-$B$8)
84			=$C$71+B84	=$B$8+(1-$B$8)*(1+($B$9*C84)^$B$10)^(-$B$11)	=(D84-$B$8)/(1-$B$8)
85			=$C$72+B85	=$B$8+(1-$B$8)*(1+($B$9*C85)^$B$10)^(-$B$11)	=(D85-$B$8)/(1-$B$8)
86			=$C$73+B86	=$B$8+(1-$B$8)*(1+($B$9*C86)^$B$10)^(-$B$11)	=(D86-$B$8)/(1-$B$8)
87			=$C$74+B87	=$B$8+(1-$B$8)*(1+($B$9*C87)^$B$10)^(-$B$11)	=(D87-$B$8)/(1-$B$8)
88			=$C$75+B88	=$B$8+(1-$B$8)*(1+($B$9*C88)^$B$10)^(-$B$11)	=(D88-$B$8)/(1-$B$8)
89			=$C$76+B89	=$B$8+(1-$B$8)*(1+($B$9*C89)^$B$10)^(-$B$11)	=(D89-$B$8)/(1-$B$8)
90			=$C$77+B90	=$B$8+(1-$B$8)*(1+($B$9*C90)^$B$10)^(-$B$11)	=(D90-$B$8)/(1-$B$8)
91			=$C$78+B91	=$B$8+(1-$B$8)*(1+($B$9*C91)^$B$10)^(-$B$11)	=(D91-$B$8)/(1-$B$8)
92			=$C$79+B92	=$B$8+(1-$B$8)*(1+($B$9*C92)^$B$10)^(-$B$11)	=(D92-$B$8)/(1-$B$8)
93			=C47		
94					
95					
96					
97					
98					
99					
100					
101					f1

	F	G
68	ITERATION (Newton-Raphson: F=n dS/dt-dq/dx Pw_new = Pw_old - F/(dF/dP) ALL entry is determined at t+1	
69	k(P)	k_avg_z(P)
70	0	0
71	=$B$6*((E70+E71)/2)^0.5*(1-(1-((E70+E71)/2)^($B$10/($B$10-1)))^(($B$10-1)/$B$10))^2	=2*F71*F72/(F71+F72)
72	=$B$6*((E71+E72)/2)^0.5*(1-(1-((E71+E72)/2)^($B$10/($B$10-1)))^(($B$10-1)/$B$10))^2	=2*F72*F73/(F72+F73)
73	=$B$6*((E72+E73)/2)^0.5*(1-(1-((E72+E73)/2)^($B$10/($B$10-1)))^(($B$10-1)/$B$10))^2	=2*F73*F74/(F73+F74)
74	=$B$6*((E73+E74)/2)^0.5*(1-(1-((E73+E74)/2)^($B$10/($B$10-1)))^(($B$10-1)/$B$10))^2	=2*F74*F75/(F74+F75)
75	=$B$6*((E74+E75)/2)^0.5*(1-(1-((E74+E75)/2)^($B$10/($B$10-1)))^(($B$10-1)/$B$10))^2	=2*F75*F76/(F75+F76)
76	=$B$6*((E75+E76)/2)^0.5*(1-(1-((E75+E76)/2)^($B$10/($B$10-1)))^(($B$10-1)/$B$10))^2	=2*F76*F77/(F76+F77)
77	=$B$6*((E76+E77)/2)^0.5*(1-(1-((E76+E77)/2)^($B$10/($B$10-1)))^(($B$10-1)/$B$10))^2	=2*F77*F78/(F77+F78)
78	=$B$6*((E77+E78)/2)^0.5*(1-(1-((E77+E78)/2)^($B$10/($B$10-1)))^(($B$10-1)/$B$10))^2	=2*F78*F79/(F78+F79)
79	=$B$6*((E78+E79)/2)^0.5*(1-(1-((E78+E79)/2)^($B$10/($B$10-1)))^(($B$10-1)/$B$10))^2	=2*F79*F80/(F79+F80)
80	=$B$6*E79^0.5*(1-(1-E79^($B$10/($B$10-1)))^(($B$10-1)/$B$10))^2	=F80
81		
82	k(P+dp10)	k_avg_z(P+dP10)
83	0	0
84	=$B$6*((E83+E84)/2)^0.5*(1-(1-((E83+E84)/2)^($B$10/($B$10-1)))^(($B$10-1)/$B$10))^2	=2*F84*F85/(F84+F85)
85	=$B$6*((E84+E85)/2)^0.5*(1-(1-((E84+E85)/2)^($B$10/($B$10-1)))^(($B$10-1)/$B$10))^2	=2*F85*F86/(F85+F86)
86	=$B$6*((E85+E86)/2)^0.5*(1-(1-((E85+E86)/2)^($B$10/($B$10-1)))^(($B$10-1)/$B$10))^2	=2*F86*F87/(F86+F87)
87	=$B$6*((E86+E87)/2)^0.5*(1-(1-((E86+E87)/2)^($B$10/($B$10-1)))^(($B$10-1)/$B$10))^2	=2*F87*F88/(F87+F88)
88	=$B$6*((E87+E88)/2)^0.5*(1-(1-((E87+E88)/2)^($B$10/($B$10-1)))^(($B$10-1)/$B$10))^2	=2*F88*F89/(F88+F89)
89	=$B$6*((E88+E89)/2)^0.5*(1-(1-((E88+E89)/2)^($B$10/($B$10-1)))^(($B$10-1)/$B$10))^2	=2*F89*F90/(F89+F90)
90	=$B$6*((E89+E90)/2)^0.5*(1-(1-((E89+E90)/2)^($B$10/($B$10-1)))^(($B$10-1)/$B$10))^2	=2*F90*F91/(F90+F91)
91	=$B$6*((E90+E91)/2)^0.5*(1-(1-((E90+E91)/2)^($B$10/($B$10-1)))^(($B$10-1)/$B$10))^2	=2*F91*F92/(F91+F92)
92	=$B$6*((E91+E92)/2)^0.5*(1-(1-((E91+E92)/2)^($B$10/($B$10-1)))^(($B$10-1)/$B$10))^2	=2*F92*F93/(F92+F93)
93	=$B$6*E92^0.5*(1-(1-E92^($B$10/($B$10-1)))^(($B$10-1)/$B$10))^2	=F93
94		
95		
96		
97		
98		
99		
100		
101		f2

	H	I	J
68			
69	ITERATION (Newton-Raphson: F=p.dS/dt-dq/dx, Pw_new = Pw_old - F/(dF/dP). ALL entry is determined at t+1		
70	k_avg_t(P)	Pw_avg_t(P)	q(P)
71			0
72	=(1-$B$13)*G37+$B$13*G71	=(1-$B$12)*C37+$B$12*C70	=H72*((I72-I73)/(A37-A38)-1)
73	=(1-$B$13)*G38+$B$13*G72	=(1-$B$12)*C38+$B$12*C71	=H73*((I73-I74)/(A38-A39)-1)
74	=(1-$B$13)*G39+$B$13*G73	=(1-$B$12)*C39+$B$12*C72	=H74*((I74-I75)/(A39-A40)-1)
75	=(1-$B$13)*G40+$B$13*G74	=(1-$B$12)*C40+$B$12*C73	=H75*((I75-I76)/(A40-A41)-1)
76	=(1-$B$13)*G41+$B$13*G75	=(1-$B$12)*C41+$B$12*C74	=H76*((I76-I77)/(A41-A42)-1)
77	=(1-$B$13)*G42+$B$13*G76	=(1-$B$12)*C42+$B$12*C75	=H77*((I77-I78)/(A42-A43)-1)
78	=(1-$B$13)*G43+$B$13*G77	=(1-$B$12)*C43+$B$12*C76	=H78*((I78-I79)/(A43-A44)-1)
79	=(1-$B$13)*G44+$B$13*G78	=(1-$B$12)*C44+$B$12*C77	=H79*((I79-I80)/(A44-A45)-1)
80	=(1-$B$13)*G45+$B$13*G79	=(1-$B$12)*C45+$B$12*C78	=H80*((I80-I81)/(A45-A46)-1)
81	=(1-$B$13)*G46+$B$13*G80	=(1-$B$12)*C46+$B$12*C79	=IF($B$20=0,H81*((I81-C80)/B46-1),0)
82			
83	k_avg_t(P+dP10)	Pw_avg_t(P+dp10)	q(P+dP10)
84			0
85	=(1-$B$13)*$G$37+$B$13*G84	=(1-$B$12)*$C$37+$B$12*C83	=H85*((I85-I86)/($A$37-$A$38)-1)
86	=(1-$B$13)*$G$38+$B$13*G85	=(1-$B$12)*$C$38+$B$12*C84	=H86*((I86-I87)/($A$38-$A$39)-1)
87	=(1-$B$13)*$G$39+$B$13*G86	=(1-$B$12)*$C$39+$B$12*C85	=H87*((I87-I88)/($A$39-$A$40)-1)
88	=(1-$B$13)*$G$40+$B$13*G87	=(1-$B$12)*$C$40+$B$12*C86	=H88*((I88-I89)/($A$40-$A$41)-1)
89	=(1-$B$13)*$G$41+$B$13*G88	=(1-$B$12)*$C$41+$B$12*C87	=H89*((I89-I90)/($A$41-$A$42)-1)
90	=(1-$B$13)*$G$42+$B$13*G89	=(1-$B$12)*$C$42+$B$12*C88	=H90*((I90-I91)/($A$42-$A$43)-1)
91	=(1-$B$13)*$G$43+$B$13*G90	=(1-$B$12)*$C$43+$B$12*C89	=H91*((I91-I92)/($A$43-$A$44)-1)
92	=(1-$B$13)*$G$44+$B$13*G91	=(1-$B$12)*$C$44+$B$12*C90	=H92*((I92-I93)/($A$44-$A$45)-1)
93	=(1-$B$13)*$G$45+$B$13*G92	=(1-$B$12)*$C$45+$B$12*C91	=H93*((I93-I94)/($A$45-$A$46)-1)
94	=(1-$B$13)*$G$46+$B$13*G93	=(1-$B$12)*$C$46+$B$12*C92	=IF($B$20=0,H94*((I94-C93)/$B$46-1),0)
95			
96			
97			
98			
99			
100			
101			f3

	A	B	C	D	E
102			P+dP9		
103	F=f(P+dP9)			(P+dp9)	SE(P+dp9)
103			=$C$70+B103	=$B$8+(1-$B$8)*(1+($B$9*C103)^$B$10)^(-$B$11)	=(D103-$B$8)/(1-$B$8)
104		=B71	=$C$71+B104	=$B$8+(1-$B$8)*(1+($B$9*C104)^$B$10)^(-$B$11)	=(D104-$B$8)/(1-$B$8)
105			=$C$72+B105	=$B$8+(1-$B$8)*(1+($B$9*C105)^$B$10)^(-$B$11)	=(D105-$B$8)/(1-$B$8)
106			=$C$73+B106	=$B$8+(1-$B$8)*(1+($B$9*C106)^$B$10)^(-$B$11)	=(D106-$B$8)/(1-$B$8)
107			=$C$74+B107	=$B$8+(1-$B$8)*(1+($B$9*C107)^$B$10)^(-$B$11)	=(D107-$B$8)/(1-$B$8)
108			=$C$75+B108	=$B$8+(1-$B$8)*(1+($B$9*C108)^$B$10)^(-$B$11)	=(D108-$B$8)/(1-$B$8)
109			=$C$76+B109	=$B$8+(1-$B$8)*(1+($B$9*C109)^$B$10)^(-$B$11)	=(D109-$B$8)/(1-$B$8)
110			=$C$77+B110	=$B$8+(1-$B$8)*(1+($B$9*C110)^$B$10)^(-$B$11)	=(D110-$B$8)/(1-$B$8)
111			=$C$78+B111	=$B$8+(1-$B$8)*(1+($B$9*C111)^$B$10)^(-$B$11)	=(D111-$B$8)/(1-$B$8)
112			=$C$79+B112	=$B$8+(1-$B$8)*(1+($B$9*C112)^$B$10)^(-$B$11)	=(D112-$B$8)/(1-$B$8)
113			=C80		
114					
115					
116			P+dP8	(P+dp8)	SE(P+dp8)
117	F=f(P+dP8)		=$C$70+B117	=$B$8+(1-$B$8)*(1+($B$9*C117)^$B$10)^(-$B$11)	=(D117-$B$8)/(1-$B$8)
118			=$C$71+B118	=$B$8+(1-$B$8)*(1+($B$9*C118)^$B$10)^(-$B$11)	=(D118-$B$8)/(1-$B$8)
119		=B71	=$C$72+B119	=$B$8+(1-$B$8)*(1+($B$9*C119)^$B$10)^(-$B$11)	=(D119-$B$8)/(1-$B$8)
120			=$C$73+B120	=$B$8+(1-$B$8)*(1+($B$9*C120)^$B$10)^(-$B$11)	=(D120-$B$8)/(1-$B$8)
121			=$C$74+B121	=$B$8+(1-$B$8)*(1+($B$9*C121)^$B$10)^(-$B$11)	=(D121-$B$8)/(1-$B$8)
122			=$C$75+B122	=$B$8+(1-$B$8)*(1+($B$9*C122)^$B$10)^(-$B$11)	=(D122-$B$8)/(1-$B$8)
123			=$C$76+B123	=$B$8+(1-$B$8)*(1+($B$9*C123)^$B$10)^(-$B$11)	=(D123-$B$8)/(1-$B$8)
124			=$C$77+B124	=$B$8+(1-$B$8)*(1+($B$9*C124)^$B$10)^(-$B$11)	=(D124-$B$8)/(1-$B$8)
125			=$C$78+B125	=$B$8+(1-$B$8)*(1+($B$9*C125)^$B$10)^(-$B$11)	=(D125-$B$8)/(1-$B$8)
126			=$C$79+B126	=$B$8+(1-$B$8)*(1+($B$9*C126)^$B$10)^(-$B$11)	=(D126-$B$8)/(1-$B$8)
127			=C93		
128					
129					
130					
131					
132					
133					
134					
135					

g

	F	G
102	k(P+dp9)	k_avg_z(P+dP9)
103	0	0
104	=$B$6*((E103+E104)/2)^0.5*(1-(1-((E103+E104)/2)^($B$10/($B$10-1)))^(($B$10-1)/$B$10))^2	=2*F104*F105/(F104+F105)
105	=$B$6*((E104+E105)/2)^0.5*(1-(1-((E104+E105)/2)^($B$10/($B$10-1)))^(($B$10-1)/$B$10))^2	=2*F105*F106/(F105+F106)
106	=$B$6*((E105+E106)/2)^0.5*(1-(1-((E105+E106)/2)^($B$10/($B$10-1)))^(($B$10-1)/$B$10))^2	=2*F106*F107/(F106+F107)
107	=$B$6*((E106+E107)/2)^0.5*(1-(1-((E106+E107)/2)^($B$10/($B$10-1)))^(($B$10-1)/$B$10))^2	=2*F107*F108/(F107+F108)
108	=$B$6*((E107+E108)/2)^0.5*(1-(1-((E107+E108)/2)^($B$10/($B$10-1)))^(($B$10-1)/$B$10))^2	=2*F108*F109/(F108+F109)
109	=$B$6*((E108+E109)/2)^0.5*(1-(1-((E108+E109)/2)^($B$10/($B$10-1)))^(($B$10-1)/$B$10))^2	=2*F109*F110/(F109+F110)
110	=$B$6*((E109+E110)/2)^0.5*(1-(1-((E109+E110)/2)^($B$10/($B$10-1)))^(($B$10-1)/$B$10))^2	=2*F110*F111/(F110+F111)
111	=$B$6*((E110+E111)/2)^0.5*(1-(1-((E110+E111)/2)^($B$10/($B$10-1)))^(($B$10-1)/$B$10))^2	=2*F111*F112/(F111+F112)
112	=$B$6*((E111+E112)/2)^0.5*(1-(1-((E111+E112)/2)^($B$10/($B$10-1)))^(($B$10-1)/$B$10))^2	=2*F112*F113/(F112+F113)
113	=$B$6*E112^0.5*(1-(1-E112^($B$10/($B$10-1)))^(($B$10-1)/$B$10))^2	=F113
114	0	0
115		
116		
117	k(P+dp8)	k_avg_z(P+dP8)
118	=$B$6*((E117+E118)/2)^0.5*(1-(1-((E117+E118)/2)^($B$10/($B$10-1)))^(($B$10-1)/$B$10))^2	=2*F118*F119/(F118+F119)
119	=$B$6*((E118+E119)/2)^0.5*(1-(1-((E118+E119)/2)^($B$10/($B$10-1)))^(($B$10-1)/$B$10))^2	=2*F119*F120/(F119+F120)
120	=$B$6*((E119+E120)/2)^0.5*(1-(1-((E119+E120)/2)^($B$10/($B$10-1)))^(($B$10-1)/$B$10))^2	=2*F120*F121/(F120+F121)
121	=$B$6*((E120+E121)/2)^0.5*(1-(1-((E120+E121)/2)^($B$10/($B$10-1)))^(($B$10-1)/$B$10))^2	=2*F121*F122/(F121+F122)
122	=$B$6*((E121+E122)/2)^0.5*(1-(1-((E121+E122)/2)^($B$10/($B$10-1)))^(($B$10-1)/$B$10))^2	=2*F122*F123/(F122+F123)
123	=$B$6*((E122+E123)/2)^0.5*(1-(1-((E122+E123)/2)^($B$10/($B$10-1)))^(($B$10-1)/$B$10))^2	=2*F123*F124/(F123+F124)
124	=$B$6*((E123+E124)/2)^0.5*(1-(1-((E123+E124)/2)^($B$10/($B$10-1)))^(($B$10-1)/$B$10))^2	=2*F124*F125/(F124+F125)
125	=$B$6*((E124+E125)/2)^0.5*(1-(1-((E124+E125)/2)^($B$10/($B$10-1)))^(($B$10-1)/$B$10))^2	=2*F125*F126/(F125+F126)
126	=$B$6*((E125+E126)/2)^0.5*(1-(1-((E125+E126)/2)^($B$10/($B$10-1)))^(($B$10-1)/$B$10))^2	=2*F126*F127/(F126+F127)
127	=$B$6*E126^0.5*(1-(1-E126^($B$10/($B$10-1)))^(($B$10-1)/$B$10))^2	=F127
128		
129		
130		
131		
132		
133		
134		
135		h

	H	I	J
102	k_avg_t(P+dP9)	Pw_avg_t(P+dp9)	q(P+dP9)
103			0
104	=(1-$B$13)*$G$37+$B$13*G104	=(1-$B$12)*$C$37+$B$12*C103	=H104*((I104-I105)/($A$37-$A$38)-1)
105	=(1-$B$13)*$G$38+$B$13*G105	=(1-$B$12)*$C$38+$B$12*C104	=H105*((I105-I106)/($A$38-$A$39)-1)
106	=(1-$B$13)*$G$39+$B$13*G106	=(1-$B$12)*$C$39+$B$12*C105	=H106*((I106-I107)/($A$39-$A$40)-1)
107	=(1-$B$13)*$G$40+$B$13*G107	=(1-$B$12)*$C$40+$B$12*C106	=H107*((I107-I108)/($A$40-$A$41)-1)
108	=(1-$B$13)*$G$41+$B$13*G108	=(1-$B$12)*$C$41+$B$12*C107	=H108*((I108-I109)/($A$41-$A$42)-1)
109	=(1-$B$13)*$G$42+$B$13*G109	=(1-$B$12)*$C$42+$B$12*C108	=H109*((I109-I110)/($A$42-$A$43)-1)
110	=(1-$B$13)*$G$43+$B$13*G110	=(1-$B$12)*$C$43+$B$12*C109	=H110*((I110-I111)/($A$43-$A$44)-1)
111	=(1-$B$13)*$G$44+$B$13*G111	=(1-$B$12)*$C$44+$B$12*C110	=H111*((I111-I112)/($A$44-$A$45)-1)
112	=(1-$B$13)*$G$45+$B$13*G112	=(1-$B$12)*$C$45+$B$12*C111	=H112*((I112-I113)/($A$45-$A$46)-1)
113	=(1-$B$13)*$G$46+$B$13*G113	=(1-$B$12)*$C$46+$B$12*C112	=IF($B$20=0,H113*((I113-C113)/$B$46-1),0)
114			
115	k_avg_t(P+dP8)	Pw_avg_t(P+dp8)	q(P+dP8)
116	=(1-$B$13)*$G$37+$B$13*G118	=(1-$B$12)*$C$37+$B$12*C117	0
117	=(1-$B$13)*$G$38+$B$13*G119	=(1-$B$12)*$C$38+$B$12*C118	=H116*((I116-I117)/($A$37-$A$38)-1)
118	=(1-$B$13)*$G$39+$B$13*G120	=(1-$B$12)*$C$39+$B$12*C119	=H117*((I117-I118)/($A$38-$A$39)-1)
119	=(1-$B$13)*$G$40+$B$13*G121	=(1-$B$12)*$C$40+$B$12*C120	=H118*((I118-I119)/($A$39-$A$40)-1)
120	=(1-$B$13)*$G$41+$B$13*G122	=(1-$B$12)*$C$41+$B$12*C121	=H119*((I119-I120)/($A$40-$A$41)-1)
121	=(1-$B$13)*$G$42+$B$13*G123	=(1-$B$12)*$C$42+$B$12*C122	=H120*((I120-I121)/($A$41-$A$42)-1)
122	=(1-$B$13)*$G$43+$B$13*G124	=(1-$B$12)*$C$43+$B$12*C123	=H121*((I121-I122)/($A$42-$A$43)-1)
123	=(1-$B$13)*$G$44+$B$13*G125	=(1-$B$12)*$C$44+$B$12*C124	=H122*((I122-I123)/($A$43-$A$44)-1)
124	=(1-$B$13)*$G$45+$B$13*G126	=(1-$B$12)*$C$45+$B$12*C125	=H123*((I123-I124)/($A$44-$A$45)-1)
125	=(1-$B$13)*$G$46+$B$13*G127	=(1-$B$12)*$C$46+$B$12*C126	=H124*((I124-I125)/($A$45-$A$46)-1)
126			=IF($B$20=0,H125*((I125-C127)/$B$46-1),0)
127			
128			
129			
130			
131			
132			
133			
134			
135			

	A	B	C	D	E
136			P+dP7	(P+dp7)	SE(P+dp7)
137	F=f(P+dP7)		=$C$70+B137	=$B$8+(1-$B$8)*(1+($B$9*C137)^$B$10)^(-$B$11)	=(D137-$B$8)/(1-$B$8)
138			=$C$71+B138	=$B$8+(1-$B$8)*(1+($B$9*C138)^$B$10)^(-$B$11)	=(D138-$B$8)/(1-$B$8)
139			=$C$72+B139	=$B$8+(1-$B$8)*(1+($B$9*C139)^$B$10)^(-$B$11)	=(D139-$B$8)/(1-$B$8)
140		=B71	=$C$73+B140	=$B$8+(1-$B$8)*(1+($B$9*C140)^$B$10)^(-$B$11)	=(D140-$B$8)/(1-$B$8)
141			=$C$74+B141	=$B$8+(1-$B$8)*(1+($B$9*C141)^$B$10)^(-$B$11)	=(D141-$B$8)/(1-$B$8)
142			=$C$75+B142	=$B$8+(1-$B$8)*(1+($B$9*C142)^$B$10)^(-$B$11)	=(D142-$B$8)/(1-$B$8)
143			=$C$76+B143	=$B$8+(1-$B$8)*(1+($B$9*C143)^$B$10)^(-$B$11)	=(D143-$B$8)/(1-$B$8)
144			=$C$77+B144	=$B$8+(1-$B$8)*(1+($B$9*C144)^$B$10)^(-$B$11)	=(D144-$B$8)/(1-$B$8)
145			=$C$78+B145	=$B$8+(1-$B$8)*(1+($B$9*C145)^$B$10)^(-$B$11)	=(D145-$B$8)/(1-$B$8)
146			=$C$79+B146	=$B$8+(1-$B$8)*(1+($B$9*C146)^$B$10)^(-$B$11)	=(D146-$B$8)/(1-$B$8)
147			=C113		
148					
149			P+dP6	(P+dp6)	SE(P+dp6)
150	F=f(P+dP6)		=$C$70+B150	=$B$8+(1-$B$8)*(1+($B$9*C150)^$B$10)^(-$B$11)	=(D150-$B$8)/(1-$B$8)
151			=$C$71+B151	=$B$8+(1-$B$8)*(1+($B$9*C151)^$B$10)^(-$B$11)	=(D151-$B$8)/(1-$B$8)
152			=$C$72+B152	=$B$8+(1-$B$8)*(1+($B$9*C152)^$B$10)^(-$B$11)	=(D152-$B$8)/(1-$B$8)
153			=$C$73+B153	=$B$8+(1-$B$8)*(1+($B$9*C153)^$B$10)^(-$B$11)	=(D153-$B$8)/(1-$B$8)
154		=B71	=$C$74+B154	=$B$8+(1-$B$8)*(1+($B$9*C154)^$B$10)^(-$B$11)	=(D154-$B$8)/(1-$B$8)
155			=$C$75+B155	=$B$8+(1-$B$8)*(1+($B$9*C155)^$B$10)^(-$B$11)	=(D155-$B$8)/(1-$B$8)
156			=$C$76+B156	=$B$8+(1-$B$8)*(1+($B$9*C156)^$B$10)^(-$B$11)	=(D156-$B$8)/(1-$B$8)
157			=$C$77+B157	=$B$8+(1-$B$8)*(1+($B$9*C157)^$B$10)^(-$B$11)	=(D157-$B$8)/(1-$B$8)
158			=$C$78+B158	=$B$8+(1-$B$8)*(1+($B$9*C158)^$B$10)^(-$B$11)	=(D158-$B$8)/(1-$B$8)
159			=$C$79+B159	=$B$8+(1-$B$8)*(1+($B$9*C159)^$B$10)^(-$B$11)	=(D159-$B$8)/(1-$B$8)
160			=C127		
161					
162					
163					
164					
165					
166					
167					
168					
169					
170					

	F	G
136	k(P+dp7)	k_avg_z(P+dP7)
137	0	0
138	=$B$6*((E137+E138)/2)^0.5*(1-(1-((E137+E138)/2)^($B$10/($B$10-1)))^(($B$10-1)/$B$10))^2	=2*F138*F139/(F138+F139)
139	=$B$6*((E138+E139)/2)^0.5*(1-(1-((E138+E139)/2)^($B$10/($B$10-1)))^(($B$10-1)/$B$10))^2	=2*F139*F140/(F139+F140)
140	=$B$6*((E139+E140)/2)^0.5*(1-(1-((E139+E140)/2)^($B$10/($B$10-1)))^(($B$10-1)/$B$10))^2	=2*F140*F141/(F140+F141)
141	=$B$6*((E140+E141)/2)^0.5*(1-(1-((E140+E141)/2)^($B$10/($B$10-1)))^(($B$10-1)/$B$10))^2	=2*F141*F142/(F141+F142)
142	=$B$6*((E141+E142)/2)^0.5*(1-(1-((E141+E142)/2)^($B$10/($B$10-1)))^(($B$10-1)/$B$10))^2	=2*F142*F143/(F142+F143)
143	=$B$6*((E142+E143)/2)^0.5*(1-(1-((E142+E143)/2)^($B$10/($B$10-1)))^(($B$10-1)/$B$10))^2	=2*F143*F144/(F143+F144)
144	=$B$6*((E143+E144)/2)^0.5*(1-(1-((E143+E144)/2)^($B$10/($B$10-1)))^(($B$10-1)/$B$10))^2	=2*F144*F145/(F144+F145)
145	=$B$6*((E144+E145)/2)^0.5*(1-(1-((E144+E145)/2)^($B$10/($B$10-1)))^(($B$10-1)/$B$10))^2	=2*F145*F146/(F145+F146)
146	=$B$6*((E145+E146)/2)^0.5*(1-(1-((E145+E146)/2)^($B$10/($B$10-1)))^(($B$10-1)/$B$10))^2	=2*F146*F147/(F146+F147)
147	=$B$6*E146^0.5*(1-(1-E146^($B$10/($B$10-1)))^(($B$10-1)/$B$10))^2	=F147
148		
149	k(P+dp6)	k_avg_z(P+dP6)
150	0	0
151	=$B$6*((E150+E151)/2)^0.5*(1-(1-((E150+E151)/2)^($B$10/($B$10-1)))^(($B$10-1)/$B$10))^2	=2*F151*F152/(F151+F152)
152	=$B$6*((E151+E152)/2)^0.5*(1-(1-((E151+E152)/2)^($B$10/($B$10-1)))^(($B$10-1)/$B$10))^2	=2*F152*F153/(F152+F153)
153	=$B$6*((E152+E153)/2)^0.5*(1-(1-((E152+E153)/2)^($B$10/($B$10-1)))^(($B$10-1)/$B$10))^2	=2*F153*F154/(F153+F154)
154	=$B$6*((E153+E154)/2)^0.5*(1-(1-((E153+E154)/2)^($B$10/($B$10-1)))^(($B$10-1)/$B$10))^2	=2*F154*F155/(F154+F155)
155	=$B$6*((E154+E155)/2)^0.5*(1-(1-((E154+E155)/2)^($B$10/($B$10-1)))^(($B$10-1)/$B$10))^2	=2*F155*F156/(F155+F156)
156	=$B$6*((E155+E156)/2)^0.5*(1-(1-((E155+E156)/2)^($B$10/($B$10-1)))^(($B$10-1)/$B$10))^2	=2*F156*F157/(F156+F157)
157	=$B$6*((E156+E157)/2)^0.5*(1-(1-((E156+E157)/2)^($B$10/($B$10-1)))^(($B$10-1)/$B$10))^2	=2*F157*F158/(F157+F158)
158	=$B$6*((E157+E158)/2)^0.5*(1-(1-((E157+E158)/2)^($B$10/($B$10-1)))^(($B$10-1)/$B$10))^2	=2*F158*F159/(F158+F159)
159	=$B$6*((E158+E159)/2)^0.5*(1-(1-((E158+E159)/2)^($B$10/($B$10-1)))^(($B$10-1)/$B$10))^2	=2*F159*F160/(F159+F160)
160	=$B$6*E159^0.5*(1-(1-E159^($B$10/($B$10-1)))^(($B$10-1)/$B$10))^2	=F160
161		
162		
163		
164		
165		
166		
167		
168		
169		
170		k

	H	I	J
136	k_avg_t(P+dP7)	Pw_avg_t(P+dp7)	q(P+dP7)
137	=(1-$B$13)*$G$37+$B$13*G138	=(1-$B$12)*$C$37+$B$12*C137	0
138	=(1-$B$13)*$G$38+$B$13*G139	=(1-$B$12)*$C$38+$B$12*C138	=H137*((I137-I138)/($A$37-$A$38)-1)
139	=(1-$B$13)*$G$39+$B$13*G140	=(1-$B$12)*$C$39+$B$12*C139	=H138*((I138-I139)/($A$38-$A$39)-1)
140	=(1-$B$13)*$G$40+$B$13*G141	=(1-$B$12)*$C$40+$B$12*C140	=H139*((I139-I140)/($A$39-$A$40)-1)
141	=(1-$B$13)*$G$41+$B$13*G142	=(1-$B$12)*$C$41+$B$12*C141	=H140*((I140-I141)/($A$40-$A$41)-1)
142	=(1-$B$13)*$G$42+$B$13*G143	=(1-$B$12)*$C$42+$B$12*C142	=H141*((I141-I142)/($A$41-$A$42)-1)
143	=(1-$B$13)*$G$43+$B$13*G144	=(1-$B$12)*$C$43+$B$12*C143	=H142*((I142-I143)/($A$42-$A$43)-1)
144	=(1-$B$13)*$G$44+$B$13*G145	=(1-$B$12)*$C$44+$B$12*C144	=H143*((I143-I144)/($A$43-$A$44)-1)
145	=(1-$B$13)*$G$45+$B$13*G146	=(1-$B$12)*$C$45+$B$12*C145	=H144*((I144-I145)/($A$44-$A$45)-1)
146	=(1-$B$13)*$G$46+$B$13*G147	=(1-$B$12)*$C$46+$B$12*C146	=H145*((I145-I146)/($A$45-$A$46)-1)
147			=IF($B$20=0,H146*((I146-C147)/$B$46-1),0)
148			
149	k_avg_t(P+dP6)	Pw_avg_t(P+dp6)	q(P+dP6)
150	=(1-$B$13)*$G$37+$B$13*G151	=(1-$B$12)*$C$37+$B$12*C150	0
151	=(1-$B$13)*$G$38+$B$13*G152	=(1-$B$12)*$C$38+$B$12*C151	=H150*((I150-I151)/($A$37-$A$38)-1)
152	=(1-$B$13)*$G$39+$B$13*G153	=(1-$B$12)*$C$39+$B$12*C152	=H151*((I151-I152)/($A$38-$A$39)-1)
153	=(1-$B$13)*$G$40+$B$13*G154	=(1-$B$12)*$C$40+$B$12*C153	=H152*((I152-I153)/($A$39-$A$40)-1)
154	=(1-$B$13)*$G$41+$B$13*G155	=(1-$B$12)*$C$41+$B$12*C154	=H153*((I153-I154)/($A$40-$A$41)-1)
155	=(1-$B$13)*$G$42+$B$13*G156	=(1-$B$12)*$C$42+$B$12*C155	=H154*((I154-I155)/($A$41-$A$42)-1)
156	=(1-$B$13)*$G$43+$B$13*G157	=(1-$B$12)*$C$43+$B$12*C156	=H155*((I155-I156)/($A$42-$A$43)-1)
157	=(1-$B$13)*$G$44+$B$13*G158	=(1-$B$12)*$C$44+$B$12*C157	=H156*((I156-I157)/($A$43-$A$44)-1)
158	=(1-$B$13)*$G$45+$B$13*G159	=(1-$B$12)*$C$45+$B$12*C158	=H157*((I157-I158)/($A$44-$A$45)-1)
159	=(1-$B$13)*$G$46+$B$13*G160	=(1-$B$12)*$C$46+$B$12*C159	=H158*((I158-I159)/($A$45-$A$46)-1)
160			=IF($B$20=0,H159*((I159-C160)/$B$46-1),0)
161			
162			
163			
164			
165			
166			
167			
168			
169			
170			

	A	B	C	D	E
171			P+dP5	(P+dp5)	SE(P+dp5)
172	F=f(P+dP5)		=$C$70+B172	=$B$8+(1-$B$8)*(1+($B$9*C172)^$B$10)^(-$B$11)	=(D172-$B$8)/(1-$B$8)
173			=$C$71+B173	=$B$8+(1-$B$8)*(1+($B$9*C173)^$B$10)^(-$B$11)	=(D173-$B$8)/(1-$B$8)
174			=$C$72+B174	=$B$8+(1-$B$8)*(1+($B$9*C174)^$B$10)^(-$B$11)	=(D174-$B$8)/(1-$B$8)
175			=$C$73+B175	=$B$8+(1-$B$8)*(1+($B$9*C175)^$B$10)^(-$B$11)	=(D175-$B$8)/(1-$B$8)
176			=$C$74+B176	=$B$8+(1-$B$8)*(1+($B$9*C176)^$B$10)^(-$B$11)	=(D176-$B$8)/(1-$B$8)
177		=B71	=$C$75+B177	=$B$8+(1-$B$8)*(1+($B$9*C177)^$B$10)^(-$B$11)	=(D177-$B$8)/(1-$B$8)
178			=$C$76+B178	=$B$8+(1-$B$8)*(1+($B$9*C178)^$B$10)^(-$B$11)	=(D178-$B$8)/(1-$B$8)
179			=$C$77+B179	=$B$8+(1-$B$8)*(1+($B$9*C179)^$B$10)^(-$B$11)	=(D179-$B$8)/(1-$B$8)
180			=$C$78+B180	=$B$8+(1-$B$8)*(1+($B$9*C180)^$B$10)^(-$B$11)	=(D180-$B$8)/(1-$B$8)
181			=$C$79+B181	=$B$8+(1-$B$8)*(1+($B$9*C181)^$B$10)^(-$B$11)	=(D181-$B$8)/(1-$B$8)
182			=C147		
183					
184			P+dP4	(P+dp4)	SE(P+dp4)
185	F=f(P+dP4)		=$C$70+B185	=$B$8+(1-$B$8)*(1+($B$9*C185)^$B$10)^(-$B$11)	=(D185-$B$8)/(1-$B$8)
186			=$C$71+B186	=$B$8+(1-$B$8)*(1+($B$9*C186)^$B$10)^(-$B$11)	=(D186-$B$8)/(1-$B$8)
187			=$C$72+B187	=$B$8+(1-$B$8)*(1+($B$9*C187)^$B$10)^(-$B$11)	=(D187-$B$8)/(1-$B$8)
188			=$C$73+B188	=$B$8+(1-$B$8)*(1+($B$9*C188)^$B$10)^(-$B$11)	=(D188-$B$8)/(1-$B$8)
189			=$C$74+B189	=$B$8+(1-$B$8)*(1+($B$9*C189)^$B$10)^(-$B$11)	=(D189-$B$8)/(1-$B$8)
190			=$C$75+B190	=$B$8+(1-$B$8)*(1+($B$9*C190)^$B$10)^(-$B$11)	=(D190-$B$8)/(1-$B$8)
191		=B71	=$C$76+B191	=$B$8+(1-$B$8)*(1+($B$9*C191)^$B$10)^(-$B$11)	=(D191-$B$8)/(1-$B$8)
192			=$C$77+B192	=$B$8+(1-$B$8)*(1+($B$9*C192)^$B$10)^(-$B$11)	=(D192-$B$8)/(1-$B$8)
193			=$C$78+B193	=$B$8+(1-$B$8)*(1+($B$9*C193)^$B$10)^(-$B$11)	=(D193-$B$8)/(1-$B$8)
194			=$C$79+B194	=$B$8+(1-$B$8)*(1+($B$9*C194)^$B$10)^(-$B$11)	=(D194-$B$8)/(1-$B$8)
195			=C160		
196					
197					
198					
199					
200					
201					
202					
203					m

	F	G
171	k(P+dp5)	k_avg_z(P+dP5)
172	0	0
173	=$B$6*((E172+E173)/2)^0.5*(1-(1-((E172+E173)/2)^($B$10/($B$10-1)))^(($B$10-1)/$B$10))^2	=2*F173*F174/(F173+F174)
174	=$B$6*((E173+E174)/2)^0.5*(1-(1-((E173+E174)/2)^($B$10/($B$10-1)))^(($B$10-1)/$B$10))^2	=2*F174*F175/(F174+F175)
175	=$B$6*((E174+E175)/2)^0.5*(1-(1-((E174+E175)/2)^($B$10/($B$10-1)))^(($B$10-1)/$B$10))^2	=2*F175*F176/(F175+F176)
176	=$B$6*((E175+E176)/2)^0.5*(1-(1-((E175+E176)/2)^($B$10/($B$10-1)))^(($B$10-1)/$B$10))^2	=2*F176*F177/(F176+F177)
177	=$B$6*((E176+E177)/2)^0.5*(1-(1-((E176+E177)/2)^($B$10/($B$10-1)))^(($B$10-1)/$B$10))^2	=2*F177*F178/(F177+F178)
178	=$B$6*((E177+E178)/2)^0.5*(1-(1-((E177+E178)/2)^($B$10/($B$10-1)))^(($B$10-1)/$B$10))^2	=2*F178*F179/(F178+F179)
179	=$B$6*((E178+E179)/2)^0.5*(1-(1-((E178+E179)/2)^($B$10/($B$10-1)))^(($B$10-1)/$B$10))^2	=2*F179*F180/(F179+F180)
180	=$B$6*((E179+E180)/2)^0.5*(1-(1-((E179+E180)/2)^($B$10/($B$10-1)))^(($B$10-1)/$B$10))^2	=2*F180*F181/(F180+F181)
181	=$B$6*((E180+E181)/2)^0.5*(1-(1-((E180+E181)/2)^($B$10/($B$10-1)))^(($B$10-1)/$B$10))^2	=2*F181*F182/(F181+F182)
182	=$B$6*E181^0.5*(1-(1-E181^($B$10/($B$10-1)))^(($B$10-1)/$B$10))^2	=F182
183		
184	k(P+dp4)	k_avg_z(P+dP4)
185	0	0
186	=$B$6*((E185+E186)/2)^0.5*(1-(1-((E185+E186)/2)^($B$10/($B$10-1)))^(($B$10-1)/$B$10))^2	=2*F186*F187/(F186+F187)
187	=$B$6*((E186+E187)/2)^0.5*(1-(1-((E186+E187)/2)^($B$10/($B$10-1)))^(($B$10-1)/$B$10))^2	=2*F187*F188/(F187+F188)
188	=$B$6*((E187+E188)/2)^0.5*(1-(1-((E187+E188)/2)^($B$10/($B$10-1)))^(($B$10-1)/$B$10))^2	=2*F188*F189/(F188+F189)
189	=$B$6*((E188+E189)/2)^0.5*(1-(1-((E188+E189)/2)^($B$10/($B$10-1)))^(($B$10-1)/$B$10))^2	=2*F189*F190/(F189+F190)
190	=$B$6*((E189+E190)/2)^0.5*(1-(1-((E189+E190)/2)^($B$10/($B$10-1)))^(($B$10-1)/$B$10))^2	=2*F190*F191/(F190+F191)
191	=$B$6*((E190+E191)/2)^0.5*(1-(1-((E190+E191)/2)^($B$10/($B$10-1)))^(($B$10-1)/$B$10))^2	=2*F191*F192/(F191+F192)
192	=$B$6*((E191+E192)/2)^0.5*(1-(1-((E191+E192)/2)^($B$10/($B$10-1)))^(($B$10-1)/$B$10))^2	=2*F192*F193/(F192+F193)
193	=$B$6*((E192+E193)/2)^0.5*(1-(1-((E192+E193)/2)^($B$10/($B$10-1)))^(($B$10-1)/$B$10))^2	=2*F193*F194/(F193+F194)
194	=$B$6*((E193+E194)/2)^0.5*(1-(1-((E193+E194)/2)^($B$10/($B$10-1)))^(($B$10-1)/$B$10))^2	=2*F194*F195/(F194+F195)
195	=$B$6*E194^0.5*(1-(1-E194^($B$10/($B$10-1)))^(($B$10-1)/$B$10))^2	=F195
196		
197		
198		
199		
200		
201		
202		
203		n

	H	I	J
171	k_avg_t(P+dP5)	Pw_avg_t(P+dp5)	q(P+dP5)
172	=(1-$B$13)*$G$37+$B$13*G173	=(1-$B$12)*$C$37+$B$12*C172	0
173	=(1-$B$13)*$G$38+$B$13*G174	=(1-$B$12)*$C$38+$B$12*C173	=H172*((I172-I173)/($A$37-$A$38)-1)
174	=(1-$B$13)*$G$39+$B$13*G175	=(1-$B$12)*$C$39+$B$12*C174	=H173*((I173-I174)/($A$38-$A$39)-1)
175	=(1-$B$13)*$G$40+$B$13*G176	=(1-$B$12)*$C$40+$B$12*C175	=H174*((I174-I175)/($A$39-$A$40)-1)
176	=(1-$B$13)*$G$41+$B$13*G177	=(1-$B$12)*$C$41+$B$12*C176	=H175*((I175-I176)/($A$40-$A$41)-1)
177	=(1-$B$13)*$G$42+$B$13*G178	=(1-$B$12)*$C$42+$B$12*C177	=H176*((I176-I177)/($A$41-$A$42)-1)
178	=(1-$B$13)*$G$43+$B$13*G179	=(1-$B$12)*$C$43+$B$12*C178	=H177*((I177-I178)/($A$42-$A$43)-1)
179	=(1-$B$13)*$G$44+$B$13*G180	=(1-$B$12)*$C$44+$B$12*C179	=H178*((I178-I179)/($A$43-$A$44)-1)
180	=(1-$B$13)*$G$45+$B$13*G181	=(1-$B$12)*$C$45+$B$12*C180	=H179*((I179-I180)/($A$44-$A$45)-1)
181	=(1-$B$13)*$G$46+$B$13*G182	=(1-$B$12)*$C$46+$B$12*C181	=H180*((I180-I181)/($A$45-$A$46)-1)
182			=IF($B$20=0,H181*((I181-C182)/$B$46-1),0)
183			
184	k_avg_t(P+dP4)	Pw_avg_t(P+dp4)	q(P+dP4)
185	=(1-$B$13)*$G$37+$B$13*G186	=(1-$B$12)*$C$37+$B$12*C185	0
186	=(1-$B$13)*$G$38+$B$13*G187	=(1-$B$12)*$C$38+$B$12*C186	=H185*((I185-I186)/($A$37-$A$38)-1)
187	=(1-$B$13)*$G$39+$B$13*G188	=(1-$B$12)*$C$39+$B$12*C187	=H186*((I186-I187)/($A$38-$A$39)-1)
188	=(1-$B$13)*$G$40+$B$13*G189	=(1-$B$12)*$C$40+$B$12*C188	=H187*((I187-I188)/($A$39-$A$40)-1)
189	=(1-$B$13)*$G$41+$B$13*G190	=(1-$B$12)*$C$41+$B$12*C189	=H188*((I188-I189)/($A$40-$A$41)-1)
190	=(1-$B$13)*$G$42+$B$13*G191	=(1-$B$12)*$C$42+$B$12*C190	=H189*((I189-I190)/($A$41-$A$42)-1)
191	=(1-$B$13)*$G$43+$B$13*G192	=(1-$B$12)*$C$43+$B$12*C191	=H190*((I190-I191)/($A$42-$A$43)-1)
192	=(1-$B$13)*$G$44+$B$13*G193	=(1-$B$12)*$C$44+$B$12*C192	=H191*((I191-I192)/($A$43-$A$44)-1)
193	=(1-$B$13)*$G$45+$B$13*G194	=(1-$B$12)*$C$45+$B$12*C193	=H192*((I192-I193)/($A$44-$A$45)-1)
194	=(1-$B$13)*$G$46+$B$13*G195	=(1-$B$12)*$C$46+$B$12*C194	=H193*((I193-I194)/($A$45-$A$46)-1)
195			=IF($B$20=0,H194*((I194-C195)/$B$46-1),0)
196			
197			
198			
199			
200			
201			
202			
203			0

	A	B	C	D	E
204			P+dP3	(P+dp3)	SE(P+dp3)
205	F=f(P+dP3)		=$C$70+B205	=$B$8+(1-$B$8)*(1+($B$9*C205)^$B$10)^(-$B$11)	=(D205-$B$8)/(1-$B$8)
206			=$C$71+B206	=$B$8+(1-$B$8)*(1+($B$9*C206)^$B$10)^(-$B$11)	=(D206-$B$8)/(1-$B$8)
207			=$C$72+B207	=$B$8+(1-$B$8)*(1+($B$9*C207)^$B$10)^(-$B$11)	=(D207-$B$8)/(1-$B$8)
208			=$C$73+B208	=$B$8+(1-$B$8)*(1+($B$9*C208)^$B$10)^(-$B$11)	=(D208-$B$8)/(1-$B$8)
209			=$C$74+B209	=$B$8+(1-$B$8)*(1+($B$9*C209)^$B$10)^(-$B$11)	=(D209-$B$8)/(1-$B$8)
210			=$C$75+B210	=$B$8+(1-$B$8)*(1+($B$9*C210)^$B$10)^(-$B$11)	=(D210-$B$8)/(1-$B$8)
211			=$C$76+B211	=$B$8+(1-$B$8)*(1+($B$9*C211)^$B$10)^(-$B$11)	=(D211-$B$8)/(1-$B$8)
212		=B71	=$C$77+B212	=$B$8+(1-$B$8)*(1+($B$9*C212)^$B$10)^(-$B$11)	=(D212-$B$8)/(1-$B$8)
213			=$C$78+B213	=$B$8+(1-$B$8)*(1+($B$9*C213)^$B$10)^(-$B$11)	=(D213-$B$8)/(1-$B$8)
214			=$C$79+B214	=$B$8+(1-$B$8)*(1+($B$9*C214)^$B$10)^(-$B$11)	=(D214-$B$8)/(1-$B$8)
215			=C182		
216					
217			P+dP2	(P+dp2)	SE(P+dp2)
218	F=f(P+dP2)		=$C$70+B218	=$B$8+(1-$B$8)*(1+($B$9*C218)^$B$10)^(-$B$11)	=(D218-$B$8)/(1-$B$8)
219			=$C$71+B219	=$B$8+(1-$B$8)*(1+($B$9*C219)^$B$10)^(-$B$11)	=(D219-$B$8)/(1-$B$8)
220			=$C$72+B220	=$B$8+(1-$B$8)*(1+($B$9*C220)^$B$10)^(-$B$11)	=(D220-$B$8)/(1-$B$8)
221			=$C$73+B221	=$B$8+(1-$B$8)*(1+($B$9*C221)^$B$10)^(-$B$11)	=(D221-$B$8)/(1-$B$8)
222			=$C$74+B222	=$B$8+(1-$B$8)*(1+($B$9*C222)^$B$10)^(-$B$11)	=(D222-$B$8)/(1-$B$8)
223			=$C$75+B223	=$B$8+(1-$B$8)*(1+($B$9*C223)^$B$10)^(-$B$11)	=(D223-$B$8)/(1-$B$8)
224			=$C$76+B224	=$B$8+(1-$B$8)*(1+($B$9*C224)^$B$10)^(-$B$11)	=(D224-$B$8)/(1-$B$8)
225			=$C$77+B225	=$B$8+(1-$B$8)*(1+($B$9*C225)^$B$10)^(-$B$11)	=(D225-$B$8)/(1-$B$8)
226		=B71	=$C$78+B226	=$B$8+(1-$B$8)*(1+($B$9*C226)^$B$10)^(-$B$11)	=(D226-$B$8)/(1-$B$8)
227			=$C$79+B227	=$B$8+(1-$B$8)*(1+($B$9*C227)^$B$10)^(-$B$11)	=(D227-$B$8)/(1-$B$8)
228			=C195		
229					
230					
231					
232					
233					
234					
235					
236					P

	F	G
204	k(P+dp3)	k_avg_z(P+dP3)
205	0	0
206	=$B$6*((E205+E206)/2)^0.5*(1-(1-((E205+E206)/2)^($B$10/($B$10-1)))^(($B$10-1)/$B$10))^2	=2*F206*F207/(F206+F207)
207	=$B$6*((E206+E207)/2)^0.5*(1-(1-((E206+E207)/2)^($B$10/($B$10-1)))^(($B$10-1)/$B$10))^2	=2*F207*F208/(F207+F208)
208	=$B$6*((E207+E208)/2)^0.5*(1-(1-((E207+E208)/2)^($B$10/($B$10-1)))^(($B$10-1)/$B$10))^2	=2*F208*F209/(F208+F209)
209	=$B$6*((E208+E209)/2)^0.5*(1-(1-((E208+E209)/2)^($B$10/($B$10-1)))^(($B$10-1)/$B$10))^2	=2*F209*F210/(F209+F210)
210	=$B$6*((E209+E210)/2)^0.5*(1-(1-((E209+E210)/2)^($B$10/($B$10-1)))^(($B$10-1)/$B$10))^2	=2*F210*F211/(F210+F211)
211	=$B$6*((E210+E211)/2)^0.5*(1-(1-((E210+E211)/2)^($B$10/($B$10-1)))^(($B$10-1)/$B$10))^2	=2*F211*F212/(F211+F212)
212	=$B$6*((E211+E212)/2)^0.5*(1-(1-((E211+E212)/2)^($B$10/($B$10-1)))^(($B$10-1)/$B$10))^2	=2*F212*F213/(F212+F213)
213	=$B$6*((E212+E213)/2)^0.5*(1-(1-((E212+E213)/2)^($B$10/($B$10-1)))^(($B$10-1)/$B$10))^2	=2*F213*F214/(F213+F214)
214	=$B$6*((E213+E214)/2)^0.5*(1-(1-((E213+E214)/2)^($B$10/($B$10-1)))^(($B$10-1)/$B$10))^2	=2*F214*F215/(F214+F215)
215	=$B$6*E214^0.5*(1-(1-E214^($B$10/($B$10-1)))^(($B$10-1)/$B$10))^2	=F215
216		
217	k(P+dp2)	k_avg_z(P+dP2)
218	0	0
219	=$B$6*((E218+E219)/2)^0.5*(1-(1-((E218+E219)/2)^($B$10/($B$10-1)))^(($B$10-1)/$B$10))^2	=2*F219*F220/(F219+F220)
220	=$B$6*((E219+E220)/2)^0.5*(1-(1-((E219+E220)/2)^($B$10/($B$10-1)))^(($B$10-1)/$B$10))^2	=2*F220*F221/(F220+F221)
221	=$B$6*((E220+E221)/2)^0.5*(1-(1-((E220+E221)/2)^($B$10/($B$10-1)))^(($B$10-1)/$B$10))^2	=2*F221*F222/(F221+F222)
222	=$B$6*((E221+E222)/2)^0.5*(1-(1-((E221+E222)/2)^($B$10/($B$10-1)))^(($B$10-1)/$B$10))^2	=2*F222*F223/(F222+F223)
223	=$B$6*((E222+E223)/2)^0.5*(1-(1-((E222+E223)/2)^($B$10/($B$10-1)))^(($B$10-1)/$B$10))^2	=2*F223*F224/(F223+F224)
224	=$B$6*((E223+E224)/2)^0.5*(1-(1-((E223+E224)/2)^($B$10/($B$10-1)))^(($B$10-1)/$B$10))^2	=2*F224*F225/(F224+F225)
225	=$B$6*((E224+E225)/2)^0.5*(1-(1-((E224+E225)/2)^($B$10/($B$10-1)))^(($B$10-1)/$B$10))^2	=2*F225*F226/(F225+F226)
226	=$B$6*((E225+E226)/2)^0.5*(1-(1-((E225+E226)/2)^($B$10/($B$10-1)))^(($B$10-1)/$B$10))^2	=2*F226*F227/(F226+F227)
227	=$B$6*((E226+E227)/2)^0.5*(1-(1-((E226+E227)/2)^($B$10/($B$10-1)))^(($B$10-1)/$B$10))^2	=2*F227*F228/(F227+F228)
228	=$B$6*E227^0.5*(1-(1-E227^($B$10/($B$10-1)))^(($B$10-1)/$B$10))^2	=F228
229		
230		
231		
232		
233		
234		
235		
236		q

	H	I	J
204	k_avg_t(P+dP3)	Pw_avg_t(P+dp3)	q(P+dP3)
205	=(1-$B$13)*$G$37+$B$13*G206	=(1-$B$12)*$C$37+$B$12*C205	0
206	=(1-$B$13)*$G$38+$B$13*G207	=(1-$B$12)*$C$38+$B$12*C206	=H205*((I205-I206)/($A$37-$A$38)-1)
207	=(1-$B$13)*$G$39+$B$13*G208	=(1-$B$12)*$C$39+$B$12*C207	=H206*((I206-I207)/($A$38-$A$39)-1)
208	=(1-$B$13)*$G$40+$B$13*G209	=(1-$B$12)*$C$40+$B$12*C208	=H207*((I207-I208)/($A$39-$A$40)-1)
209	=(1-$B$13)*$G$41+$B$13*G210	=(1-$B$12)*$C$41+$B$12*C209	=H208*((I208-I209)/($A$40-$A$41)-1)
210	=(1-$B$13)*$G$42+$B$13*G211	=(1-$B$12)*$C$42+$B$12*C210	=H209*((I209-I210)/($A$41-$A$42)-1)
211	=(1-$B$13)*$G$43+$B$13*G212	=(1-$B$12)*$C$43+$B$12*C211	=H210*((I210-I211)/($A$42-$A$43)-1)
212	=(1-$B$13)*$G$44+$B$13*G213	=(1-$B$12)*$C$44+$B$12*C212	=H211*((I211-I212)/($A$43-$A$44)-1)
213	=(1-$B$13)*$G$45+$B$13*G214	=(1-$B$12)*$C$45+$B$12*C213	=H212*((I212-I213)/($A$44-$A$45)-1)
214	=(1-$B$13)*$G$46+$B$13*G215	=(1-$B$12)*$C$46+$B$12*C214	=H213*((I213-I214)/($A$45-$A$46)-1)
215			=IF($B$20=0,H214*((I214-C215)/$B$46-1),0)
216			
217	k_avg_t(P+dP2)	Pw_avg_t(P+dp2)	q(P+dP2)
218	=(1-$B$13)*$G$37+$B$13*G219	=(1-$B$12)*$C$37+$B$12*C218	0
219	=(1-$B$13)*$G$38+$B$13*G220	=(1-$B$12)*$C$38+$B$12*C219	=H218*((I218-I219)/($A$37-$A$38)-1)
220	=(1-$B$13)*$G$39+$B$13*G221	=(1-$B$12)*$C$39+$B$12*C220	=H219*((I219-I220)/($A$38-$A$39)-1)
221	=(1-$B$13)*$G$40+$B$13*G222	=(1-$B$12)*$C$40+$B$12*C221	=H220*((I220-I221)/($A$39-$A$40)-1)
222	=(1-$B$13)*$G$41+$B$13*G223	=(1-$B$12)*$C$41+$B$12*C222	=H221*((I221-I222)/($A$40-$A$41)-1)
223	=(1-$B$13)*$G$42+$B$13*G224	=(1-$B$12)*$C$42+$B$12*C223	=H222*((I222-I223)/($A$41-$A$42)-1)
224	=(1-$B$13)*$G$43+$B$13*G225	=(1-$B$12)*$C$43+$B$12*C224	=H223*((I223-I224)/($A$42-$A$43)-1)
225	=(1-$B$13)*$G$44+$B$13*G226	=(1-$B$12)*$C$44+$B$12*C225	=H224*((I224-I225)/($A$43-$A$44)-1)
226	=(1-$B$13)*$G$45+$B$13*G227	=(1-$B$12)*$C$45+$B$12*C226	=H225*((I225-I226)/($A$44-$A$45)-1)
227	=(1-$B$13)*$G$46+$B$13*G228	=(1-$B$12)*$C$46+$B$12*C227	=H226*((I226-I227)/($A$45-$A$46)-1)
228			=IF($B$20=0,H227*((I227-C228)/$B$46-1),0)
229			
230			
231			
232			
233			
234			
235			
236			

	A	B	C	D	E
237			P+dP1	(P+dp1)	SE(P+dp1)
238	F=f(P+dP1)		=$C$70+B238	=$B$8+(1-$B$8)*(1+($B$9*C238)^$B$10)^(-$B$11)	=(D238-$B$8)/(1-$B$8)
239			=$C$71+B239	=$B$8+(1-$B$8)*(1+($B$9*C239)^$B$10)^(-$B$11)	=(D239-$B$8)/(1-$B$8)
240			=$C$72+B240	=$B$8+(1-$B$8)*(1+($B$9*C240)^$B$10)^(-$B$11)	=(D240-$B$8)/(1-$B$8)
241			=$C$73+B241	=$B$8+(1-$B$8)*(1+($B$9*C241)^$B$10)^(-$B$11)	=(D241-$B$8)/(1-$B$8)
242			=$C$74+B242	=$B$8+(1-$B$8)*(1+($B$9*C242)^$B$10)^(-$B$11)	=(D242-$B$8)/(1-$B$8)
243			=$C$75+B243	=$B$8+(1-$B$8)*(1+($B$9*C243)^$B$10)^(-$B$11)	=(D243-$B$8)/(1-$B$8)
244			=$C$76+B244	=$B$8+(1-$B$8)*(1+($B$9*C244)^$B$10)^(-$B$11)	=(D244-$B$8)/(1-$B$8)
245			=$C$77+B245	=$B$8+(1-$B$8)*(1+($B$9*C245)^$B$10)^(-$B$11)	=(D245-$B$8)/(1-$B$8)
246			=$C$78+B246	=$B$8+(1-$B$8)*(1+($B$9*C246)^$B$10)^(-$B$11)	=(D246-$B$8)/(1-$B$8)
247		=B71	=$C$79+B247	=$B$8+(1-$B$8)*(1+($B$9*C247)^$B$10)^(-$B$11)	=(D247-$B$8)/(1-$B$8)
248			=C215		
249					
250					
251					
252					
253					
254					
255					
256					
257					
258					
259					
260					
261					
262					
263					
264					
265					
266					
267					
268					
269					
270					
271					
272					s

	F	G
237	k(P+dp1)	k_avg_z(P+dP1)
238	0	0
239	=$B$6*((E238+E239)/2)^0.5*(1-(1-((E238+E239)/2)^($B$10/($B$10-1)))^(($B$10-1)/$B$10))^2	=2*F239*F240/(F239+F240)
240	=$B$6*((E239+E240)/2)^0.5*(1-(1-((E239+E240)/2)^($B$10/($B$10-1)))^(($B$10-1)/$B$10))^2	=2*F240*F241/(F240+F241)
241	=$B$6*((E240+E241)/2)^0.5*(1-(1-((E240+E241)/2)^($B$10/($B$10-1)))^(($B$10-1)/$B$10))^2	=2*F241*F242/(F241+F242)
242	=$B$6*((E241+E242)/2)^0.5*(1-(1-((E241+E242)/2)^($B$10/($B$10-1)))^(($B$10-1)/$B$10))^2	=2*F242*F243/(F242+F243)
243	=$B$6*((E242+E243)/2)^0.5*(1-(1-((E242+E243)/2)^($B$10/($B$10-1)))^(($B$10-1)/$B$10))^2	=2*F243*F244/(F243+F244)
244	=$B$6*((E243+E244)/2)^0.5*(1-(1-((E243+E244)/2)^($B$10/($B$10-1)))^(($B$10-1)/$B$10))^2	=2*F244*F245/(F244+F245)
245	=$B$6*((E244+E245)/2)^0.5*(1-(1-((E244+E245)/2)^($B$10/($B$10-1)))^(($B$10-1)/$B$10))^2	=2*F245*F246/(F245+F246)
246	=$B$6*((E245+E246)/2)^0.5*(1-(1-((E245+E246)/2)^($B$10/($B$10-1)))^(($B$10-1)/$B$10))^2	=2*F246*F247/(F246+F247)
247	=$B$6*((E246+E247)/2)^0.5*(1-(1-((E246+E247)/2)^($B$10/($B$10-1)))^(($B$10-1)/$B$10))^2	=2*F247*F248/(F247+F248)
248	=$B$6*E247^0.5*(1-(1-E247^($B$10/($B$10-1)))^(($B$10-1)/$B$10))^2	=F248
249		
250		
251		
252		
253		
254		
255		
256		
257		
258		
259		
260		
261		
262		
263		
264		
265		
266		
267		
268		
269		
270		
271		
272		t

	H	I	J
237	k_avg_t(P+dP1)	Pw_avg_t(P+dp1)	q(P+dP1)
238	=(1-$B$13)*$G$37+$B$13*G239	=(1-$B$12)*$C$37+$B$12*C238	0
239	=(1-$B$13)*$G$38+$B$13*G240	=(1-$B$12)*$C$38+$B$12*C239	=H238*((I238-I239)/($A$37-$A$38)-1)
240	=(1-$B$13)*$G$39+$B$13*G241	=(1-$B$12)*$C$39+$B$12*C240	=H239*((I239-I240)/($A$38-$A$39)-1)
241	=(1-$B$13)*$G$40+$B$13*G242	=(1-$B$12)*$C$40+$B$12*C241	=H240*((I240-I241)/($A$39-$A$40)-1)
242	=(1-$B$13)*$G$41+$B$13*G243	=(1-$B$12)*$C$41+$B$12*C242	=H241*((I241-I242)/($A$40-$A$41)-1)
243	=(1-$B$13)*$G$42+$B$13*G244	=(1-$B$12)*$C$42+$B$12*C243	=H242*((I242-I243)/($A$41-$A$42)-1)
244	=(1-$B$13)*$G$43+$B$13*G245	=(1-$B$12)*$C$43+$B$12*C244	=H243*((I243-I244)/($A$42-$A$43)-1)
245	=(1-$B$13)*$G$44+$B$13*G246	=(1-$B$12)*$C$44+$B$12*C245	=H244*((I244-I245)/($A$43-$A$44)-1)
246	=(1-$B$13)*$G$45+$B$13*G247	=(1-$B$12)*$C$45+$B$12*C246	=H245*((I245-I246)/($A$44-$A$45)-1)
247	=(1-$B$13)*$G$46+$B$13*G248	=(1-$B$12)*$C$46+$B$12*C247	=H246*((I246-I247)/($A$45-$A$46)-1)
248			=IF($B$20=0,H247*((I247-C248)/$B$46-1),0)
249			
250			
251			
252			
253			
254			
255			
256			
257			
258			
259			
260			
261			
262			
263			
264			
265			
266			
267			
268			
269			
270			
271			
272			

	K	L	M	N
68	p*dS(P)/dt	dq(P)/dx	p*dS(P+dP9)/dt	dq(P+dP9)/dx
69				
70	=$B$7*(D37-D70)/$C$29	=(J71-J72)/(A36-A37)	=$B$7*($D$37-D103)/$C$29	=(J103-J104)/($A$36-$A$37)
71	=$B$7*(D38-D71)/$C$29	=(J72-J73)/(A37-A38)	=$B$7*($D$38-D104)/$C$29	=(J104-J105)/($A$37-$A$38)
72	=$B$7*(D39-D72)/$C$29	=(J73-J74)/(A38-A39)	=$B$7*($D$39-D105)/$C$29	=(J105-J106)/($A$38-$A$39)
73	=$B$7*(D40-D73)/$C$29	=(J74-J75)/(A39-A40)	=$B$7*($D$40-D106)/$C$29	=(J106-J107)/($A$39-$A$40)
74	=$B$7*(D41-D74)/$C$29	=(J75-J76)/(A40-A41)	=$B$7*($D$41-D107)/$C$29	=(J107-J108)/($A$40-$A$41)
75	=$B$7*(D42-D75)/$C$29	=(J76-J77)/(A41-A42)	=$B$7*($D$42-D108)/$C$29	=(J108-J109)/($A$41-$A$42)
76	=$B$7*(D43-D76)/$C$29	=(J77-J78)/(A42-A43)	=$B$7*($D$43-D109)/$C$29	=(J109-J110)/($A$42-$A$43)
77	=$B$7*(D44-D77)/$C$29	=(J78-J79)/(A43-A44)	=$B$7*($D$44-D110)/$C$29	=(J110-J111)/($A$43-$A$44)
78	=$B$7*(D45-D78)/$C$29	=(J79-J80)/(A44-A45)	=$B$7*($D$45-D111)/$C$29	=(J111-J112)/($A$44-$A$45)
79	=$B$7*(D46-D79)/$C$29	=(J80-J81)/(A45-A46)	=$B$7*($D$46-D112)/$C$29	=(J112-J113)/($A$45-$A$46)
80				
81	p*dS(P+dP10)/dt	dq(P+dP10)/dx	p*dS(P+dP8)/dt	dq(P+dP8)/dx
82				
83	=$B$7*($D$37-D83)/$C$29	=(J84-J85)/($A$36-$A$37)	=$B$7*($D$37-D117)/$C$29	=(J116-J117)/($A$36-$A$37)
84	=$B$7*($D$38-D84)/$C$29	=(J85-J86)/($A$37-$A$38)	=$B$7*($D$38-D118)/$C$29	=(J117-J118)/($A$37-$A$38)
85	=$B$7*($D$39-D85)/$C$29	=(J86-J87)/($A$38-$A$39)	=$B$7*($D$39-D119)/$C$29	=(J118-J119)/($A$38-$A$39)
86	=$B$7*($D$40-D86)/$C$29	=(J87-J88)/($A$39-$A$40)	=$B$7*($D$40-D120)/$C$29	=(J119-J120)/($A$39-$A$40)
87	=$B$7*($D$41-D87)/$C$29	=(J88-J89)/($A$40-$A$41)	=$B$7*($D$41-D121)/$C$29	=(J120-J121)/($A$40-$A$41)
88	=$B$7*($D$42-D88)/$C$29	=(J89-J90)/($A$41-$A$42)	=$B$7*($D$42-D122)/$C$29	=(J121-J122)/($A$41-$A$42)
89	=$B$7*($D$43-D89)/$C$29	=(J90-J91)/($A$42-$A$43)	=$B$7*($D$43-D123)/$C$29	=(J122-J123)/($A$42-$A$43)
90	=$B$7*($D$44-D90)/$C$29	=(J91-J92)/($A$43-$A$44)	=$B$7*($D$44-D124)/$C$29	=(J123-J124)/($A$43-$A$44)
91	=$B$7*($D$45-D91)/$C$29	=(J92-J93)/($A$44-$A$45)	=$B$7*($D$45-D125)/$C$29	=(J124-J125)/($A$44-$A$45)
92	=$B$7*($D$46-D92)/$C$29	=(J93-J94)/($A$45-$A$46)	=$B$7*($D$46-D126)/$C$29	=(J125-J126)/($A$45-$A$46)
93				
94				
95				
96				
97				
98				
99				
100				
101				v

	K	L	M	N
102	p*dS(P+dP7)/dt	dq(P+dP7)/dx	p*dS(P+dP5)/dt	dq(P+dP5)/dx
103				
104	=$B$7*($D$37-D137)/$C$29	=(J137-J138)/($A$36-$A$37)	=$B$7*($D$37-D172)/$C$29	=(J172-J173)/($A$36-$A$37)
105	=$B$7*($D$38-D138)/$C$29	=(J138-J139)/($A$37-$A$38)	=$B$7*($D$38-D173)/$C$29	=(J173-J174)/($A$37-$A$38)
106	=$B$7*($D$39-D139)/$C$29	=(J139-J140)/($A$38-$A$39)	=$B$7*($D$39-D174)/$C$29	=(J174-J175)/($A$38-$A$39)
107	=$B$7*($D$40-D140)/$C$29	=(J140-J141)/($A$39-$A$40)	=$B$7*($D$40-D175)/$C$29	=(J175-J176)/($A$39-$A$40)
108	=$B$7*($D$41-D141)/$C$29	=(J141-J142)/($A$40-$A$41)	=$B$7*($D$41-D176)/$C$29	=(J176-J177)/($A$40-$A$41)
109	=$B$7*($D$42-D142)/$C$29	=(J142-J143)/($A$41-$A$42)	=$B$7*($D$42-D177)/$C$29	=(J177-J178)/($A$41-$A$42)
110	=$B$7*($D$43-D143)/$C$29	=(J143-J144)/($A$42-$A$43)	=$B$7*($D$43-D178)/$C$29	=(J178-J179)/($A$42-$A$43)
111	=$B$7*($D$44-D144)/$C$29	=(J144-J145)/($A$43-$A$44)	=$B$7*($D$44-D179)/$C$29	=(J179-J180)/($A$43-$A$44)
112	=$B$7*($D$45-D145)/$C$29	=(J145-J146)/($A$44-$A$45)	=$B$7*($D$45-D180)/$C$29	=(J180-J181)/($A$44-$A$45)
113	=$B$7*($D$46-D146)/$C$29	=(J146-J147)/($A$45-$A$46)	=$B$7*($D$46-D181)/$C$29	=(J181-J182)/($A$45-$A$46)
114				
115	p*dS(P+dP6)/dt	dq(P+dP6)/dx	p*dS(P+dP4)/dt	dq(P+dP4)/dx
116				
117	=$B$7*($D$37-D150)/$C$29	=(J150-J151)/($A$36-$A$37)	=$B$7*($D$37-D185)/$C$29	=(J185-J186)/($A$36-$A$37)
118	=$B$7*($D$38-D151)/$C$29	=(J151-J152)/($A$37-$A$38)	=$B$7*($D$38-D186)/$C$29	=(J186-J187)/($A$37-$A$38)
119	=$B$7*($D$39-D152)/$C$29	=(J152-J153)/($A$38-$A$39)	=$B$7*($D$39-D187)/$C$29	=(J187-J188)/($A$38-$A$39)
120	=$B$7*($D$40-D153)/$C$29	=(J153-J154)/($A$39-$A$40)	=$B$7*($D$40-D188)/$C$29	=(J188-J189)/($A$39-$A$40)
121	=$B$7*($D$41-D154)/$C$29	=(J154-J155)/($A$40-$A$41)	=$B$7*($D$41-D189)/$C$29	=(J189-J190)/($A$40-$A$41)
122	=$B$7*($D$42-D155)/$C$29	=(J155-J156)/($A$41-$A$42)	=$B$7*($D$42-D190)/$C$29	=(J190-J191)/($A$41-$A$42)
123	=$B$7*($D$43-D156)/$C$29	=(J156-J157)/($A$42-$A$43)	=$B$7*($D$43-D191)/$C$29	=(J191-J192)/($A$42-$A$43)
124	=$B$7*($D$44-D157)/$C$29	=(J157-J158)/($A$43-$A$44)	=$B$7*($D$44-D192)/$C$29	=(J192-J193)/($A$43-$A$44)
125	=$B$7*($D$45-D158)/$C$29	=(J158-J159)/($A$44-$A$45)	=$B$7*($D$45-D193)/$C$29	=(J193-J194)/($A$44-$A$45)
126	=$B$7*($D$46-D159)/$C$29	=(J159-J160)/($A$45-$A$46)	=$B$7*($D$46-D194)/$C$29	=(J194-J195)/($A$45-$A$46)
127				
128				
129				
130				
131				
132				
133				
134				
135				w

	K	L	M	N
136	p*dS(P+dP3)/dt	dq(P+dP3)/dx	p*dS(P+dP1)/dt	dq(P+dP1)/dx
137				
138	=$B$7*($D$37-D205)/$C$29	=(J205-J206)/($A$36-$A$37)	=$B$7*($D$37-D238)/$C$29	=(J238-J239)/($A$36-$A$37)
139	=$B$7*($D$38-D206)/$C$29	=(J206-J207)/($A$37-$A$38)	=$B$7*($D$38-D239)/$C$29	=(J239-J240)/($A$37-$A$38)
140	=$B$7*($D$39-D207)/$C$29	=(J207-J208)/($A$38-$A$39)	=$B$7*($D$39-D240)/$C$29	=(J240-J241)/($A$38-$A$39)
141	=$B$7*($D$40-D208)/$C$29	=(J208-J209)/($A$39-$A$40)	=$B$7*($D$40-D241)/$C$29	=(J241-J242)/($A$39-$A$40)
142	=$B$7*($D$41-D209)/$C$29	=(J209-J210)/($A$40-$A$41)	=$B$7*($D$41-D242)/$C$29	=(J242-J243)/($A$40-$A$41)
143	=$B$7*($D$42-D210)/$C$29	=(J210-J211)/($A$41-$A$42)	=$B$7*($D$42-D243)/$C$29	=(J243-J244)/($A$41-$A$42)
144	=$B$7*($D$43-D211)/$C$29	=(J211-J212)/($A$42-$A$43)	=$B$7*($D$43-D244)/$C$29	=(J244-J245)/($A$42-$A$43)
145	=$B$7*($D$44-D212)/$C$29	=(J212-J213)/($A$43-$A$44)	=$B$7*($D$44-D245)/$C$29	=(J245-J246)/($A$43-$A$44)
146	=$B$7*($D$45-D213)/$C$29	=(J213-J214)/($A$44-$A$45)	=$B$7*($D$45-D246)/$C$29	=(J246-J247)/($A$44-$A$45)
147	=$B$7*($D$46-D214)/$C$29	=(J214-J215)/($A$45-$A$46)	=$B$7*($D$46-D247)/$C$29	=(J247-J248)/($A$45-$A$46)
148				
149	p*dS(P+dP2)/dt	dq(P+dP2)/dx		
150				
151	=$B$7*($D$37-D218)/$C$29	=(J218-J219)/($A$36-$A$37)		
152	=$B$7*($D$38-D219)/$C$29	=(J219-J220)/($A$37-$A$38)		
153	=$B$7*($D$39-D220)/$C$29	=(J220-J221)/($A$38-$A$39)		
154	=$B$7*($D$40-D221)/$C$29	=(J221-J222)/($A$39-$A$40)		
155	=$B$7*($D$41-D222)/$C$29	=(J222-J223)/($A$40-$A$41)		
156	=$B$7*($D$42-D223)/$C$29	=(J223-J224)/($A$41-$A$42)		
157	=$B$7*($D$43-D224)/$C$29	=(J224-J225)/($A$42-$A$43)		
158	=$B$7*($D$44-D225)/$C$29	=(J225-J226)/($A$43-$A$44)		
159	=$B$7*($D$45-D226)/$C$29	=(J226-J227)/($A$44-$A$45)		
160	=$B$7*($D$46-D227)/$C$29	=(J227-J228)/($A$45-$A$46)		
161				
162				
163				
164				
165				
166				
167				
168				
169				
170				x

	A
1	
2	**DoIteration**
3	dummy=0
4	IterNum=0
5	Converge=TRUE
6	=WHILE(TRUE)
7	= SET.NAME("ErrValOld",ErrVal)
8	= SET.NAME("ErrVal",GET.CELL(5,'[CELL.XLW]Wrk sht'!$C$32))
9	= IF(OR(ErrVal<0.005,ABS(ErrVal)-ABS(ErrValOld)<0.0005))
10	= BREAK()
11	= END.IF()
12	= CopyForNextIteration()
13	= SET.NAME("IterNum",IterNum+1)
14	= IF(IterNum>10)
15	= SET.NAME("Converge",FALSE)
16	= BREAK()
17	= END.IF()
18	=NEXT()
19	=CopyForNextIteration()
20	=RETURN(Converge)
21	
22	**CopyInitGuess**
23	dummy=0
24	=ECHO(FALSE)
25	=FORMULA(GET.CELL(5,'[CELL.XLW]Wrk sht'!I37),'[CELL.XLW]Wrk sht'!C70)
26	=FORMULA(GET.CELL(5,'[CELL.XLW]Wrk sht'!I38),'[CELL.XLW]Wrk sht'!C71)
27	=FORMULA(GET.CELL(5,'[CELL.XLW]Wrk sht'!I39),'[CELL.XLW]Wrk sht'!C72)
28	=FORMULA(GET.CELL(5,'[CELL.XLW]Wrk sht'!I40),'[CELL.XLW]Wrk sht'!C73)
29	=FORMULA(GET.CELL(5,'[CELL.XLW]Wrk sht'!I41),'[CELL.XLW]Wrk sht'!C74)
30	=FORMULA(GET.CELL(5,'[CELL.XLW]Wrk sht'!I42),'[CELL.XLW]Wrk sht'!C75)
31	=FORMULA(GET.CELL(5,'[CELL.XLW]Wrk sht'!I43),'[CELL.XLW]Wrk sht'!C76)
32	=FORMULA(GET.CELL(5,'[CELL.XLW]Wrk sht'!I44),'[CELL.XLW]Wrk sht'!C77)
33	=FORMULA(GET.CELL(5,'[CELL.XLW]Wrk sht'!I45),'[CELL.XLW]Wrk sht'!C78)
34	=FORMULA(GET.CELL(5,'[CELL.XLW]Wrk sht'!I46),'[CELL.XLW]Wrk sht'!C79)
35	=ECHO(TRUE)
36	=RETURN()
37	
38	**CopyForNextIteration**
39	dummy=0
40	=ECHO(FALSE)
41	=FORMULA(GET.CELL(5,'[CELL.XLW]Wrk sht'!Y58),'[CELL.XLW]Wrk sht'!C70)
42	=FORMULA(GET.CELL(5,'[CELL.XLW]Wrk sht'!Y59),'[CELL.XLW]Wrk sht'!C71)
43	=FORMULA(GET.CELL(5,'[CELL.XLW]Wrk sht'!Y60),'[CELL.XLW]Wrk sht'!C72)
44	=FORMULA(GET.CELL(5,'[CELL.XLW]Wrk sht'!Y61),'[CELL.XLW]Wrk sht'!C73)
45	=FORMULA(GET.CELL(5,'[CELL.XLW]Wrk sht'!Y62),'[CELL.XLW]Wrk sht'!C74)
46	=FORMULA(GET.CELL(5,'[CELL.XLW]Wrk sht'!Y63),'[CELL.XLW]Wrk sht'!C75)
47	=FORMULA(GET.CELL(5,'[CELL.XLW]Wrk sht'!Y64),'[CELL.XLW]Wrk sht'!C76)
48	=FORMULA(GET.CELL(5,'[CELL.XLW]Wrk sht'!Y65),'[CELL.XLW]Wrk sht'!C77)
49	=FORMULA(GET.CELL(5,'[CELL.XLW]Wrk sht'!Y66),'[CELL.XLW]Wrk sht'!C78)
50	=FORMULA(GET.CELL(5,'[CELL.XLW]Wrk sht'!Y67),'[CELL.XLW]Wrk sht'!C79)
51	=ECHO(TRUE)
52	=RETURN()
53	
54	**CopyForNextTimeStep**
55	dummy=0
56	=ECHO(FALSE)
57	=FORMULA(GET.CELL(5,'[CELL.XLW]Wrk sht'!C70),'[CELL.XLW]Wrk sht'!C37)
58	=FORMULA(GET.CELL(5,'[CELL.XLW]Wrk sht'!C71),'[CELL.XLW]Wrk sht'!C38)
59	=FORMULA(GET.CELL(5,'[CELL.XLW]Wrk sht'!C72),'[CELL.XLW]Wrk sht'!C39)
60	=FORMULA(GET.CELL(5,'[CELL.XLW]Wrk sht'!C73),'[CELL.XLW]Wrk sht'!C40)
61	=FORMULA(GET.CELL(5,'[CELL.XLW]Wrk sht'!C74),'[CELL.XLW]Wrk sht'!C41)
62	=FORMULA(GET.CELL(5,'[CELL.XLW]Wrk sht'!C75),'[CELL.XLW]Wrk sht'!C42)

```
     A
63   =FORMULA(GET.CELL(5,'[CELL.XLW]Wrk sht'!C76),'[CELL.XLW]Wrk sht'!C43)
64   =FORMULA(GET.CELL(5,'[CELL.XLW]Wrk sht'!C77),'[CELL.XLW]Wrk sht'!C44)
65   =FORMULA(GET.CELL(5,'[CELL.XLW]Wrk sht'!C78),'[CELL.XLW]Wrk sht'!C45)
66   =FORMULA(GET.CELL(5,'[CELL.XLW]Wrk sht'!C79),'[CELL.XLW]Wrk sht'!C46)
67   =ECHO(TRUE)
68   =RETURN()
69
70   CalcDt
71   dummy=0
72   =SET.NAME("tFact",tFact*2)
73   =WHILE(TRUE)
74   =    SET.NAME("dt",GET.CELL(5,'[CELL.XLW]Wrk sht'!$J$47)*tFact)
75   =    FORMULA(dt,'[CELL.XLW]Wrk sht'!$C$29)
76   =   IF(OR(ISERROR('[CELL.XLW]Wrk sht'!$L$59),ISERROR('[CELL.XLW]Wrk sht'!$L$46)))
77   =         SET.NAME("tFact",tFact/2)
78   =   ELSE.IF(OR(GET.CELL(5,'[CELL.XLW]Wrk sht'!$H$60)>=1,GET.CELL(5,'[CELL.XLW]Wrk sht'!$H$47)>=1))
79   =         SET.NAME("tFact",tFact/2)
80   =   ELSE.IF(OR(GET.CELL(5,'[CELL.XLW]Wrk sht'!$L$59)>2,GET.CELL(5,'[CELL.XLW]Wrk sht'!$L$46)>2))
81   =         SET.NAME("tFact",tFact/2)
82   =    ELSE.IF(AND(NOT(RedistMode),'[CELL.XLW]Wrk sht'!$I$46>'[CELL.XLW]Wrk sht'!$C$47+0.15))
83   =         SET.NAME("tFact",tFact/2)
84   =   ELSE()
85   =             IF(AND(NOT(RedistMode),ABS(GET.CELL(5,'[CELL.XLW]Wrk sht'!$F$26))>=ABS(dq)))
86   =              IF(AND(ElTime>0,ABS(GET.CELL(5,'[CELL.XLW]Wrk sht'!$F$26)-dq)>0.000001))
87   =                 SET.NAME("tFact",tFact/2)
88   =              ELSE()
89   =                 BREAK()
90   =              END.IF()
91   =             ELSE()
92   =               BREAK()
93   =             END.IF()
94   =   END.IF()
95   =NEXT()
96   =IF(AND(ElTime>0,dt>=0.1*ElTime))
97   =     SET.NAME("dt",0.1*ElTime)
98   =     FORMULA(dt,'[CELL.XLW]Wrk sht'!$C$29)
99   =END.IF()
100  =RETURN()
101
102  RecordResult()
103  dummy=0
104  =SET.NAME("TotalTime",GET.CELL(5,'[CELL.XLW]Wrk sht'!$C$26))
105  =IF(OR(LastPrint,TotalTime>tPrint+10^(INT(LOG(ElTime+0.0000001))-1)))
106  =    FORMULA(GET.CELL(5,'[CELL.XLW]Wrk sht'!$C$26),OFFSET([CELL.XLW]Result!$A$6,RecCount,0,1,1))
107  =    FORMULA(GET.CELL(5,'[CELL.XLW]Wrk sht'!$C$31),OFFSET([CELL.XLW]Result!$A$6,RecCount,1,1,1))
108  =    FORMULA(GET.CELL(5,'[CELL.XLW]Wrk sht'!$C$79),OFFSET([CELL.XLW]Result!$A$6,RecCount,2,1,1))
109  =    FORMULA(GET.CELL(5,'[CELL.XLW]Wrk sht'!$D$79),OFFSET([CELL.XLW]Result!$A$6,RecCount,3,1,1))
110  =    FORMULA(GET.CELL(5,'[CELL.XLW]Wrk sht'!$C$78),OFFSET([CELL.XLW]Result!$A$6,RecCount,4,1,1))
111  =    FORMULA(GET.CELL(5,'[CELL.XLW]Wrk sht'!$D$78),OFFSET([CELL.XLW]Result!$A$6,RecCount,5,1,1))
112  =    FORMULA(GET.CELL(5,'[CELL.XLW]Wrk sht'!$C$77),OFFSET([CELL.XLW]Result!$A$6,RecCount,6,1,1))
113  =    FORMULA(GET.CELL(5,'[CELL.XLW]Wrk sht'!$D$77),OFFSET([CELL.XLW]Result!$A$6,RecCount,7,1,1))
114  =    FORMULA(GET.CELL(5,'[CELL.XLW]Wrk sht'!$C$76),OFFSET([CELL.XLW]Result!$A$6,RecCount,8,1,1))
115  =    FORMULA(GET.CELL(5,'[CELL.XLW]Wrk sht'!$D$76),OFFSET([CELL.XLW]Result!$A$6,RecCount,9,1,1))
116  =    FORMULA(GET.CELL(5,'[CELL.XLW]Wrk sht'!$C$75),OFFSET([CELL.XLW]Result!$A$6,RecCount,10,1,1))
117  =    FORMULA(GET.CELL(5,'[CELL.XLW]Wrk sht'!$D$75),OFFSET([CELL.XLW]Result!$A$6,RecCount,11,1,1))
118  =    FORMULA(GET.CELL(5,'[CELL.XLW]Wrk sht'!$C$74),OFFSET([CELL.XLW]Result!$A$6,RecCount,12,1,1))
119  =    FORMULA(GET.CELL(5,'[CELL.XLW]Wrk sht'!$D$74),OFFSET([CELL.XLW]Result!$A$6,RecCount,13,1,1))
120  =    FORMULA(GET.CELL(5,'[CELL.XLW]Wrk sht'!$C$73),OFFSET([CELL.XLW]Result!$A$6,RecCount,14,1,1))
121  =    FORMULA(GET.CELL(5,'[CELL.XLW]Wrk sht'!$D$73),OFFSET([CELL.XLW]Result!$A$6,RecCount,15,1,1))
122  =    FORMULA(GET.CELL(5,'[CELL.XLW]Wrk sht'!$C$72),OFFSET([CELL.XLW]Result!$A$6,RecCount,16,1,1))
123  =    FORMULA(GET.CELL(5,'[CELL.XLW]Wrk sht'!$D$72),OFFSET([CELL.XLW]Result!$A$6,RecCount,17,1,1))
124  =    FORMULA(GET.CELL(5,'[CELL.XLW]Wrk sht'!$C$71),OFFSET([CELL.XLW]Result!$A$6,RecCount,18,1,1))
```

	A
125	= FORMULA(GET.CELL(5,'[CELL.XLW]Wrk sht'!$D$71),OFFSET([CELL.XLW]Result!$A$6,RecCount,19,1,1))
126	= FORMULA(GET.CELL(5,'[CELL.XLW]Wrk sht'!$C$70).OFFSET([CELL.XLW]Result!$A$6.RecCount,20,1,1))
127	= FORMULA(GET.CELL(5,'[CELL.XLW]Wrk sht'!$D$70).OFFSET([CELL.XLW]Result!$A$6.RecCount,21.1,1))
128	= FORMULA(GET.CELL(5,'[CELL.XLW]Wrk sht'!$C$30).OFFSET([CELL.XLW]Result!$A$6,RecCount,22,1,1))
129	= FORMULA(GET.CELL(5,'[CELL.XLW]Wrk sht'!$C$32),OFFSET([CELL.XLW]Result!$A$6,RecCount,23,1,1))
130	= SET.NAME("RecCount",RecCount+1)
131	= SET.NAME("tPrint",tPrint+10^(INT(LOG(ElTime+0.0000001))-1))
132	=END.IF()
133	=RETURN()
134	
135	**RecordInitCond**
136	dummy=0
137	=FORMULA(GET.CELL(5,'[CELL.XLW]Wrk sht'!$C$26),[CELL.XLW]Result!$A$6)
138	=FORMULA(GET.CELL(5,'[CELL.XLW]Wrk sht'!$C$31),[CELL.XLW]Result!$B$6)
139	=FORMULA(GET.CELL(5,'[CELL.XLW]Wrk sht'!$C$46),[CELL.XLW]Result!$C$6)
140	=FORMULA(GET.CELL(5,'[CELL.XLW]Wrk sht'!$D$46),[CELL.XLW]Result!$D$6)
141	=FORMULA(GET.CELL(5,'[CELL.XLW]Wrk sht'!$C$45),[CELL.XLW]Result!$E$6)
142	=FORMULA(GET.CELL(5,'[CELL.XLW]Wrk sht'!$D$45),[CELL.XLW]Result!$F$6)
143	=FORMULA(GET.CELL(5,'[CELL.XLW]Wrk sht'!$C$44),[CELL.XLW]Result!$G$6)
144	=FORMULA(GET.CELL(5,'[CELL.XLW]Wrk sht'!$D$44),[CELL.XLW]Result!$H$6)
145	=FORMULA(GET.CELL(5,'[CELL.XLW]Wrk sht'!$C$43),[CELL.XLW]Result!$I$6)
146	=FORMULA(GET.CELL(5,'[CELL.XLW]Wrk sht'!$D$43),[CELL.XLW]Result!$J$6)
147	=FORMULA(GET.CELL(5,'[CELL.XLW]Wrk sht'!$C$42),[CELL.XLW]Result!$K$6)
148	=FORMULA(GET.CELL(5,'[CELL.XLW]Wrk sht'!$D$42),[CELL.XLW]Result!$L$6)
149	=FORMULA(GET.CELL(5,'[CELL.XLW]Wrk sht'!$C$41),[CELL.XLW]Result!$M$6)
150	=FORMULA(GET.CELL(5,'[CELL.XLW]Wrk sht'!$D$41),[CELL.XLW]Result!$N$6)
151	=FORMULA(GET.CELL(5,'[CELL.XLW]Wrk sht'!$C$40),[CELL.XLW]Result!$O$6)
152	=FORMULA(GET.CELL(5,'[CELL.XLW]Wrk sht'!$D$40),[CELL.XLW]Result!$P$6)
153	=FORMULA(GET.CELL(5,'[CELL.XLW]Wrk sht'!$C$39),[CELL.XLW]Result!$Q$6)
154	=FORMULA(GET.CELL(5,'[CELL.XLW]Wrk sht'!$D$39),[CELL.XLW]Result!$R$6)
155	=FORMULA(GET.CELL(5,'[CELL.XLW]Wrk sht'!$C$38),[CELL.XLW]Result!$S$6)
156	=FORMULA(GET.CELL(5,'[CELL.XLW]Wrk sht'!$D$38),[CELL.XLW]Result!$T$6)
157	=FORMULA(GET.CELL(5,'[CELL.XLW]Wrk sht'!$C$37),[CELL.XLW]Result!$U$6)
158	=FORMULA(GET.CELL(5,'[CELL.XLW]Wrk sht'!$D$37),[CELL.XLW]Result!$V$6)
159	=FORMULA(GET.CELL(5,'[CELL.XLW]Wrk sht'!$C$30),[CELL.XLW]Result!$W$6)
160	=FORMULA(GET.CELL(5,'[CELL.XLW]Wrk sht'!$C$32),[CELL.XLW]Result!$X$6)
161	=RETURN()

	B
1	
2	**SetScenario**
3	dummy=0
4	=IF(DIALOG.BOX(D2:J34))
5	= IF(J4=2)
6	= IF(J7)
7	= InitHydrostatic()
8	= END.IF()
9	= IF(J11)
10	= FORMULA(J12,'[CELL.XLW]Wrk sht'!$C$18)
11	= END.IF()
12	= END.IF()
13	= IF(J34)
14	= Reset()
15	= END.IF()
16	= Simulate()
17	=END.IF()
18	=RETURN()
19	
20	**JustContinue**
21	=Simulate()
22	=RETURN()
23	
24	**InitHydrostatic**
25	dummy=0
26	=SET.NAME("PBot",J9)
27	=FORMULA(PBot,'[CELL.XLW]Wrk sht'!$C$19)
28	ZMax=3
29	=ECHO(FALSE)
30	=FOR("i",1,10)
31	= SET.NAME("ZHi",ZMax-ZMax/10*(i-1))
32	= SET.NAME("ZLo",ZHi-ZMax/10)
33	= SET.NAME("Zi",(ZHi+ZLo)/2)
34	= FORMULA(PBot+Zi,OFFSET('[CELL.XLW]Wrk sht'!$C$37,i-1,0,1,1))
35	=NEXT()
36	=ECHO(TRUE)
37	=FORMULA(0.01,'[CELL.XLW]Wrk sht'!$C$29)
38	tFact=0.001
39	=CopyInitGuess()
40	=DoIteration()
41	=RETURN()
42	
43	**Reset**
44	dummy=0
45	Outflow=0
46	dV=100000
47	RecCount=0
48	ElTime=0
49	RedisTime=0
50	DesatTime=0
51	TotalTime=0
52	CheckSlope=FALSE
53	RedistMode=FALSE
54	tPrint=0
55	LastPrint=FALSE
56	Area='[CELL.XLW]Wrk sht'!$C$16
57	=FORMULA(TotalTime,'[CELL.XLW]Wrk sht'!C26)
58	=FORMULA(DesatTime,'[CELL.XLW]Wrk sht'!C27)
59	=FORMULA(RedisTime,'[CELL.XLW]Wrk sht'!C28)
60	=FORMULA(Outflow,'[CELL.XLW]Wrk sht'!$C$31)
61	=FORMULA(0,'[CELL.XLW]Wrk sht'!$B$20)
62	=RecordInitCond()

```
     B
63   =RETURN()
64
65   Simulate
66   dummy=0
67   =WHILE(TRUE)
68   =  CopyForNextTimeStep()
69   =  CalcDt()
70   =  CopyInitGuess()
71   =  DoIteration()
72   =  SET.NAME("ElTime",ElTime+dt)
73   =   IF(RedistMode)
74   =        SET.NAME("RedisTime",RedisTime+dt)
75   =    ELSE()
76   =        SET.NAME("DesatTime",DesatTime+dt)
77   =   END.IF()
78   =   SET.NAME("TotalTime",TotalTime+dt)
79   =  SET.NAME("dq",GET.CELL(5,'[CELL.XLW]Wrk sht'!$J$81))
80   =  SET.NAME("dV",ABS(dq)*dt*Area)
81   =  SET.NAME("Outflow",Outflow+dV)
82   =  SET.NAME("Slopet",'[CELL.XLW]Wrk sht'!$C$30)
83   =  FORMULA(TotalTime,'[CELL.XLW]Wrk sht'!C26)
84   =  FORMULA(DesatTime,'[CELL.XLW]Wrk sht'!C27)
85   =  FORMULA(RedisTime,'[CELL.XLW]Wrk sht'!C28)
86   =  FORMULA(Outflow,'[CELL.XLW]Wrk sht'!$C$31)
87   =  IF(MaxIsReached())
88   =      SET.NAME("LastPrint",TRUE)
89   =      RecordResult()
90   =      BREAK()
91   =  END.IF()
92   =  IF(AND(J15,OR(AND(J16=1,TotalTime>J19),AND(J16=2,Outflow>J20))))
93   =      IF(NOT(RedistMode))
94   =        SET.NAME("RedistMode",TRUE)
95   =        SET.NAME("ElTime",0)
96   =        SET.NAME("tFact",0.00001)
97   =        FORMULA(1,'[CELL.XLW]Wrk sht'!$B$20)
98   =     END.IF()
99   =  END.IF()
100  =   RecordResult()
101  =NEXT()
102  =RETURN()
103
104  MaxIsReached
105  dummy=0
106  =IF(AND(J24,TotalTime>J27))
107  =     SET.NAME("RCode",TRUE)
108  =ELSE.IF(AND(J25,Outflow>J28))
109  =     SET.NAME("RCode",TRUE)
110  =ELSE.IF(AND(AND(J26,CheckSlope),ABS(Slopet-1)<ABS(1-J29)))
111  =         SET.NAME("RCode",TRUE)
112  =ELSE()
113  =      IF(AND(NOT(CheckSlope),Slopet<0))
114  =          SET.NAME("CheckSlope",TRUE)
115  =     END.IF()
116  =     SET.NAME("RCode",FALSE)
117  =END.IF()
118  =RETURN(RCode)
119
120
121
122
123
124
```

	C	D	E	F	G	H	I	J	K
1							**Scenario Dialog box**		
2					323	341	SIMULATION SCENARIO		
3		14			296	109	Initial Condition		
4		11						2	
5		12					Continue current state		IC continue
6		12					Change to		IC change
7		13	41	53			Hydrostatic profile with	TRUE	IC hydrostatic
8		5	102	72			Pw @ z=0 :		
9		8	184	70	65			35	PBot
10		5	255	72			cm		
11		13	41	92			Applied suction :	TRUE	IC suction
12		8	184	91	65			50	PSuc
13		5	255	94			cm		
14		14	9	116	300	76	Redistribution Criteria		
15		13					Switch to redistribution at	TRUE	
16		11						2	
17		12	40				Elapse time :		Rd elapse time
18		12					Outflow :		Rd outflow
19		8	159	142	65			10	tInitRd
20		8	159	163	65			0.945	qInitRd
21		5	234	144			sec		
22		5	234	165			cm3		
23		14	9	196	299	80	Stop Simulation when		
24		13	25	210			Elapse time:	FALS	Stop at t
25		13	25	231			Outflow :	FALS	Stop outflow
26		13	25	252			Slope :	TRUE	Stop slope
27		8	136	210	73			570	Maxt
28		8	136	231	73			0.945	MaxOutflow
29		8	136	252	74			1.000	MaxSlope
30		5	220	212			second		
31		5	220	233			cm3		
32		1	58	311	88		OK		
33		2	176	311	88		Cancel		
34		13	97	286			Reset Time/OutFlow	TRUE	
35									
36									
37									
38									
39									
40									
41									
42									
43									
44									
45									
46									
47									
48									
49									
50									
51									
52									
53									
54									
55									
56									
57									
58									
59									
60									
61									
62									

B. PRESSURE-SATURATION DATA OBTAINED USING SATURATION EQUILIBRIUM METHOD

B.1. Air-Water Data
B.2. Air-Oil Data

PROJECT	ME-109a
SOIL TYPE	Metea <850u
SYSTEM	Air oil
PROC. NOTE	Reff. for air-oil
DATE	09-Jul-90
rho	1.622 @ 20 deg

PREPARATION DATA 1

Weight of water absorbed by filter paper

SAMPLE NO	WEIGHT OF Air Dry	Saturated	Oil absorbed
1	0.162	0.6832	0.5212
2	0.184	0.7808	0.5968
			0.559

PREPARATION DATA 2

Initial Moisture Content

SAMPLE NO	Tin	Air dry + Tin	Oven dry + Tin	Init. Moisture
1	1.379	5.304	5.250	0.014
2	1.387	3.551	3.510	0.019
3	1.378	2.398	2.382	0.016
				0.016399478

PREPARATION DATA 3 (in gram)

CAPS: 3.994 gram

CELL LABEL	RING	ALL CELL PART	SATURATED CELL,CAPS BOTTOM FILLED	8 AT THE END OF EXPERIMENT
	<1>	<2>	<3>	<4>
1	70.43	409.45	582.44	549.23
2	70.31	406.71	582.05	#N/A
3	70.59	407.70	582.95	549.71
4	71.96	407.59	583.03	550.16
5	70.54	406.52	583.13	550.95

NOTE: Col <1>: Wing nuts + Washer + Rimg + Upper part+ Lwr part + Ovn dry plate + 2 AD Filter paper

Col <3>: <2> +bottom caps + saturated soil+space bellow filled

FINAL PROC DATA

For Residual Moisture Calculation

CELL LABEL	TIN	TIN, BRAS RING, MO-IST SMPL	TIN, BRAS RING, OVN DRY SMPL
	<5>	<6>	<7>
1	6.97	186.89	176.37
2	7.71	#N/A	#N/A
3	6.97	187.03	176.45
4	6.82	188.61	177.84
5	6.91	187.84	176.64

PRESSURE DATA

Pressure :	7.5	7.5	15	15	30	30
Date :	12-Jul	13-Jul	13-Jul	14-Jul	14-Jul	16-Jul
Time :	01:14 PM	11:28 AM	11:29 AM	12:25 PM	02:47 PM	10:20 AM
Temperature :	22	23	23	23	23	23
Step:	--START--	---END---	--START--	---END---	--START--	---END---
CELL	<8a>	<8a>	<8b>	<8b>	<8c>	<8c>
1	9.74	11.87	11.87	21.01	9.47	21.40
2	9.55	11.14	11.14	19.61	9.48	19.65
3	10.65	15.60	15.60	24.12	9.18	17.70
4	10.43	12.11	12.11	20.96	9.30	19.13
5	9.12	11.10	11.10	19.21	10.31	20.72

Pressure :	40	40	50	50	75	75
Date :	16-Jul	17-Jul	17-Jul	18-Jul	18-Jul	19-Jul
Time :	12:16 PM	10:20 AM	10:27 AM	11:50 AM	11:50 AM	09:16 AM
Temperature :	23	23	23	23	23	23
Step:	--START--	---END---	--START--	---END---	--START--	---END---
CELL	<8d>	<8d>	<8e>	<8e>	<8f>	<8f>
1	9.54	12.45	12.45	16.76	16.76	17.62
2	9.34	#N/A	#N/A	#N/A	#N/A	#N/A
3	9.66	13.16	13.16	15.82	15.82	17.65
4	9.07	13.88	13.88	17.14	17.14	18.09
5	10.50	16.31	16.31	18.49	18.49	19.14

Pressure :	100	100	238	238
Date :	19-Jul	20-Jul	20-Jul	21-Jul
Time :	10:39 AM	10:33 AM	10:39 AM	10:33 AM
Temperature :	23	23	23	23
Step:	--START--	---END---	--START--	---END---
CELL	<8g>	<8g>	<8h>	<8h>
1	9.62	11.52	11.52	12.29
2	#N/A	#N/A	#N/A	#N/A
3	9.65	12.17	12.17	12.41
4	9.09	10.67	10.67	11.97
5	10.14	11.85	11.85	12.82

DATA REDUCTION 1

Bulk Density

CELL	OVEN DRY SOIL WGT	BULK DENSITY
	<9>	<10>
1	98.97	1.453
2	#N/A	#N/A
3	98.89	1.452
4	99.06	1.454
5	99.19	1.456

Note: Ring Vol: 68.119 cm3

DATA REDUCTION 2

Residual Moisture Content

CELL	RESIDUAL MOISTURE CONTENT	INITIAL MOISTURE CONTENT	WATER RELEASED	WATER COLLECTED	MASS BALLANCE
	<11>=6-7	<12>=11+13	<13>=3-4	<14>=sum(d8)	<15>=(14-13)/12
1	10.52	43.73	33.21	33.95	1.69
2	#N/A	#N/A	#N/A	#N/A	#N/A
3	10.58	43.82	33.24	32.74	-1.14
4	10.77	43.64	32.87	32.26	-1.40
5	11.20	43.38	32.18	31.82	-0.83

WEIGHT OF MOISTURE LOSS

PRE:	7.5	15	30	40	50	75	100	238
CELL								
AT EACH STEP								
1	2.13	9.14	11.93	2.91	4.31	0.86	1.90	0.77
2	1.59	8.47	10.17	#N/A	#N/A	#N/A	#N/A	#N/A
3	4.95	8.52	8.52	3.50	2.66	1.83	2.52	0.24
4	1.68	8.85	9.83	4.81	3.26	0.95	1.58	1.30
5	1.98	8.11	10.41	5.81	2.18	0.65	1.71	0.97
ACCUMULATIVE								
1	2.13	9.14	11.93	2.91	4.31	0.86	1.90	0.77
2	3.72	17.61	22.10	#N/A	#N/A	#N/A	#N/A	#N/A
3	7.08	17.66	20.45	6.41	6.97	2.69	4.42	1.01
4	3.81	17.99	21.76	7.72	7.57	1.81	3.48	2.07
5	4.11	17.25	22.34	8.72	6.49	1.51	3.61	1.74

VOLUMETRIC MOISTURE CONTENT

PRE:	1E-07	7.5	15	30	40	50	75	100	238
CELL									
1	0.402	0.383	0.300	0.193	0.166	0.127	0.119	0.102	0.095
2	#N/A	#N/A	#N/A	#N/A	#N/A	#N/A	#N/A	#N/A	#N/A
3	0.392	0.347	0.270	0.193	0.161	0.137	0.121	0.098	0.096
4	0.389	0.374	0.294	0.205	0.162	0.132	0.124	0.109	0.097
5	0.389	0.371	0.298	0.204	0.151	0.132	0.126	0.110	0.101
AVG	#N/A	#N/A	#N/A	#N/A	#N/A	#N/A	#N/A	#N/A	#N/A
STD'	#N/A	#N/A	#N/A	#N/A	#N/A	#N/A	#N/A	#N/A	#N/A

DEGREE OF SATURATION

1	1.00	0.95	0.75	0.48	0.41	0.32	0.30	0.25	0.24
2	#N/A	#N/A	#N/A	#N/A	#N/A	#N/A	#N/A	#N/A	#N/A
3	1.00	0.89	0.69	0.49	0.41	0.35	0.31	0.25	0.24
4	1.00	0.96	0.76	0.53	0.42	0.34	0.32	0.28	0.25
5	1.00	0.95	0.77	0.52	0.39	0.34	0.32	0.28	0.26

PROJECT	ME-109
SOIL TYPE	Metea
SYSTEM	Air Water
PROC. NOTE	Replica #1 of 108 reff. for aw
DATE	29-Sep-90
rho	1.021 @ 20 deg

PREPARATION DATA 1

Weight of water absorbed by filter paper

SAMPLE NO	WEIGHT OF Air Dry	Saturated	Water absorbed
1	0.171	0.427	0.256
2	0.194	0.488	0.294
			0.275

PREPARATION DATA 2

Initial Moisture Content

SAMPLE NO	Tin	Moist soil+Tin	Oven dry + Tin	Init. Moisture
1	0.920	7.210	6.860	0.059
2	0.920	3.280	3.150	0.058
3	0.910	4.190	4.040	0.048
				0.055047282

PREPARATION DATA 3 (in gram)

CAPS: 8.201 gram

CELL . LABEL	RING	ALL CELL PART	SATURATED CELL,CAPS OTTOM FILLE	8 AT THE END OF EXPERIMENT
	<1>	<2>	<3>	<4>
1	70.39	399.76	552.99	532.29
2	73.27	396.88	555.03	532.23
3	69.43	397.74	555.70	534.13
4	72.81	397.08	553.85	533.78
5	73.50	393.05	552.38	531.33

NOTE: Col <1>: Wing nuts + Washer + Rimg + Upper part+ Lwr part + Ovn dry plate + 2 AD Filter paper

Col <3>: <2> +bottom caps + saturated soil+space bellow

FINAL PROC DATA

For Residual Moisture Calculation

CELL LABEL	TIN	TIN, BRAS RING, MO-IST SMPL	TIN, BRAS RING, OVN DRY SMPL
	<5>	<6>	<7>
1	3.83	177.51	172.51
2	3.83	180.44	174.43
3	3.83	176.40	171.74
4	3.81	180.52	175.99
5	3.81	181.36	176.19

DATA REDUCTION 2

Residual Moisture Content

CELL	.RESIDUAL MOISTURE CONTENT	INITIAL MOISTURE CONTENT	WATER RELEASED	WATER COLLECTED	MASS BALLANCE
	<11>=6-7	<12>=11+13	<13>=3-4	<14>=sum(d8)	<15>=(14-13)/12
1	5.00	25.70	20.70	21.13	1.68
2	6.01	28.81	22.80	22.53	-0.94
3	4.66	26.23	21.57	21.12	-1.72
4	4.53	24.60	20.07	20.19	0.49
5	5.17	26.22	21.05	21.70	2.48

WEIGHT OF MOISTURE LOSS

PRESS CELL	17	49	66	89	117	167	317	717
AT EACH STEP								
1	0.73	5.60	6.97	1.97	1.42	2.07	2.04	0.33
2	0.92	1.72	8.80	5.03	2.74	1.18	2.06	0.08
3	0.60	6.40	6.40	1.53	2.69	0.93	1.80	0.77
4	0.96	5.99	6.64	1.43	2.01	1.13	1.74	0.29
5	1.09	1.02	9.62	4.03	1.72	0.95	2.56	0.71
ACCUMULATIVE								
1	0.73	6.33	13.30	15.27	16.69	18.76	20.80	21.13
2	0.92	2.64	11.44	16.47	19.21	20.39	22.45	22.53
3	0.60	7.00	13.40	14.93	17.62	18.55	20.35	21.12
4	0.96	6.95	13.59	15.02	17.03	18.16	19.90	20.19
5	1.09	2.11	11.73	15.76	17.48	18.43	20.99	21.70

VOLUMETRIC MOISTURE CONTENT

PRESS CELL	0	17	49	66	89	117	167	317	717
1	0.384	0.373	0.291	0.188	0.159	0.139	0.108	0.078	0.073
2	0.419	0.406	0.380	0.251	0.177	0.137	0.120	0.089	0.088
3	0.378	0.370	0.276	0.182	0.159	0.120	0.106	0.080	0.068
4	0.363	0.349	0.261	0.163	0.142	0.113	0.096	0.071	0.067
5	0.394	0.378	0.363	0.222	0.163	0.138	0.124	0.086	0.076
AVG	0.388	0.375	0.314	0.201	0.160	0.129	0.111	0.081	0.075
STDV	0.019	0.018	0.048	0.031	0.011	0.011	0.010	0.007	0.008

DEGREE OF SATURATION

1	1.00	0.97	0.76	0.49	0.42	0.36	0.28	0.20	0.19
2	1.00	0.97	0.91	0.60	0.42	0.33	0.29	0.21	0.21
3	1.00	0.98	0.73	0.48	0.42	0.32	0.28	0.21	0.18
4	1.00	0.96	0.72	0.45	0.39	0.31	0.27	0.20	0.18
5	1.00	0.96	0.92	0.56	0.41	0.35	0.31	0.22	0.19

PRESSURE DATA

Pressure :	17		49		66	
Date :	01-Aug	02-Aug	02-Aug	03-Aug	03-Aug	05-Aug
Time :	01:40 PM	11:28 AM	11:28 AM	11:17 AM	11:17 AM	01:30 AM
Temperature :	22	23	23	23	23	23
Step:	--START--	---END---	--START--	---END---	--START--	---END---
CELL						
1	10.40	11.13	11.13	16.73	9.35	16.32
2	9.37	10.29	10.29	12.01	9.86	18.66
3	9.65	10.25	10.25	16.65	9.45	15.85
4	10.01	10.97	10.97	16.96	10.12	16.76
5	9.32	10.41	10.41	11.43	9.18	18.80

Pressure :	89		117		167	
Date :	05-Aug	06-Aug	06-Aug	07-Aug	07-Aug	08-Aug
Time :	01:30 AM	11:34 AM	11:34 AM	01:57 PM	01:57 PM	01:57 PM
Temperature :	23	23	23	23	23	23
Step:	--START--	---END---	--START--	---END---	--START--	---END---
CELL						
1	9.65	11.62	11.62	13.04	13.04	15.11
2	9.12	14.15	14.15	16.89	16.89	18.07
3	9.56	11.09	11.09	13.78	13.78	14.71
4	9.88	11.31	11.31	13.32	13.32	14.45
5	9.21	13.24	13.24	14.96	14.96	15.91

Pressure :	317		717	
Date :	08-Aug	09-Aug	09-Aug	10-Aug
Time :	01:57 PM	12:50 PM	12:50 PM	12:50 PM
Temperature :	23	23	23	23
Step:	--START--	---END---	--START--	---END---
CELL				
1	15.11	17.15	9.43	9.76
2	18.07	20.13	9.45	9.53
3	14.71	16.51	10.05	10.82
4	14.45	16.19	10.11	10.40
5	15.91	18.47	9.32	10.03

DATA REDUCTION 1

Bulk Density

CELL	OVEN DR SOIL WG	BULK DENSITY
	<9>	<10>
1	98.29	1.443
2	97.33	1.429
3	98.48	1.446
4	99.37	1.459
5	98.88	1.452

Note: Ring Vol: 68.119

C. REGRESSION OUTPUT

SPSS Result
Air-Water System

A. Saturation Equilibrium

A.1. Cell 1

```
Nonlinear Regression Summary Statistics     Dependent Variable SE_S1
  Source                      DF  Sum of Squares  Mean Square
  Regression                   3         3.21827       1.07276
  Residual                     6   2.095629E-03   3.492714E-04
  Uncorrected Total            9         3.22037
  (Corrected Total)            8          .79303
  R squared = 1 - Residual SS / Corrected SS =     .99736

                                                Asymptotic 95 %
                               Asymptotic     Confidence Interval
  Parameter    Estimate        Std. Error     Lower          Upper
  SR          .185867309     .016738882    .144908741    .226825877
  A           .023725148     .001067714    .021112546    .026337751
  N          2.608953612     .153587725   2.233137989   2.984769236

  Asymptotic Correlation Matrix of the Parameter Estimates
                  SR         A          N
  SR          1.0000     -.1204      .7100
  A           -.1204     1.0000     -.6550
  N            .7100     -.6550     1.0000
```

A.2. Cell 2

```
Nonlinear Regression Summary Statistics     Dependent Variable SE_S2
  Source                      DF  Sum of Squares  Mean Square
  Regression                   3         3.59751       1.19917
  Residual                     6   1.829279E-03   3.048798E-04
  Uncorrected Total            9         3.59934
  (Corrected Total)            8          .85753
  R squared = 1 - Residual SS / Corrected SS =     .99787

                                                Asymptotic 95 %
                               Asymptotic     Confidence Interval
  Parameter    Estimate        Std. Error     Lower          Upper
  SR          .223956252     .012046083    .194480548    .253431956
  A           .017169866     .000465797    .016030102    .018309629
  N          3.759266303     .232879374   3.189431003   4.329101604

  Asymptotic Correlation Matrix of the Parameter Estimates
                  SR         A          N
  SR          1.0000      .0872      .5541
  A            .0872     1.0000     -.5472
  N            .5541     -.5472     1.0000
```

A.3. Cell 3

```
Nonlinear Regression Summary Statistics     Dependent Variable SE_S3
  Source                      DF  Sum of Squares  Mean Square
  Regression                   3         3.13448       1.04483
  Residual                     6   2.192198E-03   3.653664E-04
  Uncorrected Total            9         3.13667
  (Corrected Total)            8          .80941
  R squared = 1 - Residual SS / Corrected SS =     .99729
```

```
                                          Asymptotic 95 %
                             Asymptotic     Confidence Interval
Parameter     Estimate       Std. Error     Lower          Upper
SR            .179457012     .016845170    .138238366     .220675657
A             .024686491     .001141628    .021893028     .027479954
N            2.611190050     .156043455   2.229365469    2.993014630

Asymptotic Correlation Matrix of the Parameter Estimates
                  SR          A           N
SR             1.0000      -.1260       .7096
A              -.1260      1.0000      -.6586
N               .7096      -.6586      1.0000
```

A.4. Cell 4

```
Nonlinear Regression Summary Statistics      Dependent Variable SE_S4
  Source                      DF   Sum of Squares   Mean Square
  Regression                   3          3.01430       1.00477
  Residual                     6     1.613228E-03  2.688714E-04
  Uncorrected Total            9          3.01592
  (Corrected Total)            8           .82072
  R squared = 1 - Residual SS / Corrected SS =      .99803

                                          Asymptotic 95 %
                             Asymptotic     Confidence Interval
Parameter     Estimate       Std. Error     Lower          Upper
SR            .175272285     .013755495    .141613801     .208930769
A             .025508022     .000986397    .023094396     .027921649
N            2.681842856     .137600831   2.345145753    3.018539960

Asymptotic Correlation Matrix of the Parameter Estimates
                  SR          A           N
SR             1.0000      -.1170       .6982
A              -.1170      1.0000      -.6552
N               .6982      -.6552      1.0000
```

A.5. Cell 5

```
Nonlinear Regression Summary Statistics      Dependent Variable SE_S5
  Source                      DF   Sum of Squares   Mean Square
  Regression                   3          3.53873       1.17958
  Residual                     6     7.839523E-03  1.306587E-03
  Uncorrected Total            9          3.54657
  (Corrected Total)            8           .86994
  R squared = 1 - Residual SS / Corrected SS =      .99099

                                          Asymptotic 95 %
                             Asymptotic     Confidence Interval
Parameter     Estimate       Std. Error     Lower          Upper
SR            .219392728     .025020222    .158170451     .280615005
A             .017738378     .001020385    .015241585     .020235171
N            3.674507015     .461516478   2.545216874    4.803797155

Asymptotic Correlation Matrix of the Parameter Estimates
                  SR          A           N
SR             1.0000       .0830       .5612
A               .0830      1.0000      -.5479
N               .5612      -.5479      1.0000
```

A.6. SE all

```
Nonlinear Regression Summary Statistics     Dependent Variable SE_S
  Source                  DF  Sum of Squares  Mean Square
  Regression               3        16.45007      5.48336
  Residual                42          .06880   1.637981E-03
  Uncorrected Total       45        16.51887
  (Corrected Total)       44         4.17228
  R squared = 1 - Residual SS / Corrected SS =     .98351

                                              Asymptotic 95 %
                               Asymptotic     Confidence Interval
  Parameter    Estimate        Std. Error     Lower          Upper
  SR           .193063491     .014628308    .163542370    .222584612
  A            .021273045     .000791200    .019676340    .022869751
  N           2.907024543     .168339440   2.567301800   3.246747286

  Asymptotic Correlation Matrix of the Parameter Estimates
                     SR           A           N
  SR              1.0000      -.0372       .6603
  A               -.0372      1.0000      -.6124
  N                .6603      -.6124      1.0000
```

B. Presure Equilibrium

B.1. Cell 1

```
Nonlinear Regression Summary Statistics     Dependent Variable PE_S1
  Source                  DF  Sum of Squares  Mean Square
  Regression               3         8.72360      2.90787
  Residual                15          .01589   1.059621E-03
  Uncorrected Total       18         8.73949
  (Corrected Total)       17         1.17524
  R squared = 1 - Residual SS / Corrected SS =     .98648

                                              Asymptotic 95 %
                               Asymptotic     Confidence Interval
  Parameter    Estimate        Std. Error     Lower          Upper
  SR           .265765467     .022804424    .217158987    .314371947
  A            .021889159     .000655873    .020491200    .023287119
  N           3.134065543     .258524024   2.583034630   3.685096456

  Asymptotic Correlation Matrix of the Parameter Estimates
                     SR           A           N
  SR              1.0000       .3154       .7042
  A                .3154      1.0000      -.1477
  N                .7042      -.1477      1.0000
```

B.2. Cell 2

```
Nonlinear Regression Summary Statistics     Dependent Variable PE_S2
  Source                  DF  Sum of Squares  Mean Square
  Regression               3         8.18419      2.72806
  Residual                15          .01149   7.657700E-04
  Uncorrected Total       18         8.19568
  (Corrected Total)       17         1.15263
  R squared = 1 - Residual SS / Corrected SS =     .99003
```

```
                                         Asymptotic 95 %
                          Asymptotic    Confidence Interval
Parameter    Estimate     Std. Error     Lower        Upper
SR          .265465274    .016785044   .229688800    .301241747
A           .024563224    .000477704   .023545022    .025581426
N          3.943358281    .271261578  3.365177913   4.521538649

Asymptotic Correlation Matrix of the Parameter Estimates
                SR          A          N
SR          1.0000      .3820      .6094
A            .3820     1.0000     -.1490
N            .6094     -.1490     1.0000
```

B.3. Cell 3

```
Nonlinear Regression Summary Statistics     Dependent Variable PE_S3
  Source                  DF  Sum of Squares  Mean Square
  Regression               3        8.46954       2.82318
  Residual                15         .01051   7.008422E-04
  Uncorrected Total       18        8.48006
  (Corrected Total)       17         .94411
  R squared = 1 - Residual SS / Corrected SS =     .98887

                                         Asymptotic 95 %
                          Asymptotic    Confidence Interval
Parameter    Estimate     Std. Error     Lower        Upper
SR          .236929406    .025652718   .182251932    .291606881
A           .023017836    .000700355   .021525065    .024510607
N          2.724943257    .165280030  2.372657212   3.077229303

Asymptotic Correlation Matrix of the Parameter Estimates
                SR          A          N
SR          1.0000      .3217      .7502
A            .3217     1.0000     -.2121
N            .7502     -.2121     1.0000
```

B.4. Cell 4

```
Nonlinear Regression Summary Statistics     Dependent Variable PE_S4
  Source                  DF  Sum of Squares  Mean Square
  Regression               3        8.76843       2.92281
  Residual                15         .02138   1.425210E-03
  Uncorrected Total       18        8.78981
  (Corrected Total)       17         .98161
  R squared = 1 - Residual SS / Corrected SS =     .97822

                                         Asymptotic 95 %
                          Asymptotic    Confidence Interval
Parameter    Estimate     Std. Error     Lower        Upper
SR          .224802526    .025355605   .170758333    .278846720
A           .020010398    .000487883   .018970500    .021050296
N          3.908730532    .361630200  3.137934007   4.679527058

Asymptotic Correlation Matrix of the Parameter Estimates
                SR          A          N
SR          1.0000      .4754      .4657
A            .4754     1.0000     -.2153
N            .4657     -.2153     1.0000
```

B.5. Cell 5

```
Nonlinear Regression Summary Statistics     Dependent Variable PE_S5
  Source                  DF  Sum of Squares  Mean Square
  Regression               3        8.37428        2.79143
  Residual                15         .01095   7.299417E-04
  Uncorrected Total       18        8.38523
  (Corrected Total)       17        1.00163
  R squared = 1 - Residual SS / Corrected SS =     .98907

                                              Asymptotic 95 %
                              Asymptotic     Confidence Interval
  Parameter   Estimate      Std. Error      Lower         Upper
  SR          .213951001    .023159461    .164587779    .263314223
  A           .019195945    .000491686    .018147941    .020243949
  N          2.996441761    .184490669   2.603209209   3.389674313

  Asymptotic Correlation Matrix of the Parameter Estimates
                   SR          A          N
  SR           1.0000      .3411      .6888
  A             .3411     1.0000     -.2401
  N             .6888     -.2401     1.0000
```

B.6. Cell 6

```
Nonlinear Regression Summary Statistics     Dependent Variable PE_S6
  Source                  DF  Sum of Squares  Mean Square
  Regression               3        8.31781        2.77260
  Residual                15         .03086   2.057608E-03
  Uncorrected Total       18        8.34867
  (Corrected Total)       17        1.30710
  R squared = 1 - Residual SS / Corrected SS =     .97639

                                              Asymptotic 95 %
                              Asymptotic     Confidence Interval
  Parameter   Estimate      Std. Error      Lower         Upper
  SR          .237359602    .024306009    .185552570    .289166635
  A           .023323244    .000740512    .021744879    .024901608
  N          3.721848523    .483569795   2.691143904   4.752553142

  Asymptotic Correlation Matrix of the Parameter Estimates
                   SR          A          N
  SR           1.0000      .2700      .5130
  A             .2700     1.0000     -.3104
  N             .5130     -.3104     1.0000
```

B.7. Cell 7

```
Nonlinear Regression Summary Statistics     Dependent Variable PE_S7
  Source                  DF  Sum of Squares  Mean Square
  Regression               3        7.42435        2.47478
  Residual                15         .05292   3.528294E-03
  Uncorrected Total       18        7.47728
  (Corrected Total)       17        1.12329
  R squared = 1 - Residual SS / Corrected SS =     .95288

                                              Asymptotic 95 %
                              Asymptotic     Confidence Interval
  Parameter   Estimate      Std. Error      Lower         Upper
  SR          .221494731    .039091195    .138173821    .304815641
  A           .020132438    .000656554    .018733025    .021531851
  N          4.317164518    .764616195   2.687423678   5.946905358
```

```
  Asymptotic Correlation Matrix of the Parameter Estimates
                   SR          A          N
  SR           1.0000      .3580      .6546
  A             .3580     1.0000     -.1672
  N             .6546     -.1672     1.0000
```

B.8. PE All

```
Nonlinear Regression Summary Statistics     Dependent Variable PE_S
  Source                 DF  Sum of Squares  Mean Square
  Regression              3       58.08456       19.36152
  Residual              123         .33164   2.696268E-03
  Uncorrected Total     126       58.41620
  (Corrected Total)     125        7.73521
  R squared = 1 - Residual SS / Corrected SS =      .95713

                                             Asymptotic 95 %
                               Asymptotic     Confidence Interval
  Parameter    Estimate        Std. Error     Lower          Upper
  SR            .229495938     .014684055    .200429752    .258562125
  A             .021847051     .000383119    .021088691    .022605412
  N            3.120371145     .147475130   2.828453167   3.412289123

  Asymptotic Correlation Matrix of the Parameter Estimates
                   SR          A          N
  SR           1.0000      .2799      .6713
  A             .2799     1.0000     -.2870
  N             .6713     -.2870     1.0000
```

C. Pooled SE and PE data

```
Nonlinear Regression Summary Statistics     Dependent Variable S
  Source                 DF  Sum of Squares  Mean Square
  Regression              3       74.52789       24.84263
  Residual              168         .40717   2.423657E-03
  Uncorrected Total     171       74.93507
  (Corrected Total)     170       12.31172
  R squared = 1 - Residual SS / Corrected SS =      .96693

                                             Asymptotic 95 %
                               Asymptotic     Confidence Interval
  Parameter    Estimate        Std. Error     Lower          Upper
  SR            .213898288     .010906972    .192365905    .235430670
  A             .021689960     .000335702    .021027223    .022352698
  N            3.021016281     .110100837   2.803656840   3.238375722

  Asymptotic Correlation Matrix of the Parameter Estimates
                   SR          A          N
  SR           1.0000      .1848      .6725
  A             .1848     1.0000     -.3740
  N             .6725     -.3740     1.0000
```

SPSS Result
Air-Oil System

A. Saturation Equilibrium

A.1. Cell 1

```
  Nonlinear Regression Summary Statistics     Dependent Variable SS1
  Source                 DF  Sum of Squares  Mean Square
  Regression              3         3.14637        1.04879
  Residual                6   1.654965E-03  2.758274E-04
  Uncorrected Total       9         3.14803
  (Corrected Total)       8          .73555
  R squared = 1 - Residual SS / Corrected SS =     .99775

                                           Asymptotic 95 %
                          Asymptotic     Confidence Interval
  Parameter   Estimate    Std. Error     Lower         Upper
  SR          .216736677   .015467300  .178889556  .254583797
  A           .062351208   .002559450  .056088460  .068613957
  N          2.618260450   .140317205 2.274916619 2.961604281

  Asymptotic Correlation Matrix of the Parameter Estimates
                SR         A         N
  SR          1.0000    -.0595     .7526
  A           -.0595    1.0000    -.5531
  N            .7526    -.5531    1.0000
```

A.2. Cell 2

```
Nonlinear Regression Summary Statistics     Dependent Variable SS2
  Source                 DF  Sum of Squares  Mean Square
  Regression              3         3.04630        1.01543
  Residual                6   1.396263E-03  2.327105E-04
  Uncorrected Total       9         3.04769
  (Corrected Total)       8          .61374
  R squared = 1 - Residual SS / Corrected SS =     .99772

                                           Asymptotic 95 %
                          Asymptotic     Confidence Interval
  Parameter   Estimate    Std. Error     Lower         Upper
  SR          .208232505   .019519642  .160469662  .255995348
  A           .079441789   .004012099  .069624537  .089259041
  N          2.134933754   .105663076 1.876385521 2.393481986

  Asymptotic Correlation Matrix of the Parameter Estimates
                SR         A         N
  SR          1.0000    -.2380     .8413
  A           -.2380    1.0000    -.6373
  N            .8413    -.6373    1.0000
--------------------------------------------------------------------
```

A.3. Cell 3

```
Nonlinear Regression Summary Statistics     Dependent Variable SS3
  Source                 DF  Sum of Squares  Mean Square
  Regression              3         3.29934        1.09978
  Residual                6   2.044807E-03  3.408012E-04
  Uncorrected Total       9         3.30139
  (Corrected Total)       8          .69184
  R squared = 1 - Residual SS / Corrected SS =     .99704

                                           Asymptotic 95 %
                          Asymptotic     Confidence Interval
```

```
 Parameter   Estimate    Std. Error     Lower         Upper
 SR          .237269389   .017900322   .193468879   .281069900
 A           .060570293   .002899210   .053476182   .067664404
 N          2.574162336   .157311212  2.189235666  2.959089006

 Asymptotic Correlation Matrix of the Parameter Estimates
                 SR         A          N
 SR          1.0000    -.0662      .7579
 A           -.0662    1.0000     -.5611
 N            .7579    -.5611     1.0000
```

A.4. Cell 4

```
Nonlinear Regression Summary Statistics     Dependent Variable SS4
  Source                 DF  Sum of Squares  Mean Square
  Regression              3        3.31058        1.10353
  Residual                6   2.165306E-03   3.608844E-04
  Uncorrected Total       9        3.31275
  (Corrected Total)       8         .67805
  R squared = 1 - Residual SS / Corrected SS =     .99681

                                           Asymptotic 95 %
                          Asymptotic     Confidence Interval
  Parameter   Estimate    Std. Error     Lower         Upper
  SR          .256779702   .016891314   .215448146   .298111257
  A           .060096911   .002837410   .053154018   .067039803
  N          2.721194994   .176107274  2.290276017  3.152113971

  Asymptotic Correlation Matrix of the Parameter Estimates
                  SR         A          N
  SR          1.0000    -.0316      .7354
  A           -.0316    1.0000     -.5389
  N            .7354    -.5389     1.0000
```

A.5. SE ALL

```
Nonlinear Regression Summary Statistics     Dependent Variable SS_ALL
  Source                 DF  Sum of Squares  Mean Square
  Regression              3       12.79225        4.26408
  Residual               33         .01760   5.334762E-04
  Uncorrected Total      36       12.80986
  (Corrected Total)      35        2.72315
  R squared = 1 - Residual SS / Corrected SS =     .99354

                                           Asymptotic 95 %
                          Asymptotic     Confidence Interval
  Parameter   Estimate    Std. Error     Lower         Upper
  SR          .230852388   .011515977   .207422957   .254281820
  A           .064636301   .001999256   .060568785   .068703818
  N          2.495353457   .094577587  2.302933909  2.687773005

  Asymptotic Correlation Matrix of the Parameter Estimates
                  SR         A          N
  SR          1.0000    -.0941      .7733
  A           -.0941    1.0000     -.5712
  N            .7733    -.5712     1.0000
-----------------------------------------------------------------
```

B. Presure Equilibrium

B.1. Cell 1

```
Nonlinear Regression Summary Statistics     Dependent Variable PS1
  Source                  DF  Sum of Squares  Mean Square
  Regression               3        6.80869        2.26956
  Residual                10         .02558   2.557503E-03
  Uncorrected Total       13        6.83426
  (Corrected Total)       12         .78736
  R squared = 1 - Residual SS / Corrected SS =     .96752

                                              Asymptotic 95 %
                               Asymptotic    Confidence Interval
  Parameter    Estimate        Std. Error     Lower         Upper
  SR           .216224062      .064561620   .072371808    .360076315
  A            .067541880      .005856179   .054493500    .080590260
  N           2.312055769      .301804838  1.639592684   2.984518853

  Asymptotic Correlation Matrix of the Parameter Estimates
                   SR          A          N
  SR           1.0000      .2226      .7835
  A             .2226     1.0000     -.2716
  N             .7835     -.2716     1.0000
```

B.2. Cell 2

```
Nonlinear Regression Summary Statistics     Dependent Variable PS2
  Source                  DF  Sum of Squares  Mean Square
  Regression               3        6.40744        2.13581
  Residual                10         .01025   1.024532E-03
  Uncorrected Total       13        6.41768
  (Corrected Total)       12         .97341
  R squared = 1 - Residual SS / Corrected SS =     .98947

                                              Asymptotic 95 %
                               Asymptotic    Confidence Interval
  Parameter    Estimate        Std. Error     Lower         Upper
  SR           .222122383      .022709674   .171522076    .272722689
  A            .052948823      .001498861   .049609152    .056288493
  N           4.068471978      .344772143  3.300271770   4.836672186

  Asymptotic Correlation Matrix of the Parameter Estimates
                   SR          A          N
  SR           1.0000      .3767      .4367
  A             .3767     1.0000     -.3795
  N             .4367     -.3795     1.0000
```

B.3. Cell 3

```
Nonlinear Regression Summary Statistics     Dependent Variable PS3
  Source                  DF  Sum of Squares  Mean Square
  Regression               3        6.54829        2.18276
  Residual                10   5.794601E-03   5.794601E-04
  Uncorrected Total       13        6.55409
  (Corrected Total)       12         .85967
  R squared = 1 - Residual SS / Corrected SS =     .99326
```

```
                                          Asymptotic 95 %
                            Asymptotic     Confidence Interval
Parameter    Estimate       Std. Error     Lower         Upper
SR           .240359759     .021526053    .192396725    .288322793
A            .068707315     .001834661    .064619436    .072795193
N           3.177073165     .207895561   2.713852990   3.640293341

Asymptotic Correlation Matrix of the Parameter Estimates
                   SR          A          N
SR             1.0000      .3517      .6682
A               .3517     1.0000     -.1998
N               .6682     -.1998     1.0000
```

B.4. Cell 4

```
Nonlinear Regression Summary Statistics     Dependent Variable PS4
  Source                    DF  Sum of Squares  Mean Square
  Regression                 3        6.27705       2.09235
  Residual                  10   2.939531E-03   2.939531E-04
  Uncorrected Total         13        6.27999
  (Corrected Total)         12         .82741
  R squared = 1 - Residual SS / Corrected SS =      .99645

                                          Asymptotic 95 %
                            Asymptotic     Confidence Interval
Parameter    Estimate       Std. Error     Lower         Upper
SR           .270039190     .018093034    .229725398    .310352982
A            .058346729     .001846515    .054232436    .062461022
N           2.464993945     .122208989   2.192695348   2.737292541

Asymptotic Correlation Matrix of the Parameter Estimates
                   SR          A          N
SR             1.0000      .0668      .7907
A               .0668     1.0000     -.4043
N               .7907     -.4043     1.0000
```

B.5. PE All

```
Nonlinear Regression Summary Statistics     Dependent Variable PS_ALL
  Source                    DF  Sum of Squares  Mean Square
  Regression                 3       25.93174       8.64391
  Residual                  49         .15428   3.148614E-03
  Uncorrected Total         52       26.08602
  (Corrected Total)         51        3.45833
  R squared = 1 - Residual SS / Corrected SS =      .95539

                                          Asymptotic 95 %
                            Asymptotic     Confidence Interval
Parameter    Estimate       Std. Error     Lower         Upper
SR           .256510471     .024897608    .206476855    .306544088
A            .063704804     .002514772    .058651180    .068758429
N           2.797045959     .206964647   2.381134929   3.212956988
Asymptotic Correlation Matrix of the Parameter Estimates

                   SR          A          N
SR             1.0000      .2279      .6752
A               .2279     1.0000     -.3471
N               .6752     -.3471     1.0000
```

C. Pooled SE and PE data

```
Nonlinear Regression Summary Statistics     Dependent Variable S_TOTAL
  Source                   DF  Sum of Squares  Mean Square
  Regression                3       38.72051       12.90684
  Residual                 85         .17537   2.063226E-03
  Uncorrected Total        88       38.89588
  (Corrected Total)        87        6.54283
  R squared = 1 - Residual SS / Corrected SS =     .97320

                                              Asymptotic 95 %
                             Asymptotic     Confidence Interval
  Parameter    Estimate      Std. Error     Lower           Upper
  SR           .245726009    .014516142    .216864030    .274587988
  A            .064034385    .001806441    .060442697    .067626074
  N           2.659540349    .123329373   2.414328515   2.904752183

  Asymptotic Correlation Matrix of the Parameter Estimates
                    SR          A          N
  SR            1.0000      .0716      .7271
  A              .0716     1.0000     -.4429
  N              .7271     -.4429     1.0000
```

D. INTERFACIAL TENSION DATA

- D.1. Air-Water System - Metea Soil
- D.2. Oil-wter System - Metea Soil
- D.3. Air-Oil System - Metea Soil
- D.4. Air-Water System - Ottawa Sand
- D.5. Oil-Water System - Ottawa Sand
- D.6. Air-Oil System - Ottawa Sand

Air: (-)
Water: air-water experiment (ME 114 and ME 115)

	me 114 #1/a			me 114 #2/a		
Density=	0.974			0.9836		
Mag Coef=	49.325			50		
	de	ds	γ	de	ds	γ
	109.3	59.8	71.85	111.6	61.8	71.34
	109.1	60.2	70.02	111.4	61.8	70.75
	109.1	60	70.63	111.5	62	70.45
	110	60.6	71.48	111.1	61.7	70.17
	109.9	60.7	70.87	110.9	62	68.72
	109.9	60.5	71.49	110.9	61.6	69.89
	110	61.5	68.79	111.3	61.9	70.16
	110.2	61.3	69.95	111.1	62.1	69.00
	110.2	61.6	69.07	111.1	61.9	69.59
	110	61	70.26	110.7	61.2	70.50
	110.1	61	70.56	110.7	61.1	70.80
	110	61.1	69.96	110.9	61.3	70.78
	109.8	61	69.68	111	61.8	69.59
	109.8	60.9	69.98	111	62	69.01
	109.8	60.8	70.28	111	61.8	69.59
	109.9	60.9	70.27	111	61.8	69.59
	109.7	60.7	70.28	110.9	61.8	69.30
	109.9	60.5	71.49	111	61.8	69.59
AVG			70.38			69.93
STDEV			0.802			0.707

	me 114 #3/a			me 114 #4/a		
Density=	0.9818			0.9766		
Mag Coef=	50.2			49.975		
	de	ds	γ	de	ds	γ
	110	61	68.38	111.1	62.5	67.44
	109.9	61.4	66.94	111.1	62.2	68.29
	109.9	61.2	67.52	111	62.1	68.30
	110.2	61.4	67.79	111.1	62.6	67.16
	110.1	61.4	67.51	111.1	62.7	66.88
	110	61.1	68.09	110.9	62.6	66.61
	110	61.4	67.22	110.9	61.9	68.59
	109.5	61	66.96	110.8	61.7	68.88
	110	61.3	67.51	111	61.8	69.16
	110.2	61	68.95	111	62	68.58
	110.2	61.5	67.50	110.9	61.8	68.88
	110.1	61.5	67.22	110.9	61.9	68.59
	109.8	61.1	67.52	110.3	62.5	65.23
	109.8	61	67.81	110.3	62.4	65.51
	109.5	61.4	65.83	110.4	62.4	65.78
	110	61.8	66.10	110.8	62.2	67.45
	109.9	61.8	65.82	110.9	62.2	67.73
	110	61.8	66.10	110.9	62.3	67.45
AVG			67.26			67.58
STDEV			0.841			1.171

Air: (-)
Water: air-water experiment (ME 114 and ME 115)

	me 115 #1/a			me 115 #2/a		
Density=	0.9576			0.9738		
Mag Coef=	50			49.875		
	de	ds	γ	de	ds	γ
	110.6	60.9	69.23	110	61	68.71
	110.5	61.1	68.35	110	60.9	69.00
	110.5	61.1	68.35	110	61	68.71
	110.9	61	69.80	111.1	61.8	69.53
	110.9	61.1	69.50	111.2	61.6	70.41
	110.9	61.2	69.21	111.1	61.6	70.12
	110.6	61	68.93	110.7	61.2	70.14
	110.6	61.2	68.35	110.6	61.4	69.26
	110.7	61.1	68.93	110.7	61.2	70.14
	110.9	61.4	68.62	111	62	68.66
	111	61.6	68.32	110.9	62.2	67.81
	111	61.7	68.04	111	62	68.66
	110.6	61.1	68.64	110.9	61.9	68.67
	110.7	61	69.22	110.9	61.8	68.96
	110.6	61.2	68.35	110.9	62	68.38
	110.7	61.1	68.93	110.6	61.7	68.39
	110.8	61.1	69.21	110.4	62	66.97
	110.7	61.3	68.34	110.6	62	67.53
AVG			68.80			68.89
STDEV			0.478			0.912

AVG	68.65
STDEV	1.51
N	144.00
t-95	3.411228

	me 115 #3/a			me 115 #4/a		
Density=	0.9721			0.9804		
Mag Coef=	46.66			50.325		
	de	ds	γ	de	ds	γ
	103.1	57.7	67.22	110.5	61.9	66.78
	103.1	57.8	66.92	110.6	62	66.78
	103.1	58	66.32	110.5	61.9	66.78
	103.2	57.8	67.22	112.1	62.5	69.58
	103.2	57.7	67.52	112.2	62.5	69.87
	103.3	57.8	67.52	112.2	62.5	69.87
	103.1	57.6	67.52	112.1	62.5	69.58
	103.1	57.8	66.92	112.3	62.6	69.86
	103.2	57.6	67.83	112.1	62	71.05
	103.1	57.9	66.62	112.1	62.7	69.00
	103.1	57.9	66.62	112.1	62.9	68.43
	103.1	58	66.32	112.2	62.8	69.00
	103	57.9	66.32	112.4	62.5	70.44
	103	57.9	66.32	112.3	62.5	70.15
	103	57.7	66.92	112.3	62.7	69.57
	103.1	57.8	66.92	111.9	62.1	70.17
	103	57.8	66.62	112	61.6	71.96
	103	57.8	66.62	111.9	61.8	71.06
AVG			66.90			69.44
STDEV			0.465			1.431

Oil : Air-oil experiment (ME 124)
Water: oil-water experiment (ME 125)

	#1			#2		
Density=	0.6028			0.5988		
Mag Coef=	43.5			41.75		
	de	ds	γ	de	ds	γ
	93.5	53	38.15	91	52	38.16
	93.5	53.1	37.96	91.1	51.7	38.94
	93.5	53	38.15	91	51.9	38.35
	91.5	52.5	35.40	89.2	51.2	36.24
	91.5	52.5	35.40	89.1	51.5	35.51
	91.6	52.2	36.11	89.3	51.2	36.43
	96.9	54.5	41.82	93.5	52.6	41.96
	96.9	55	40.84	93.7	52.2	43.23
	96.9	54.7	41.42	93.5	52.9	41.35
AVG			38.36			38.91
STDEV			2.365			2.575

	#3			#4		
Density=	0.6068			0.5916		
Mag Coef=	42.817			42.95		
	de	ds	γ	de	ds	γ
	93.5	52.1	41.45	93.4	54.1	36.22
	93.5	52.3	41.04	93.2	54	36.04
	93.5	52.4	40.83	93.3	53.9	36.39
	90.5	51.4	36.95	94	54	37.49
	90.7	51.2	37.71	94	54	37.49
	90.5	51.2	37.33	94.1	54	37.67
	92.7	52.9	38.29	93.1	52.8	38.03
	92.6	52.6	38.67	93	52.7	38.03
	92.5	52.8	38.10	93	52.8	37.84
		AVG	38.93	95.1	54.3	38.99
		STDEV	1.619	95.1	54.1	39.36
				95.1	54.5	38.61
				95.7	54.5	39.75
				95.9	54.5	40.14
				95.8	53.9	41.11
				96.1	55.1	39.38
				96.2	54.8	40.14
				96.2	55.1	39.57
					AVG	38.46
					STDEV	1.454
					AVG	38.62
					STDEV	1.97815
					N	45
					t-95	4.590717

Air: (-)
Oil: air-oil experiment (ME 118)

	me 118 oa # 1			me 118 oa # 2		
Density=	1.598			1.5982		
Mag Coef=	46.824			46.432		
	de	ds	γ	de	ds	γ
	60.1	39.8	24.01	60.9	39.9	25.78
	60.1	39.7	24.16	60.9	39.9	25.78
	60.1	39.4	24.65	60.9	39.7	26.13
	60.5	39.5	25.25	60.7	40.1	25.06
	60.5	39.5	25.25	60.9	39.7	26.13
	60.5	39.5	25.25	60.9	39.9	25.78
	60.5	39.5	25.25	60.9	40.0	25.62
	60.4	39.1	25.73	60.9	40.0	25.62
	60.5	39.3	25.59	60.9	39.9	25.78
AVG			25.02			25.74
STDEV			0.571			0.297

	me 118 oa # 3			me 118 oa # 4		
Density=	1.5746			1.5867		
Mag Coef=	46.396			46.204		
	de	ds	γ	de	ds	γ
	60.6	39.5	25.53	60.9	40.8	24.38
	60.4	39.8	24.65	61.1	40.7	24.92
	60.6	39.5	25.53	61.1	40.8	24.76
	60.5	39.6	25.17	61.0	40.1	25.71
	60.5	39.4	25.51	61.1	39.9	26.25
	60.4	39.5	25.15	61.9	40.2	27.33
	60.7	39.6	25.56	61.0	41.0	24.26
	60.5	39.8	24.84	61.0	41.0	24.26
	60.6	39.8	25.03	61.1	40.9	24.60
AVG			25.22			25.16
STDEV			0.317			0.999

AVG	25.29
STDEV	0.69
N	27.00
t-95	1.650296

Air : (-)
Water: Oil-Water experiment (OS 121 and OS 122)

	os 121 ow #1/a			os 121 ow #2/a		
Density=	0.9844			0.9773		
Mag Coef=	45.975			46		
	de	ds	γ	de	ds	γ
	102.8	56.1	74.43	102.8	56.9	71.15
	102.6	56.6	72.09	102.9	56.7	72.12
	102.7	56.4	73.08	102.9	56.8	71.79
	102.6	56.9	71.10	103.0	56.6	72.78
	102.6	56.5	72.42	102.9	56.6	72.45
	102.6	56.9	71.10	103.1	56.1	74.81
	103.0	57.0	72.06	102.9	57.0	71.14
	102.9	57.2	71.08	102.9	56.9	71.46
	102.9	56.9	72.06	103.0	57.0	71.46
AVG			72.16			72.13
STDEV			1.028			1.089

	os 121 ow #3/a			os 121 ow #4/a		
Density=	0.9769			0.9824		
Mag Coef=	46.275			46.325		
	de	ds	γ	de	ds	γ
	103.3	57.3	70.56	103.8	57.2	72.73
	103.5	56.8	72.84	103.9	57.1	73.38
	103.5	57.0	72.17	103.9	56.9	74.06
	103.7	57.3	71.83	103.4	57.5	70.48
	103.5	57.5	70.55	103.5	57.5	70.79
	103.6	57.1	72.16	103.2	57.4	70.17
	103.4	57.1	71.53	103.8	57.9	70.46
	103.3	57.7	69.30	103.9	57.9	70.77
	103.3	57.1	71.21	104.0	57.6	72.06
AVG			71.35			71.66
STDEV			1.017			1.358

	os 122 ow # 1/a			os 122 ow # 2/a		
Density=	0.9824			0.9832		
Mag Coef=	46.2			46.25		
	de	ds	γ	de	ds	γ
	103.0	57.0	71.21	103.1	56.7	72.42
	103.0	57.1	70.89	103.1	57.0	71.43
	103.1	56.9	71.86	103.1	56.9	71.76
	101.6	57.2	66.25	103.1	56.7	72.42
	101.7	56.9	67.47	103.0	56.6	72.43
	101.9	56.9	68.09	103.0	57.0	71.11
	103.0	57.5	69.61	103.0	57.0	71.11
	102.9	57.5	69.30	103.1	56.8	72.09
	103.0	57.4	69.93	103.1	56.9	71.76
AVG			69.40			71.84
STDEV			1.738			0.507

Air : (-)
Water: Oil-Water experiment (OS 121 and OS 122)

	os 122 ow # 3/a			os 122 ow #4/a		
Density=	0.979			0.9816		
Mag Coef=	47.175			47.675		
	de	ds	γ	de	ds	γ
	106.0	58.5	72.60	105.9	58.0	72.57
	106.0	58.8	71.64	105.9	57.9	72.89
	106.0	58.7	71.96	105.8	58.0	72.25
	106.0	59.0	71.01	105.9	57.5	74.22
	106.0	58.9	71.32	105.7	57.9	72.26
	105.9	58.9	71.01	105.9	57.8	73.22
	106.0	59.0	71.01	105.9	58.0	72.57
	106.0	58.7	71.96	105.9	57.8	73.22
	105.9	59.0	70.70	105.9	58.1	72.24
AVG			71.47			72.83
STDEV			0.580			0.613

AVG	72.14
STDEV	1.432
N	72
t-95	1.661245

Oil : Air-oil experiment (OS 123)
Water: oil-water experiment (OS 122)

	os 122 ow #1			os 122 ow #2		
Density=	0.6179			0.6048		
Mag Coef=	40.825			44.1		
	de	ds	γ	de	ds	γ
	83.1	46.0	37.31	87.9	46.8	38.74
	83.0	46.0	37.10	87.8	46.8	38.54
	83.1	45.9	37.52	87.8	47.0	38.12
	84.2	46.2	39.19	87.2	47.0	36.93
	84.5	46.2	39.84	87.1	46.8	37.15
	84.2	46.0	39.64	87.1	47.0	36.74
	82.8	46.0	36.69	88.8	48.2	37.61
	82.8	46.2	36.28	88.8	48.0	38.02
	82.7	45.9	36.70	88.8	48.2	37.61
AVG			37.81			37.72
STDEV			1.292			0.658

	os 122 ow #3			os 122 ow #4		
Density=	0.6133			0.5827		
Mag Coef=	40.15			43.2		
	de	ds	γ	de	ds	γ
	88.1	50.9	38.49	91.8	50.1	39.79
	88.1	51.6	37.14	91.9	50.1	39.99
	88.0	51.0	38.09	92.0	50.1	40.19
	86.1	50.1	36.08	89.6	48.9	37.90
	86.1	50.0	36.27	89.3	48.7	37.72
	86.0	50.0	36.08	89.4	49.0	37.32
	87.9	51.0	37.89	91.9	50.1	39.99
	87.9	51.0	37.89	91.9	50.0	40.20
	88.0	50.9	38.29	91.9	50.0	40.20
AVG			37.36			39.25
STDEV			0.928			1.152

AVG	38.03
STDEV	1.281291
N	36
t-95	3.00074

Air : (-)
Oil : air-oil experiment (OS 123)

	os 123 ao #1/a			os 123 ao #2/a		
Density=	1.6013			1.5851		
Mag Coef=	47.775			47.275		
	de	ds	γ	de	ds	γ
	62.0	40.5	25.49	62.6	40.9	26.26
	62.1	40.5	25.68	62.7	40.9	26.45
	62.1	40.4	25.85	62.7	40.9	26.45
	62.2	40.7	25.54	62.1	40.6	25.79
	62.3	40.5	26.06	62.2	40.4	26.32
	62.2	40.7	25.54	62.1	40.2	26.47
	62.1	40.6	25.51	62.8	40.8	26.82
	62.1	40.2	26.19	62.7	40.9	26.45
	62.2	40.2	26.38	62.6	40.7	26.60
AVG			25.80			26.40
STDEV			0.314			0.262

	os 123 ao # 3/a			os 123 oa #4/a		
Density=	1.5913			1.5647		
Mag Coef=	46.3			46.25		
	de	ds	γ	de	ds	γ
	62.9	40.5	28.83	61.9	40.1	27.07
	62.6	40.7	27.84	61.8	40.0	27.05
	62.7	40.8	27.86	61.8	40.3	26.52
	61.9	40.9	26.09	61.5	40.0	26.45
	62.0	40.7	26.62	61.6	40.1	26.47
	62.0	40.9	26.28	61.5	40.0	26.45
	62.0	40.5	26.97	61.1	40.3	25.16
	62.0	40.6	26.80	61.1	40.1	25.50
	62.0	40.5	26.97	61.1	40.1	25.50
AVG			27.14			26.24
STDEV			0.825			0.653

AVG	26.40
STDEV	0.75
N	36.00
t-95	1.7623

E. PRESSURE-SATURATION DATA OBTAINED USING PRESSURE EQUILIBRIUM METHOD

E.1. Air-Water Data - Metea Soil.
E.2. Oil-Water Data - Metea Soil.
E.3. Air-Oil Data - Metea Soil.
E.4. Air-Water Data - Ottawa Sand.
E.5. Oil-Water Data - Ottawa Sand
E.6. Air-Oil Data - Ottawa Sand.

ME 114
System A-W
Soil METEA

NO	CELL WEIGHT					TIN			
	EMPTY	PACKED	SATU-RATED	DRAINED		EMPTY	INIT SOIL & RING	OVEN DRY SOIL & RING	RING
				ALL PART	W/O RING & SAMPLE				
<1>	<2>	<3>	<3>	<4>	<5>	<6>	<7>	<8>	<9>
1	394.79	498.63	560.16	534.82	333.45	3.72	182.30	174.70	72.59
2	393.28	497.26	560.47	532.82	333.05	3.68	181.92	174.90	72.61
3	397.01	500.90	562.65	533.48	335.23	3.65	181.06	174.63	72.40
4	396.96	500.87	560.72	532.98	335.34	3.71	182.05	174.76	72.61

Note Caps for column :

<3> = 16.090 gr
<4> = 8.103 gr
<5> = 7.793 gr

NO	Drained Water	Collected Water	Mass Ballance	Residual Water	Absorbed Water	Weight of Soil	Bulk Density
	<10>	<11>	<12>	<13>	<14>	<15>	<16>
1	17.353	20.598	-13.00 %	7.60	24.953	98.390	1.444384
2	19.663	20.224	-2.10 %	7.02	26.683	98.610	1.447614
3*	21.183	20.841	1.24 %	6.43	27.613	98.578	1.447144
4	19.753	20.831	-3.99 %	7.29	27.043	98.437	1.445074

ME114-#1			ME114-#2			ME114-#3			ME114-#4		
W-start	W-end	Volt	W-start	W-end	Volt	W-start	W-end	Volt	W-start	W-end	Volt
		2.253			-9.376			10.505			3.606
9.787	10.685	1.730	9.978	10.183	-9.245	9.967	10.597	10.392	8.988	9.935	3.491
10.685	11.700	1.560	10.183	11.311	-9.145	10.597	11.644	10.263	9.935	11.128	3.334
11.700	12.680	1.550	11.311	12.351	-9.025	11.644	12.918	10.192	11.128	12.050	3.322
12.680	13.689	1.571	12.351	13.401	-8.997	12.918	13.990	10.175	12.050	13.249	3.223
13.689	14.738	1.520	13.401	14.279	-8.947	13.990	14.920	10.118	13.249	14.142	3.254
14.727	15.625	1.520	14.727	15.428	-8.942	14.195	15.796	10.134	14.136	15.259	3.186
15.625	16.761	1.537	15.428	16.397	-8.946	15.796	16.838	10.109	15.259	16.144	3.200
10.138	11.181	1.525	9.613	10.858	-8.933	9.678	10.613	10.115	9.578	10.666	3.174
11.181	11.718	1.491	10.858	12.604	-8.876	10.253	12.253	10.041	10.666	12.056	3.110
11.685	13.977	1.387	12.569	14.263	-8.791	12.197	14.625	9.968	12.047	12.941	2.999
13.977	13.980	1.366	14.263	16.718	-8.629	14.625	15.305	9.934	12.941	15.838	2.865
10.578	11.488	1.262	10.153	12.153	-8.321	9.940	11.949	9.832	10.066	11.016	2.740
11.488	12.507	1.145	12.153	13.431	-8.125	11.949	13.847	9.635	11.016	11.770	2.720
12.493	13.947	0.980	13.415	14.201	-7.935	13.816	14.845	9.434	11.762	12.127	2.642
10.290	13.290	0.735	10.235	10.740	-7.833	10.069	10.464	9.361	10.137	11.902	2.467
10.696	12.332	-0.006	10.219	12.359	-4.812	9.953	11.495	6.986	9.879	10.523	1.942
12.315	14.034	-2.534	10.841	11.245	-3.214	11.473	11.802	6.641	10.714	13.636	-3.110

Calibration

ME114-#1			ME114-#2			ME114-#3			ME114-#4		
P	V-data	V-reg	P	V-data	V-reg	P	V-data	V-reg	P	V-data	V-reg
25	1.78	1.89	25	-9.31	-9.11	25	10.26	10.25	25	3.33	3.35
75	1.18	1.18	75	-8.71	-8.57	75	9.74	9.73	75	2.87	2.85
125	0.52	0.46	125	-8.10	-8.03	125	9.29	9.22	125	2.38	2.34
225	-0.83	-0.97	225	-6.81	-6.95	225	8.25	8.19	225	1.36	1.32
425	-3.65	-3.83	425	-4.59	-4.79	425	6.21	6.14	425	-0.64	-0.70
625	-6.62	-6.70	625	-2.71	-2.63	625	4.14	4.09	625	-2.68	-2.73
825	-9.69	-9.56	825	-0.95	-0.48	825	2.00	2.03	825	-4.79	-4.76
625	-6.77	-6.70	625	-2.59	-2.63	625	4.06	4.09	625	-2.76	-2.73
425	-3.85	-3.83	425	-4.36	-4.79	425	6.08	6.14	425	-0.75	-0.70
225	-0.97	-0.97	225	-6.66	-6.95	225	8.13	8.19	225	1.30	1.32
25	1.76	1.89	25	-9.27	-9.11	25	10.16	10.25	25	3.29	3.35
	-69.82509	157.2298		92.72211	869.2977		-97.38256	1022.989		-98.6732	355.7387

ME114-#1			ME114-#2			ME114-#3			ME114-#4		
dW	MC	Pc	dW	MC	Pc	dW	MC	Pc	dW	MC	Pc
	0.366	-0.09		0.392	-0.06		0.405	-0.01		0.397	-0.08
0.898	0.353	36.43	0.205	0.389	12.08	0.630	0.396	10.99	0.947	0.383	11.27
1.015	0.338	48.30	1.128	0.372	21.35	1.047	0.381	23.55	1.193	0.366	26.76
0.980	0.324	49.00	1.040	0.357	32.48	1.274	0.362	30.47	0.922	0.352	27.95
1.009	0.309	47.53	1.050	0.341	35.08	1.072	0.346	32.12	1.199	0.334	37.71
1.049	0.294	51.10	0.878	0.329	39.71	0.930	0.333	37.67	0.893	0.321	34.66
0.898	0.280	51.10	0.701	0.318	40.18	1.601	0.309	36.11	1.123	0.305	41.37
1.136	0.264	49.91	0.969	0.304	39.81	1.042	0.294	38.55	0.885	0.292	39.98
1.043	0.248	50.75	1.245	0.286	41.01	0.935	0.280	37.96	1.088	0.276	42.55
0.537	0.241	53.12	1.746	0.260	46.30	2.000	0.251	45.17	1.390	0.255	48.87
2.292	0.207	60.38	1.694	0.235	54.18	2.428	0.215	52.28	0.894	0.242	59.82
0.003	0.207	61.85	2.455	0.199	69.20	0.680	0.205	55.59	2.897	0.200	73.04
0.910	0.194	69.11	2.000	0.170	97.76	2.009	0.176	65.52	0.950	0.186	85.37
1.019	0.179	77.28	1.278	0.151	115.93	1.898	0.148	84.71	0.754	0.175	87.35
1.454	0.157	88.80	0.786	0.140	133.55	1.029	0.133	104.28	0.365	0.169	95.04
3.000	0.113	105.91	0.505	0.132	143.01	0.395	0.127	111.39	1.765	0.144	112.31
1.636	0.089	157.65	2.140	0.101	423.12	1.542	0.104	342.67	0.644	0.134	164.12
1.719	0.064	334.17	0.404	0.095	571.29	0.329	0.099	376.27	2.922	0.091	662.61
20.598	0.366	0.00	20.224	0.392	0.00	20.841	0.405	0.00	20.831	0.397	0.00

ME114-#1		ME114-#2		ME114-#3		ME114-#4	
S	P	S	P	S	P	S	P
1.00	0.00	1.00	0.00	1.00	0.00	1.00	0.00
0.96	36.43	0.99	12.08	0.98	10.99	0.97	11.27
0.92	48.30	0.95	21.35	0.94	23.55	0.92	26.76
0.88	49.00	0.91	32.48	0.89	30.47	0.89	27.95
0.84	47.53	0.87	35.08	0.85	32.12	0.84	37.71
0.80	51.10	0.84	39.71	0.82	37.67	0.81	34.66
0.77	51.10	0.81	40.18	0.76	36.11	0.77	41.37
0.72	49.91	0.78	39.81	0.72	38.55	0.74	39.98
0.68	50.75	0.73	41.01	0.69	37.96	0.70	42.55
0.66	53.12	0.66	46.30	0.62	45.17	0.64	48.87
0.56	60.38	0.60	54.18	0.53	52.28	0.61	59.82
0.56	61.85	0.51	69.20	0.51	55.59	0.50	73.04
0.53	69.11	0.43	97.76	0.43	65.52	0.47	85.37
0.49	77.28	0.39	115.93	0.36	84.71	0.44	87.35
0.43	88.80	0.36	133.55	0.33	104.28	0.43	95.04
0.31	105.91	0.34	143.01	0.31	111.39	0.36	112.31
0.24	157.65	0.26	423.12	0.26	342.67	0.34	164.12
0.17	334.17	0.24	571.29	0.25	376.27	0.23	662.61

ME 115
System A-W
Soil METEA

NO	CELL WEIGHT					TIN			
	EMPTY	PACKED	SATU-RATED	DRAINED		EMPTY	INIT SOIL & RING	OVEN DRY SOIL & RING	RING
				ALL PART	W/O RING & SAMPLE				
<1>	<2>	<3>	<3>	<4>	<5>	<6>	<7>	<8>	<9>
1	394.62	499.83	563.03	532.11	334.05	3.69	180.20	174.13	72.48
2	394.19	499.26	562.82	532.88	333.98	3.75	180.92	174.71	72.63
3	396.98	502.01	563.95	534.01	334.31	3.61	180.06	174.84	72.51
4	397.02	501.97	563.22	533.18	334.23	3.69	180.15	174.76	72.59

Note Caps for column :

<3> = 16.090 gr
<4> = 8.113 gr
<5> = 7.793 gr

NO	Drained Water	Collected Water	Mass Ballance	Residual Water	Absorbed Water	Weight of Soil	Bulk Density
	<10>	<11>	<12>	<13>	<14>	<15>	<16>
1	22.943	22.428	1.78 %	6.07	29.013	97.959	1.438057
2	21.963	22.523	-1.99 %	6.21	28.173	98.326	1.443445
3*	21.963	21.610	1.30 %	5.22	27.183	98.718	1.449199
4*	22.063	22.022	0.15 %	5.39	27.453	98.481	1.44572

ME115-#1			ME115-#2			ME115-#3			ME115-#4		
W-start	W-end	Volt	W-start	W-end	Volt	W-start	W-end	Volt	W-start	W-end	Volt
		2.248			-9.376			10.555			3.611
9.090	10.564	1.970	10.221	11.546	-9.212	10.141	11.543	10.448	9.056	10.142	3.510
10.564	11.897	1.860	11.546	12.543	-9.051	11.543	12.663	10.337	10.142	12.228	3.234
11.897	12.399	1.757	12.543	13.943	-8.981	12.663	13.435	10.228	12.228	13.656	3.130
12.399	13.998	1.622	13.943	14.222	-8.933	13.435	14.761	10.119	13.656	14.710	3.134
13.998	14.121	1.612	14.222	15.221	-8.883	14.761	15.201	10.120	14.710	15.613	3.128
14.121	15.025	1.628	15.221	16.705	-8.867	15.201	16.521	10.111	15.613	16.982	3.112
10.122	11.654	1.601	10.023	11.567	-8.859	9.981	10.789	10.110	8.829	9.910	3.105
11.654	12.381	1.618	11.567	12.811	-8.823	10.789	11.987	10.073	9.910	10.676	3.108
13.381	14.441	1.575	12.811	13.654	-8.755	11.987	13.010	10.081	10.676	12.339	3.105
14.441	15.876	1.492	13.654	14.998	-8.699	13.010	15.329	10.017	12.339	13.510	3.080
9.543	10.423	1.470	10.114	11.253	-8.601	10.061	11.379	9.968	13.510	14.598	3.005
10.423	11.781	1.331	11.253	12.986	-8.514	11.379	13.879	9.822	14.598	15.973	2.871
11.668	11.907	1.330	12.986	13.998	-8.387	13.879	15.287	9.321	9.870	11.611	2.678
11.907	14.753	1.290	13.998	15.479	-8.214	15.287	18.675	8.884	11.611	14.217	2.595
9.070	13.991	0.573	10.090	11.567	-8.033	11.113	11.979	8.061	14.217	15.410	2.213
13.291	14.532	-2.596	11.567	14.001	-6.907	11.979	12.078	6.874	15.410	16.518	1.737
14.332	14.586	-5.876	14.001	15.789	-2.411	12.078	12.381	4.415	16.518	16.822	-1.621

Calibration

ME115-#1			ME115-#2			ME115-#3			ME115-#4		
P	**V-data**	**V-reg**	**P**	**V-data**	**V-reg**	**P**	**V-data**	**V-reg**	**P**	**V-data**	**V-reg**
25	1.78	1.89	25	-9.31	-9.11	25	10.26	10.25	25	3.33	3.35
75	1.18	1.18	75	-8.71	-8.57	75	9.74	9.73	75	2.87	2.85
125	0.52	0.46	125	-8.10	-8.03	125	9.29	9.22	125	2.38	2.34
225	-0.83	-0.97	225	-6.81	-6.95	225	8.25	8.19	225	1.36	1.32
425	-3.65	-3.83	425	-4.59	-4.79	425	6.21	6.14	425	-0.64	-0.70
625	-6.62	-6.70	625	-2.71	-2.63	625	4.14	4.09	625	-2.68	-2.73
825	-9.69	-9.56	825	-0.95	-0.48	825	2.00	2.03	825	-4.79	-4.76
625	-6.77	-6.70	625	-2.59	-2.63	625	4.06	4.09	625	-2.76	-2.73
425	-3.85	-3.83	425	-4.36	-4.79	425	6.08	6.14	425	-0.75	-0.70
225	-0.97	-0.97	225	-6.66	-6.95	225	8.13	8.19	225	1.30	1.32
25	1.76	1.89	25	-9.27	-9.11	25	10.16	10.25	25	3.29	3.35
	-69.82509	157.2298		92.72211	869.2977		-97.38256	1022.989		-98.6732	355.7387

ME115-#1			ME115-#2			ME115-#3			ME115-#4		
dW	MC	Pc	dW	MC	Pc	dW	MC	Pc	dW	MC	Pc
	0.426	0.263		0.414	-0.065		0.399	-4.884		0.403	-0.570
1.474	0.404	19.674	1.325	0.394	15.142	1.402	0.378	5.536	1.086	0.387	9.396
1.333	0.385	27.355	0.997	0.379	30.070	1.120	0.362	16.345	2.086	0.356	36.630
0.502	0.377	34.547	1.400	0.359	36.560	0.772	0.351	26.960	1.428	0.335	46.892
1.599	0.354	43.974	0.279	0.355	41.011	1.326	0.331	37.575	1.054	0.320	46.497
0.123	0.352	44.672	0.999	0.340	45.647	0.440	0.325	37.477	0.903	0.307	47.089
0.904	0.339	43.555	1.484	0.318	47.131	1.320	0.305	38.354	1.369	0.287	48.668
1.532	0.316	45.440	1.544	0.296	47.873	0.808	0.294	38.451	1.081	0.271	49.358
0.727	0.306	44.253	1.244	0.277	51.211	1.198	0.276	42.054	0.766	0.260	49.062
1.060	0.290	47.255	0.843	0.265	57.516	1.023	0.261	41.275	1.663	0.235	49.358
1.435	0.269	53.051	1.344	0.245	62.708	2.319	0.227	47.508	1.171	0.218	51.825
0.880	0.256	54.587	1.139	0.229	71.795	1.318	0.208	52.280	1.088	0.202	59.226
1.358	0.236	64.293	1.733	0.203	79.862	2.500	0.171	66.497	1.375	0.182	72.448
0.239	0.233	64.362	1.012	0.188	91.637	1.408	0.150	115.286	1.741	0.156	91.492
2.846	0.191	67.155	1.481	0.167	107.678	3.388	0.100	157.842	2.606	0.118	99.682
4.921	0.119	117.220	1.477	0.145	124.461	0.866	0.088	237.988	1.193	0.100	137.375
1.241	0.100	338.496	2.434	0.109	228.866	0.099	0.086	353.581	1.108	0.084	184.343
0.254	0.097	567.522	1.788	0.083	645.745	0.303	0.082	593.045	0.304	0.080	515.688
22.428	0.426	0.263	22.523	0.414	0.000	21.610	0.389	0.000	22.022	0.402	0.000

ME115-#1		ME115-#2		ME115-#3		ME115-#4	
S	P	S	P	S	P	S	P
1.00	0.26	1.00	0.00	1.00	0.00	1.00	0.00
0.95	19.67	0.95	15.14	0.97	5.54	0.96	9.40
0.90	27.36	0.92	30.07	0.93	16.35	0.89	36.63
0.89	34.55	0.87	36.56	0.90	26.96	0.83	46.89
0.83	43.97	0.86	41.01	0.85	37.57	0.80	46.50
0.83	44.67	0.82	45.65	0.83	37.48	0.76	47.09
0.80	43.55	0.77	47.13	0.78	38.35	0.71	48.67
0.74	45.44	0.72	47.87	0.75	38.45	0.67	49.36
0.72	44.25	0.67	51.21	0.71	42.05	0.65	49.06
0.68	47.26	0.64	57.52	0.67	41.28	0.58	49.36
0.63	53.05	0.59	62.71	0.58	47.51	0.54	51.83
0.60	54.59	0.55	71.79	0.53	52.28	0.50	59.23
0.55	64.29	0.49	79.86	0.44	66.50	0.45	72.45
0.55	64.36	0.46	91.64	0.39	115.29	0.39	91.49
0.45	67.16	0.40	107.68	0.26	157.84	0.29	99.68
0.28	117.22	0.35	124.46	0.23	237.99	0.25	137.37
0.24	338.50	0.26	228.87	0.22	353.58	0.21	184.34
0.23	567.52	0.20	645.74	0.21	593.04	0.20	515.69

ME 116
System 0-W
Soil METEA

NO	CELL WEIGHT							TIN			
			SATURATED CELL		DRAINED				INIT	OVEN DRY	
	EMPTY	PACKED	WATER	WATER & TOP OIL	ALL PART	w/o TOP OIL	w/o RING & SAMPLE	EMPTY	SOIL & RING	SOIL & RING	RING
<1>	<2>	<3>	<4>		<5>	<6>	<7>	<8>	<9>	<10>	<11>
1	402.24	502.85	555.71	574.88	569.65	566.71	351.08	3.72	216.12	172.50	70.16
2	402.98	503.83	555.70	573.90	571.42	568.80	352.47	3.69	216.45	172.58	70.18
3	402.17	503.05	556.07	574.94	571.38	568.58	351.62	3.66	216.70	172.58	70.40
4	400.62	501.47	555.27	571.28	568.11	566.82	349.58	3.72	217.56	173.54	71.06
	Caps:		8.06	16.16	16.107		16.107				

NO	Collected Water	Cell weight at the end		Mass Ballance	Residual Water	Absorbed Water	Weight of Soil	Bulk Density
		by data 1	by data 2					
	<12>	<13>	<14>	<15>	<16>	<17>	<18>	<19>
1	20.57	571.52	569.65	-7.19 %	5.36	25.93	98.615	1.447687
2*	21.30	570.99	571.42	1.62 %	5.42	26.71	98.713	1.449126
3*	20.21	571.35	571.38	0.11 %	7.29	27.50	98.522	1.446322
4*	21.35	568.40	568.11	-1.06 %	6.17	27.52	98.766	1.449904

Note: -1.060957

rho-oil = 1.622

<13> = <4> - <12> . (1- rho oil)

ME116-#1			ME116-#2			ME116-#3			ME116-#4		
W-start	W-end	Volt	W-start	W-end	Volt	W-start	W-end	Volt	W-start	W-end	Volt
		9.928			-9.729			10.394			4.440
10.543	11.489	9.690	10.165	11.164	-9.647	10.063	11.946	10.327	10.034	11.354	4.340
11.489	12.603	9.689	11.164	12.212	-9.611	11.946	12.051	10.306	11.354	12.585	4.329
12.603	13.600	9.753	12.212	13.202	-9.562	12.051	13.015	10.283	12.585	13.331	4.316
13.600	14.535	9.784	13.202	14.194	-9.522	13.015	13.975	10.265	13.331	14.255	4.301
14.535	15.496	9.708	14.194	15.157	-9.508	13.975	15.010	10.253	14.255	15.290	4.292
15.496	16.419	9.677	15.157	16.792	-9.487	15.010	15.837	10.237	15.290	16.212	4.285
16.419	17.385	9.653	16.792	17.755	-9.476	15.837	16.821	10.228	16.212	17.094	4.278
10.556	12.226	9.634	10.210	12.345	-9.454	11.144	12.355	10.214	10.564	12.470	4.251
12.226	14.425	9.594	12.345	14.153	-9.420	12.355	13.939	10.208	12.470	14.307	4.222
14.425	15.125	9.586	14.153	16.138	-9.383	13.939	16.067	10.186	14.307	16.605	4.184
15.125	16.196	9.557	16.138	18.192	-9.276	16.067	17.703	10.169	16.605	18.149	4.111
10.605	11.372	9.535	10.116	12.104	-9.140	9.926	11.939	10.091	10.423	12.303	3.983
11.372	11.946	9.530	12.104	13.410	-8.965	11.939	13.332	9.979	12.303	13.791	3.869
11.946	12.441	9.495	13.410	14.635	-8.808	13.332	14.042	9.908	13.791	14.596	3.782
10.650	13.840	9.394	11.144	12.136	-8.308	10.058	11.866	9.630	11.109	12.680	3.475
10.924	13.987	9.120	10.154	10.368	-6.477	9.937	10.906	9.204	10.273	11.236	2.559

Calibration

ME116-#1			ME116-#2			ME116-#3			ME116-#4		
P	**V-data**	**V-reg**	**P**	**V-data**	**V-reg**	**P**	**V-data**	**V-reg**	**P**	**V-data**	**V-reg**
0	9.84	9.87	0	-9.76	-9.77	0	10.41	10.41	0	4.44	4.45
30	9.48	9.45	30	-9.40	-9.36	25	10.19	10.11	26	4.20	4.18
50	9.21	9.17	50	-9.14	-9.09	50	9.96	9.91	50	4.00	4.01
76	8.85	8.81	75	-8.81	-8.74	70	9.74	9.65	75	3.78	3.78
100	8.52	8.47	100	-8.49	-8.41	75	9.51	9.41	100	3.58	3.57
150	7.80	7.77	152	-7.83	-7.73	100	9.05	8.90	150	3.14	3.13
200	7.07	7.07	201	-6.93	-7.06	199	8.58	8.40	200	2.68	2.69
150	7.73	7.77	152	-7.75	-7.73	149	9.02	8.90	149	3.14	3.13
100	8.45	8.47	100	-8.34	-8.41	100	9.47	9.41	102	3.56	3.57
50	9.15	9.17	50	-8.98	-9.09	75	9.71	9.91	51	4.00	4.01
0	9.84	9.87	0	-9.70	-9.77	1	10.37	10.41	1	4.45	4.45
	-71.51367	705.9433		73.67094	719.8336		-99.77075	1038.381		-114.0087	506.802

ME116-#1			ME116-#2			ME116-#3			ME116-#4		
dW	MC	Pc	dW	MC	Pc	dW	MC	Pc	dW	MC	Pc
	0.381	-4.044		0.392	3.089		0.404	1.364		0.404	0.603
0.946	0.367	12.976	0.999	0.377	9.130	1.883	0.376	8.049	1.320	0.385	12.004
1.114	0.350	13.047	1.048	0.362	11.782	0.105	0.375	10.144	1.231	0.367	13.258
0.997	0.336	8.471	0.990	0.348	15.392	0.964	0.360	12.439	0.746	0.356	14.741
0.935	0.322	6.254	0.992	0.333	18.339	0.960	0.346	14.235	0.924	0.342	16.451
0.961	0.308	11.689	0.963	0.319	19.370	1.035	0.331	15.432	1.035	0.327	17.477
0.923	0.294	13.906	1.635	0.295	20.917	0.827	0.319	17.028	0.922	0.313	18.275
0.966	0.280	15.622	0.963	0.281	21.728	0.984	0.304	17.926	0.882	0.300	19.073
1.670	0.256	16.981	2.135	0.249	23.348	1.211	0.287	19.323	1.906	0.272	22.151
2.199	0.223	19.841	1.808	0.223	25.853	1.584	0.263	19.921	1.837	0.245	25.457
0.700	0.213	20.413	1.985	0.194	28.579	2.128	0.232	22.116	2.298	0.212	29.790
1.071	0.197	22.487	2.054	0.164	36.462	1.636	0.208	23.812	1.544	0.189	38.112
0.767	0.186	24.060	1.988	0.134	46.481	2.013	0.179	31.595	1.880	0.161	52.705
0.574	0.178	24.418	1.306	0.115	59.374	1.393	0.158	42.769	1.488	0.140	65.702
0.495	0.170	26.921	1.225	0.097	70.940	0.710	0.148	49.853	0.805	0.128	75.621
3.190	0.124	34.144	0.992	0.083	107.775	1.808	0.121	77.589	1.571	0.105	110.622
3.063	0.079	53.739	0.214	0.080	242.667	0.969	0.107	120.091	0.963	0.091	215.054
20.571	0.377	0.000	21.297	0.392	3.089	20.210	0.404	1.364	21.352	0.404	0.603

ME116-#1		ME116-#2		ME116-#3		ME116-#4	
S	P	S	P	S	P	S	P
1.00	0.00	1.00	3.09	1.00	1.36	1.00	0.60
0.97	12.98	0.96	9.13	0.93	8.05	0.95	12.00
0.93	13.05	0.92	11.78	0.93	10.14	0.91	13.26
0.89	8.47	0.89	15.39	0.89	12.44	0.88	14.74
0.85	6.25	0.85	18.34	0.86	14.23	0.85	16.45
0.82	11.69	0.81	19.37	0.82	15.43	0.81	17.48
0.78	13.91	0.75	20.92	0.79	17.03	0.78	18.27
0.74	15.62	0.72	21.73	0.75	17.93	0.74	19.07
0.68	16.98	0.64	23.35	0.71	19.32	0.67	22.15
0.59	19.84	0.57	25.85	0.65	19.92	0.61	25.46
0.56	20.41	0.49	28.58	0.58	22.12	0.52	29.79
0.52	22.49	0.42	36.46	0.52	23.81	0.47	38.11
0.49	24.06	0.34	46.48	0.44	31.59	0.40	52.71
0.47	24.42	0.29	59.37	0.39	42.77	0.35	65.70
0.45	26.92	0.25	70.94	0.37	49.85	0.32	75.62
0.33	34.14	0.21	107.78	0.30	77.59	0.26	110.62
0.21	53.74	0.20	242.67	0.27	120.09	0.22	215.05

ME 117
System 0-W
Soil METEA

NO	CELL WEIGHT							TIN			
	EMPTY	PACKED	SATURATED CELL		DRAINED			EMPTY	INIT SOIL & RING	OVEN DRY SOIL & RING	RING
			WATER	WATER & TOP OIL	ALL PART	w/o TOP OIL	w/o RING & SAMPLE				
<1>	<2>	<3>	<4>		<5>	<6>	<7>	<8>	<9>	<10>	<11>
1	402.32	503.41	552.99	571.42	568.44	567.03	350.32	3.87	214.30	172.51	70.16
2	403.10	503.74	552.63	572.21	568.13	565.13	351.72	3.82	213.74	172.38	70.18
3	402.17	503.04	551.69	571.98	566.20	565.53	351.32	3.79	214.27	172.61	70.40
4	400.86	501.70	555.25	568.67	#N/A	#N/A	#N/A	#N/A	#N/A	#N/A	#N/A
Caps:			8.06	16.16	16.107		16.107				

NO	Collected Water	Cell weight at the end by data 1	Cell weight at the end by data 2	Mass Ballance	Residual Water	Absorbed Water	Weight of Soil	Bulk Density
	<12>	<13>	<14>	<15>	<16>	<17>	<18>	<19>
1	20.21	567.83	568.44	2.30 %	6.37	26.58	98.479	1.445691
2	17.90	567.18	568.13	3.75 %	7.34	25.24	98.382	1.444267
3	15.57	565.51	566.20	2.87 %	8.61	24.19	98.418	1.444795
4	#N/A	#N/A	#N/A	#N/A	#N/A	#N/A	#N/A	#N/A

Note:
rho-oil = 1.622
<13> = <4> - <12> . (1- rho oil)

ME117-#1			ME117-#1			ME117-#1			ME117-#1		
W-start	W-end	Volt	W-start	W-end	Volt	W-start	W-end	Volt	W-start	W-end	Volt
		9.823			-12.571			10.279			#N/A
11.509	13.671	9.657	10.519	12.657	-12.520	10.562	12.218	10.254	#N/A	#N/A	#N/A
13.671	15.411	9.554	12.657	14.869	-12.471	12.218	14.422	10.254	#N/A	#N/A	#N/A
15.411	17.476	9.540	14.869	16.719	-12.474	14.422	16.442	10.262	#N/A	#N/A	#N/A
17.476	19.451	9.520	16.719	18.732	-12.450	16.442	18.384	10.256	#N/A	#N/A	#N/A
11.431	14.282	9.503	10.655	13.581	-12.399	10.373	13.261	10.230	#N/A	#N/A	#N/A
14.282	17.202	9.424	13.581	15.733	-12.298	13.261	15.005	10.149	#N/A	#N/A	#N/A
10.239	13.465	9.250	10.597	12.268	-12.168	11.604	11.999	10.053	#N/A	#N/A	#N/A
13.465	14.787	8.962	12.268	13.395	-12.020	11.999	13.215	9.889	#N/A	#N/A	#N/A
12.539	13.653	8.682	10.570	11.927	-11.485	10.270	11.372	9.760	#N/A	#N/A	#N/A
13.653	14.483	8.390	11.927	12.382	-11.270	11.327	11.734	9.645	#N/A	#N/A	#N/A

Calibration

ME117-#1			ME117-#1			ME117-#1			ME117-#1		
P	V-data	V-reg	P	V-data	V-reg	P	V-data	V-reg	P	V-data	V-reg
0	9.82	9.86	0	-12.77	-12.78	0	10.49	10.49	0	4.44	4.45
30	9.47	9.44	30	-12.41	-12.38	35	10.27	10.18	26	4.20	4.18
50	9.19	9.16	50	-12.15	-12.10	50	10.04	9.98	50	4.00	4.01
76	8.84	8.79	75	-11.82	-11.75	50	9.82	9.72	75	3.78	3.78
100	8.50	8.46	100	-11.50	-11.43	75	9.59	9.47	100	3.58	3.57
150	7.78	7.76	152	-10.84	-10.75	100	9.13	8.97	150	3.14	3.13
200	7.05	7.06	201	-9.95	-10.07	199	8.66	8.46	200	2.68	2.69
150	7.71	7.76	152	-10.76	-10.75	149	9.10	8.97	149	3.14	3.13
100	8.43	8.46	100	-11.36	-11.43	100	9.55	9.47	102	3.56	3.57
50	9.13	9.16	50	-11.99	-12.10	75	9.79	9.98	51	4.00	4.01
0	9.83	9.86	0	-12.72	-12.78	1	10.45	10.49	1	4.45	4.45
	-71.51367	704.8706		73.67094	941.7305		-98.76872	1035.715		-114.0087	506.802

ME117-#1			ME117-#1			ME117-#1			ME117-#1		
dW	MC	Pc	dW	MC	Pc	dW	MC	Pc	dW	MC	Pc
	0.390	2.392		0.370	15.613		0.355	20.472		#N/A	#N/A
2.162	0.358	14.263	2.138	0.339	19.370	1.656	0.331	22.941	#N/A	#N/A	#N/A
1.740	0.333	21.629	2.212	0.307	22.980	2.204	0.298	22.941	#N/A	#N/A	#N/A
2.065	0.303	22.630	1.850	0.279	22.759	2.020	0.269	22.151	#N/A	#N/A	#N/A
1.975	0.274	24.060	2.013	0.250	24.527	1.942	0.240	22.743	#N/A	#N/A	#N/A
2.851	0.232	25.276	2.926	0.207	28.284	2.888	0.198	25.311	#N/A	#N/A	#N/A
2.920	0.189	30.926	2.152	0.175	35.725	1.744	0.172	33.312	#N/A	#N/A	#N/A
3.226	0.142	43.369	1.671	0.151	45.302	0.395	0.166	42.794	#N/A	#N/A	#N/A
1.322	0.122	63.965	1.127	0.134	56.206	1.216	0.149	58.992	#N/A	#N/A	#N/A
1.114	0.106	83.989	1.357	0.114	95.620	1.102	0.132	71.733	#N/A	#N/A	#N/A
0.830	0.094	104.871	0.455	0.108	111.459	0.407	0.126	83.091	#N/A	#N/A	#N/A
20.205			17.901			15.574			#N/A		

ME 118
System A-O
Soil METEA
Oil-rho 1.622

NO	CELL WEIGHT					TIN			RING
	EMPTY	PACKED	SATU-RATED	DRAINED		EMPTY	INIT SOIL & RING	OVEN DRY SOIL & RING	
				ALL PART	W/O RING & SAMPLE				
<1>	<2>	<3>	<3>	<4>	<5>	<6>	<7>	<8>	<9>
1	402.43	503.78	577.84	543.58		3.86	184.97	174.42	72.57
2	401.80	502.10	576.79	542.23		3.82	185.18	174.40	72.59
3	401.83	502.05	576.74	542.41		3.79	185.16	174.69	72.83
4	400.74	500.80	574.49	541.74		3.85	185.36	174.54	72.61
			16.15	8.06					

Note Caps for column :

<3> = 8.110 gr
<4> = 7.793 gr
<5> = 7.793 gr

NO	Drained Oil	Collected Oil	Mass Ballance	Residual Oil	Absorbed Oil	Weight of Soil	Bulk Density
	<10>	<11>	<12>	<13>	<14>	<15>	<16>
1*	33.94	33.88	0.14 %	10.55	44.49	97.991	1.438527
2*	34.24	35.20	-2.13 %	10.78	45.023	97.993	1.438556
3*	34.01	34.26	-0.56 %	10.47	44.483	98.072	1.439716
4	32.43	31.41	2.37 %	10.82	43.253	98.079	1.439819

ME118-#1			ME118-#2			ME118-#3			ME118-#4		
W-start	W-end	Volt	W-start	W-end	Volt	W-start	W-end	Volt	W-start	W-end	Volt
		9.995			5.479			-3.790			7.283
9.736	11.250	9.788	10.331	11.576	5.748	9.536	11.412	-4.090	9.543	10.916	7.119
11.250	13.790	9.669	11.576	12.601	5.930	11.412	12.529	-4.094	10.916	12.539	7.000
13.790	14.096	9.628	12.601	14.753	5.926	12.529	14.148	-4.174	12.539	13.938	6.970
14.096	16.224	9.685	14.753	17.336	6.019	14.148	16.591	-4.200	13.632	16.632	6.868
16.224	20.004	9.668	17.336	22.742	6.188	16.591	20.990	-4.280	16.632	21.739	6.784
9.623	12.742	9.585	10.095	13.241	6.202	9.901	13.367	-4.320	9.102	13.506	6.621
13.222	16.142	9.414	13.241	16.279	6.304	13.367	16.255	-4.390	13.506	16.447	6.426
16.142	19.753	9.301	16.279	19.838	6.339	16.255	19.242	-4.450	16.447	18.719	6.223
19.753	22.897	9.210	19.838	23.054	6.540	19.242	22.678	-4.680	18.719	21.819	5.934
13.567	17.564	8.971	12.116	17.844	6.614	11.587	14.864	-4.850	12.095	14.835	5.441
17.564	19.710	8.403	17.844	20.952	9.069	14.864	19.626	-5.330	14.835	15.496	4.774
13.221	17.897	5.897	13.142	14.140	13.544	12.586	14.576	-8.330	12.729	15.515	1.790

Calibration

#1			#2			#3			#4		
P	V-data	V-reg	P	V-data	V-reg	P	V-data	V-reg	P	V-data	V-reg
0	9.47	9.90	0	5.70	5.57	0	-3.80	-3.88	0	7.26	7.24
25	9.28	9.31	29	6.46	6.53	24	-4.51	-4.59	25	6.81	6.59
50	8.80	8.73	52	7.09	7.30	52	-5.31	-5.42	50	5.79	5.93
75	8.29	8.15	78	7.87	8.16	71	-5.86	-5.98	75	5.33	5.28
100	7.78	7.56	100	8.59	8.89	104	-6.83	-6.95	101	4.66	4.60
150	6.59	6.39	150	10.33	10.55	150	-8.21	-8.31	150	3.38	3.31
200	5.34	5.23	200	12.07	12.22	200	-9.74	-9.79	200	2.09	2.00
300	2.61	2.89	300	15.90	15.54	301	-12.81	-12.78	301	-0.66	-0.64
193	5.41	5.39	199	12.08	12.18	197	-9.80	-9.70	200	1.94	2.00
101	7.66	7.54	92	8.71	8.63	102	-7.02	-6.90	100	4.55	4.62
51	8.73	8.71	53	7.45	7.33	52	-5.59	-5.42	50	5.85	5.93
0	9.75	9.90	0	6.21	5.57	0	-4.13	-3.88	0	7.11	7.24
	-42.81072	423.7423		30.08064	-167.4496		-33.81624	-131.1726		-38.19555	276.5762

ME118-#1			ME118#2			ME118-#3			ME118-#4		
dW	MC	Pc	dW	MC	Pc	dW	MC	Pc	dW	MC	Pc
	0.403	-4.151		0.407	-2.638		0.403	-3.009		0.391	-1.602
1.514	0.389	4.711	1.245	0.396	5.454	1.876	0.386	7.136	1.373	0.379	4.662
2.540	0.366	9.805	1.025	0.387	10.929	1.117	0.376	7.271	1.623	0.364	9.207
0.306	0.363	11.561	2.152	0.367	10.808	1.619	0.361	9.976	1.399	0.352	10.353
2.128	0.344	9.120	2.583	0.344	13.606	2.443	0.339	10.856	3.000	0.325	14.249
3.780	0.310	9.848	5.406	0.295	18.689	4.399	0.299	13.561	5.107	0.278	17.458
3.119	0.282	13.402	3.146	0.267	19.110	3.466	0.268	14.914	4.404	0.238	23.683
2.920	0.255	20.722	3.038	0.239	22.179	2.888	0.241	17.281	2.941	0.212	31.132
3.611	0.222	25.560	3.559	0.207	23.232	2.987	0.214	19.310	2.272	0.191	38.885
3.144	0.194	29.456	3.216	0.178	29.278	3.436	0.183	27.087	3.100	0.163	49.924
3.997	0.158	39.687	5.728	0.126	31.504	3.277	0.154	32.836	2.740	0.138	68.754
2.146	0.138	64.004	3.108	0.098	105.352	4.762	0.111	49.068	0.661	0.132	94.231
4.676	0.096	171.287	0.998	0.089	239.963	1.990	0.093	150.517	2.786	0.107	208.206
33.881	0.396	0.000	35.204	0.404	0.000	34.260	0.398	0.000	31.406	0.388	0.000

ME811-#1		ME811-#2		ME811-#3		ME811-#4	
S	P	S	P	S	P	S	P
1.00	0.00	1.00	0.00	1.00	0.00	1.00	0.00
0.98	4.71	0.98	5.45	0.97	7.14	0.98	4.66
0.92	9.81	0.96	10.93	0.94	7.27	0.94	9.21
0.92	11.56	0.91	10.81	0.91	9.98	0.91	10.35
0.87	9.12	0.85	13.61	0.85	10.86	0.84	14.25
0.78	9.85	0.73	18.69	0.75	13.56	0.72	17.46
0.71	13.40	0.66	19.11	0.67	14.91	0.61	23.68
0.64	20.72	0.59	22.18	0.61	17.28	0.55	31.13
0.56	25.56	0.51	23.23	0.54	19.31	0.49	38.89
0.49	29.46	0.44	29.28	0.46	27.09	0.42	49.92
0.40	39.69	0.31	31.50	0.39	32.84	0.36	68.75
0.35	64.00	0.24	105.35	0.28	49.07	0.34	94.23
0.24	171.29	0.22	239.96	0.23	150.52	0.28	208.21

OS 119

System **A-W**

Soil **OTAWA**

NO	CELL WEIGHT					TIN			
				DRAINED			INIT	OVEN DRY	
	EMPTY	PACKED	SATU-RATED	ALL PART	W/O RING & SAMPLE	EMPTY	SOIL & RING	SOIL & RING	RING
<1>	<2>	<3>	<3>	<4>	<5>	<6>	<7>	<8>	<9>
1	#N/A	#N/A	#N/A	#N/A	#N/A	#N/A	#N/A	#N/A	#N/A
2	403.46	517.63	565.12	542.55	353.97	3.89	192.47	190.62	72.61
3	402.60	516.77	565.47	542.30	353.93	3.77	192.14	190.22	72.83
4	#N/A	#N/A	#N/A	#N/A	#N/A	#N/A	#N/A	#N/A	#N/A

Note Caps for column :

<3> = 8.840 gr

<4> = 8.650 gr

<5> = 7.793 gr

NO	Drained Water	Collected Water	Mass Ballance	Residual Water	Absorbed Water	Weight of Soil	Bulk Density
	<10>	<11>	<12>	<13>	<14>	<15>	<16>
1	#N/A	#N/A	#N/A	#N/A	#N/A	#N/A	#N/A
2	22.38	22.20	0.76 %	1.85	24.23	114.12	1.675304
3	22.98	23.27	-1.18 %	1.92	24.90	113.62	1.667963
4	#N/A	#N/A	#N/A	#N/A	#N/A	#N/A	#N/A

OS119-#1			OS119-#2			OS119-#3			OS119-#4		
W-start	W-end	Volt	W-start	W-end	Volt	W-start	W-end	Volt	W-start	W-end	Volt
		#N/A			0.007			0.040			#N/A
#N/A	#N/A	#N/A	8.750	9.607	0.210	8.516	9.489	0.150	#N/A	#N/A	#N/A
#N/A	#N/A	#N/A	9.607	10.447	0.270	9.489	10.082	0.160	#N/A	#N/A	#N/A
#N/A	#N/A	#N/A	10.447	11.050	0.320	10.082	10.749	0.180	#N/A	#N/A	#N/A
#N/A	#N/A	#N/A	11.050	11.642	0.390	10.749	11.486	0.200	#N/A	#N/A	#N/A
#N/A	#N/A	#N/A	11.642	13.244	0.480	11.486	13.137	0.210	#N/A	#N/A	#N/A
#N/A	#N/A	#N/A	13.244	15.271	0.520	13.137	15.030	0.220	#N/A	#N/A	#N/A
#N/A	#N/A	#N/A	15.271	19.125	0.590	15.030	18.947	0.240	#N/A	#N/A	#N/A
#N/A	#N/A	#N/A	9.952	12.792	0.680	8.651	12.584	0.280	#N/A	#N/A	#N/A
#N/A	#N/A	#N/A	12.792	16.780	0.740	12.584	16.709	0.330	#N/A	#N/A	#N/A
#N/A	#N/A	#N/A	16.780	18.513	0.910	16.709	17.938	0.370	#N/A	#N/A	#N/A
#N/A	#N/A	#N/A	9.615	11.224	1.040	9.680	11.333	0.390	#N/A	#N/A	#N/A
#N/A	#N/A	#N/A	11.213	11.816	1.640	10.322	11.802	0.850	#N/A	#N/A	#N/A
#N/A	#N/A	#N/A	11.816	12.335	3.430	11.802	12.208	1.600	#N/A	#N/A	#N/A
#N/A	#N/A	#N/A	13.328	13.478	5.840	12.198	11.928	2.740	#N/A	#N/A	#N/A
#N/A	#N/A	#N/A	13.478	13.858	8.000	11.928	12.214	3.840	#N/A	#N/A	#N/A
#N/A	#N/A	#N/A	#N/A	#N/A	#N/A	#N/A	#N/A	#N/A	#N/A	#N/A	#N/A
#N/A	#N/A	#N/A	#N/A	#N/A	#N/A	#N/A	#N/A	#N/A	#N/A	#N/A	#N/A

Calibration

OS119-#1			OS119-#2			OS119-#3			OS119-#4		
P	V-data	P-reg	P	V-data	P-reg	P	V-data	P-reg	P	V-data	P-reg
0	0.01	1.99	0	0.10	-2.83	0	0.04	2.32	0	0.01	-1.23
10	0.10	10.92	10	0.30	7.37	10	0.13	11.27	10	0.08	5.87
25	0.24	24.80	25	0.60	22.67	25	0.26	24.19	25	0.30	28.18
50	0.49	49.60	50	1.07	46.64	50	0.48	46.07	50	0.52	50.50
75	0.74	74.40	75	1.65	76.22	75	0.77	74.90	75	0.75	73.83
100	0.98	98.21	100	2.11	99.68	100	0.99	96.77	100	1.04	103.25
150	1.48	147.81	150	3.16	153.23	150	1.53	150.46	150	1.50	149.91
200	1.99	198.39	200	4.12	202.19	200	2.03	200.17	200	1.98	198.60
300	3.01	299.57	300	6.00	298.07	300	3.04	300.59	300	2.96	298.01
400	4.05	402.73	400	7.88	393.95	400	4.04	400.01	400	3.96	399.44
200	2.00	199.39	200	4.22	207.29	200	2.03	200.17	200	2.02	202.66
100	1.00	100.19	100	2.24	106.31	100	1.04	101.74	100	1.03	102.23
0	0.01	1.99	0	0.14	-0.79	0	0.03	1.33	0	0.01	-1.23
	99.19415	0.998016		50.99949	-7.928676		99.42356	-1.656972		101.4373	-2.248216

OS119-#1			OS119-#2			OS119-#3			OS119-#4		
dW	**S**	**Pc**	**dW**	**S**	**Pc**	**dW**	**S**	**Pc**	**dW**	**S**	**Pc**
	#N/A	#N/A		0.356	-7.572		0.366	2.320		#N/A	#N/A
#N/A	#N/A	#N/A	0.857	0.343	2.781	0.973	0.351	13.257	#N/A	#N/A	#N/A
#N/A	#N/A	#N/A	0.840	0.331	5.841	0.593	0.343	14.251	#N/A	#N/A	#N/A
#N/A	#N/A	#N/A	0.603	0.322	8.391	0.667	0.333	16.239	#N/A	#N/A	#N/A
#N/A	#N/A	#N/A	0.592	0.313	11.961	0.737	0.322	18.228	#N/A	#N/A	#N/A
#N/A	#N/A	#N/A	1.602	0.290	16.551	1.651	0.298	19.222	#N/A	#N/A	#N/A
#N/A	#N/A	#N/A	2.027	0.260	18.591	1.893	0.270	20.216	#N/A	#N/A	#N/A
#N/A	#N/A	#N/A	3.854	0.203	22.161	3.917	0.212	22.205	#N/A	#N/A	#N/A
#N/A	#N/A	#N/A	2.840	0.162	26.751	3.933	0.155	26.182	#N/A	#N/A	#N/A
#N/A	#N/A	#N/A	3.988	0.103	29.811	4.125	0.094	31.153	#N/A	#N/A	#N/A
#N/A	#N/A	#N/A	1.733	0.078	38.481	1.229	0.076	35.130	#N/A	#N/A	#N/A
#N/A	#N/A	#N/A	1.609	0.054	45.111	1.653	0.052	37.118	#N/A	#N/A	#N/A
#N/A	#N/A	#N/A	0.603	0.045	75.710	1.480	0.030	82.853	#N/A	#N/A	#N/A
#N/A	#N/A	#N/A	0.519	0.038	167.000	0.406	0.024	157.421	#N/A	#N/A	#N/A
#N/A	#N/A	#N/A	0.150	0.035	289.908	-0.270	0.028	270.764	#N/A	#N/A	#N/A
#N/A	#N/A	#N/A	0.380	0.030	400.067	0.286	0.024	380.130	#N/A	#N/A	#N/A
#N/A	#N/A	#N/A							#N/A	#N/A	#N/A
#N/A	#N/A	#N/A							#N/A	#N/A	#N/A
#N/A			22.197	0.346	0.000	23.273			#N/A		

OS-119#1		OS-119#2		OS-119#3		OS-119#4	
S	P	S	P	S	P	S	P
		1.00	0.00	1.00	0.00		
		0.99	2.78	0.96	13.26		
		0.95	5.84	0.94	14.25		
		0.93	8.39	0.91	16.24		
		0.90	11.96	0.88	18.23		
		0.84	16.55	0.81	19.22		
		0.75	18.59	0.74	20.22		
		0.59	22.16	0.58	22.20		
		0.47	26.75	0.42	26.18		
		0.30	29.81	0.26	31.15		
		0.22	38.48	0.21	35.13		
		0.16	45.11	0.14	37.12		
		0.13	75.71	0.08	82.85		
		0.11	167.00	0.07	157.42		
		0.10	289.91	0.08	270.76		
		0.09	400.07	0.07	380.13		

OS 120
System **A-W**
Soil **OTAWA SAND**

NO	CELL WEIGHT					TIN			
	EMPTY	PACKED	SATU-RATED	DRAINED		EMPTY	INIT SOIL & RING	OVEN DRY SOIL & RING	RING
				ALL PART	W/O RING & SAMPLE				
<1>	<2>	<3>	<3>	<4>	<5>	<6>	<7>	<8>	<9>
1	400.63	515.85	563.55	542.20	351.99	3.88	194.09	191.48	73.42
2	403.33	517.74	568.02	543.26	353.86	3.83	193.23	190.69	72.60
3	404.41	518.70	566.57	543.88	354.56	3.78	193.10	190.84	72.83
4	404.76	518.27	565.97	543.75	353.23	3.86	194.38	190.68	72.57

Note Caps for column :

<3> = 8.150 gr
<4> = 8.056 gr
<5> = 7.793 gr

NO	Drained Water	Collected Water	Mass Ballance	Residual Water	Absorbed Water	Weight of Soil	Bulk Density
	<10>	<11>	<12>	<13>	<14>	<15>	<16>
1	21.256	21.228	0.12 %	2.61	23.866	114.184	1.676243
2	24.666	25.044	-1.39 %	2.54	27.206	114.256	1.677300
3	22.596	22.116	1.93 %	2.26	24.856	114.227	1.676874
4	22.127	22.293	-0.64 %	3.70	25.827	114.254	1.677271

OS120-#1			OS120-#2			OS120-#3			OS120-#4		
W-start	W-end	Volt	W-start	W-end	Volt	W-start	W-end	Volt	W-start	W-end	Volt
		0.014			2.720			0.100			0.250
4.728	5.254	0.140	4.729	5.246	2.750	4.746	5.280	0.150	4.709	5.262	0.300
5.254	5.694	0.170	5.246	5.736	2.790	5.280	5.765	0.180	5.262	5.763	0.320
4.778	5.294	0.180	4.744	5.296	2.840	4.795	5.346	0.180	5.736	5.754	0.330
5.294	5.690	0.180	5.296	5.751	2.940	5.346	5.791	0.190	5.754	5.762	0.330
4.747	5.267	0.170	4.736	5.312	3.010	4.852	5.336	0.190	4.783	5.285	0.340
5.267	5.707	0.210	5.312	5.729	3.030	5.336	5.789	0.190	5.285	5.770	0.350
9.509	10.675	0.220	8.735	10.694	3.120	8.428	9.605	0.180	8.950	10.025	0.340
10.675	11.673	0.230	10.694	11.748	3.200	9.605	10.576	0.170	10.025	11.212	0.350
11.673	12.618	0.240	11.748	12.819	3.250	10.576	11.613	0.190	11.212	12.186	0.350
12.618	13.783	0.250	12.819	13.883	3.290	11.613	12.615	0.200	12.186	13.241	0.360
13.783	14.754	0.260	13.883	14.860	3.330	12.615	13.763	0.200	13.241	14.149	0.360
14.754	15.731	0.280	14.860	15.964	3.380	13.763	14.773	0.210	14.149	15.157	0.370
15.731	16.711	0.260	15.964	16.954	3.420	14.773	15.917	0.210	15.157	16.237	0.360
16.711	17.631	0.270	16.954	17.812	3.450	15.917	16.791	0.220	16.237	17.217	0.370
17.631	18.766	0.280	17.812	19.052	3.510	16.791	17.745	0.220	17.217	18.265	0.380
18.766	19.657	0.290	8.666	10.923	3.590	17.745	18.816	0.230	18.265	19.182	0.380
9.001	11.761	0.280	10.923	12.904	3.660	8.330	10.576	0.240	9.125	11.145	0.420
11.761	13.626	0.350	12.904	15.772	3.780	10.576	14.421	0.320	11.145	14.406	0.440
13.626	14.476	0.380	15.772	16.924	3.820	14.421	15.366	0.370	11.406	14.811	0.540
8.610	10.405	0.390	9.067	10.960	4.080	8.496	9.162	0.390	8.967	9.278	0.550
10.405	10.676	0.540	10.096	10.580	4.170	9.162	9.497	0.420	9.278	9.487	0.580
10.676	10.902	0.610	10.580	11.095	4.230	9.497	9.789	0.470	9.487	9.683	0.610
10.902	11.042	0.650	11.095	11.295	4.280	9.789	9.946	0.640	9.683	10.094	0.770
11.042	11.187	1.010	11.295	11.506	4.610	9.946	10.089	0.850	10.094	10.202	0.880
11.187	11.377	1.590	11.506	11.665	5.060	10.089	10.236	1.170	10.202	10.275	0.920
11.377	11.640	1.640	11.665	11.902	6.240	10.236	10.445	1.370	10.075	10.323	1.020
11.640	11.861	2.470	11.902	12.071	8.310	10.445	10.603	2.170	10.323	10.524	1.530

Calibration

OS120-#1			OS120-#2			OS120-#3			OS120-#4		
P	V-data	P-reg	P	V-data	P-reg	P	V-data	P-reg	P	V-data	P-reg
600	6.00	596.69	600	7.44	595.67	600	5.96	592.93	600	6.00	601.63
500	5.05	500.33	500	6.73	505.92	500	5.07	503.54	500	5.03	500.25
400	4.06	401.15	400	5.92	403.53	400	4.09	405.10	400	4.05	397.82
300	3.09	303.08	300	5.09	298.61	300	3.05	300.64	300	3.11	299.58
200	2.08	200.77	200	4.23	189.90	200	2.06	201.20	200	2.15	199.25
100	1.09	100.78	100	3.36	79.93	100	1.05	99.75	100	1.20	99.96
50	0.61	52.86	50	2.92	24.31	50	0.54	48.53	50	0.73	50.84
0	0.03	-5.66	0	3.14	52.12	0	0.04	-1.70	0	0.25	0.67
	100.8956	-8.687786	2	126.4078	-344.8018	-0.04	100.4442	-5.713659		104.5134	-25.45533

OS120-#1			OS120-#2			OS120-#3			OS120-#4		
dW	MC	Pc	dW	MC	Pc	dW	MC	Pc	dW	MC	Pc
	0.350	-7.275		0.399	-0.973		0.365	4.331		0.379	0.673
0.526	0.343	5.438	0.517	0.392	2.820	0.534	0.357	9.353	0.553	0.371	5.899
0.440	0.336	8.464	0.490	0.385	7.876	0.485	0.350	12.366	0.501	0.364	7.989
0.516	0.329	9.473	0.552	0.377	14.196	0.551	0.342	12.366	0.018	0.363	9.034
0.396	0.323	9.473	0.455	0.370	26.837	0.445	0.335	13.371	0.008	0.363	9.034
0.520	0.315	8.464	0.576	0.361	35.686	0.484	0.328	13.371	0.502	0.356	10.079
0.440	0.309	12.500	0.417	0.355	38.214	0.453	0.322	13.371	0.485	0.349	11.124
1.166	0.292	13.509	1.959	0.326	49.590	1.177	0.304	12.366	1.075	0.333	10.079
0.998	0.277	14.518	1.054	0.311	59.703	0.971	0.290	11.362	1.187	0.316	11.124
0.945	0.263	15.527	1.071	0.295	66.024	1.037	0.275	13.371	0.974	0.301	11.124
1.165	0.246	16.536	1.064	0.280	71.080	1.002	0.260	14.375	1.055	0.286	12.170
0.971	0.232	17.545	0.977	0.265	76.136	1.148	0.243	14.375	0.908	0.272	12.170
0.977	0.217	19.563	1.104	0.249	82.457	1.010	0.228	15.380	1.008	0.258	13.215
0.980	0.203	17.545	0.990	0.235	87.513	1.144	0.212	15.380	1.080	0.242	12.170
0.920	0.189	18.554	0.858	0.222	91.305	0.874	0.199	16.384	0.980	0.227	13.215
1.135	0.173	19.563	1.240	0.204	98.890	0.954	0.185	16.384	1.048	0.212	14.260
0.891	0.160	20.572	2.257	0.171	109.002	1.071	0.169	17.388	0.917	0.199	14.260
2.760	0.119	19.563	1.981	0.142	117.851	2.246	0.136	18.393	2.020	0.169	18.440
1.865	0.092	26.626	2.868	0.099	133.020	3.845	0.080	26.428	3.261	0.121	20.531
0.850	0.079	29.653	1.152	0.083	138.076	0.945	0.066	31.451	3.405	0.071	30.982
1.795	0.053	30.662	1.893	0.055	170.942	0.666	0.056	33.460	0.311	0.067	32.027
0.271	0.049	45.796	0.484	0.048	182.319	0.335	0.051	36.473	0.209	0.063	35.162
0.226	0.046	52.859	0.515	0.040	189.903	0.292	0.047	41.495	0.196	0.061	38.298
0.140	0.044	56.894	0.200	0.037	196.224	0.157	0.044	58.571	0.411	0.055	55.020
0.145	0.042	93.217	0.211	0.034	237.938	0.143	0.042	79.664	0.108	0.053	66.516
0.190	0.039	151.736	0.159	0.032	294.822	0.147	0.040	111.806	0.073	0.052	70.697
0.263	0.035	156.781	0.237	0.028	443.983	0.209	0.037	131.895	0.248	0.048	81.148
0.221	0.032	240.524	0.169	0.026	705.647	0.158	0.035	212.250	0.201	0.045	134.450
21.228	0.346	0.000	25.044			22.116			22.293		

OS120-#1		OS120-#2		OS120-#3		OS120-#4	
S	P	S	P	S	P	S	P
0.99	5.44	0.98	2.82	0.98	9.35	0.98	5.90
0.97	8.46	0.96	7.88	0.96	12.37	0.96	7.99
0.95	9.47	0.94	14.20	0.94	12.37	0.96	9.03
0.93	9.47	0.93	26.84	0.92	13.37	0.96	9.03
0.91	8.46	0.90	35.69	0.90	13.37	0.94	10.08
0.89	12.50	0.89	38.21	0.88	13.37	0.92	11.12
0.84	13.51	0.82	49.59	0.83	12.37	0.88	10.08
0.80	14.52	0.78	59.70	0.79	11.36	0.83	11.12
0.76	15.53	0.74	66.02	0.75	13.37	0.79	11.12
0.71	16.54	0.70	71.08	0.71	14.38	0.75	12.17
0.67	17.55	0.66	76.14	0.67	14.38	0.72	12.17
0.63	19.56	0.62	82.46	0.63	15.38	0.68	13.21
0.59	17.55	0.59	87.51	0.58	15.38	0.64	12.17
0.55	18.55	0.56	91.31	0.54	16.38	0.60	13.21
0.50	19.56	0.51	98.89	0.51	16.38	0.56	14.26
0.46	20.57	0.43	109.00	0.46	17.39	0.52	14.26
0.34	19.56	0.35	117.85	0.37	18.39	0.45	18.44
0.27	26.63	0.25	133.02	0.22	26.43	0.32	20.53
0.23	29.65	0.21	138.08	0.18	31.45	0.19	30.98
0.15	30.66	0.14	170.94	0.15	33.46	0.18	32.03
0.14	45.80	0.12	182.32	0.14	36.47	0.17	35.16
0.13	52.86	0.10	189.90	0.13	41.50	0.16	38.30
0.13	56.89	0.09	196.22	0.12	58.57	0.14	55.02
0.12	93.22	0.09	237.94	0.12	79.66	0.14	66.52
0.11	151.74	0.08	294.82	0.11	111.81	0.14	70.70
0.10	156.78	0.07	443.98	0.10	131.89	0.13	81.15
0.09	240.52	0.06	705.65	0.10	212.25	0.12	134.45

OS 121
System **O-W**
Soil **OTAWA SAND**

NO	CELL WEIGHT							TIN			
			SATURATED CELL		DRAINED						
	EMPTY	PACKED	WATER	WATER & TOP OIL	ALL PART	w/o TOP OIL	w/o RING & SAMPLE	EMPTY	INIT SOIL & RING	OVEN DRY SOIL & RING	RING
<1>	<2>	<3>	<4>		<5>	<6>	<7>	<8>	<9>	<10>	<11>
1	399.74	514.07	566.41	578.65	591.75	563.71	362.56	3.87	224.57	190.74	72.64
2	399.46	513.82	564.58	578.41	591.10	564.80	361.02	3.82	223.79	190.42	72.57
3	401.67	516.02	564.09	580.60	593.47	563.58	360.20	3.79	223.79	191.27	73.26
4	403.62	517.99	566.57	582.16	595.78	563.82	362.13	3.87	224.24	191.55	73.52
Caps:			8.06	16.16	16.107		16.107				

NO	Collected Water	Cell weight at the end		Mass Ballance	Residual Water	Absorbed Water	Weight of Soil	Bulk Density
		by data 1	by data 2					
	<12>	<13>	<14>	<15>	<16>	<17>	<18>	<19>
1	22.11	576.24	575.64	-2.44 %	2.32	24.43	114.230	1.676918
2	21.86	575.85	574.99	-3.55 %	2.28	24.15	114.033	1.674026
3	21.42	577.76	577.36	-1.66 %	2.64	24.06	114.217	1.676727
4	21.68	579.49	579.67	0.75 %	3.31	24.99	114.162	1.67592

Note:
rho-oil = 1.622
<13> = <4> - <12> . (1- rho oil)

OS121-#1			OS21-#2			O121-#3			O121-#4		
W-start	W-end	Volt	W-start	W-end	Volt	W-start	W-end	Volt	W-start	W-end	Volt
		-0.020			4.960			0.020			0.000
4.758	5.050	0.080	4.752	5.077	5.000	4.768	5.060	0.035	4.820	5.118	0.044
5.050	5.312	0.085	5.077	5.295	5.010	5.060	5.304	0.039	5.118	5.355	0.049
5.312	5.527	0.090	5.295	5.523	5.020	5.304	5.560	0.041	5.355	5.555	0.050
5.527	5.767	0.094	5.523	5.729	5.020	5.560	5.785	0.043	5.555	5.794	0.056
4.806	5.068	0.096	4.765	5.074	5.030	4.804	5.115	0.053	4.827	5.124	0.060
5.068	5.338	0.098	5.074	5.305	5.030	5.115	5.330	0.053	5.124	5.364	0.060
5.338	5.576	0.100	5.305	5.506	5.030	5.330	5.568	0.055	5.364	5.567	0.070
5.572	5.880	0.100	5.506	6.744	5.030	5.568	6.798	0.055	5.567	6.792	0.070
4.863	5.136	0.110	4.775	5.082	5.040	4.774	5.114	0.070	4.872	5.153	0.070
5.136	5.374	0.110	5.082	5.317	5.040	5.114	5.332	0.070	5.153	5.369	0.070
5.374	5.568	0.110	5.317	5.528	5.040	5.332	5.549	0.070	5.369	5.601	0.074
5.568	5.802	0.110	5.528	5.751	5.040	5.549	5.814	0.070	5.601	5.838	0.076
9.275	10.639	0.100	8.448	9.846	5.040	8.408	9.846	0.080	8.842	10.244	0.081
10.639	11.736	0.120	9.846	11.141	5.050	9.846	10.886	0.080	10.244	11.152	0.088
11.736	14.912	0.122	11.141	13.824	5.060	10.886	13.896	0.100	11.152	14.137	0.096
14.912	17.693	0.128	13.824	16.869	5.070	13.896	17.010	0.130	14.137	17.280	0.100
17.693	19.656	0.138	16.869	19.182	5.080	17.010	19.774	0.160	17.280	19.077	0.100
9.600	13.727	0.180	8.578	11.035	5.090	8.470	12.202	0.240	8.929	12.135	0.120
9.512	10.358	0.190	8.053	9.328	5.120	8.637	9.185	0.260	8.465	9.758	0.130
10.358	10.715	0.200	9.328	9.830	5.130	9.185	9.541	0.270	9.758	10.178	0.150
10.715	11.140	0.270	9.830	10.263	5.130	9.541	9.801	0.350	10.178	10.584	0.160
11.140	11.876	0.280	10.263	10.908	5.140	9.801	10.184	0.400	10.584	11.091	0.180
11.876	12.729	0.330	10.908	11.645	5.170	10.184	10.529	0.440	11.091	11.596	0.220
12.729	13.196	0.390	11.645	12.476	5.270	10.529	10.752	0.660	11.596	11.944	0.260
13.196	13.968	0.730	12.076	12.394	5.540	10.752	10.905	0.730	11.944	12.800	0.499
9.484	10.336	0.840	8.689	9.893	5.680	8.509	9.394	0.790	9.068	10.400	0.580

Calibration

OS121-#1			OS21-#2			O121-#3			O121-#4		
P	**V-data**	**P-reg**	**P**	**V-data**	**P-reg**	**P**	**V-data**	**P-reg**	**P**	**V-data**	**P-reg**
150	1.58	152.42	150	6.55	150.95	150	1.50	152.89	150	1.50	151.40
0	0.09	4.74	0	5.01	4.12	0	0.02	4.92	0	0.01	2.34
10	0.15	10.68	10	5.08	10.79	10	0.09	11.92	10	0.09	10.34
20	0.23	18.61	20	5.17	19.38	20	0.17	19.92	20	0.19	20.35
30	0.33	28.52	30	5.27	28.91	30	0.26	28.92	30	0.29	30.35
40	0.43	38.44	40	5.34	35.58	40	0.34	36.91	40	0.38	39.36
50	0.53	48.35	50	5.44	45.12	50	0.44	46.91	50	0.46	47.36
75	0.77	72.14	75	5.74	73.72	75	0.69	71.91	75	0.73	74.37
100	1.03	97.91	100	6.02	100.42	100	0.96	98.90	100	0.96	97.38
150	1.57	151.43	150	6.56	151.90	150	1.48	150.89	150	1.50	151.40
0	0.06	1.76	0	5.01	4.12	0	-0.02	0.92	0	-0.01	0.34
	99.12022	-4.185807		95.34115	-473.5386		99.9768	2.9216		100.0431	1.339719

OS121-#1			OS21-#2			O121-#3			O121-#4		
dW	S	Pc	dW	S	Pc	dW	S	Pc	dW	S	Pc
	0.359	-6.17		0.354	-0.65		0.353	4.92		0.367	1.34
0.292	0.354	3.74	0.325	0.350	3.17	0.292	0.349	6.42	0.298	0.363	5.74
0.262	0.351	4.24	0.218	0.347	4.12	0.244	0.345	6.82	0.237	0.359	6.24
0.215	0.347	4.74	0.228	0.343	5.07	0.256	0.342	7.02	0.200	0.356	6.34
0.240	0.344	5.13	0.206	0.340	5.07	0.225	0.338	7.22	0.239	0.353	6.94
0.262	0.340	5.33	0.309	0.336	6.03	0.311	0.334	8.22	0.297	0.348	7.34
0.270	0.336	5.53	0.231	0.332	6.03	0.215	0.331	8.22	0.240	0.345	7.34
0.238	0.333	5.73	0.201	0.329	6.03	0.238	0.327	8.42	0.203	0.342	8.34
0.308	0.328	5.73	1.238	0.311	6.03	1.230	0.309	8.42	1.225	0.324	8.34
0.273	0.324	6.72	0.307	0.307	6.98	0.340	0.304	9.92	0.281	0.320	8.34
0.238	0.320	6.72	0.235	0.303	6.98	0.218	0.301	9.92	0.216	0.316	8.34
0.194	0.318	6.72	0.211	0.300	6.98	0.217	0.298	9.92	0.232	0.313	8.74
0.234	0.314	6.72	0.223	0.297	6.98	0.265	0.294	9.92	0.237	0.310	8.94
1.364	0.294	5.73	1.398	0.276	6.98	1.438	0.273	10.92	1.402	0.289	9.44
1.097	0.278	7.71	1.295	0.257	7.93	1.040	0.257	10.92	0.908	0.276	10.14
3.176	0.231	7.91	2.683	0.218	8.89	3.010	0.213	12.92	2.985	0.232	10.94
2.781	0.191	8.50	3.045	0.173	9.84	3.114	0.167	15.92	3.143	0.186	11.34
1.963	0.162	9.49	2.313	0.139	10.79	2.764	0.127	18.92	1.797	0.159	11.34
4.127	0.101	13.66	2.457	0.103	11.75	3.732	0.072	26.92	3.206	0.112	13.34
0.846	0.089	14.65	1.275	0.084	14.61	0.548	0.064	28.92	1.293	0.093	14.35
0.357	0.084	15.64	0.502	0.077	15.56	0.356	0.059	29.92	0.420	0.087	16.35
0.425	0.077	22.58	0.433	0.071	15.56	0.260	0.055	37.91	0.406	0.081	17.35
0.853	0.065	23.57	0.645	0.061	16.51	0.383	0.049	42.91	0.507	0.074	19.35
0.467	0.058	28.52	0.737	0.050	19.38	0.345	0.044	46.91	0.505	0.066	23.35
0.772	0.047	34.47	0.831	0.038	28.91	0.223	0.041	68.91	0.348	0.061	27.35
0.852	0.034	68.17	0.318	0.034	54.65	0.153	0.039	75.90	0.856	0.049	51.26
22.106	0.356	0.000	21.864	0.354	0.000	21.417	0.367	0.000	21.681	0.368	0.000

OS121-#1		OS121-#2		OS121-#3		OS121-#4	
S	P	S	P	S	P	S	P
1.00	3.74	0.99	3.17	0.95	6.42	0.98	5.74
0.98	4.24	0.98	4.12	0.94	6.82	0.98	6.24
0.98	4.74	0.97	5.07	0.93	7.02	0.97	6.34
0.97	5.13	0.96	5.07	0.92	7.22	0.96	6.94
0.96	5.33	0.95	6.03	0.91	8.22	0.95	7.34
0.94	5.53	0.94	6.03	0.90	8.22	0.94	7.34
0.93	5.73	0.93	6.03	0.89	8.42	0.93	8.34
0.92	5.73	0.88	6.03	0.84	8.42	0.88	8.34
0.91	6.72	0.87	6.98	0.83	9.92	0.87	8.34
0.90	6.72	0.86	6.98	0.82	9.92	0.86	8.34
0.89	6.72	0.85	6.98	0.81	9.92	0.85	8.74
0.88	6.72	0.84	6.98	0.80	9.92	0.84	8.94
0.83	5.73	0.78	6.98	0.74	10.92	0.78	9.44
0.78	7.71	0.73	7.93	0.70	10.92	0.75	10.14
0.65	7.91	0.62	8.89	0.58	12.92	0.63	10.94
0.54	8.50	0.49	9.84	0.46	15.92	0.50	11.34
0.45	9.49	0.39	10.79	0.35	18.92	0.43	11.34
0.28	13.66	0.29	11.75	0.20	26.92	0.30	13.34
0.25	14.65	0.24	14.61	0.17	28.92	0.25	14.35
0.23	15.64	0.22	15.56	0.16	29.92	0.24	16.35
0.22	22.58	0.20	15.56	0.15	37.91	0.22	17.35
0.18	23.57	0.17	16.51	0.13	42.91	0.20	19.35
0.16	28.52	0.14	19.38	0.12	46.91	0.18	23.35
0.13	34.47	0.11	28.91	0.11	68.91	0.17	27.35
0.10	68.17	0.09	54.65	0.11	75.90	0.13	51.26

OS 122
System O-W
Soil OTAWA SAND

NO	CELL WEIGHT							TIN			RING
	EMPTY	PACKED	SATURATED CELL		DRAINED			EMPTY	INIT SOIL & RING	OVEN DRY SOIL & RING	
			WATER	WATER & TOP OIL	ALL PART	w/o TOP OIL	w/o RING & SAMPLE				
<1>	<2>	<3>	<4>		<5>	<6>	<7>	<8>	<9>	<10>	<11>
1	403.72	518.13	567.91	582.83	596.21		362.33	3.86	226.99	191.54	73.44
2	402.21	516.61	565.58	581.90	594.76		362.38	3.84	226.02	190.71	72.59
3	402.15	516.55	565.67	581.81	594.87		361.96	3.79	226.28	190.77	72.84
4	401.03	515.46	565.58	580.95	593.95		361.69	3.86	225.98	190.74	72.60
Caps:			8.038	16.08	16.096		16.096				

NO	Collected Water	Cell weight at the end		Mass Ballance	Residual Water	Absorbed Water	Weight of Soil	Bulk Density
		by data 1	by data 2					
	<12>	<13>	<14>	<15>	<16>	<17>	<18>	<19>
1	22.82	580.94	580.11	-3.30 %	2.31	25.13	114.238	1.677036
2	21.54	579.22	578.66	-2.32 %	2.29	23.83	114.282	1.677682
3	21.87	579.33	578.77	-2.31 %	2.36	24.23	114.142	1.675626
4	21.76	578.40	577.85	-2.24 %	2.77	24.52	114.276	1.677594

Note:
rho-oil = 1.622
<13> = <4> - <12> . (1- rho oil)

OS122-#1			OS122-#2			OS122-#3			OS122-#4		
W-start	W-end	Volt	W-start	W-end	Volt	W-start	W-end	Volt	W-start	W-end	Volt
		0.058			6.020			0.010			-0.050
4.724	4.909	0.068	4.925	5.046	6.030	4.898	5.021	0.017	4.828	4.975	0.026
4.909	4.969	0.069	5.046	5.125	6.040	5.021	5.079	0.022	4.975	5.092	0.024
4.969	5.089	0.070	5.125	5.214	6.040	5.079	5.264	0.035	5.092	5.177	0.031
5.089	5.181	0.070	5.214	5.295	6.040	5.264	5.347	0.039	5.177	5.272	0.038
5.181	5.300	0.080	5.295	5.379	6.040	5.347	5.452	0.042	5.272	5.351	0.043
5.300	5.359	0.080	5.379	5.478	6.050	5.452	5.533	0.045	5.351	5.447	0.045
5.359	5.491	0.080	5.478	5.561	6.050	5.533	5.567	0.049	5.447	5.538	0.047
5.491	5.559	0.080	5.561	5.653	6.050	5.657	5.742	0.050	5.538	5.622	0.049
5.559	5.638	0.080	5.653	5.729	6.050	5.742	5.821	0.052	5.622	5.711	0.050
5.368	5.739	0.085	5.729	5.830	6.050	5.821	5.935	0.053	5.711	5.797	0.050
4.777	5.049	0.092	4.832	5.172	6.049	4.334	5.234	0.052	4.855	5.144	0.052
5.049	5.321	0.095	5.172	5.395	6.054	5.234	5.461	0.056	5.144	5.376	0.053
5.321	5.522	0.104	5.395	5.602	6.062	5.461	5.712	0.058	5.376	5.592	0.055
5.522	5.758	0.105	5.602	5.816	6.066	5.712	5.904	0.058	5.592	5.817	0.057
4.803	5.317	0.106	4.846	5.401	6.068	4.912	5.468	0.059	4.855	5.368	0.058
5.317	5.771	0.110	5.401	5.829	6.067	5.468	5.895	0.062	5.368	5.817	0.058
9.672	12.088	0.120	8.468	10.630	6.070	8.100	10.842	0.060	8.882	11.365	0.064
12.088	15.679	0.130	10.630	13.766	6.080	10.842	14.171	0.062	11.365	14.375	0.078
15.679	20.032	0.160	13.766	18.856	6.100	14.171	19.680	0.090	14.375	19.129	0.117
9.750	13.952	0.190	8.807	12.833	6.120	8.745	12.166	0.090	9.026	14.494	0.180
13.052	14.563	0.200	12.833	14.210	6.160	12.166	12.627	0.100	14.494	15.102	0.190
14.563	15.074	0.220	14.210	14.687	6.190	12.627	13.181	0.100	15.102	15.596	0.200
9.649	10.613	0.230	8.055	9.197	6.230	8.611	9.309	0.110	9.052	9.615	0.220
10.613	11.017	0.250	9.197	9.810	6.260	9.309	9.676	0.140	9.615	9.860	0.230
11.017	12.026	0.310	9.810	10.025	6.290	9.676	10.412	0.290	9.860	10.605	0.290
12.026	12.649	0.660	10.025	10.455	6.350	10.412	10.747	0.530	10.605	10.935	0.540

Calibration

OS122-#1			OS122-#2			OS122-#3			OS122-#4		
P	V-data	P-reg	P	V-data	P-reg	P	V-data	P-reg	P	V-data	P-reg
0	0.05	-0.41	0	6.02	2.96	0	0.03	2.36	0	0.02	0.21
10	0.15	9.60	10	6.10	10.94	10	0.12	11.39	10	0.11	9.24
20	0.25	19.62	20	6.19	19.91	20	0.20	19.41	20	0.21	19.28
30	0.36	30.63	30	6.30	30.87	30	0.29	28.43	30	0.31	29.32
40	0.46	40.65	40	6.38	38.85	40	0.39	38.46	40	0.42	40.37
50	0.55	49.66	50	6.46	46.82	50	0.48	47.49	50	0.52	50.41
75	0.80	74.70	75	6.68	68.76	75	0.73	72.56	75	0.77	75.51
100	1.05	99.74	100	6.97	97.67	100	1.00	99.63	100	1.02	100.61
150	1.55	149.81	150	7.54	154.79	150	1.53	152.78	150	1.50	148.81
100	1.06	100.74	100	7.00	100.66	100	1.01	100.64	100	1.02	100.61
50	0.55	49.66	50	6.49	49.82	50	0.49	48.49	50	0.52	50.41
0	0.06	0.59	0	6.02	2.96	0	0.04	3.36	0	0.02	0.21
	100.1518	-5.220177		99.68734	-597.16		100.28	-0.64722		100.4049	-1.800644

OS122-#1			OS122-#2			OS122-#3			OS122-#4		
dW	MC	Pc	dW	MC	Pc	dW	MC	Pc	dW	MC	Pc
	0.369	0.589		0.350	2.962		0.356	0.356		0.360	-6.821
0.185	0.366	1.590	0.121	0.348	3.959	0.123	0.354	1.058	0.147	0.358	0.810
0.060	0.365	1.690	0.079	0.347	4.956	0.058	0.353	1.559	0.117	0.356	0.609
0.120	0.364	1.790	0.089	0.346	4.956	0.185	0.350	2.863	0.085	0.355	1.312
0.092	0.362	1.790	0.081	0.344	4.956	0.083	0.349	3.264	0.095	0.353	2.015
0.119	0.360	2.792	0.084	0.343	4.956	0.105	0.348	3.565	0.079	0.352	2.517
0.059	0.360	2.792	0.099	0.342	5.953	0.081	0.346	3.865	0.096	0.351	2.718
0.132	0.358	2.792	0.083	0.341	5.953	0.034	0.346	4.266	0.091	0.350	2.918
0.068	0.357	2.792	0.092	0.339	5.953	0.085	0.345	4.367	0.084	0.348	3.119
0.079	0.356	2.792	0.076	0.338	5.953	0.079	0.343	4.567	0.089	0.347	3.220
0.371	0.350	3.293	0.101	0.337	5.953	0.114	0.342	4.668	0.086	0.346	3.220
0.272	0.346	3.994	0.340	0.332	5.853	0.900	0.329	4.567	0.289	0.342	3.420
0.272	0.342	4.294	0.223	0.328	6.352	0.227	0.325	4.968	0.232	0.338	3.521
0.201	0.339	5.196	0.207	0.325	7.149	0.251	0.322	5.169	0.216	0.335	3.722
0.236	0.336	5.296	0.214	0.322	7.548	0.192	0.319	5.169	0.225	0.332	3.922
0.514	0.328	5.396	0.555	0.314	7.747	0.556	0.311	5.269	0.513	0.324	4.023
0.454	0.321	5.797	0.428	0.308	7.648	0.427	0.304	5.570	0.449	0.318	4.023
2.416	0.286	6.798	2.162	0.276	7.947	2.742	0.264	5.370	2.483	0.281	4.625
3.591	0.233	7.800	3.136	0.230	8.944	3.329	0.215	5.570	3.010	0.237	6.031
4.353	0.169	10.804	5.090	0.155	10.937	5.509	0.134	8.378	4.754	0.167	9.947
4.202	0.108	13.809	4.026	0.096	12.931	3.421	0.084	8.378	5.468	0.087	16.272
1.511	0.086	14.810	1.377	0.076	16.919	0.461	0.077	9.381	0.608	0.078	17.276
0.511	0.078	16.813	0.477	0.069	19.909	0.554	0.069	9.381	0.494	0.071	18.280
0.964	0.071	17.815	1.142	0.052	23.897	0.554	0.069	9.381	0.494	0.071	18.280
0.404	0.065	19.818	0.613	0.043	26.887	0.698	0.059	10.384	0.563	0.062	20.288
1.009	0.051	25.827	0.215	0.040	29.878	0.367	0.054	13.392	0.245	0.059	21.292
0.623	0.041	60.880	0.430	0.034	35.859	0.736	0.043	28.434	0.745	0.048	27.317
22.818			21.540			21.871			21.757	0.358	0.000

OS122-#1		OS122-#2		OS122-#3		OS122-#4	
S	P	S	P	S	P	S	P
0.99	1.59	0.99	3.96	0.99	1.06	1.00	0.81
0.99	1.69	0.99	4.96	0.99	1.56	0.99	0.61
0.99	1.79	0.99	4.96	0.98	2.86	0.99	1.31
0.98	1.79	0.98	4.96	0.98	3.26	0.99	2.01
0.98	2.79	0.98	4.96	0.98	3.56	0.98	2.52
0.97	2.79	0.98	5.95	0.97	3.87	0.98	2.72
0.97	2.79	0.97	5.95	0.97	4.27	0.98	2.92
0.97	2.79	0.97	5.95	0.97	4.37	0.97	3.12
0.96	2.79	0.97	5.95	0.97	4.57	0.97	3.22
0.95	3.29	0.96	5.95	0.96	4.67	0.97	3.22
0.94	3.99	0.95	5.85	0.92	4.57	0.95	3.42
0.93	4.29	0.94	6.35	0.91	4.97	0.94	3.52
0.92	5.20	0.93	7.15	0.90	5.17	0.94	3.72
0.91	5.30	0.92	7.55	0.90	5.17	0.93	3.92
0.89	5.40	0.90	7.75	0.87	5.27	0.91	4.02
0.87	5.80	0.88	7.65	0.86	5.57	0.89	4.02
0.78	6.80	0.79	7.95	0.74	5.37	0.78	4.63
0.63	7.80	0.66	8.94	0.60	5.57	0.66	6.03
0.46	10.80	0.44	10.94	0.38	8.38	0.47	9.95
0.29	13.81	0.27	12.93	0.24	8.38	0.24	16.27
0.23	14.81	0.22	16.92	0.22	9.38	0.22	17.28
0.21	16.81	0.20	19.91	0.19	9.38	0.20	18.28
0.19	17.81	0.15	23.90	0.19	9.38	0.20	18.28
0.18	19.82	0.12	26.89	0.17	10.38	0.17	20.29
0.14	25.83	0.11	29.88	0.15	13.39	0.16	21.29
0.11	60.88	0.10	35.86	0.12	28.43	0.13	27.32

OS 123
System **A-O**
Soil **OTAWA SAND**
Oil-rho **1.622**

NO	CELL WEIGHT					TIN			
				DRAINED					
	EMPTY	PACKED	SATU-RATED	ALL PART	W/O RING & SAMPLE	EMPTY	INIT SOIL & RING	OVEN DRY SOIL & RING	RING
<1>	<2>	<3>	<3>	<4>	<5>	<6>	<7>	<8>	<9>
1	400.51	514.85	590.51	556.01		3.86	196.13	190.69	72.63
2	397.37	511.91	585.61	549.71		3.84	192.83	188.30	70.21
3	401.88	516.36	585.55	552.74		3.86	195.12	191.31	73.26
4	403.78	518.39	590.60	554.52		3.84	196.22	191.69	73.51

Note Caps for column :
<3> = 8.110 gr
<4> = 7.793 gr
<5> = 7.793 gr

NO	Drained oil	Collected Oil	Mass Ballance	Residual Oil	Absorbed Oil	Weight of Soil	Bulk Density
	<10>	<11>	<12>	<13>	<14>	<15>	<16>
1	34.18	33.93	0.64 %	5.44	39.623	114.200	1.676478
2	35.58	34.52	2.64 %	4.53	40.109	114.250	1.677212
3	32.49	32.26	0.65 %	3.81	36.3	114.190	1.676331
4	35.76	34.96	1.99 %	4.53	40.293	114.340	1.678533

OS123-#1			OS123-#2			OS123-#3			OS123-#4		
W-start	W-end	Volt	W-start	W-end	Volt	W-start	W-end	Volt	W-start	W-end	Volt
		0.023			1.030			0.030			-0.040
4.819	5.030	0.050	4.793	5.057	1.040	4.954	5.191	0.050	4.820	5.014	-0.010
5.030	5.228	0.090	5.057	5.249	1.040	5.191	5.407	0.060	5.014	5.148	0.001
5.228	5.496	0.100	5.249	5.528	1.050	5.407	5.658	0.070	5.148	5.348	0.010
5.496	5.790	0.100	5.528	5.780	1.060	5.658	5.960	0.070	5.348	5.637	0.030
5.790	6.033	0.100	5.642	5.916	1.060	5.960	6.253	0.070	5.637	5.901	0.030
6.033	6.242	0.100	5.916	6.254	1.060	6.253	6.446	0.070	5.901	6.141	0.040
6.242	6.386	0.100	6.254	6.484	1.060	6.446	6.643	0.080	6.141	6.347	0.050
10.736	11.731	0.110	10.904	12.281	1.070	11.051	12.614	0.090	11.689	13.370	0.120
12.141	14.008	0.120	12.281	14.148	1.070	12.614	14.235	0.100	13.370	14.620	0.160
14.008	15.660	0.120	14.148	15.623	1.070	14.235	15.797	0.110	14.620	16.204	0.210
15.660	17.257	0.130	15.629	16.991	1.080	15.797	17.475	0.100	16.204	17.701	0.250
17.257	18.814	0.130	16.991	18.769	1.100	17.475	19.047	0.110	17.701	19.443	0.300
18.814	23.336	0.150	18.769	23.211	1.100	19.047	23.602	0.110	19.443	23.840	0.410
23.336	28.046	0.160	23.211	27.889	1.110	23.602	27.376	0.120	23.840	28.595	0.480
11.258	15.435	0.180	11.258	15.560	1.130	11.080	15.582	0.130	11.810	16.247	0.550
15.435	20.161	0.190	15.560	19.911	1.150	15.582	20.373	0.160	16.247	20.785	0.600
20.161	23.353	0.230	19.911	23.064	1.160	20.373	22.183	0.170	20.785	23.782	0.680
11.363	12.479	0.250	11.107	12.685	1.170	11.155	13.960	0.320	11.915	13.197	0.720
12.419	13.190	0.280	12.685	13.370	1.190	13.960	13.982	0.580	13.197	14.292	0.790
13.190	13.589	0.290	13.370	14.581	1.350	13.982	13.994	0.660	14.292	14.810	0.800
13.589	14.076	0.360	14.581	14.909	1.490	13.994	14.147	0.900	14.810	15.221	1.010
11.317	11.823	0.430	11.302	11.356	1.850	10.959	11.074	0.990	11.803	12.200	1.390
11.823	11.912	1.660	11.356	11.407	1.960	11.074	11.105	1.270	12.200	13.054	1.460

Calibration

OS123-#1			OS123-#2			OS123-#3			OS123-#4		
P	V-data	V-reg	P	V-data	V-reg	P	V-data	V-reg	P	V-data	V-reg
0	0.06	0.06	0	1.05	1.03	0	0.22	0.04	0	0.23	-0.02
25	0.31	0.31	25	1.30	1.30	25	0.35	0.34	25	0.39	0.33
50	0.56	0.56	50	1.56	1.57	50	0.54	0.65	50	0.58	0.68
75	0.81	0.80	75	1.82	1.84	75	0.83	0.95	75	0.83	1.03
100	1.06	1.05	100	2.09	2.10	100	1.20	1.26	100	1.20	1.38
150	1.50	1.55	150	2.66	2.64	150	1.96	1.87	150	2.23	2.07
200	2.08	2.05									
	100.4042	-5.796996		93.21461	-96.14819		81.98284	-3.018748		71.59949	1.511129

OS123-#1			OS123-#2			OS123-#3			OS123-#4		
dW	MC	Pc	dW	MC	Pc	dW	MC	Pc	dW	MC	Pc
	0.359	-3.488		0.363	-0.137		0.329	-0.559		0.365	-1.353
0.211	0.357	-0.777	0.264	0.361	0.795	0.237	0.326	1.080	0.194	0.363	0.795
0.198	0.355	3.239	0.192	0.359	0.795	0.216	0.324	1.900	0.134	0.362	1.583
0.268	0.352	4.243	0.279	0.356	1.727	0.251	0.322	2.720	0.200	0.360	2.227
0.294	0.350	4.243	0.252	0.354	2.659	0.302	0.319	2.720	0.289	0.357	3.659
0.243	0.348	4.243	0.274	0.352	2.659	0.293	0.317	2.720	0.264	0.355	3.659
0.209	0.346	4.243	0.338	0.349	2.659	0.193	0.315	2.720	0.240	0.353	4.375
0.144	0.344	4.243	0.230	0.346	2.659	0.197	0.313	3.540	0.206	0.351	5.091
0.995	0.335	5.247	1.377	0.334	3.591	1.563	0.299	4.360	1.681	0.336	10.103
1.867	0.319	6.252	1.867	0.317	3.591	1.621	0.284	5.180	1.250	0.324	12.967
1.652	0.304	6.252	1.475	0.304	3.591	1.562	0.270	5.999	1.584	0.310	16.547
1.597	0.289	7.256	1.362	0.291	4.524	1.678	0.255	5.180	1.497	0.296	19.411
1.557	0.275	7.256	1.778	0.275	6.388	1.572	0.241	5.999	1.742	0.281	22.991
4.522	0.234	9.264	4.442	0.235	6.388	4.555	0.200	5.999	4.397	0.241	30.867
4.710	0.191	10.268	4.678	0.193	7.320	3.774	0.166	6.819	4.755	0.198	35.879
4.177	0.154	12.276	4.302	0.154	9.184	4.502	0.125	7.639	4.437	0.158	40.891
4.726	0.111	13.280	4.351	0.114	11.049	4.791	0.081	10.099	4.538	0.117	44.471
3.192	0.082	17.296	3.153	0.086	11.981	1.810	0.065	10.918	2.997	0.089	50.199
1.116	0.072	19.304	1.578	0.072	12.913	2.805	0.040	23.216	1.282	0.078	53.063
0.771	0.065	22.316	0.685	0.065	14.777	0.022	0.039	44.531	1.095	0.068	58.075
0.399	0.061	23.320	1.211	0.054	29.692	0.012	0.039	51.090	0.518	0.063	58.791
0.487	0.057	30.349	0.328	0.052	42.742	0.153	0.038	70.766	0.411	0.060	73.827
0.506	0.052	37.377	0.054	0.051	76.299	0.115	0.037	78.144	0.397	0.056	101.034
0.089	0.052	160.874	0.051	0.051	86.552	0.031	0.037	101.099	0.854	0.048	106.046
33.930	0.356	0	34.521	0.363	0	32.255	0.328	0	34.962	0.364	0

OS23-#1		OS23-#2		OS23-#3		OS23-#4	
S	P	S	P	S	P	S	P
1.00	-0.78	0.99	0.80	1.00	1.08	1.00	0.80
1.00	3.24	0.99	0.80	0.99	1.90	0.99	1.58
0.99	4.24	0.98	1.73	0.98	2.72	0.99	2.23
0.98	4.24	0.98	2.66	0.97	2.72	0.98	3.66
0.98	4.24	0.97	2.66	0.97	2.72	0.98	3.66
0.97	4.24	0.96	2.66	0.96	2.72	0.97	4.38
0.97	4.24	0.96	2.66	0.96	3.54	0.97	5.09
0.94	5.25	0.92	3.59	0.91	4.36	0.92	10.10
0.89	6.25	0.87	3.59	0.87	5.18	0.89	12.97
0.85	6.25	0.84	3.59	0.82	6.00	0.85	16.55
0.81	7.26	0.80	4.52	0.78	5.18	0.82	19.41
0.77	7.26	0.76	6.39	0.73	6.00	0.77	22.99
0.66	9.26	0.65	6.39	0.61	6.00	0.66	30.87
0.54	10.27	0.53	7.32	0.50	6.82	0.54	35.88
0.43	12.28	0.42	9.18	0.38	7.64	0.43	40.89
0.31	13.28	0.32	11.05	0.25	10.10	0.32	44.47
0.23	17.30	0.24	11.98	0.20	10.92	0.25	50.20
0.20	19.30	0.20	12.91	0.12	23.22	0.21	53.06
0.18	22.32	0.18	14.78	0.12	44.53	0.19	58.07
0.17	23.32	0.15	29.69	0.12	51.09	0.17	58.79
0.16	30.35	0.14	42.74	0.12	70.77	0.16	73.83
0.15	37.38	0.14	76.30	0.11	78.14	0.15	101.03
0.14	160.87	0.14	86.55	0.11	101.10	0.13	106.05